

Universidad de Cantabria
Facultad de Medicina
Departamento de Biología Molecular
Instituto de Biomedicina y Biotecnología de Cantabria
(IBBTEC)



**Mecanismo y Regulación de la Citoquinesis en la
Levadura *Saccharomyces cerevisiae***

**Mechanism and Regulation of Cytokinesis in budding
yeast *Saccharomyces cerevisiae***

Tesis doctoral presentada por
Iago Molist Pérez
para optar al Grado de Doctor por la
Universidad de Cantabria
Abril 2017

El Dr. Alberto Sánchez Díaz, Profesor Contratado Doctor en la Facultad de Medicina de la Universidad de Cantabria y el Instituto de Biomedicina y Biotecnología de la Universidad de Cantabria y la Dra. Magdalena Foltman, investigadora postdoctoral en la Facultad de Medicina de la Universidad de Cantabria y el Instituto de Biomedicina y Biotecnología de la Universidad de Cantabria.

CERTIFICAN:

Que el Licenciado Iago Molist Pérez ha realizado bajo su dirección el presente trabajo de Tesis Doctoral titulado:

**Mecanismo y Regulación de la Citoquinesis en la Levadura
*Saccharomyces cerevisiae***

**Mechanism and Regulation of Cytokinesis in budding yeast
*Saccharomyces cerevisiae***

Que consideran que este trabajo reúne los requisitos de originalidad y calidad científica necesarios para su presentación como Memoria de Doctorado por el interesado, al objeto de poder optar al grado de Doctor por la Universidad de Cantabria.

Y para que conste y surta los efectos oportunos, firman el presente certificado.

Santander, Abril de 2017

Fdo. Alberto Sánchez

Fdo. Magdalena Foltman

Esta Tesis ha sido realizada en el Instituto de Biomedicina y Biotecnología de Cantabria (IBBTEC) y la Facultad de Medicina de la Universidad de Cantabria en Santander, Cantabria.

La financiación necesaria para la realización de esta Tesis ha sido aportada por el Ministerio de Economía y Competitividad, gracias a la ayuda predoctoral de formación de personal investigador (FPI) BES-2012-058697, asociada al proyecto BFU2011-23193.

七転び八起き

Acknowledgements.

En primer lugar, me gustaría agradecer a mis supervisores el Dr. Alberto Sánchez y la Dra. Magdalena Foltman por darme la oportunidad de iniciarme en la ciencia, comenzar una carrera científica; así como sus consejos y su infinita paciencia conmigo. Me gustaría también mencionar a una estudiante en concreto que estuvo en el laboratorio, Marina. Tanto Magda como tú habéis sido compañeras de laboratorio increíbles, y amigas con las que he pasado muy buenos ratos tanto dentro como fuera del laboratorio. Finalmente, me gustaría agradecer a Yasmina por el tiempo que pasamos juntos; aunque no mucho, disfruté mucho el tiempo contigo en el laboratorio. ¡Mucho ánimo con tu tesis, que sé que lo harás genial!

Mis años en el IBBTEC no habrían sido los mismo sin la gente de los diferentes grupos que compartimos el edificio. Me gustaría agradecer todas las charlas (científicas o no) y la polimerasa de Thaidy y los Alcoholicocos; los consejos sobre *Bitchia* y charlas amorosas con Laura; los viajes en bus y las cañas con MdT; la ruta de senderismo en Los Tojos que nunca olvidaré con Marina, Lucía, Maña, Marcos, etc.; el repostear con Coral; las golosinas de Pepi; los apocalipsis zombies con medio IBBTEC; las purificaciones de anticuerpos...

I would also like to thank my British supervisor Dr. Bernadette Byrne during my placement at London. Your guidance and patience are truly inspiring, and I am tremendously grateful for the opportunity I had in your lab. Finally, my placement would not have been the same without my lab mates. I would like to specially mention Nikki, whose constant help, optimism and friendship truly mean a lot to me.

Esta sección no estaría completa sin mencionar a algunos amigos que siempre han estado ahí, en persona o en la distancia.

Aos meus amigos de Santiago; Miguel, Pau, Alba, María, Luís, etc. Cada vez que volvo á terra as cousas non cambian, e espero que siga así por moito tempo. Igualmente, a unha persoa moi especial do instituto, Elena. No Reino Unido ou na China, sen importar as circunstancias, ninguén cambiará a nosa tradición do chocolate con churros onda as señoras. Non o cambiaría por nada do mundo.

Pour mes amis en Belgique (maar alleen in Franstalig België), je sais que pour toi Coralie ta thèse se passera bien, et je te souhaite beaucoup de chance pour ce qui t'attend après. Aussi, tous les gars du CHE, je rêve toujours de passer plus de temps avec vous; je sais que vos projets futurs se réaliseront! Pour le moment... mariez-vous! J'veux aller à vos mariages pour avoir une excuse pour retourner en Belgique.

I en català em surt directament el nom de una persona, en ジョアン様. Sé que t'anirà bé a les teves aventures com a postdoc a 東京, i no et preocupis que, tard o d'hora, la visita promesa arribarà. がんばって amb la recerca, la gent com tu es mereix que els seus projectes es facin realitat. I nosaltres encara tenim la nostra companyia productora de gayasa pendent...

En Santander, no sería justo no mencionar a los Monos... y todas las tardes/noches de juegos de mesa y helados. Santander no sería lo mismo sin vosotros. Igualmente, todas las conversaciones y téis en el piso de Hannah, Dan y Sid... o en el Río de la Pila. Vosotros modelasteis mi inglés para que mejorase día a día, y os convertisteis en buenos amigos.

Finally, I would like to thank a couple of groups that have been my rocks in London. My Londoner life would not be the same without my ex-flatmates and friends Camilla, Tania and Donna. I love you lots! Also, the London Gaymers. You are an amazing project that has allowed me to meet like-minded people and enjoy my life in the UK so much. And also to Andrew... for a lot more spring strolls, travels and morning coffees together.

Para acabar, quiero agradecer todo el apoyo de mi familia, sobre todo de mis padres y mi hermana. Aunque no siempre nos lo demostremos, os quiero un montón.

Abbreviations.

AD	Activation Domain
Aid	Auxin-inducible degron
APC	Anaphase promoting complex
APS	Ammonium persulfate
ATP	Adenosine triphosphate
BLAST	Basic local alignment search tool
BSA	Bovine serum albumin
C2	Protein kinase C conserved region 2
Cdc	Cell division cycle
CDK	Cycle-dependent kinase
CHD	Calponin-homology domain
CON1/2	Conserved region 1/2
COPII	Coat protein II
CRB	Cell resuspension buffer
cryoEM	Cryo-electron microscopy
Cyk3	Cytokinesis 3
DBD	DNA-binding domain
DD	Aspartic acid-aspartic acid
DDM	Dodecylmaltoside
DM	Decylmaltoside
DMNG	Decyl maltoside neopentyl glycol
DMSO	Dimethyl sulfoxide
DNA	Deoxyribonucleic acid
DTT	Dithiothreitol
ECL	Enhanced chemiluminescence
EDTA	Ethylenediaminetetraacetic acid
EM	Electron microscopy
ER	Endoplasmic reticulum
ESCRT	Endosomal sorting complexes required for transport
F-actin	Filamentous actin
F-BAR	Fer/Cip4-Bin/Amphiphysin/Rvs domain
FACS	Fluorescence-activated cell sorting

FEAR	Cdc-fourteen early anaphase release
FSEC	Fluorescent size-exclusion chromatography
GAP	GTPase-activating protein
GDP	Guanosine diphosphate
GEF	Guanine nucleotide exchange factor
GFP	Green fluorescent protein
GlcNAc	N-acetylglucosamine
GNG6	Glucose neopentyl glycol 6
GRD	GAP-related domain
GTP	Guanosine triphosphate
HEPES	4-(2-hydroxyethyl)-1-piperazineethanesulfonic acid
Hof1	Homologue of fifteen
hphNT	Hygromycin resistance gene
HRP	Horseradish peroxidase
IAA	Indole acetic acid
Inn1	Ingression
IP	Immunoprecipitation
IPC	Ingression progression complex
IPTG	Isopropyl β -D-1-thiogalactopyranoside
IQGAP	Isoleucine-glutamine-GAP
kanMX	Geneticin resistance gene
LB	Luria-Bertani
LMNG	Lauryl maltoside neopentyl glycol
MEN	Mitosis exit network
Mid1	Medial ring protein 1
Mlc1	Myosin light chain 1
MOPS	3-(N-morpholino) propanesulfonic acid
MRB	Membrane resuspension buffer
MWCO	Molecular weight cut-off
MYC	Cellular myelocytomatosis oncogene epitope
NAA	Naphtalene acetic acid
NM	Nonylmaltoside
NP-40	Nonidet P-40

OD ₆₀₀	Optical density measured at 600nm of wavelength
PAGE	Polyacrylamide gel electrophoresis
PBS	Phosphate-buffered saline
PCR	Polymerase chain reaction
PNGase	Peptide:N-glycosidase F
PPB	Preprophase band
PXXP	Proline-rich motif
RGct	Ras-GAP C-terminus
RhoA	Ras homolog gene family, member A
RNA	Ribonucleic acid
RNase A	Ribonuclease A
RNAi	RNA interference
ROCK	Rho-associated protein kinase
RSM	Rich sporulation medium
SC	Synthetic complete
SDS	Sodium dodecyl sulphate
SEC	Size-exclusion chromatography
SH3	SRC Homology 3 domain
Sic1	Substrate/subunit inhibitor of cyclin-dependent protein kinase
SIN	Septation Initiation Network
TAP	Tandem-Affinity Purification
TBST	Tris-buffered saline Tween
TCA	Trichloroacetic acid
td	Temperature-sensitive degron
TE	Tris-EDTA
TEM	Transmission electron microscopy
TEMED	Tetramethylethylenediamine
TEV	Tobacco Etch Virus nuclear-inclusion-an endopeptidase
TG	Transglutaminase domain
Tris	Tris (hydroxymethyl) aminomethane
UD-MNG	Undecyl maltoside neopentyl glycol
UDP	Uridine diphosphate
YP	Yeast extract, Peptone

YPD	Yeast extract, Peptone, Dextrose
YPDA	Yeast extract, Peptone, Dextrose, Adenine
YPGal	Yeast extract, Peptone, Galactose
YPGalA	Yeast extract, Peptone, Galactose, Adenine
YPRaff	Yeast extract, Peptone, Raffinose
YPRaffA	Yeast extract, Peptone, Raffinose, Adenine
YSB	Yeast Solubilisation Buffer

ACKNOWLEDGEMENTS	9
ABBREVIATIONS	11
I. FIGURE LIST	17
II. TABLE LIST	19
1. INTRODUCTION	21
1.1 GENERAL INTRODUCTION.....	23
1.2 HISTORICAL BACKGROUND.....	24
1.3 CYTOKINESIS IN EUKARYOTIC ORGANISMS.....	28
1.4 CYTOKINESIS IN HIGHER PLANTS.....	29
1.5 CYTOKINESIS IN ANIMAL CELLS.....	29
1.6 CYTOKINESIS IN FISSION YEAST.....	31
1.7 CYTOKINESIS IN BUDDING YEAST.....	32
1.7.1 <i>Cyk3</i> and <i>transglutaminase-like</i> domains.....	37
1.7.2 <i>Chitin synthase Chs2</i> and <i>extracellular matrix (ECM)</i> remodelling.....	39
1.8 AIMS OF THIS THESIS.....	42
2. MATERIALS AND METHODS	43
2.1 DNA METHODS.....	45
2.1.1 <i>Genomic DNA extraction from yeast</i>	45
2.1.2 <i>Polymerase Chain Reaction (PCR)</i>	45
2.1.3 <i>Restriction enzyme digestion of PCR products and plasmids</i>	45
2.1.4 <i>Ligation of PCR products into plasmids</i>	45
2.1.5 <i>Transformation of E. coli</i>	46
2.1.6 <i>Plasmid DNA isolation from E. coli</i>	46
2.1.7 <i>DNA sequencing</i>	50
2.2 YEAST METHODS.....	50
2.2.1 <i>Yeast transformation</i>	50
2.2.2 <i>Mating strains to isolate diploids</i>	51
2.2.3 <i>Tetrad analysis</i>	51
2.2.4 <i>Dilution spotting assay</i>	58
2.2.5 <i>Yeast two-hybrid assay</i>	58
2.2.6 <i>Growth and synchronisation of yeast strains</i>	58
2.2.7 <i>Small-scale membrane protein expression</i>	59
2.2.8 <i>Growth of yeast strains for large-scale Chs2 protein production</i>	60
2.2.9 <i>FACS and binucleate cells counting</i>	60
2.3 PROTEIN METHODS.....	60
2.3.1 <i>Small-scale membrane preparation</i>	60
2.3.2 <i>Membrane preparation for Chs2 purification</i>	61
2.3.3 <i>Fluorescent size-exclusion chromatography (FSEC)</i>	61
2.3.4 <i>Large-scale Chs2 protein purification</i>	61
2.3.5 <i>Trichloroacetic acid (TCA) precipitation of proteins</i>	62
2.3.6 <i>Immunoblotting</i>	63
2.3.7 <i>Immunoprecipitation of protein complexes</i>	64
2.3.8 <i>Growth of E. coli cultures for protein expression</i>	65
2.3.9 <i>E. coli native purification</i>	65
2.3.10 <i>E. coli denaturing purification</i>	66
2.3.11 <i>Antigen purification</i>	66
2.3.12 <i>Antibody purification</i>	66
2.4 MICROSCOPY METHODS.....	67
3. RESULTS	69
3.1 BIOCHEMICAL STUDIES ON CHITIN SYNTHASE 2 - PURIFICATION AND STABILITY OF CHS2 PROTEIN.....	71
3.2 IDENTIFICATION OF CYK3 PROTEIN AS A COMPONENT OF THE INGRESSION PROGRESSION COMPLEX. ...	80

3.3 CHITIN SYNTHASE CHS2 IS ABLE TO DIRECTLY INTERACT WITH CYTOKINETIC PROTEIN CYK3.	83
3.4 GENERATING CONDITIONAL MUTANTS TO INACTIVATE CYK3. LACK OF CYK3 PROTEIN PRODUCES A CELL DIVISION DEFECT.	86
3.5 STUDYING THE DEFECTS ASSOCIATED WITH CYK3-DEPLETED CELLS.....	90
3.6 GENERATING THE TOOL TO DETERMINE CYK3 FUNCTION.....	92
3.7 SH3 DOMAIN OF CYK3 IS UNABLE TO INTERACT WITH CHS2, BUT IT IS IMPORTANT FOR CYK3 LOCALISATION AT THE SITE OF DIVISION.	95
3.8 CYK3 REGULATES THE FUNCTION OF CHS2.....	98
3.9 SYNTHETIC LETHALITY OF <i>C2-HOF1</i> AND LACK OF CYK3 IS RESCUED BY A HYPERMORPHIC ALLELE OF <i>CHS2</i> AND REVEALS AN UNEXPECTED ROLE FOR INN1 C-TERMINUS.....	107
3.10 DEFECTS IN PRIMARY SEPTUM DEPOSITION CAUSE THE LETHALITY ASSOCIATED TO DEPLETION OF CYK3 IN <i>C2-HOF1</i> CELLS	114
4. DISCUSSION.....	121
4.1 A PROTEIN COMPLEX COORDINATES CYTOKINESIS IN BUDDING YEAST.	123
4.2 IS CHS2 CONSERVED THROUGHOUT EVOLUTION?	124
4.3 WORKING WITH MEMBRANE PROTEIN CHS2, A NOT-SO-EASY TASK.....	126
4.4 CYK3 AS A CRUCIAL CYTOKINETIC REGULATOR.....	128
5. CONCLUSIONS	131
6. RESUMEN	137
7. REFERENCES	143

I. Figure list.

Figure 1.1 Cytokinesis in eukaryotic organisms.	28
Figure 1.2 Cytokinesis in higher plants.	29
Figure 1.3 Cytokinesis in higher eukaryotes.	30
Figure 1.4 Cytokinesis in <i>S. pombe</i> .	31
Figure 1.5 Cytokinesis in <i>S. cerevisiae</i> .	33
Figure 1.6 The Mitosis Exit Network (MEN).	34
Figure 1.7 Alignment of the transglutaminase-like domains.	38
Figure 1.8 Timing of arrival of major cytokinetic regulators to the site of division.	39
Figure 3.1 Expression and solubilisation of chitin synthase Chs2.	72
Figure 3.2 Assessment of Chs2 solubility in different detergents.	74
Figure 3.3 Expression and purification of Chs2 protein.	76
Figure 3.4 Purification of Chs2 after co-expression with Inn1 protein in <i>cdc15-2</i> or <i>cdc14-1</i> background.	77
Figure 3.5 Ingression Progression Complexes (IPCs) are formed at the end of cytokinesis to coordinate actomyosin ring contraction, primary septum formation and membrane ingression.	80
Figure 3.6 Raising anti-Cyk3, anti-Chs2 and anti-Hof1 antibodies.	81
Figure 3.7 Cyk3 is able to interact with Chs2 in yeast extracts from cells undergoing cytokinesis.	84
Figure 3.8 Chs2 and Cyk3 are able to directly interact when purified from an <i>E. coli</i> expression system.	85
Figure 3.9 Degradation of Cyk3 using auxin degron does not yield a tight phenotype.	87
Figure 3.10 Double temperature and auxin degron (<i>td-aid</i>) provides an excellent tool for studying the role of Cyk3 protein.	89
Figure 3.11 Upon the depletion of Cyk3 protein, a temporary accumulation of Inn1-GFP occurs, indicating a defect in cell division.	90
Figure 3.12 Upon the depletion of Cyk3 protein, chitin synthase Chs2 protein can localise at the site of division.	91
Figure 3.13 <i>C2-HOF1</i> is synthetically lethal with <i>td-cyk3-aid</i> .	94
Figure 3.14 SH3 domain of Cyk3 does not bind to Chs2.	96
Figure 3.15 Lack of SH3 domain prevents localisation of Cyk3.	97
Figure 3.16 Different fragments of Cyk3 are able to interact with a fragment of Chs2	98

containing the catalytic domain in a yeast two-hybrid assay.	
Figure 3.17 Chs2 and a fragment of Cyk3 are able to interact directly when purified from an <i>E. coli</i> expression system.	100
Figure 3.18 Conserved residues in the transglutaminase-like domain are important for Cyk3 function.	101
Figure 3.19 Simultaneous mutation of two conserved residues H563 and D578 to alanines abolishes Cyk3 function.	103
Figure 3.20 Overexpression of transglutaminase-like domain mutant <i>cyk3-2A</i> unables cells to lay down thicker primary septa.	104
Figure 3.21 Deposition of thicker primary septa upon overexpression of Cyk3 is not due to Chs2 localisation.	106
Figure 3.22 The synthetic lethal combination of <i>C2-HOF1</i> and the lack of <i>CYK3</i> is rescued by the hypermorphic allele of Chs2, <i>CHS2-V377I</i> .	108
Figure 3.23 C-terminus of Inn1 and Cyk3 do not share a common function.	109
Figure 3.24 C-terminus of Inn1 is not able to compensate the lack of Cyk3 in <i>C2-HOF1</i> cells.	111
Figure 3.25 C-terminus domain of Inn1 is responsible for the synthetic lethality in <i>C2-HOF1</i> cells lacking Cyk3 function because of misregulation of Chs2 protein.	113
Figure 3.26 Actomyosin ring is assembled and disassembled in <i>C2-HOF1</i> cells lacking Cyk3.	115
Figure 3.27 Inn1-GFP accumulates in cells lacking functional <i>CYK3</i> in the presence of <i>C2-HOF1</i> .	117
Figure 3.28 Inn1 is able to localise prematurely in the site of division in cells devoid of Cyk3 in a <i>C2-HOF1</i> background.	119
Figure 3.29 <i>C2-HOF1</i> cells depleted for Cyk3 are unable to lay down primary septa.	120
Figure 4.1 Model for the activation of chitin synthase Chs2.	123
Figure 4.2 Hyaluronan synthases share homology with chitin synthase Chs2.	125

II. Table list.

Table 1.1 Cytokinesis is a conserved process throughout evolution.	28
Table 1.2 Comparison of primary septum synthases from fission (Bgs1) and budding (Chs2) yeast.	40
Table 2.1 Oligonucleotides used in this study.	47
Table 2.2 Plasmids used in this study.	49
Table 2.3 Yeast strains used in this study.	52
Table 2.4 Constructs made by one-step PCR.	57
Table 4.1 Glycosyltransferase enzymes involved in cell division in different organisms.	124

1. INTRODUCTION

1.1 General introduction.

Cytokinesis is the final stage of the cell cycle in which a cell is physically divided into two daughter cells, each of them enclosed by a plasma membrane and surrounded by the extracellular matrix (ECM). Cytokinesis in most organisms is based on the formation of a contractile, actomyosin-based ring in the cell equator. This way, cells ensure an even separation of DNA and organelles between mother and daughter cells.

The study of cytokinesis has always been an important research topic, since the continuity of life depends on continuous cell proliferation, in a cycle that alternates the replication of the genetic material and its partition between mother and daughter cells, known as the cell cycle. At the end of the cell cycle, cells segregate the replicated DNA in a process called mitosis, and in a coordinated manner cells divide the cytoplasm between mother and daughter cells in a process called cytokinesis.

Although organisms have evolved to develop very different abilities to cope with different environments, key steps of cytokinesis are conserved amongst the evolutionary distant species to achieve this goal (Balasubramanian *et al.* 2004, Pollard 2010).

Due to the evolutionary conservation of the process, the use of budding yeast *Saccharomyces cerevisiae* to understand how cells divide has presented and still presents

many advantages. Disciplines such as genetics, biochemistry and cellular biology have used budding yeast extensively. The ability of budding yeast to undergo efficient homologous recombination using a limited number of base pairs has made budding yeast an excellent model with which to carry out different genetic alterations. The use of budding yeast allows researchers to determine fundamental aspects of eukaryotic biology in a fast and precise manner, and these can be later confirmed in experiments using mammalian cells.

Successful cytokinesis is needed for cell proliferation, so it is not surprising that affecting cytokinesis in different organisms leads to a lethal phenotype. It has been shown in *Saccharomyces cerevisiae* (Watts *et al.* 1987, VerPlank and Li 2005) and fission yeast *Schizosaccharomyces pombe* (Kitayama *et al.* 1997, Cortes *et al.* 2007) that cytokinesis failure leads to cell death owing to depletion of either type-II myosin (Watts *et al.* 1987) or members of the enzyme family, called glycosyltransferases, that remodel extracellular matrix during cytokinesis (Shaw *et al.* 1991, VerPlank and Li 2005). This is also the case in higher eukaryotes, such as in worm *Caenorhabditis elegans*, in which cytokinesis failure due to lack of myosin function or activity of a special glycosyltransferase (Chondroitin synthase ChSy, T24D1.1) leads to an early embryonic

death (Guo and Kemphues 1996, Mizuguchi *et al.* 2003).

Invariably, cytokinesis failure leads to the formation of genetically unstable tetraploid cells with multiple centromeres (Fujiwara *et al.* 2005, Nakayama and Inoue 2016). Fujiwara *et al.* have demonstrated that tetraploid cells (but not diploid cells) are able to induce tumour formation when injected into nude mice.

Interestingly, some skeletal muscle cells undergo mitosis but not cytokinesis, giving rise to genetically stable multinucleated cells, in which the number of nuclei is thought to be related with hypertrophy and atrophy (Blaauw *et al.* 2013). More importantly, smooth muscle tissue also shows some degree of polyploidy that increases with age and is related to senescence (Barrett *et al.* 1983, Yang *et al.* 2007).

Additionally, the formation of polyploid liver hepatocytes has been related to the protection against genetic damage and the functional capacity of the liver (Duncan 2013, Gentric and Desdouets 2014, Fortier *et al.* 2017). Finally, formation of polyploid cells is necessary for wound healing and tissue repair (Losick 2016).

Abnormal cell division is not restricted to generation of polyploidy, but it can also lead to an asymmetric division. Consequently, mother and daughter cells would differ in size and/or cytoplasmic content, leading to different fates (Rhyu *et al.* 1994).

For instance, in neuroblasts of fruit fly *Drosophila melanogaster* there is an asymmetric protein disposition, which leads to a different fate between mother and daughter cells (Yu *et al.* 2006, Chia *et al.* 2008). This asymmetric division is crucial for their function, as transplanting neuroblasts lacking functional proteins required for the asymmetry into a wild type fly leads to tumour formation and death (Caussinus and Gonzalez 2005, Beaucher *et al.* 2007, Homem and Knoblich 2012).

In higher eukaryotes, one of the most striking examples of asymmetric cell division is the formation of the polar bodies in oocytes. During oocyte maturation, an asymmetric division takes place, from which a large egg and a small polar body arise (Yi and Li 2012, Sun and Kim 2013). Other cell types that divide asymmetrically can be found in the hair follicles (Zhang *et al.* 2010) and the mammary glands (Santoro *et al.* 2016).

Cytokinesis is a key step in cell cycle, so the discovery of the mechanisms regulating cytokinesis is a fundamental aspect in cell biology. It is essential to understand how proteins involved in cytokinesis work and how misregulation of the way they function could promote division failure.

1.2 Historical background

A major question to be asked by early cytologists was whether mitosis and cytokinesis were dependent or independent processes.

In the early 20th century, botanist Eduard Strasburger addressed this issue by studying alga *Cladophora glomerata*. This alga performs several rounds of mitosis that is followed by cytokinesis to separate all daughter cells. This strongly suggested that cytokinesis and mitosis were independent processes (Strasburger 1913). The importance of cytokinesis was established when Boveri proposed that tumours could develop either because of abnormal division of the centrosomes or by suppression of cell division, which would then lead to tetraploidy (Boveri 2008) (English translation).

In order to perform early experiments studying the cytokinesis, fertilised marine invertebrate eggs were used as a model, as they were easy to obtain, large in size and they are also symmetrical, transparent and synchronous in their first divisions.

In higher eukaryotes, the first visible change that occurs during cytokinesis is the formation of a cleavage furrow in cell surface, physically marking the site of division. This pucker further deepens rapidly, until it completely divides mother and daughter cells. In the early 1910s, Yatsu showed that once the cleavage furrow is undergoing contraction, it requires neither the nucleus nor the aster, as removing these structures did not block the furrow to continue (Yatsu 1908, Yatsu 1912).

The trigger of this cleavage furrow was discovered in 1916, when Conklin showed in eggs of the sea snail *Crepidula* that the

position of the ingression furrow depends on the localisation of the mitotic spindle. Consequently, it was shown that when the mitotic spindle position was shifted, the position of the division plane was forever changed (Conklin 1916).

Later on, Chambers and Kopac used another approach (Chambers and Kopac 1937). They injected an oil drop in the cytoplasm of dividing sea urchin eggs to show that, when that drop was at the cleavage site of a dividing cell, constriction continued despite of the fact that the droplet had displaced the mitotic apparatus. This reinforced the theory that the mitotic apparatus is not needed after the onset of contraction.

In order to discover when the mitotic spindle plays its role in the formation of the cleavage furrow, Beams and Evans used colchicine, which blocks microtubule polymerisation (Beams and Evans 1940). They showed that cleavage could take place only if the disruption happened in anaphase or later, suggesting that cleavage furrow plays a role earlier in the cell cycle. This finding was confirmed later by Mitchinson (Mitchinson 1953).

In order to overcome any doubt that the mitotic spindle is not necessary after the formation of the cleavage furrow, Hiramoto designed a different experiment, in which he sucked the mitotic apparatus from the eggs at different stages of the cell cycle (Hiramoto 1956). Removal of the mitotic apparatus

before anaphase blocked the cleavage, but the blockage did not happen when the mitotic apparatus was removed upon anaphase or later on. He also confirmed the experiments performed by Chambers and Kopac (Hiramoto 1965), by injecting oil at different stages of the cell cycle to displace the mitotic apparatus, showing that indeed the mitotic apparatus determined the site of division.

After confirming that the mitotic spindle is indeed responsible for the formation of the cleavage furrow, researchers did not know which part of the cleavage furrow was responsible for this process. This question was addressed by Ray Rappaport, who designed an experiment using sea urchin *Echinorachnius* eggs. After pressing them with a glass bead to produce a doughnut-shaped cell, the eggs were left to divide. The first division created a horseshoe-shaped binucleate cell that, after further division, produced a group of uninucleate cells through three cleavage furrows: one for each of the two spindles, and a third one between the asters separating the two spindles (that is, without any chromosomes in between). This suggested that it is the zone of convergence of the asters that determines the position of the cleavage furrow (Rappaport 1961).

Several theories were developed in order to understand how the cleavage furrow was formed. Theories appeared suggesting that mitosis and cytokinesis are caused by the same mechanism, that is, a physically active

mitotic apparatus. Asters would directly attach to the surface, and the tension transmitted to them would be proportional to their length; consequently, longer asters would pull stronger on the equatorial surface, pulling it inwards (Chambers 1922, Gray 1931).

On the other hand, it was proposed that it is the contraction of a tightening band in the equator of the cell that causes the division (Lewis 1939). Several possibilities were tested. Equatorial tension increase would suggest that the necessary forces for cytokinesis would result from a contraction of a superficial layer in the cell equator (Lewis 1939, Marsland 1954). Polar tension decrease would suggest that cytokinesis is caused by a decrease of tension in the poles of the cell, consequently inducing furrow formation (Wolpert 1960, White and Borisy 1983).

In order to distinguish between these possibilities, a thorough understanding of the structure of the cleavage furrow was necessary. In order to do that, Mercer and Wolpert examined the cleavage site of dividing sea urchin eggs under transmission electron microscopy (TEM). Indeed, the site of division was rich in tubular-shaped material (Mercer and Wolpert 1958). Later on, Rappaport showed that the force generated by the furrow was enough for cleavage and, most importantly, proved that it is very similar to the contractile capability of an actomyosin thread (Rappaport 1967), pointing out towards a possible actomyosin-based composition.

It was tempting to suggest that contraction was happening due to an interaction of F-actin with myosin. In the 1950s it had been postulated that muscle contraction occurred because of an interaction between F-actin and myosin in the skeletal muscle sarcomeres (Huxley and Hanson 1954), providing a possible mechanism. Indeed, a protein with the same characteristics as actin had been purified from sea urchin eggs undergoing cytokinesis (Miki-Noumura and Kondo 1970). A year later, actin-like filaments were observed in the cleavage furrow of newt eggs (Perry *et al.* 1971). To prove this hypothesis, Schroeder incubated dividing HeLa cells with meromyosin, a myosin fragment that binds to F-actin. When observing these cells under transmission electron microscopy, the thickness of the contractile ring increased, strongly suggesting that it contains F-actin (Schroeder 1973).

Later on, in starfish and sea urchin eggs, Mabuchi found that a form of myosin was present beneath the cell surface, and that it could react with muscle actin in the same way as muscle actin with muscle myosin in the presence of ATP (Mabuchi 1973, Mabuchi 1974). A bit later, presence of myosin in the cleavage furrow of dividing HeLa cells was confirmed (Fujiwara and Pollard 1976). Subsequently, it was demonstrated that both actin and myosin co-localised at the cleavage furrow (Fujiwara and Pollard 1978).

Finally, to check whether the mechanism of division depends on actin-myosin interaction, anti-myosin antibodies were injected into dividing cells. The experiment showed that anti-myosin antibodies effectively blocked cytokinesis yet not affecting mitosis (Mabuchi and Okuno 1977).

From the 1970s, our understanding of cell division has steadily grown thanks to the development of different techniques. A major breakthrough was the genetic study undertaken by Hartwell (Hartwell *et al.* 1970) in which he identified previously unknown temperature-sensitive mutants in budding yeast. Amongst them he found several alleles that were unable to complete cytokinesis after mitosis, leading to the formation of multinucleated cells. The mutated genes, *cdc3*, *cdc10*, *cdc11* and *cdc12*, were later shown to encode septins, proteins that form a structural scaffold needed for cytokinesis. The same approach was taken by Nurse and colleagues to identify genes related to cell cycle progression in fission yeast (Nurse *et al.* 1976).

Other molecular techniques developed later on had huge impact on shaping our understanding of the cytokinesis process. Amongst them, development of techniques such as fluorescence and confocal microscopy has tremendously contributed to our understanding of cytokinesis, thanks to the use of fluorescent proteins, such as GFP (Chalfie

Table 1.1: Cytokinesis is a conserved process throughout evolution.

	Higher eukaryotes	<i>S. cerevisiae</i>	<i>S. pombe</i>
Myosin	Myosin-II	Myo1	Myo2
Rho-GTPase	RhoA	Rho1	Rho1
Formin	Cyk1 (nematodes) mDia2 (mice)	Bni1 Bnr1	Cdc12
Polo-like kinase	Plk1	Cdc5	Plo1
Phosphatase	Cdc14A	Cdc14	Clp1

et al. 1994). In addition, high throughput techniques like genomics and proteomics have advanced our knowledge about cytokinesis. Also, the development of higher resolution electron microscopy such as cryo-EM and electron tomography had contributed to a better understanding of cytokinesis (Bertin *et al.* 2008) and they shaped the available information about how an eukaryotic cell is able to divide.

1.3 Cytokinesis in eukaryotic organisms.

In this section we will cover the mechanism of cytokinesis in eukaryotic organisms. However, we would like to mention that prokaryotic organisms also build a contractile ring, which is based on a GTPase protein named FtsZ, that forms the so-called Z-ring at the middle of the cell and guides septum formation in *Escherichia coli* (Bi and

Lutkenhaus 1991, Lyu *et al.* 2016, Vedyaykin *et al.* 2016).

Amongst eukaryotic organisms, cytokinesis is a highly conserved process (Table 1.1). However, different eukaryotes have evolved slightly different approaches due to their biology (Figure 1.1). Several differences arose in cell division between budding yeast and animal cells, which will be described in more detail in the relevant section. On the one hand, the cue and timing for selection of the site of division is different;

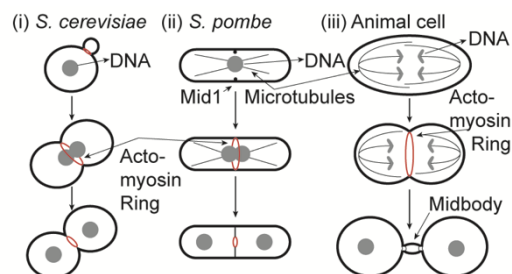


Figure 1.1: Cytokinesis in eukaryotic organisms.

Different organisms select their division sites upon different signals, at different stages of the cell cycle.

- (i) *Saccharomyces cerevisiae*.
- (ii) *Schizosaccharomyces pombe*.
- (iii) Animal cell.

whereas in budding yeast cleavage site selection occurs in G₁, where the new bud is about to emerge; in animal cells it occurs during anaphase according to the spindle position. On the other hand, whereas budding yeast show a closed division without breakage of the nuclear envelope, an open division happens in animal cells. Finally, during abscission, a new structure called the midbody is formed in animal cells, unlike what occurs in budding yeast.

Despite these differences, both organisms rely on the formation of actomyosin ring for successful cytokinesis. Higher plants, however, have developed a different cytokinesis strategy when compared to yeast or animal cells, so their particular cytokinesis mechanism will be discussed first. Below we will explain how higher plants, animal cells and yeast perform cytokinesis. There are mainly two yeast models that have been used for the study of cell division, *S. pombe* and *S. cerevisiae*, of which we will share molecular details.

1.4 Cytokinesis in higher plants.

In higher plants, cytokinesis occurs in the absence of a contractile actomyosin ring. This is consistent with the fact that the model higher plant *Arabidopsis thaliana* does not code in its genome neither type-II myosin, one of the major actomyosin ring components, nor septins, which form an important scaffold for

cytokinesis (Arabidopsis 2000). The plant cell builds instead a new cell wall (called the cell plate) at the site of division, using material from the Golgi apparatus (Figure 1.2).

The selection of the division site is determined before prophase by the so-called preprophase band (PPB) (Pickett-Heaps JD 1966, Müller and Jürgens 2015). It consists of an actin and microtubules band underneath the cell cortex.

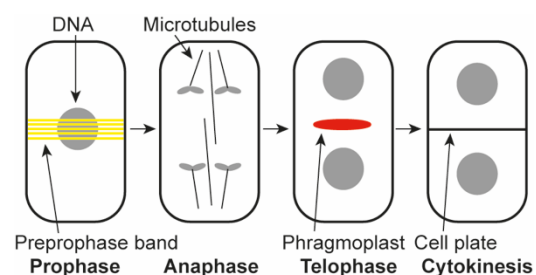


Figure 1.2: Cytokinesis in higher plants.

Yellow: pre-prophase band. Grey: DNA. Red: Phragmoplast. Black: Cell wall.

The preprophase band disassembles after mitotic entry, but induces signals, such as Pok1 and Pok2 (Lipka *et al.* 2014) that guide the formation of a new cell wall between the mother and daughter cell, which is called the phragmoplast. These signals guide the fusion of the cell plate with the parental membrane (Müller *et al.* 2006, Lipka *et al.* 2014), dividing mother and daughter cells.

1.5 Cytokinesis in animal cells.

In animal cells, cytokinesis can be separated into different stages (Figure 1.3).

First, mitotic spindle determines the position of the cleavage site. Subsequently, cells assemble a contractile ring underneath

the plasma membrane. Once cells have segregated their chromosomes, actomyosin ring contraction is initiated, which drives ingression of the plasma membrane. This process needs to be coupled necessarily with ECM remodelling. Finally, cells resolve the final step of cytokinesis in a process called abscission, which leads to the final resolution of mother and daughter cells (Balasubramanian *et al.* 2004, Barr and Gruneberg 2007).

The central spindle, an array of antiparallel microtubules that have a small degree of overlap at their plus ends, determines the cleavage site during anaphase. A protein complex centralspindlin is precisely located to the future site of division, to bundle together microtubules of opposite polarity and stabilising them to form the central spindle (Mishima *et al.* 2002, Mishima *et al.* 2004, White and Glotzer 2012). Centralspindlin recruits a key protein, Ect2 (Tatsumoto *et al.* 1999, Frenette *et al.* 2012), which is a RhoA GEF (Guanine nucleotide Exchange Factor). Ect2 is able to positively regulate the activity of the small GTPase RhoA that acts as the master regulator of cytokinesis. RhoA determines the site of division, as it is able to induce the accumulation of F-actin and myosin (Kimura *et al.* 1996, Kosako *et al.* 2000, Alberts 2001).

To stimulate the nucleation and assembly of actin filaments, active RhoA is able to trigger the function of formins. On the

other hand, active RhoA is able to stimulate myosin assembly and activity. RhoA activates Rho kinase (ROCK) and Citron kinase (Citron K), both kinases will directly phosphorylate myosin regulatory light chains (Piekny *et al.* 2005). This will activate its assembly in bipolar filaments and activate its motor activity (Kamm and Stull 1985, Matsumura *et al.* 2001, Echard *et al.* 2004).

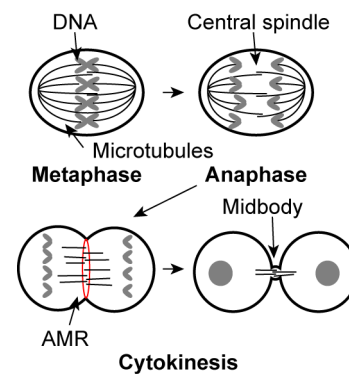


Figure 1.3: Cytokinesis in higher eukaryotes.

Black lines represent microtubules, gray represents DNA and red represents the contractile ring.

Contraction of the assembled actomyosin ring provides the force for the separation of mother and daughter cells. Studying ring contraction is extremely challenging. The use of fluorescent versions of myosin and formins has been essential to follow contraction dynamics, as GFP-tagged actin is not functional (Agbulut *et al.* 2007, Deibler *et al.* 2011). It has been described that the rate of formin loss from the contractile ring is proportional to its circumference; thus, the bigger the initial diameter, the faster the ring will contract (Wu and Pollard 2005). It has been recently proposed that membrane curvature could be responsible of the release

of actomyosin bundles from the cytokinetic ring, consequently shrinking the ring and causing the contraction (Huang *et al.* 2016).

After the actomyosin ring contraction and plasma membrane ingression, animal cells are partitioned into two daughters but remain connected initially by a narrow intracellular bridge, the so-called midbody. This structure can be observed as an electron-dense disc narrower on the sides than in the centre (Mullins and Biesele 1977) (Figure 1.3). The midbody is originated as the furrow ingression compacts antiparallel midzone bundles into a single large bundle. Midbody formation depends on the contraction of the actomyosin ring, as blocking the contractile ring by inhibiting type-II myosin with blebbistatin or actin polymerisation with latrunculin A prevents formation of this structure (Hu *et al.* 2012). The midbody is linked to the plasma membranes through septins and anillin (Kechad *et al.* 2012).

Abscission involves fusion of endomembranes, and is driven by the Endosomal Sorting Complexes Required for Transport (ESCRT) machinery, which brings membranes close enough to allow membrane fusion and finalise cytokinesis (Guizetti *et al.* 2011, Adell *et al.* 2016). The midbody structure stays in one of the daughter cells, where retaining the midbody has been related to cell division potency and its loss to cell differentiation (Ettinger *et al.* 2011).

1.6 Cytokinesis in fission

yeast.

Fission yeast *Schizosaccharomyces pombe* have a rod shape and measure around 7-14µm. Cell division in fission yeast happens in a symmetric fashion and contraction of the actomyosin ring is coupled to the simultaneous synthesis of a primary and secondary septum between mother and daughter cells (Figure 1.4) (Muñoz *et al.* 2013).

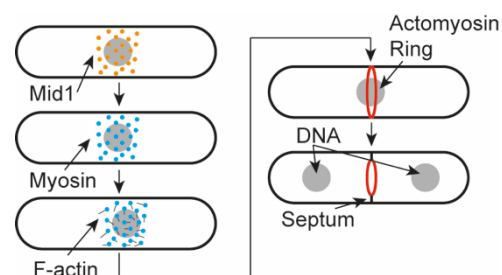


Figure 1.4: Cytokinesis in *S. pombe*.

Mid1 protein (orange) promotes the recruitment of formin and type-II myosin (cyan), that after the formation of actin filaments lead to the formation of a contractile ring.

Defining the site of division occurs in interphase, and it is determined by the position of anillin protein Mid1, that will accumulate in the equator of the cell around the interphase nucleus (Chang *et al.* 1996, Paoletti and Chang 2000).

Mid1 first recruits Cdc4 (myosin essential light chain) and Rng2 (IQGAP protein in fission yeast). Subsequently, Rng2 is able to nucleate the formation of actin filaments (Takaine *et al.* 2009, Tebbs and Pollard 2013). It also recruits further proteins, notably Myo2 (type-II myosin) and Rlc1 (myosin regulatory light chain) to build a contractile ring (Almonacid *et al.* 2011).

The trigger for mitotic exit and actomyosin ring contraction is the septation initiation network, or SIN. Thus, lack of SIN signalling leads to cytokinetic failure with multinucleated cell phenotype (Minet *et al.* 1979, Ohkura *et al.* 1995, Schmidt *et al.* 1997). Consequently, an excess of SIN signalling can lead to the opposite effect, such as the formation of a contractile ring and a septum at any point during cell cycle (Ohkura *et al.* 1995, Schmidt *et al.* 1997). This pathway relies on a kinase signalling cascade that will promote the release of Clp1 phosphatase, which will counteract the phosphorylated status caused by mitotic Cdk1 (Cueille *et al.* 2001, Trautmann *et al.* 2001).

Then, contraction of the actomyosin ring must occur, and it depends on myosin but not on actin dynamics (Mishra *et al.* 2013). For furrow ingression to occur, cell shape is essential, as in spherical protoplasts the ring is able to contract, yet it slides to either side of the cell (Mishra *et al.* 2012).

Contraction of the actomyosin ring is accompanied by the synthesis of a β -1,3 glucan septum between mother and daughter cells by Bgs1. Bgs1 is a 200 kDa essential transmembrane protein that synthesises a β -1,3 glucan septum from UDP-glucose between mother and daughter cells during cytokinesis (Cortes *et al.* 2007).

This process is coordinated by proteins such as C2-domain containing protein Fic1, transglutaminase-like domain containing

protein Cyk3 and F-BAR domain containing protein Cdc15 (Roberts-Galbraith *et al.* 2009, Roberts-Galbraith *et al.* 2010, Arasada and Pollard 2014, Ren *et al.* 2015).

1.7 Cytokinesis in budding yeast.

Budding yeast is a unicellular organism that is one of the most commonly used organisms to study cell cycle. The mechanism and regulation of cytokinesis are highly conserved throughout eukaryotes. Budding yeast cells are extremely well characterised. There is a wide collection of available mutants. Genetic manipulation is fast and easy, which allows researchers to easily create different molecular tools to study key aspects of cell biology. In addition, a rapid generation time makes it a key model organism to obtain answers to fundamental questions that help develop further research in mammalian cells (Figure 1.5).

The way eukaryotic cells decide where to place the actomyosin ring is different and it depends on the biology of each type of cells. Budding yeast cells select the division site very early in the cell cycle. The division site will be precisely located in the bud emergence site, whose location is determined at the end of each cell cycle. Therefore, the division site is located either next to the previous division site (haploid cells) or just opposite to it (diploid cells) (Chant and Pringle 1995). Proteins Bud8/9 for diploid cells; and Bud3/4 and Axl1/2

in haploid cells define this landmark for differential budding (Sanders and Field 1995). Bud selection machinery comes to the marked place by Ras-related GTPase Rsr1 module (Bender and Pringle 1989, Chant and Herskowitz 1991).

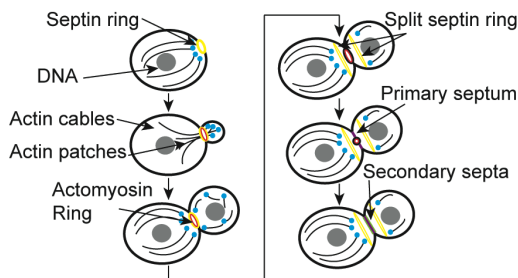


Figure 1.5: Cytokinesis in *S. cerevisiae*.

Blue dots are actin patches, black lines are actin cables. In red, site of division. Yellow represents septins, red the contractile ring. Grey represents DNA, purple represents the primary septum, green represents the secondary septum.

This module is able to interact with Rho-GTPase Cdc42 (Ziman and Johnson 1994, Smith *et al.* 2002). Cdc42 is able to regulate septin ring assembly, which will further become a scaffold for actomyosin ring assembly in cytokinesis (Bi *et al.* 1998, Lippincott and Li 1998).

Septins are filamentous GTP-binding proteins that mark the site of division (Glomb and Gronemeyer 2016). They self-assemble into rods, that then assembly themselves into filaments, forming a ring in the future site of division that works as a scaffold and as a diffusion barrier (Dobbelaere and Barral 2004). There are seven septins in budding yeast: five mitotic septins form the ring at the bud neck during cell division (Cdc3, Cdc10, Cdc11,

Cdc12, Shs1), whereas two are important for sporulating cells (Spr3, Spr28) (Gottlin-Ninfa and Kaback 1986, Holaway *et al.* 1987, De Virgilio *et al.* 1996). Mitotic septins form a collar in the site of division, whose recruitment will depend on Cdc42 (Iwase *et al.* 2006). Septins also interact with polo-like kinase Cdc5 through its N-terminus (Song and Lee 2001).

Cdc5, or Polo-like kinase, is a protein controlling many aspects of cell division, including cytokinesis. It has been shown that Cdc5 is responsible for the localisation of Tus1 and Rom2 (Yoshida *et al.* 2006), which are Rho1 GEFs that are responsible for the activation of Rho1 GTPase.

Rho1 is the master player in cell division (Madaule 1987, Drgonová *et al.* 1996), as it can activate and promote the localisation of formins to the site of division, thus nucleating the formation of actin filaments (Dong 2003). Cells use different formins at different stages of the cell cycle: Bnr1 from G1 to telophase, and Bni1 from telophase and during cytokinesis (Vallen *et al.* 2000, Sagot *et al.* 2002, Pruyne *et al.* 2004). The switch between formins depends on a special phosphatase called Cdc14, which removes Bnr1 and recruits Bni1 (Bloom *et al.* 2011), in a process explained below.

Cdc5 also plays a critical role during mitotic exit and cytokinesis entry. Cdc5 is involved in two pathways. The first of them is the FEAR (cdc Fourteen Early Anaphase

Release) pathway, and the second is the MEN (Mitosis Exit Network) pathway. The latter promotes the release of Cdc14 phosphatase from the nucleolus to remove protein phosphorylation state caused by the kinase activity associated to Cyclin/CDK complexes, which form the enzymatic motor that drives cell cycle progression. Whereas FEAR pathway is not very well understood, its importance is thought to be minor compared to MEN (Yellman and Roeder 2015). The MEN pathway is well characterised, and it consists of the GTPase Tem1, the protein kinases Cdc15, Dbf2 and Cdc5, the Dbf2 associated factor Mob1, the GTPase activating proteins Bub2 and Bfa1, the guanine-nucleotide exchange factor Lte1. It is known that the polo-like kinase Cdc5 initiates a signalling kinase cascade through Tem1, then Cdc15, and culminates with the activation of Dbf2-20/Mob1 complex (Rodriguez-Rodriguez *et al.* 2016) (Figure 1.6).

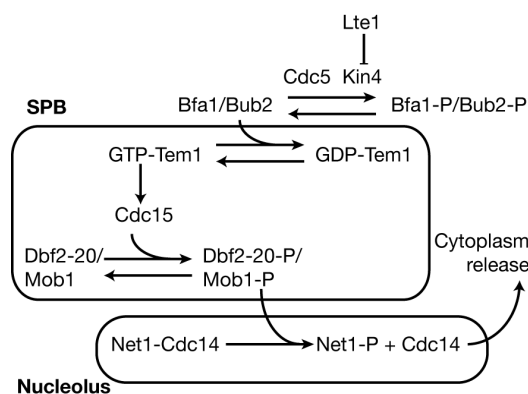


Figure 1.6: The Mitosis Exit Network (MEN).

A kinase cascade initiated by Cdc5 leads to the release from the nucleolus of the special phosphatase Cdc14, which counteracts mitotic Cdk1 activity (details in the main text).

Subsequently, Dbf2-20/Mob1 complex induces the release of Cdc14 protein from the nucleolus, as they will trigger the phosphorylation of Cdc14 protein, reducing the affinity for Net1 and thus allowing Cdc14 release from the nucleolus (Stoepel *et al.* 2005, Mohl *et al.* 2009). Cdc5 also phosphorylates Net1, decreasing its affinity for Cdc14 (Shou *et al.* 2002, Yoshida and Akio 2002). This promotes release of Cdc14 from the nucleolus to the nucleus and the cytoplasm.

Cdc14 is a Tyr and Ser/Thr phosphatase that is essential for exit from mitosis (Taylor *et al.* 1997). Cells lacking Cdc14 activity are arrested in G2/M of the cell cycle, with high kinase activity associated to mitotic Cyclin/Cdk1 complexes (Fitzpatrick *et al.* 1998). Inversely, overexpression of *CDC14* leads to an arrest in G1 phase of the cell cycle, since Cdk1 kinase activity is blocked in those cells (Visintin *et al.* 1998).

Cdc14 acts co-ordinately at three different levels to promote downregulation of Cdk1 activity and thus drive mitotic exit (Visintin *et al.* 1998):

- Cdc14 dephosphorylates a Cdk1 inhibitor called Sic1, which inhibits Cdk1 activity (Jaspersen *et al.* 1998, Visintin *et al.* 1998).
- Cdc14 dephosphorylates Swi5. Swi5 is a transcription factor that stimulates the production of Sic1, a major Cdk1 inhibitor. This dephosphorylation induces its

translocation to the nucleus, where it induces expression of *SIC1* (Visintin *et al.* 1998, Traverso *et al.* 2001).

- Cdc14 dephosphorylates Cdh1, which stabilises its association with the E3 ubiquitin ligase APC (Anaphase Promoting Complex) that triggers chromosome separation. Cdh1 is one of the activators of the APC during mitosis and promotes destruction of cyclin Clb2, which participates in the inactivation of CDK activity at the end of the cell cycle to allow mitotic exit (Visintin *et al.* 1998, Jaspersen *et al.* 1999, Bremmer *et al.* 2012).

It has been described that Cdc14 dephosphorylates key cytokinetic proteins including Iqg1, Inn1 and Chs2 (Kuilman *et al.* 2014). In addition, it has been shown that Cdc14 is essential for a rapid and efficient cytokinesis (Sanchez-Diaz *et al.* 2012). Furthermore, Cdc14 counteracts phosphorylation of key proteins at early G1 by G1 cyclins/Cdk1 complexes, which guarantee a time window for cells to perform efficiently cytokinesis (Sanchez-Diaz *et al.* 2012).

During anaphase the septin collar splits into two distinct rings. The septin ring act as a scaffold and as a diffusion barrier to compartmentalise the cortex and maintain diffusible cortical factors around the cleavage site (Dobbelaere and Barral 2004). During mitotic exit, localisation of one of the main components of the actomyosin ring, the type-II

myosin Myo1 depends on Iqg1 protein and Iqg1 will likely anchor the myosin ring to the plasma membrane (Fang *et al.* 2010). Iqg1 is the sole and essential IQGAP protein in budding yeast (Epp and Chant 1997, Osman and Cerione 1998, Abel *et al.* 2015). It temporally controls the formation of the actomyosin ring, as it is essential for the localisation of type-II myosin Myo1, as mentioned above (Fang *et al.* 2010), and in addition for the formation of the actin ring (Epp and Chant 1997, Osman and Cerione 1998, Shannon and Li 1999). It does so thanks to an N-terminal calponin-homology domain (CHD) that is able to crosslink actin filaments, and this process is dependent on its phosphorylation state (Mendes Pinto *et al.* 2012, Naylor and Morgan 2014, Miller *et al.* 2015). Furthermore, it contains a set of IQ motifs that, by binding to myosin light chain Mlc1, will promote Iqg1 recruitment to the cleavage site (Shannon and Li 2000). Finally, it contains a GAP-related domain (GRD) and a Ras-GAP C-terminus (RGCT), which are able to interact with Myo1 and are important for actomyosin ring contraction (Shannon and Li 1999).

Cdk1 and Cdc14 regulate Iqg1 function, as Cdk1 promotes its bud neck localisation (Naylor and Morgan 2014) and Cdc14 promotes actomyosin ring constriction (Miller *et al.* 2015); although its phosphorylation state does not affect arrival to the site of division of other cytokinesis

regulators such as Cyk3 or Inn1 (Naylor and Morgan 2014). Iqg1 is able to interact with cytokinesis regulators such as Hof1 (Tian *et al.* 2014) and Inn1 (Sanchez-Diaz *et al.* 2008); as well as MEN protein Tem1 (Shannon and Li 1999, Bardin and Amon 2001). Its localisation is partially dependent on Hof1, together with F-BAR protein Rvs167 (Nkosi *et al.* 2013).

Iqg1 dephosphorylation upon Cdc14 release triggers actomyosin ring contraction (Miller *et al.* 2015). The actomyosin ring disassembles as it contracts (Mendes Pinto *et al.* 2012) in a process that requires both actin depolymerisation and myosin force.

Actomyosin ring contraction is accompanied in budding yeast by the ingression of the plasma membrane and the synthesis of a chitinous septum between the mother and daughter cell, called the primary septum. It has been clearly described that actomyosin ring contraction and primary septum deposition are interdependent processes (Schmidt *et al.* 2002, VerPlank and Li 2005, Rancati *et al.* 2008). Consistently, it has been suggested that the actomyosin ring guides the deposition of the primary septum and vice-versa, as disruption of the actomyosin ring misguides primary septum formation and disruption of primary septum formation affects normal actomyosin ring contraction (Bi 2001, Schmidt *et al.* 2002, VerPlank and Li 2005, Nishihama *et al.* 2009).

Protein complexes called the Ingression Progression Complexes, or IPCs,

control the interdependency of these two processes (Foltman *et al.* 2016a). These complexes coordinate contraction of the actomyosin ring, ingression of the plasma membrane and synthesis of the primary septum. IPCs are composed not only of Myo1 and the glycosyltransferase responsible for the primary septum formation, Chs2; but also proteins Iqg1, Hof1, Inn1 and Cyk3 (Foltman *et al.* 2016a).

It was proposed that Inn1 couples actomyosin ring contraction and plasma membrane ingression, as cells that lack Inn1 are able to contract the actomyosin ring, but unable to ingress the membrane (Sanchez-Diaz *et al.* 2008). Inn1 is an essential protein, unlike its fission yeast homolog, Fic1 (Sanchez-Diaz *et al.* 2008, Roberts-Galbraith *et al.* 2009, Ren *et al.* 2014). Inn1 is a 46 kDa protein that contains a C2 domain at its N-terminus, and the rest of the protein seems to be quite unstructured. Later, Inn1 was associated with the synthesis of the primary septum by Chs2 (Nishihama *et al.* 2009, Meitinger *et al.* 2010, Devrekanli *et al.* 2012). Indeed, a hypermorphic allele of Chs2, *CHS2-V377I*, rescues the cytokinesis defect associated to cells harbouring a point mutation that inactivates Inn1 C2 domain function (Devrekanli *et al.* 2012). Inn1 protein is able to interact, through its PXXP motifs, with the SH3 domains of Cyk3 protein (Nishihama *et al.* 2009, Nkosi *et al.* 2013).

Hof1 interacts with Inn1. It has been shown that the Inn1 C-terminal domain contains proline-rich motifs (PXXP) that determine the interaction with Hof1 SH3 domain, which is located at the C-terminal end of the protein (Sanchez-Diaz *et al.* 2008, Jendretzki *et al.* 2009, Nishihama *et al.* 2009, Meitinger *et al.* 2011). At the N-terminus, Hof1 contains an F-BAR domain. This kind of domains has been shown to induce membrane curvature (Henne *et al.* 2007, Shimada *et al.* 2007, Yu and Schulten 2013). The X-ray crystal structure of F-BAR domain from Hof1 has recently been determined, which form an elongated banana-shaped dimer and is able to bind equally well to all kind of phospholipids (Moravcevic *et al.* 2015).

Hof1 arrives earlier at the site of division, associating with septins in S phase (Meitinger *et al.* 2013, Oh *et al.* 2013, Finnigan *et al.* 2016). Then, phosphorylation of Hof1 by MEN allows Hof1 release from the septin ring and its recruitment to the actomyosin ring prior to contraction (Lippincott and Li 1998, Meitinger *et al.* 2011). This phosphorylation is necessary for actomyosin ring constriction and primary septum synthesis (Meitinger *et al.* 2013).

Its interaction with both type-II myosin Myo1 (Oh *et al.* 2013) and Bnr1, a formin involved in actin nucleation (Kamei *et al.* 1998); as well as its function in membrane curvature through its F-BAR domain and its septin interaction, makes it an interesting

protein connecting the plasma membrane with the actomyosin ring.

Hof1 interacts through its SH3 domain with cytokinetic regulator Cyk3 (Labeledzka *et al.* 2012). Cyk3 is a key cytokinetic regulator, and its importance will be discussed in detail in the following section.

1.7.1 Cyk3 and transglutaminase-like domains.

Cyk3 contains a transglutaminase-like domain around the middle of the protein and an SH3 domain situated at the N-terminus. Cyk3 is a non-essential protein that was initially discovered as a dosage-suppressor for *hof1Δ* and *iqg1Δ* (Korinek *et al.* 2000, Jendretzki *et al.* 2009, Onishi *et al.* 2013). Additionally it was originally described that simultaneous deletion of both *CYK3* and *HOF1* proved to be synthetically lethal (Korinek *et al.* 2000, Onishi *et al.* 2013).

Cyk3 plays a key role during cytokinesis, as cells depleted of Cyk3 protein had a certain percentage of cytokinesis defects (10%)(Korinek *et al.* 2000). Even though actin distribution and dynamics is normal in those cells (Korinek *et al.* 2000, Nkosi *et al.* 2013), Cyk3 is required for a correct actomyosin ring contraction (Meitinger *et al.* 2013).

Cyk3 is not only involved in the actomyosin dynamics, but also in the synthesis of a septum synthesised by chitin synthase Chs2 (Sburlati and Cabib 1986, Silverman *et*

al. 1988). Overexpression of Cyk3 leads to the deposition of a thicker primary septum between mother and daughter cells (Meitinger *et al.* 2010, Oh *et al.* 2012). Furthermore, defects associated with lack of Cyk3 can be rescued by a hypermorphic allele of *CHS2*, *CHS2-V377I* (Devrekanli *et al.* 2012).

SH3 domains are crucial for protein-protein interactions through PXXP motifs (Mayer 2001). Interestingly, Cyk3 via SH3 domain interacts with PXXP motifs in Inn1 (Jendretzki *et al.* 2009, Nishihama *et al.* 2009, Labeledzka *et al.* 2012, Palani *et al.* 2012, Nkosi *et al.* 2013) and septins (Iwase *et al.* 2007). In addition, Cyk3 contains a PXXP motif itself, which interacts with the SH3 domain of Hof1 (Labeledzka *et al.* 2012).

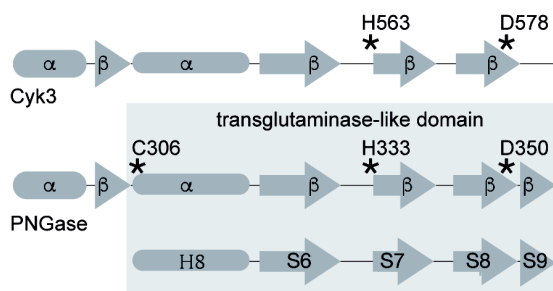


Figure 1.7: Alignment of transglutaminase-like domains.

Alignment of the transglutaminase-like domains of ScCyk3 protein and mouse PNGase.

Cyk3 transglutaminase-like domain was first shown by protein sequence alignment (Makarova *et al.* 1999) (Figure 1.7). Transglutaminases are a family of enzymes that catalyse intramolecular or intermolecular protein cross-linking between lysine and glutamine residues.

Active transglutaminases possess a catalytic triad, comprising a cysteine, a

histidine and an aspartic acid (Hettasch 1994, Micanovic *et al.* 1994); and usually catalyse the formation of links between peptide chains. An example of proteins containing these active domains are PNGases (*peptide:N-glycanases*), which were discovered in almond seed extracts in 1977 (Takahashi 1977). This family was further expanded to other plants and seeds (Sugiyama *et al.* 1983, Plummer *et al.* 1987, Berger *et al.* 1995), budding yeast (Suzuki *et al.* 2000) and higher eukaryotes such as medaka fish (Seko *et al.* 1991) and mouse (Kitajima *et al.* 1995). PNGases also occur in prokaryotic organisms, such as *Flavobacterium meningosepticum* (Elder and Alexander 1982). PNGase homolog in budding yeast, Png1, is a non-essential protein that hydrolyses β -aspartylglycosylamine bonds of asparagine-linked glycopeptides (Suzuki *et al.* 2000). Some members of the transglutaminase family are proteases, which likely arose through evolving from ancient papain-like thiol proteases (Makarova *et al.* 1999).

On the other hand, there are other members of the transglutaminase family that carry an inactive domain, namely a transglutaminase-like domain. One of those members is budding yeast Cyk3, which lacks the catalytic cysteine from the catalytic triad (Makarova *et al.* 1999). The importance of the lack of the cysteine residue is yet unknown. The relevance of the transglutaminase-like

domain Cyk3 function will be discussed further in this thesis.

It is interesting to note that the transmembrane enzyme chitin synthase Chs2 interacts directly with Cyk3 and form the IPCs, together with the group of cytokinetic factors described above (Foltman *et al.* 2016a). The timing of arrival to the site of division of major cytokinetic proteins and IPCs is summarised in Figure 1.8. In the next section we will discuss the chitin synthase Chs2 in more detail.

1.7.2 Chitin synthase Chs2 and extracellular matrix (ECM) remodelling.

The IPCs coordinate contraction of the actomyosin ring, plasma membrane ingression and the deposition of primary septa by the chitin synthase II, Chs2 (Foltman *et al.* 2016a). Chs2 protein synthesises a chitinous layer of cell wall, that is a part of the extracellular matrix in budding yeast (Table 1.2).

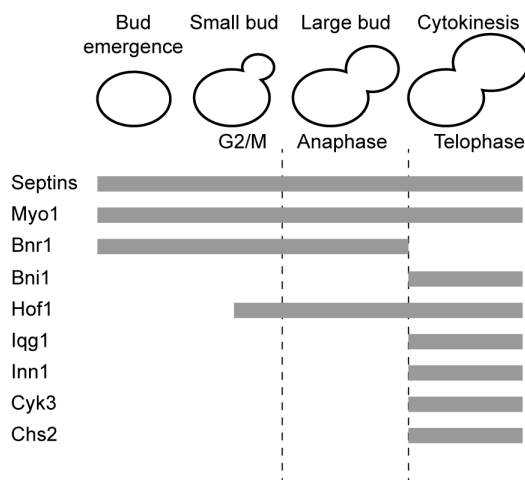


Figure 1.8: Timing of arrival of major cytokinetic regulators to the site of division.

The expression, localisation and activation of Chs2 is highly regulated to ensure Chs2 function occurs at the end of the cell cycle when cells have segregated their chromosomes and are ready to contract the actomyosin ring. The transcription of Chs2 peaks during mitosis (Choi *et al.* 1994).

Once synthesised, Chs2 protein is retained at the ER, as it is phosphorylated by Cdk1 to prevent the premature release from the ER (Zhang *et al.* 2006, Teh *et al.* 2009). Once cells have segregated their genetic material towards the cell poles, MEN signalling cascade gets activated and promote the release of the phosphatase Cdc14 from the nucleolus (Queralt and Uhlmann 2008). Subsequently, Cdc14 phosphatase dephosphorylates Chs2 (Chin *et al.* 2012), stimulating its package into COPII-coated vesicles that will be delivered to the site of division (Zhang *et al.* 2006, Teh *et al.* 2009, Chin *et al.* 2012, Jakobsen *et al.* 2013). At the late stages of cytokinesis, Dbf2 kinase, from the MEN signalling cascade has been shown to phosphorylate Chs2. This phosphorylation is needed for its correct disassembly from the actomyosin ring (Oh *et al.* 2012), linking MEN network to cytokinesis progression. Taken together, MEN is able to regulate the synthesis of primary septum through chitin synthase Chs2.

Chitin synthase II is an essential protein and belongs to the family of glycosyltransferases, enzymes that catalyse

the transfer of saccharide moieties from an activated nucleotide sugar to a glycosyl acceptor molecule. Chs2 links together molecules of UDP-N-acetylglucosamine with β -1,4 linkages to form long chains of chitin that will form the primary septum between mother and daughter cell.

Chs2 features three regions in its 963 amino acid sequence:

- N-terminal region: Which contains several Cdk-phosphorylation sites (Martinez-Rucobo *et al.* 2009, Chin *et al.* 2012). It spans amino acids 1-215, and controls the localisation of the protein: at the ER where it is phosphorylated, and at the site of division when it is dephosphorylated (Teh *et al.* 2009).
- Catalytic domain: This region contains several conserved motifs, such as

QXXRW and DD motifs, within its CON1 (Conserved region 1) domain (490-607aa); and is able to link together two monomers of UDP-N-Acetylglucosamine (Nagahashi *et al.* 1995, Yabe *et al.* 1998, Dorfmüller *et al.* 2014). Spanning amino acids 215-629, it is however, unable to synthesize long chains of chitin alone.

- Transmembrane domain: Which contains several predicted transmembrane helices, it allows the synthesis of long polysaccharide chains, thanks to its CON2 (Conserved region 2) domain (748-815aa) (Dorfmüller *et al.* 2014). It spans amino acids 629-963.

It has been shown that Chs2 needs protease treatment to be active, suggesting it is synthesised as a zymogen (Sburlati and

Table 1.2: Comparison of primary septum synthases from fission yeast (Bgs1) and budding yeast (Chs2).

	Bgs1	Chs2
Monomer	UDP-Glucose	UDP-GlcNAc
Polymer	β 1-3 Glucan	Chitin
Phosphorylation	Cdc2 (Noguchi <i>et al.</i> , 2002)	Cdk1 (Teh <i>et al.</i> , 2009) Dbf2 (Oh <i>et al.</i> , 2012)
Dephosphorylation	Clp1 (Mishra <i>et al.</i> , 2004; Arasada <i>et al.</i> , 2014)	Cdc14 (Chin <i>et al.</i> , 2012; Jakobsen <i>et al.</i> , 2014)
Actomyosin ring if protein deleted?	AMR slides and cannot contract (Mishra <i>et al.</i> , 2012)	AMR collapses (VerPlank and Li, 2005)
PS/SS synthesis	Simultaneous	Sequential

Cabib 1986, Silverman *et al.* 1988). Indeed, in order to assess Chs2 activity *in vitro*, a previous treatment with trypsin is needed (Sburlati and Cabib 1986).

After synthesis of the septum, Chs2 becomes endocytosed through clathrin-mediated endocytosis (Chin *et al.* 2016) and transported to the vacuole, where it is degraded by Pep4 protease (Chuang and Schekman 1996).

Finally, the cell must synthesise a secondary septum and degrade the primary septum to separate mother and daughter cells. This secondary septum mainly consists of β -1,3 glucan, synthesised by glucan synthases Fks1 and Fks2; and Chs3, chitin synthase III also plays a role in this process (Shaw *et al.* 1991, Douglas *et al.* 1994).

To allow cell separation, cell induces a daughter-specific genetic program initiated by the kinase Cbk1 and its regulatory subunit Mob2 (Colman-Lerner *et al.* 2001). Cbk1/Mob2 induces the specific selective localisation of the transcription factor Ace2 to the nucleus of daughter cells, where Ace2 promotes the expression of enzymes that contribute to cell separation by degrading the cell wall, such as the chitinase Cts1 (O'Conallain *et al.* 1999). Mother and daughter cells are now separated and they are able to continue independently their progression through the cell cycle (Adams 2004).

Biology of animal cells is much shared with fungal pathogens such as the budding

yeasts *Candida albicans*, *Cryptococcus neoformans*, *Cryptococcus gattii* and *Ajellomyces* (Kim and Sudbery 2011, Kronstad *et al.* 2011), so that effective anti-fungal therapies are often associated with considerable toxicity. In addition, the appearance of highly resistant strains, together with the need for effective oral formulations mean that there is a continuous need for novel therapies against fungal-specific proteins (Sable *et al.*, 2008).

Mechanism and regulation of cytokinesis are highly conserved from yeast to mammals as they all employ a contractile ring of actin and type II myosin to mediate division of the cytoplasm (Oliferenko *et al.* 2009, Pollard 2010). However, formation of the specific ECM layer, primary septum in yeast, requires a specific glycosyltransferase that can be used as target for therapeutic intervention as mammalian cells lack the specific enzymes that synthesise cell wall carbohydrates such as chitin.

Therefore Chs2 is an excellent candidate as a drug target in order to treat fungal infections, such as candidiasis, that represent a major threat in immunocompromised patients; where it can lead to colonisation of the mucosae (Kim and Sudbery 2011).

1.8 Aims of this thesis.

- To understand how chitin synthase Chs2 synthesises the primary septum, a special layer of the extracellular matrix, in coordination with the contraction of the actomyosin ring.
- To understand the function of Cyk3 protein and its importance during cell division in budding yeast.

2. MATERIALS AND METHODS

2.1 DNA methods.

2.1.1 Genomic DNA extraction from yeast.

To use as a template for PCR, genomic DNA was extracted from yeast. 10 ml cultures were grown overnight, and cell pellets were washed with water. Cells were lysed by vortexing in a lysis solution (100 mM NaCl, 10 mM Tris pH 8, 1 mM EDTA, 1% SDS, 2% Triton) containing glass beads and phenol/chloroform/isoamyl alcohol (P2069, Sigma-Aldrich). TE buffer (10 mM Tris pH 8, 1 mM EDTA) was added to the mixture, and after pelleting the insoluble fraction the supernatant was mixed with 100% ethanol to precipitate genomic DNA. The DNA was washed with 70% ethanol, and then resuspended in TE buffer containing 50 µg/ml RNase A (Sigma, R5125) and incubated for one hour at 37°C to dissolve DNA and degrade RNA. DNA was then stored at -20°C.

2.1.2 Polymerase Chain Reaction (PCR).

Amplifying DNA fragments for making plasmids or for yeast transformation was done by PCR with Prime Star polymerase (Takara, R010A), using the 5x buffer supplied with the polymerase. 100 µl reactions were performed using a 20 µM concentration of oligonucleotides.

PCR reactions to confirm correct integrations or deletions in yeast strains were

done using GoTaq® Green Master Mix (Promega, M712) or Ex-taq (Takara) according to the manufacturer's instructions.

A standard setting for PCR reactions was 94°C 2 minutes, followed by 30 cycles of 94°C 1 minute, 55°C 1 minute and 72°C 1 minute/kb, which was then followed by a final cycle of 72°C 10 minutes, before holding samples at 4°C. Oligonucleotides used in this study are listed in Table 2.1.

2.1.3 Restriction enzyme digestion of PCR products and plasmids.

PCR products and plasmids were digested with appropriate restriction enzymes according to the manufacturer's instructions. Double or sequential digestions were performed at 37°C for two hours. Between sequential digests, the DNA fragments were purified using Nucleospin Extract Columns (Macherey-Nagel, NZ740588) and eluted in 35 µl of TE.

2.1.4 Ligation of PCR products into plasmids.

Digested PCR products and plasmids were separated in a 0.8% agarose gel (Sigma, A9539) containing 0.5 µg/µl ethidium bromide (Sigma, E1510) to allow its visualisation. Bands were cut from the gel and purified with NucleoSpin Gel and PCR Clean-Up (Macherey-Nagel, 22740609.250). For each ligation reaction, 20 ng of the gel-purified

vector and 20 ng of the gel-purified insert were mixed with water in a final volume of 8 μ l, and then incubated at 45°C for five minutes to separate any annealed ends, before placing on ice for two minutes. After that, 1 μ l of T4 DNA ligase buffer and 1 μ l T4 DNA ligase were added (NEB, M0202L) and reaction was incubated for two hours at room temperature.

For pDDGFP2-based plasmids (Drew *et al.* 2008), PCR fragments containing the gene of interest were obtained, with 5' and 3' overhangs with the Smal-linearised pDDGFP2 plasmid. 3 μ l of plasmid and 5 μ l of PCR product were co-transformed by the lithium acetate method in budding yeast (explained in section 2.2.1), so that they would be ligated by homologous recombination.

2.1.5 Transformation of *E. coli*.

Transformation of plasmids into *E. coli* DH5 α and Rosetta was done following Inoue *et al.* protocol (Inoue *et al.* 1990). Briefly, 5 μ l of ligation or diluted plasmid were mixed to 100 μ l of competent cells and were incubated on ice for one hour. Cells were then heat-shocked at 42°C for two minutes, and allowed to recover on ice for five minutes. To allow cells to express the antibiotic-resistance gene, 0.5 ml of LB media (Luria-Bertani) (Becton-Dickenson, 244620; (1% (w/v) tryptone, 0.5% (w/v) yeast extract, 1% (w/v) NaCl)) were added, and cells were incubated at 37°C for 30 minutes. Finally, cells were quickly spun

down, media was removed until 100 μ l was left, and resuspended cells were plated in LB agar plates (Pronadisa, 1083.00) supplemented with the appropriate antibiotic: 100 μ g/ml ampicillin (Sigma, A9518), 30 μ g/ml kanamycin (Sigma, K1377) or 30 μ g/ml chloramphenicol (Sigma, C0378).

2.1.6 Plasmid DNA isolation from *E. coli*.

For small-scale plasmid purification, 5 ml of LB supplemented with the appropriate antibiotic was inoculated with a single colony from an *E. coli* transformation plate and incubated overnight with shaking at 37°C.

Plasmids were purified using a NucleoSpin Plasmid Miniprep Kit (Macherey-Nagel, 740588.250) according to the manufacturer's instructions. Briefly, *E. coli* cells were broken in an SDS-containing detergent, and debris and chromosomal DNA pelleted in a potassium acetate buffer. Plasmid DNA was bound to a silica membrane, washed in an ethanol buffer, and eluted in water or TE buffer. Plasmid DNA was stored at -20°C.

For large-scale plasmid purification, plasmid DNA was isolated using NucleoBond Xtra Maxi Plus (Macherey-Nagel, 74016.50) according to the manufacturer's instructions.

Plasmids used in this study are listed in Table 2.2.

Table 2.1: Oligonucleotides used in this study.

Oligo number	Sequence (5'-3')
CD4	ATCGATGAATTCGAGCTCG
CD5	CGTACGCTGCAGGTCGAC
CD9	CATATGCGCGATTGCTGATC
CD10	AATAGGTCAGGCTCTCGCTG
CD42	TCCTCTCCGTATATGTGAGC
CD45	GGCATCAGAGCAGATTGTAC
CD46	CTCCTTACGCATCTGTGCGG
CD49	ACAACGACCAAGCTCACATC
CD50	ACATTATGGGTGGTATGTTGG
CD150	CCAGTAGTAATTCACAATCC
CD188	AGATCACAGAATGCAAATGG
CD190	GCTCTGACTGATGATAATGG
CD193	AAGTTATTCAAAGTCCCTCC
CD195	TGTTAATGGACCATCATGG
CD197	AGTGGTTATACTTAAACTCC
CD200	GGCCTGATGAAATAGAGTCC
CD202	TGCTCGAATTTAATCTCTCC
CD211	AGTCATTGAATATGCCAAGG
CD218	AGTTTTCCCGTGATGGCTCC
CD244	CTGGTGCAGGCGCTGGAGCG
CD267	GTAGATCTCGAGTTATACGCACAACCATTTCAGCAAAAACGGAC
CD424	CACCCAGGCTTTACACTTTAT
CD425	TCGTATACCTAAAATAGGGGAGG
CD482	TGTGCGGTAACTTTGTCTG
CD540	GAACCTCAGTGGCAAATCC
CD542	GAACCTCAGTGGCAAATCC
CD543	AGCTATTCATCCAGCAGGCC
CD544	ACTGGACCTGTATGAACACG
CD563	GACCGAAGCGGAAGCGTTCG
CD624	CATGGGAAGTCTCTAAATTAGACTTACCAAATGTTTTCCACAAAAAGGGCCGTACG CTGCAGGTCGAC
CD625	AAATGTCAAAATATCCTAGAAAGTAATGGTTGTCATAACCTGTACATTCTATCGAT GAATTCGAGCTCG
CD626	AGATGGGAAACAGATTGTGG
CD627	AATTGCTCTACGTTTCGACG
CD653	TCGCTGACTCTGGTATTGGGTGGTCCGTTTTTGTGAATGGTTGTGCGTACGTAC GCTGCAGGTCGAC
CD654	ACTATATAGCCATATATGAGTTATGAAATTCACCTTCTGAGTAGAATGTATCGAT GAATTCGAGCTCG
CD655	CTAATCAAAGCAGTCCTACC
CD656	GATGTTAAACGGTCAATGG
CD657	ACCGCATATAATTTTAGTTCGAAACATTAAGGTTCAGTCCCGAAGTTATAATBTAA GGCGGCCAGATCTG
CD658	CTGGCCTTCACCTTAAATGGTGGCTTCAAAGATGTTAAGTTAGTGGCCATGGCAC CCGCTCCAGCGCCTG
CD659	TAATGGTGGTGCCTGTCAGG
CD660	GTACTTGAGGCTTACTATGG
CD669	ATACAAAGGCCTCGTGTGAGACTTGAAAGTGTACTACTAATATTCAGAAATTAAG

	GCGCGCCAGATCTG
CD671	ATATTATGTATGTCTCTATC
CD672	AACGAGAGTAGTTTGAGAT
CD673	GGATAGGATTAATCCCTATAATTCATTCAGCTACTGCATCAAGGTCTTCGTACG CTGCAGGTCGAC
CD674	CCCACGGCAGCGTATATCTTTCTATTTCTACTTAACAAAAATCTGACATTATCGATG AATTCGAGCTCG
CD678	ATTCCTGAGAGTTCGATTCC
CD688	CCGACCAGAGATGATATGTC
CD783	CTCCAGTTCAGTATCCTCAC
CD805	GACCGGCTTGAATGGAGATG
CD808	CCACGCCATTTGTCTTTCT
CD831	CTCTCTTGTTCCGGTTAC
CD862	ATCCTATCTAGATATTAATGGTGGTGCCTGTCAGGG
CD863	GATCGAGAATTCTATGCAAATTTAAATGTAATACGG
CD865	ATATCAGTTTGATCTACTGC
CD866	GCAAATTTAAATGTAATACG
CD896	TCAAAACTTTTCTACTATTTTTGAAGGTTGCCTACCATTTTCAGTGCTCGA CATTATGCAAATTTAAATG
CD897	GGTACTGGTGGGAATAACAAC
CD898	CCTCTTGTTCTTGAGACTGG
CD900	AGCCGTCTCAGCAGCCAACC
CD901	GCTTTGTTGATCTTTGTTGA
CD1025	TGAATACTCGAGTTATTTGTACAATTCATCCATACCATG
CD1031	GTAGATCTCGAGAAGTCGACTTAATTTTCTAAAATAACGTCAATAAATCT CCATT
CD1032	TACTGAGGATCCATGGAGCTGGTGCAGGCGCTGGAGCGGGTGCCGCAAGA TACTCAACTGTTCTGAAAAGT
CD1034	GTAGATCTCGAGAAGTCGACTTAGTTATTTACAAATTCATGAATTGGGTT GGTTA
CD1061	TTGAAGTTAACTTTGATACC
CD1104	GCCGCGTCGCCGCGCGGTTCC
CD1105	CAGTAGTATCTTTGCAAGTG
CD1163	CTGACTCTGGTATTGGGTGGTCCGTTTTTGCTGAATGGTTGTGCGTATAAATTAAG GCGCGCCAGATCTG

Table 2.2: Plasmids used in this study.

Plasmid	Backbone	Fragment	Oligos
pET28c	pET28c	-	-
pET100	pET28c	Streptag	-
pMF10	pGADT7	Clal-Chs2(1-629)-XhoI	801-802
pMF13	pET28c	NheI-Chs2(1-222)-XhoI	821-822
pMF14	pET28c	NheI-Cyk3(101-322)-XhoI	823-824
pMF22	pET28c	SpeI/NheI-Cyk3-XhoI	-
pMF36	pET100	NheI-Strep-Chs2(215-629)-XhoI	-
pMF62	pET28c	SpeI-Cyk3(475-885)-XhoI	1071-175
pMF75	pGBKT7	BamHI-Cyk3(1-594)-Sall	266-1034
pMF85	pET28c	NheI-Hof1(280-502)-XhoI	1128-1129
pMF97	pRS305GAL	SpeI-cyk3-2A-XhoI	164-267

pMF98	pRS305	XbaI-cyk3-2A-XhoI	
pMK43		KpnI-IAA17-XmaI	
pIMP5	pRS305GAL	SpeI-Cyk3-GFP-XhoI	
pIMP8	pRS305GAL	SpeI-cyk3-2A-GFP-XhoI	
pIMP9	pRS305	XbaI-Cyk3prom-Cyk3-XhoI	
pIMP10	pDDGFP2	Chs2	1179-1180
pIMP11	pDDGFP2	Chs2 (215-963aa)	1180-1181
pIMP12	pDDGFP2	C2-Chs2	1180-1182
pMP20	pYM20	KpnI-IAA17-XmaI	
pASD20	pRS305	XbaI-Inn1(Cterminus)GFP-XhoI	
pASD65	pGADT7	Clal-Chs2(215-629)-XhoI	802-803
pASD87	pGBKT7	BamHI-Cyk3(475-885)-XhoI/Sall	
pASD88	pGBKT7	BamHI-Cyk3(508-583)-XhoI/Sall	
pASD89	pGBKT7	BamHI-Cyk3(508-594)-XhoI/Sall	
pASD90	pGBKT7	BamHI-Cyk3(524-583)-XhoI/Sall	
pASD93	pGBKT7	BamHI-Cyk3(475-594)-Sall	1032-1034
pASD94	pGBKT7	BamHI-Cyk3(605-885)-XhoI/Sall	267-1069
pASD95	pGBKT7	BamHI-Cyk3(475-863)-Sall	1031-1032
pASD100	pGBKT7	BamHI-Cyk3(475-764)-Sall	1093-1032
pAD12	pET28c	XbaI-Inn1C2-5XGA-6His-NotI	219-220
pAD27	pGBKT7	BamHI-Inn1-XhoI/Sall	260-261
pAD37	pGBKT7	BamHI-Inn1(Cterm)-XhoI/Sall	261-293
pAD96	pRS305GAL	SpeI-Cyk3-XhoI	164-267
pKL643	pRS305	XbaI-Inn1(K31A)GFP-XhoI	2141-2142
pRS305	pRS305	-	

2.1.7 DNA sequencing.

DNA sequencing was carried out by Stab Vida company (www.stabvida.com). Plasmids samples were prepared in a total volume of 13 µl containing 500 ng of DNA and 30 pmol of the appropriate sequencing primer. For PCR products sequencing, the total volume was 13 µl containing 200 ng DNA and 30 pmol of the appropriate sequencing primer.

2.2 Yeast methods.

2.2.1 Yeast transformation.

All yeast strains used in this work are listed in Table 2.3 and are based on the W303 genetic background, except for the two-hybrid strain PJ69-4A (James *et al.* 1996); and the FGY217 strain and derivatives, which are based on PLY127 (Drew *et al.* 2008).

To generate strains in which either the amino or the carboxy terminus of a protein was modified with an epitope tag or a degron cassette, a single step PCR approach was used in order to modify the chromosomal locus of the corresponding gene (Kanemaki *et al.* 2003, Sanchez-Diaz *et al.* 2004, Nishimura *et al.* 2009). The PCR products were generated using two 70-base oligonucleotides specific to the gene of interest; for each oligonucleotide the first 50 nucleotides had homology to the gene of interest, and the remaining 20 nucleotides had homology to the sequences within the plasmid that was used as a template for the PCR reaction.

The PCR product was then purified over a Nucleospin Extract Colum, and 1 µg was used to transform a yeast strain. The oligonucleotides used for each strain are listed in Table 2.1, and the modified loci generated by one-step PCR transformation are listed in Table 2.4.

To generate strains where the gene was integrated as a second copy into either of the *leu2*, *his3*, *ura3* or *trp1* locus, pRS series of integrative plasmids (Sikorski and Hieter 1989) were used, where the sequences of the gene of interest was cloned into one of the pRS vector, which differ only in yeast selectable marker gene (*HIS3*, *TRP1*, *LEU2*, *URA3*). The plasmid was then linearised inside the marker gene and transformed to either haploid or diploid yeast cells.

DNA was transformed into yeast cells by the lithium-acetate method (Gietz *et al.* 1992) as described previously (Sanchez-Diaz *et al.* 2004). For linearised plasmids 100 ng was used for transformation.

Cells were streaked from their glycerol stocks into YPD media (1% yeast extract (Becton Dickenson, 212750), 2% peptone (Oxoid, LP0037), 2% glucose, 2% bacto agar (Becton Dickenson, 214010)), supplemented with 0.1 mM CuSO₄ in strains harbouring a *CUP1* copper-inducible promoter.

To select for auxotrophic markers, minimal medium plates were used (0.67% yeast nitrogen base (Becton Dickenson, 291940), 2% glucose, 2% Bacto agar)

supplemented with the appropriate combination of amino acids: 0.04 mg/ml adenine, 0.04 mg/ml histidine, 0.04 mg/ml leucine, 0.04 mg/ml tryptophan, or 0.08 mg/ml uracil.

For yeast two-hybrid experiments and time-lapse experiments, synthetic complete (SC) drop out medium was used as described previously (Sherman, 2002).

For experiments involving the auxin degron system 500 μ M NAA (1-Naphthaleneacetic acid) (Sigma, 317918), and 500 μ M IAA (3-Indoleacetic acid) (Sigma, I3750) were used in rich medium (YPD or YPGal), whereas 20 μ M NAA and IAA was used in minimal SC medium.

To select for the *kanMX* and *hphNT* drug resistance markers, YPD plates were supplemented with 50 μ g/ml geneticin (Invitrogen, 11811-031) or 100 μ g/ml hygromycin B (Autogen Bioclear, HygroGold liquid, ant-hg-5) respectively. When geneticin and hygromycin B were used to select transformants, cells were incubated in YPD media for 4-6 hours to allow drug resistance markers to be expressed before plating.

Plates were incubated for three days at 24°C or two days at 30°C before examining the colonies. Colonies were re-streaked or replicated in selective media to ensure growth of specific transformants.

2.2.2 Mating strains to isolate diploids.

After streaking out strains from the glycerol stocks, freshly streaked pairs of colonies of opposite mating type (MAT α and MAT α ; typically three days old colonies grown at 24°C in YPD media) were mixed together on a YPD plate with a drop of water. Patches were left to grow overnight at 24°C. Patches were then streaked individually on either selective media – if the two haploids contained different selection markers, or YPD, for three days at 24°C. Colonies were streaked on YPD or RSM (Rich Sporulation Medium) (0.25% yeast extract, 1.5% potassium acetate, 0.1% glucose, 2% agar and 2.4% amino acid stock) (Sanchez-Diaz *et al.* 2004) and incubated again at 24°C for three days to select for diploids, that were able to form asci in RSM media.

2.2.3 Tetrad analysis.

For sporulation of diploid strains, a freshly grown colony was spread onto an RSM plate. After three to five days of incubation at 24°C or 30°C, sporulating cells were mixed with 75 μ l of water containing 5 μ l of β -glucuronidase solution (Sigma, G7770) and incubated for 10 minutes at room temperature. Asci were dissected on YPD plates with a Carl Zeiss Axiolab micromanipulator, and after incubation for three days at 24°C plates were replica-plated into the appropriate selective medium to assign genotypes.

Table 2.3: Yeast strains used in this study.

Strain name	Genotype	Source
PJ69-4A	<i>MATa trp1-901 leu2-3,112 ura3-52 his3-200 gal4Δ gal80Δ LYS2::GAL1-HIS3 GAL2-ADE2 met2::GAL7-lacZ</i>	H. Ulrich
YAD381	<i>MATα ade2-1 ura3-1 his3-11,15 trp1-1 leu2-3,112 can1-100 CHS2-9MYC (KITRP) INN1-TAP (kanMX) pep4Δ::URA3 (URA3) ADE2+</i>	A. Devrekanli
YASDHOF1-1B	<i>MATa ade2-1 ura3-1 his3-11,15 trp1-1 leu2-3,112 can1-100 HOF1-C-GFP (KITRP1)</i>	A. Sánchez
YASD6.3C2HOF1-H	<i>MATa ade2-1 ura3-1 his3-11,15 trp1-1 leu2-3,112 can1-100 CUP1-C2-HOF1 (HIS3MX)</i>	A. Sánchez
YASD819	<i>MATa ade2-1 ura3-1 his3-11,15 trp1-1 leu2-3,112 can1-100 CHS2-C-GFP (KITRP1)</i>	A. Sánchez
YASD2061	<i>MATa ade2-1 ura3-1 his3-11,15 trp1-1 leu2-3,112 can1-100 CYK3-C-GFP (KITRP1)</i>	A. Sánchez
YASD2081	<i>MATa ade2-1 ura3-1 his3-11,15 trp1-1 leu2-3,112 can1-100 INN1-TAP (KanMX) pep4Δ::URA3 ADE2+</i>	A. Sánchez
YIMP4	<i>MATa ade2-1 ura3-1 his3-11,15 trp1-1 leu2-3,112 can1-100 / MATα ade2-1 ura3-1 his3-11,15 trp1-1 leu2-3,112 can1-100 CYK3 / cyk3-H563A-GFP (KITRP) HOF1 / CUP1-C2-HOF1 (HIS3MX)</i>	This study
YIMP5	<i>MATa ade2-1 ura3-1 his3-11,15 trp1-1 leu2-3,112 can1-100 / MATα ade2-1 ura3-1 his3-11,15 trp1-1 leu2-3,112 can1-100 CYK3 / cyk3-D578A-GFP (KITRP) HOF1 / CUP1-C2-HOF1 (HIS3MX)</i>	This study
YIMP9	<i>MATa ade2-1 ura3-1 his3-11,15 trp1-1 leu2-3,112 can1-100 / MATa ade2-1 ura3-1 his3-11,15 trp1-1 leu2-3,112 can1-100 HOF1 / CUP1-C2-HOF1 (HIS3MX) CYK3 / cyk3-C522A-GFP (KITRP)</i>	This study
YIMP11	<i>MATa ade2-1 ura3-1 his3-11,15 trp1-1 leu2-3,112 can1-100 / MATα ade2-1 ura3-1 his3-11,15 trp1-1 leu2-3,112 can1-100 HOF1 / CUP1-C2-HOF1 (HIS3MX) CHS2 / CHS2-V377I-hphNT (hphNT) CYK3 / cyk3Δ (KLTRP)</i>	This study
YIMP12	<i>MATa ade2-1 ura3-1 his3-11,15 trp1-1 leu2-3,112 can1-100 / MATα ade2-1 ura3-1 his3-11,15 trp1-1 leu2-3,112 can1-100 CHS2 / CHS2-V377I-hphNT (hphNT) CYK3 / cyk3Δ (KLTRP) HOF1 / C2(INN1)-K31A-HOF1 (HIS3MX)</i>	This study
YIMP22	<i>MATa ade2-1 ura3-1 his3-11,15 trp1-1 leu2-3,112 can1-100 / MATa ade2-1 ura3-1 his3-11,15 trp1-1 leu2-3,112 can1-100 CHS2 / CHS2-9MYC (KITRP1) CYK3 / TAP-CYK3 (kanMX)</i>	This study
YIMP35	<i>MATa ade2-1 ura3-1 his3-11,15 trp1-1 leu2-3,112 can1-100 / MATa ade2-1 ura3-1 his3-11,15 trp1-1 leu2-3,112 can1-100 HOF1 / CUP1-C2-HOF1 (HIS3MX) CYK3 / CYK3ΔSH3 (kanMX)</i>	This study
YIMP37	<i>MATa ade2-1 ura3-1 his3-11,15 trp1-1 leu2-3,112 can1-100 TAP-CYK3 (kanMX) CHS2-9MYC (KITRP1) pep4Δ::ADE2</i>	This study

	(ADE2)	
YIMP39	<i>MATa ade2-1 ura3-1 his3-11,15 trp1-1 leu2-3,112 can1-100 CHS2-9MYC (KITRP1) pep4Δ::ADE2 (ADE2)</i>	This study
YIMP41	<i>MATa ade2-1 ura3-1 his3-11,15 trp1-1 leu2-3,112 can1-100 CUP1-C2-HOF1 (HIS3MX) ura3-1::ADH1-OsTIR1-9MYC (URA3) cyk3-aid (kanMX)</i>	This study
YIMP43	<i>MATa ade2-1 ura3-1 his3-11,15 trp1-1 leu2-3,112 can1-100 CUP1-C2-HOF1 (HIS3MX) ura3-1::ADH1-OsTIR1-9MYC (URA3)</i>	This study
YIMP60	<i>MATa ade2-1 ura3-1 his3-11,15 trp1-1 leu2-3,112 can1-100 ura3-1::ADH1-OsTIR1-9MYC (URA3) cyk3-aid (kanMX)</i>	This study
YIMP73	<i>MATa ade2-1 ura3-1 his3-11,15 trp1-1 leu2-3,112 can1-100 CUP1-C2-HOF1 (HIS3MX) cyk3-aid (kanMX) ura3-1::GAL-OsTIR1-9MYC (URA3)</i>	This study
YIMP81	<i>MATa ade2-1 ura3-1 his3-11,15 trp1-1 leu2-3,112 can1-100 cyk3-aid (kanMX) ura3-1::GAL-OsTIR1-9MYC (URA3)</i>	This study
YIMP142	<i>MATa ade2-1 ura3-1 his3-11,15 trp1-1 leu2-3,112 can1-100 CUP1-C2-HOF1 (HIS3MX) cyk3-aid (kanMX) td-inn1-aid(Trp,KanMX) ura3-1::ADH1-OsTIR1-9MYC (URA3) leu2-3,112::pRS305-Prom+ORF-INN1-GFP-K31A (LEU2)</i>	This study
YIMP147	<i>MATa ade2-1 ura3-1 his3-11,15 trp1-1 leu2-3,112 can1-100 CUP1-C2-HOF1 (HIS3MX) td-inn1-aid(Trp,KanMX) ura3-1::ADH1-OsTIR1-9MYC (URA3) leu2-3,112::pRS305-Prom+ORF-INN1-GFP-K31A (LEU2)</i>	This study
YIMP149	<i>MATa ade2-1 ura3-1 his3-11,15 trp1-1 leu2-3,112 can1-100 td-inn1-aid (Trp,KanMX) ura3-1::ADH1-OsTIR1-9MYC (URA3) leu2-3,112::pRS305-Prom+ORF-INN1-GFP-K31A (LEU2)</i>	This study
YIMP155	<i>MATa ade2-1 ura3-1 his3-11,15 trp1-1 leu2-3,112 can1-100 / MATα ade2-1 ura3-1 his3-11,15 trp1-1 leu2-3,112 can1-100 CYK3 / CYK3ΔSH3-GFP (KITRP1, kanMX) HOF1 / CUP1-C2-HOF1 (HIS3MX)</i>	This study
YIMP168	<i>MATa ade2-1 ura3-1 his3-11,15 trp1-1 leu2-3,112 can1-100 / MATa ade2-1 ura3-1 his3-11,15 trp1-1 leu2-3,112 can1-100 HOF1 / CUP1-C2-HOF1 (HIS3MX) CYK3 / cyk3-C542A-GFP (KITRP)</i>	This study
YIMP196	<i>MATa ade2-1 ura3-1 his3-11,15 trp1-1 leu2-3,112 can1-100 INN1-yEGFP (kanMX) C2-HOF1 (HIS3) ura3-1::GAL-OsTIR1-9MYC (URA3) ubr1Δ::GAL-UBR1 (HIS3)</i>	This study
YIMP197	<i>MATa ade2-1 ura3-1 his3-11,15 trp1-1 leu2-3,112 can1-100 INN1-yEGFP (kanMX) ura3-1::GAL-OsTIR1-9MYC (URA3) ubr1Δ::GAL-UBR1 (HIS3) td-cyk3-aid (KITRP1, hphNT)</i>	This study
YIMP198	<i>MATa ade2-1 ura3-1 his3-11,15 trp1-1 leu2-3,112 can1-100 INN1-yEGFP (kanMX) C2-HOF1 (HIS3) ura3-1::GAL-OsTIR1-9MYC (URA3) ubr1Δ::GAL-UBR1 (HIS3) td-cyk3-aid (KITRP1, hphNT)</i>	This study
YIMP206	<i>MATa ade2-1 ura3-1 his3-11,15 trp1-1 leu2-3,112 can1-100 ura3-1::GAL-OsTIR1-9MYC (URA3) ubr1Δ::GAL-UBR1 (HIS3) CHS2-C-GFP (KITRP1)</i>	This study
YIMP207	<i>MATa ade2-1 ura3-1 his3-11,15 trp1-1 leu2-3,112 can1-100</i>	This study

	<i>INN1-yEGFP (kanMX) ubr1Δ::GAL-UBR1 (HIS3) ura3-1::GAL-OsTIR1-9MYC (URA3)</i>	
YIMP209	<i>MATa ade2-1 ura3-1 his3-11,15 trp1-1 leu2-3,112 can1-100 C2-HOF1 (HIS3) ura3-1::GAL-OsTIR1-9MYC (URA3) ubr1Δ::GAL-UBR1 (HIS3) td-cyk3-aid (KITRP1, hphNT) MYO1-C-GFP (KITRP1)</i>	This study
YIMP210	<i>MATa ade2-1 ura3-1 his3-11,15 trp1-1 leu2-3,112 can1-100 / MATa ade2-1 ura3-1 his3-11,15 trp1-1 leu2-3,112 can1-100 HOF1 / CUP1-C2-HOF1 (HIS3MX) RVS167 / rvs167Δ (hphNT)</i>	This study
YIMP218	<i>MATa ade2-1 ura3-1 his3-11,15 trp1-1 leu2-3,112 can1-100 chs3Δ (URA3) GAL-CYK3 (LEU2)</i>	This study
YIMP231	<i>MATa ade2-1 ura3-1 his3-11,15 trp1-1 leu2-3,112 can1-100 ura3-1::GAL-OsTIR1-9MYC (URA3) ubr1Δ::GAL-UBR1 (HIS3)</i>	This study
YIMP234	<i>MATa ade2-1 ura3-1 his3-11,15 trp1-1 leu2-3,112 can1-100 C2-HOF1 (HIS3) ura3-1::GAL-OsTIR1-9MYC (URA3) ubr1Δ::GAL-UBR1 (HIS3) chs3Δ (URA3)</i>	This study
YIMP235	<i>MATa ade2-1 ura3-1 his3-11,15 trp1-1 leu2-3,112 can1-100 chs3Δ (URA3) leu2-3,112::GAL-CYK3-GFP (LEU2)</i>	This study
YIMP237	<i>MATa ade2-1 ura3-1 his3-11,15 trp1-1 leu2-3,112 can1-100 / MATa ade2-1 ura3-1 his3-11,15 trp1-1 leu2-3,112 can1-100 HOF1 / CUP1-C2-HOF1 (HIS3MX) CYK3 / cyk3Δ (hphNT)</i>	This study
YIMP240	<i>MATa ade2-1 ura3-1 his3-11,15 trp1-1 leu2-3,112 can1-100 CUP1-C2-HOF1 (HIS3MX) cyk3-aid (kanMX) td-inn1-aid (Trp,KanMX) ura3-1::ADH1-OsTIR1-9MYC (URA3)</i>	This study
YIMP242	<i>MATa ade2-1 ura3-1 his3-11,15 trp1-1 leu2-3,112 can1-100 CUP1-C2-HOF1 (HIS3MX) td-inn1-aid (Trp,KanMX) ura3-1::ADH1-OsTIR1-9MYC (URA3)</i>	This study
YIMP246	<i>MATa ade2-1 ura3-1 his3-11,15 trp1-1 leu2-3,112 can1-100 C2-HOF1 (HIS3) ura3-1::GAL-OsTIR1-9MYC (URA3) ubr1Δ::GAL-UBR1 (HIS3) chs3Δ (URA3) td-cyk3-aid (KITRP, hphNT)</i>	This study
YIMP247	<i>MATa ade2-1 ura3-1 his3-11,15 trp1-1 leu2-3,112 can1-100 ura3-1::GAL-OsTIR1-9MYC (URA3) ubr1Δ::GAL-UBR1 (HIS3) td-cyk3-aid (KITRP1, hphNT) chs3Δ (URA3)</i>	This study
YIMP248	<i>MATa ade2-1 ura3-1 his3-11,15 trp1-1 leu2-3,112 can1-100 ura3-1::GAL-OsTIR1-9MYC (URA3) ubr1Δ::GAL-UBR1 (HIS3) chs3Δ (URA3)</i>	This study
YIMP249	<i>MATa ade2-1 ura3-1 his3-11,15 trp1-1 leu2-3,112 can1-100 CUP1-C2-HOF1 (HIS3MX) td-inn1-aid (Trp,KanMX) ura3-1::ADH1-OsTIR1-9MYC (URA3) leu2-3,112::pRS305-Prom+INN1-Cterminus-GFP (LEU2)</i>	This study
YIMP250	<i>MATa ade2-1 ura3-1 his3-11,15 trp1-1 leu2-3,112 can1-100 CUP1-C2-HOF1 (HIS3MX) cyk3-aid (kanMX) td-inn1-aid (Trp,KanMX) ura3-1::ADH1-OsTIR1-9MYC (URA3) leu2-3,112::pRS305-Prom+INN1-Cterminus-GFP (LEU2)</i>	This study
YIMP257	<i>MATα ade2-1 ura3-1 his3-11,15 trp1-1 leu2-3,112 can1-100 CUP1-C2-HOF1 (HIS3MX) cyk3-aid (kanMX) ura3-</i>	This study

	1::GAL-OsTIR1-9MYC (URA3) CHS2-V377I-hphNT (hphNT)	
YIMP258	MATa <i>ade2-1 ura3-1 his3-11,15 trp1-1 leu2-3,112 can1-100</i> CUP1-C2-HOF1 (HIS3MX) <i>ura3-1::GAL-OsTIR1-9MYC (URA3) CHS2-V377I-hphNT (hphNT)</i>	This study
YIMP306	MATa <i>ade2-1 ura3-1 his3-11,15 trp1-1 leu2-3,112 can1-100</i> <i>cyk3-aid (kanMX) td-inn1-aid (Trp,KanMX) ura3-1::ADH1-OsTIR1-9MYC (URA3)</i>	This study
YIMP308	MATa <i>ade2-1 ura3-1 his3-11,15 trp1-1 leu2-3,112 can1-100</i> <i>cyk3-aid (kanMX) td-inn1-aid (Trp,KanMX) ura3-1::ADH1-OsTIR1-9MYC (URA3) CHS2-V377I-hphNT (hphNT)</i>	This study
YIMP310	MATa <i>ade2-1 ura3-1 his3-11,15 trp1-1 leu2-3,112 can1-100</i> CUP1-C2-HOF1 (HIS3MX) <i>cyk3-aid (kanMX) td-inn1-aid (Trp,KanMX) ura3-1::ADH1-OsTIR1-9MYC (URA3) CHS2-V377I-hphNT (hphNT)</i>	This study
YIMP324	MATa <i>ade2-1 ura3-1 his3-11,15 trp1-1 leu2-3,112 can1-100 td-inn1-aid (Trp,KanMX) ura3-1::ADH1-OsTIR1-9MYC (URA3)</i>	This study
YIMP325	MATa <i>ade2-1 ura3-1 his3-11,15 trp1-1 leu2-3,112 can1-100 td-inn1-aid (Trp,KanMX) ura3-1::ADH1-OsTIR1-9MYC (URA3) CHS2-V377I-hphNT (hphNT)</i>	This study
YIMP388	MATa <i>ade2-1 ura3-1 his3-11,15 trp1-1 leu2-3,112 can1-100</i> / MATa <i>ade2-1 ura3-1 his3-11,15 trp1-1 leu2-3,112 can1-100</i> CYK3 / <i>cyk3Δ (hphNT) INN1 / inn1Δ (KITRP1) HOF1 / CUP1-C2-HOF1 (HIS3MX) CHS2 / CHS2-V377I-kanMX</i>	This study
YIMP390	MATa <i>ade2-1 ura3-1 his3-11,15 trp1-1 leu2-3,112 can1-100</i> / MATa <i>ade2-1 ura3-1 his3-11,15 trp1-1 leu2-3,112 can1-100</i> CYK3 / <i>cyk3Δ (hphNT) INN1 / inn1Δ (KITRP1) HOF1 / CUP1-C2-HOF1 (HIS3MX) CHS2 / CHS2-V377I-kanMX</i>	This study
YIMP391	MATa <i>ade2-1 ura3-1 his3-11,15 trp1-1 leu2-3,112 can1-100</i> / MATa <i>ade2-1 ura3-1 his3-11,15 trp1-1 leu2-3,112 can1-100</i> HOF1 / CUP1-C2-HOF1 (HIS3MX) <i>SHO1 / sho1Δ (hphNT)</i>	This study
YIMP409	MATa <i>ade2-1 ura3-1 his3-11,15 trp1-1 leu2-3,112 can1-100</i> CUP1-C2-HOF1-GFP (HIS3MX, KITRP1)	This study
YIMP415	MATa <i>ade2-1 ura3-1 his3-11,15 trp1-1 leu2-3,112 can1-100</i> INN1-yEGFP (kanMX) C2-HOF1 (HIS3) <i>ura3-1::GAL-OsTIR1-9MYC (URA3) ubr1Δ::GAL-UBR1 (HIS3) td-cyk3-aid (KITRP1, hphNT) leu2-3,112::pRS305-empty</i>	This study
YIMP416	MATa <i>ade2-1 ura3-1 his3-11,15 trp1-1 leu2-3,112 can1-100</i> INN1-yEGFP (kanMX) C2-HOF1 (HIS3) <i>ura3-1::GAL-OsTIR1-9MYC (URA3) ubr1Δ::GAL-UBR1 (HIS3) td-cyk3-aid (KITRP1, hphNT) leu2-3,112::pRS305-cyk3-H563A-D578A</i>	This study
YIMP417	MATa <i>ade2-1 ura3-1 his3-11,15 trp1-1 leu2-3,112 can1-100</i> INN1-yEGFP (kanMX) C2-HOF1 (HIS3) <i>ura3-1::GAL-OsTIR1-9MYC (URA3) ubr1Δ::GAL-UBR1 (HIS3) td-cyk3-aid (KITRP1, hphNT) leu2-3,112::pRS305-CYK3</i>	This study
YIMP423	MATa <i>ade2-1 ura3-1 his3-11,15 trp1-1 leu2-3,112 can1-100</i> CHS2-C-GFP (KITRP1) <i>leu2::pRS305-GAL-cyk3-H563A-D578A</i>	This study

YIMP428	<i>MATa ade2-1 ura3-1 his3-11,15 trp1-1 leu2-3,112 can1-100 / MATα ade2-1 ura3-1 his3-11,15 trp1-1 leu2-3,112 can1-100 CHS2 / CHS2-C-GFP (KITRP1) HOF1 / C2-HOF1 (HIS3MX) CYK3 / td-cyk3-aid (KITRP1, hphNT)</i>	This study
YIMP452	<i>MATa ade2-1 ura3-1 his3-11,15 trp1-1 leu2-3,112 can1-100 C2-HOF1 (HIS3) ura3-1::GAL-OsTIR1-9MYC (URA3) ubr1Δ::GAL-UBR1 (HIS3) MYO1-C-GFP (KITRP1) SPC42-Cter-EQFP (HIS3)</i>	This study
YIMP457	<i>MATa ura3-52 lys2Δ201 pep4Δ pDDGFP-CHS2-TEV-GFP-8HIS (URA3)</i>	This study
YIMP458	<i>MATa ade2-1 ura3-1 his3-11,15 trp1-1 leu2-3,112 can1-100 pep4Δ::ADE2 pDDGFP-CHS2-TEV-GFP-8HIS (URA3)</i>	This study
YIMP459	<i>MATa ura3-52 lys2Δ201 pep4Δ pDDGFP-CHS2(215-963)-TEV-GFP-8HIS (URA3)</i>	This study
YIMP460	<i>MATa ura3-52 lys2Δ201 pep4Δ pDDGFP-C2-CHS2-TEV-GFP-8HIS (URA3)</i>	This study
YIMP461	<i>MATa ade2-1 ura3-1 his3-11,15 trp1-1 leu2-3,112 can1-100 cdc14-1 leu2-3,112 ::pRS305-GAL-INN1 (LEU2) pep4Δ::ADE2 pDDGFP-CHS2-TEV-GFP-8HIS (URA3)</i>	This study
YIMP462	<i>MATa ade2-1 ura3-1 his3-11,15 trp1-1 leu2-3,112 can1-100 cdc15-2 leu2-3,112 ::pRS305-GAL-INN1 (LEU2) pep4Δ::ADE2 pDDGFP-CHS2-TEV-GFP-8HIS (URA3)</i>	This study
YIMP463	<i>MATa ade2-1 ura3-1 his3-11,15 trp1-1 leu2-3,112 can1-100 leu2-3,112 ::pRS305-GAL-INN1 (LEU2) pep4Δ::ADE2 pDDGFP-CHS2-TEV-GFP-8HIS (URA3)</i>	This study
YIMP466	<i>MATa ade2-1 ura3-1 his3-11,15 trp1-1 leu2-3,112 can1-100 / MATα ade2-1 ura3-1 his3-11,15 trp1-1 leu2-3,112 can1-100 HOF1 / CUP1-C2-HOF1 (HIS3MX) CHS2 / CHS2-V377I-kanMX CYK3 / cyk3-H563A-D578A-hphNT (hphNT)</i>	This study
YJW15	<i>MATa ade2-1 ura3-1 his3-11,15 trp1-1 leu2-3,112 can1-100 ura3-1::ADH1-OsTIR1-9MYC (URA3)</i>	M. Kanemaki
YMF38	<i>MATa ade2-1 ura3-1 his3-11,15 trp1-1 leu2-3,112 can1-100 CHS2-9MYC (KITRP) INN1-TAP (kanMX) pep4Δ::URA3 (URA3) ADE2+</i>	M. Foltman
YMF76	<i>MATa ade2-1 ura3-1 his3-11,15 trp1-1 leu2-3,112 can1-100 / MATa ade2-1 ura3-1 his3-11,15 trp1-1 leu2-3,112 can1-100 CYK3/ CYK3-TAP (HIS3MX) CHS2/CHS2-9MYC (KITRP1)</i>	M. Foltman
YMF79	<i>MATa ade2-1 ura3-1 his3-11,15 trp1-1 leu2-3,112 can1-100 CHS2-9MYC (KITRP1) leu2-3,112::TETO2-CTAP4 (LEU2) pep4Δ::URA3 (URA3) ADE2+</i>	M. Foltman
YMF319	<i>MATa ade2-1 ura3-1 his3-11,15 trp1-1 leu2-3,112 can1-100 ubr1Δ::GAL-UBR1 (HIS3) ura3-1::ADH1-OsTIR1-9MYC (URA3) td-inn1-aid (KITRP-kanMX) CYK3-C-GFP (KITRP1)</i>	M. Foltman
YMF322	<i>MATa ade2-1 ura3-1 his3-11,15 trp1-1 leu2-3,112 can1-100 ubr1Δ::GAL-UBR1 (HIS3) ura3-1::ADH1-OsTIR1-9MYC (URA3) CYK3-C-GFP (KITRP1)</i>	M. Foltman
YMF334	<i>MATa ade2-1 ura3-1 his3-11,15 trp1-1 leu2-3,112 can1-100 C2-HOF1 (HIS3) ura3-1::GAL-OsTIR1-9MYC (URA3) ubr1Δ::GAL-UBR1 (HIS3)</i>	M. Foltman

YMF335	<i>MATa ade2-1 ura3-1 his3-11,15 trp1-1 leu2-3,112 can1-100 ura3-1::GAL-OsTIR1-9MYC (URA3) ubr1Δ::GAL-UBR1 (HIS3) td-cyk3-aid (KITRP1, hphNT)</i>	M. Foltman
YMF343	<i>MATa ade2-1 ura3-1 his3-11,15 trp1-1 leu2-3,112 can1-100 ura3-1::GAL-OsTIR1-9MYC (URA3) ubr1Δ::GAL-UBR1 (HIS3) td-cyk3-aid (KITRP1, hphNT) CHS2-C-GFP (KITRP1)</i>	M. Foltman
YMF356	<i>MATa ade2-1 ura3-1 his3-11,15 trp1-1 leu2-3,112 can1-100 C2-HOF1 (HIS3) ura3-1::GAL-OsTIR1-9MYC (URA3) ubr1Δ::GAL-UBR1 (HIS3) td-cyk3-aid (KITRP1, hphNT)</i>	M. Foltman
YMF475	<i>MATa ade2-1 ura3-1 his3-11,15 trp1-1 leu2-3,112 can1-100 CYK3ΔSH3-GFP (KITRP1, hphNT) leu2-3,112::pRS305-GAL-CYK3 (LEU2)</i>	M. Foltman
YMF505	<i>MATa ade2-1 ura3-1 his3-11,15 trp1-1 leu2-3,112 can1-100 chs3Δ (URA3)</i>	M. Foltman
YMF576	<i>MATa ade2-1 ura3-1 his3-11,15 trp1-1 leu2-3,112 can1-100 chs3Δ (URA3) leu2-3,112::pRS305-GAL-CYK3-H563A-D578A-GFP (LEU2)</i>	M. Foltman
YMF610	<i>MATa ade2-1 ura3-1 his3-11,15 trp1-1 leu2-3,112 can1-100 CHS2-C-GFP (KITRP1) leu2-3,112::GAL-CYK3(LEU2)</i>	M. Foltman
YMF669	<i>MATa ade2-1 ura3-1 his3-11,15 trp1-1 leu2-3,112 can1-100/MATa ade2-1 ura3-1 his3-11,15 trp1-1 leu2-3,112 can1-100 HOF1/CUP1-C2-HOF1 (HIS3MX) CYK3/cyk3-H563A-D578A-GFP (KITRP)</i>	M. Foltman
YNK40	<i>MATa ade2-1 ura3-1 his3-11,15 trp1-1 leu2-3,112 can1-100 ura3-1::GAL-OsTIR1-9MYC (URA3)</i>	M. Kanemaki
W303-1a	<i>MATa ade2-1 ura3-1 his3-11,15 trp1-1 leu2-3,112 can1-100</i>	Rodney Rothstein

Table 2.4: Constructs made by one-step PCR.

Construct	Template plasmid	Oligos	Oligos checking
TAP-CYK3	pASD69 (kanMX)	657, 658	659, 660, 540, 542
cyk3-aid	pMK43 (kanMX)	653, 654	655, 656, 540, 542
td-cyk3-aid	pMP20 (hphNT)	653, 654	656, 188, 9, 10
C2-HOF1-GFP	pYM26 (K.I.TRP1)	673, 674	211, 543, 150, 672
cyk3ΔSH3-GFP	pASD69 (kanMX)	657, 896	657, 660, 540, 542

2.2.4 Dilution spotting assay.

For each strain, one fresh colony was diluted in 1 ml of PBS, counted in a haemocytometer and diluted in PBS until cell concentration was 3.33×10^6 cells per ml. Tenfold dilutions were made, and 15 μ l drops containing 50000, 5000, 500 or 50 cells were pipetted on the appropriate plates under different conditions and incubated for several days at the appropriate temperature. Plates were scanned on each day using EPSON perfection V700 PHOTO scanner.

2.2.5 Yeast two-hybrid assay.

Genes coding for the proteins or protein truncations of interest were fused to the activation domain (AD) or the DNA binding domain (DBD) were co-transformed into the yeast strain PJ69-4A (Hybrigenics), using 500 ng of each plasmid. Transformed yeast cells were grown on selective SC plates lacking tryptophan (for the DBD plasmid) and leucine (for the AD plasmid) for at least two days at 30°C. For each transformation, six colonies were picked and restreaked onto fresh SC – Leu – Trp plates, and then grown for two more days. Next, six colonies from each plate were mixed and resuspended in 1 ml of PBS, before processing for ‘dilution spotting assay’ as described previously using SC plates lacking tryptophan and leucine (‘non-selective’ medium) and SC plates lacking tryptophan, leucine and histidine (‘selective’ medium).

2.2.6 Growth and synchronisation of yeast strains.

For each strain, one fresh colony was inoculated into YP media supplemented with 2% raffinose or 2% glucose according to the experiment, and grown overnight. The following morning, cells were counted in a haemocytometer and diluted to 0.4×10^7 cells/ml.

Synchronisation in G1 phase of the cell cycle was induced by adding mating pheromone (alpha factor) to a final concentration of 7.5 μ g/ml when cells reached 0.7×10^7 cells/ml. After two hours, additional mating pheromone was added to a final concentration of 2.5 μ g/ml every 30 minutes until 90% of the cells were arrested as non-budded cells, which was observed by phase-contrast microscopy. For wild type cells, G1 block typically takes around 3 hours in YPD media and 3.5 hours on YPRaff (Foltman *et al.* 2016b).

Synchronisation in G2/M was performed by adding nocodazole to a final concentration of 5 μ g/ml, until 90% of the cells were arrested as large-budded cells. For wild type cells, G2/M arrest takes around 3 hours in YPD and 3.5 hours in YPRaff (Foltman *et al.* 2016b).

To release cells from the arrest, they were pelleted, washed twice and re-suspended in fresh medium lacking mating pheromone or nocodazole.

In degron experiments, carbon source was changed from raffinose to galactose to induce the expression of E3 ubiquitin ligases *UBR1* and/or *TIR1*. For auxin degron degradation of the protein of interest, degradation was induced by addition of auxins NAA and IAA to a final concentration of 500 μ M.

We used calcofluor (Fluorescent Brightener 28; Sigma; F3543) to stain the primary septa of live cells. Calcofluor was added 35 minutes after release from G1 block to a final concentration of 50 μ g/ml and the culture was further incubated for at least 60 minutes.

We used aniline blue (Fluka, 95290) to stain the secondary septa of live cells. Aniline was added 35 minutes after release from G1 block to a final concentration of 0.05% (w/v) and the culture was further incubated for at least 60 minutes.

When cells were grown for time-lapse experiments, release from G2/M phase of the cell cycle was performed by washing and resuspending cells in SC-based media supplemented with 2% sucrose and 2% galactose, as well as supplemented with auxins NAA and IAA to a final concentration of 20 μ M. After release, cells were grown in an IBIDI cells in focus 15 micro-slide (8 well 80827 glass bottom) slide. Slides were coated with a 5 mg/ml solution of concanavalin A (Sigma, L7647), washed with water, and dried for 30 minutes, to allow cells to attach to the

slide during the time-lapse video microscopy experiment.

2.2.7 Small-scale membrane protein expression.

Cells were inoculated in 5 ml of minimal media lacking uracil (6.7 g/L yeast nitrogen base lacking amino acids, 2 g/L amino acid mix lacking uracil) to allow retention of the 2 μ pDDGFP2 plasmid encoding Chs2 protein in 50 ml aerated tubes (Sigma, Z761028) at 24°C or 30°C according to the experiment. The day after, cells were diluted to an OD₆₀₀ of 0.15 (0.33 \times 10⁷ cells/ml) in 10 ml of minimal media lacking uracil supplemented with 0.1% glucose. Cells were allowed to grow to an OD₆₀₀ of 0.6 (1.4 \times 10⁷ cells/ml), and protein expression was induced by addition of galactose to a final concentration of 2%.

After 22 hours of expression, cells were harvested at 3,000 \times g, and resuspended in 200 μ l of YSB buffer (50 mM Tris pH 7.5, 10% glycerol, 5 mM EDTA, 1X Roche Complete protease inhibitors (04693132001)). Cell expression was checked by reading GFP counts from the 200 μ l sample in a clear-bottom 96-well plate using fluorescence reader SpectraMax M2e (Molecular Devices) using an excitation wavelength of 470nm and an emission wavelength of 512nm (Drew *et al.* 2008).

2.2.8 Growth of yeast strains for large-scale Chs2 protein production.

To induce the expression of membrane protein Chs2 a three day-old colony of *GAL-CHS2-GFP-8HIS pep4Δ* (YIMP457) or *GAL-CHS2-GFP-8HIS GAL-INN1 cdc15-2 pep4Δ* (YIMP462) was inoculated into minimal media lacking uracil (6.7 g/L yeast nitrogen base lacking amino acids, 2 g/L amino acid mix lacking uracil) supplemented with 2% glucose overnight at 30°C or 24°C, according to the experiment. The day after, cells were diluted to an OD₆₀₀ of 0.15 (0.33×10⁷ cells/ml) in minimal media lacking uracil supplemented with 0.1% glucose. Cells were allowed to grow to an OD₆₀₀ of 0.6 (1.4×10⁷ cells/ml), and protein expression was induced by addition of galactose to a final concentration of 2% as described in section 2.2.7. The culture volume for large-scale production was 12 litres per culture.

After allowing the cells to produce the protein of interest for 22h, cells were pelleted, resuspended in CRB buffer (50 mM Tris-HCl pH 7.5, 1 mM EDTA, 0.6 M sorbitol), flash-frozen in liquid nitrogen and stored at -80°C.

2.2.9 FACS and binucleate cells counting.

1 ml sample of cells from the culture of interest were spun down, and pellet was resuspended in 1 ml of 70% ethanol.

To prepare fixed cells for FACS or binucleate cells counting, 100 µl aliquots of fixed cells were rehydrated in 50 mM sodium citrate. Hydrated cells were spun down, and pellet was resuspended in 50 mM sodium citrate buffer supplemented with 0.1 mg/ml RNase A (Sigma, R5125). Samples were incubated for two hours at 37°C to degrade RNA.

After that, cells were spun down, and resuspended in 5 mg/ml pepsin (AMS Biotechnology, 31820.01) in 50 mM HCl. Finally, cells were spun down and resuspended in 50 mM sodium citrate supplemented with 2 µg/ml propidium iodide (Sigma, P4170) to allow DNA visualisation. Prior to observation, cells were sonicated twice for four seconds, to release any cell clumps. At this stage cells were processed on a FACScan (BD FACScan) and generated plots were analysed with CellQuest software (BD Cell Quest Pro). Additionally, the number of binucleate cells was assessed by counting 100 cells from each time point in a fluorescence microscope using a rhodamine-specific filter to visualise propidium iodide-stained nuclei.

2.3 Protein methods.

2.3.1 Small-scale membrane preparation.

Cells from the small-scale expression trials were broken with glass beads (BioSpec, 11079105) by vortexing at 4°C for 10 minutes.

Unbroken cells were removed by centrifugation at $14100 \times g$ for 30 seconds, and membranes were purified by centrifugation at $14100 \times g$ for one hour. Membrane pellet was resuspended in 50 μ l of YSB buffer (50 mM Tris pH 7.5, 10% glycerol, 5 mM EDTA, 1X Roche Complete protease inhibitors (04693132001)).

2.3.2 Membrane preparation for Chs2 purification.

Cell pellets from twelve litres cultures of *GAL-CHS2-GFP-8HIS pep4 Δ* (YIMP457) or *GAL-CHS2-GFP-8HIS GAL-INN1 cdc15-2 pep4 Δ* (YIMP462) were defrosted from -80°C and one protease inhibitor tablet (Roche, 04693132001), dissolved in 10 ml of CRB buffer, was added. Cells were broken with a cell disruptor (Constant Systems) after several cycles at 25, 30, 33, 36 and 39 kpsi. Unbroken cells were removed by centrifugation at $10000 \times g$ for 10 minutes, and membranes were purified from the supernatant by centrifugation at $100,000 \times g$ for 2 hours. Membranes were resuspended in MRB buffer (20 mM Tris-HCl pH 7.5, 0.3 M sucrose, 0.1 mM CaCl_2), flash-frozen in liquid nitrogen and stored at -80°C .

2.3.3 Fluorescent size-exclusion chromatography (FSEC).

To assess the solubilisation and stability of Chs2 in a range of detergents, 3.5 mg of total membrane proteins were mixed with PBS and and 1% (w/v) of the detergent of

choice to a final volume of 1 ml. Mixture was left to solubilise with gentle rocking at 4°C for one hour, and insoluble material was centrifuged down at $14,100 \times g$ for one hour.

Solubilised material was loaded onto a 24 ml size-exclusion Superose 6 Increase 10/300 GL column (GE Healthcare, 29-0915-96). 200 μ m fractions were collected in a clear bottom 96-well plate, and fluorescence was read using fluorescence reader SpectraMax M2e (Molecular Devices) using an excitation wavelength of 470nm and an emission wavelength of 512nm.

2.3.4 Large-scale Chs2 protein purification.

Membranes from six litres of yeast culture expressing Chs2 were solubilised for one hour at 4°C in solubilisation buffer (PBS 1X, 10% glycerol, 100 mM NaCl, 1% DDM, 5 mM DTT) containing one tablet of protease inhibitors diluted in 10 ml of water (Roche, 04693132001). Insoluble membranes were removed by centrifugation at $100000 \times g$ for 45 minutes. To the supernatant, a final concentration of 10 mM imidazole was added to prevent unspecific binding to the resin.

Protein was loaded to two 5 ml HisTrap resin columns (GE Healthcare, 17-5248-02) equilibrated with wash buffer (PBS 1X, 10% glycerol, 100 mM NaCl, 0.03% DDM, 5 mM DTT, 10mM imidazole) with a peristaltic pump. Bound protein was washed with 100 ml of wash buffer with 10 mM, 30 mM and 50 mM

imidazole to remove non-specifically bound proteins. Elution was performed with elution buffer (PBS 1X, 10% glycerol, 0.03% DDM, 5 mM DTT, 350 mM imidazole). 1 ml of 3.5 mg/ml TEV protease was added to the eluate to cleave GFP and His tags, and protein was dialysed overnight at 4°C in a 12-14 MWCO dialysis tubing (Spectra/Por, 132680) in dialysis buffer (20 mM Tris-HCl pH 7.5, 10% glycerol, 100 mM NaCl, 0.03% DDM, 5 mM DTT).

The day after, dialysed protein was clarified by centrifuging at 4000 × g for 10 minutes at 4°C, and then filtered through a 0.2 µm syringe filter (Pall, 4612). Imidazole was added to a final concentration of 15 mM, and cleaved tags were removed by reverse purification in a 5 ml HisTrap column equilibrated in dialysis buffer supplemented with 15 mM imidazole. Flow-through containing the protein of interest, was concentrated to 500 µl (Millipore, UFC910024), protein aggregates spun down at 14100 × g for 10 minutes, then injected into a 24 ml size-exclusion Superdex 200 10/300 GL column (GE Healthcare, 28990944) equilibrated in gel-filtration buffer (20 mM Tris pH 7.5, 150 mM NaCl, 0.03% DDM, 5 mM DTT) as a final purification step.

Protein peaks were separated on a 12% Tris-glycine gel (Thermo-Fisher, WT0121BOX) to check for purity and stained with InstantBlue (Sigma, ISB1L) and protein band was cut and sent to the mass-

spectrometry facility at the University of Saint-Andrews (Scotland) for identification. Sample was reduced, alkylated and digested with trypsin. The resulting peptides were analysed by MALDI MS and the spectra were searched against NCBI using Mascot.

The protein was analysed by immunoblotting to confirm the identity of the band.

2.3.5 Trichloroacetic acid (TCA) precipitation of proteins.

Approximately 10⁸ cells were pelleted by centrifugation at 200 × g for three minutes. After washing cells with water to eliminate media residues, pellets were frozen at -20°C.

To make the extracts, pellets were thawed and resuspended in 300 µl of 20% TCA, to which 300 µl of glass beads (BioSpec, 11079105) were added, and cells were lysed by vortexing for one minute. Extract was transferred to a new tube, and glass beads washed again with 300 µl 5% TCA.

Pooled extracts were centrifuged at 200 × g for 10 minutes, after which a protein pellet is formed. Pellet was resuspended in high pH Laemmli buffer (regular 1x Laemmli buffer + 150 µl Tris base/ml), and sample was boiled at 95°C for four minutes. Unbroken cells were removed by centrifugation at 200 × g for 10 minutes, after which the supernatant was frozen at -20°C.

2.3.6 Immunoblotting.

For gel separation of proteins, either handcasted SDS polyacrylamide gels or precast NuPAGE gels were used (Invitrogen; 8% gels, WG1002BOX; 4-12% gels WG1402BOX).

Running gel was made of 375 mM Tris pH 8.8, 0.1% SDS (Fisher, BP1311), 0.1% APS (Fisher, 17874), 0.1% TEMED (Sigma, T9281) and 7.5-10% acrylamide solution (acrylamide:bis-acrylamide 37.5:1 Protogel, National Diagnostics, EC-890) according to the size of the protein of interest.

Stacking gel was composed of 125 mM Tris pH 6.8, 0.1% SDS, 0.05% APS, 0.1% TEMED and 3.9% acrylamide. SDS-PAGE Running buffer (0.3% Tris base, 1.44% glycine and 0.1% SDS) was used to run gels at 130V for one and a half to two hours.

Gels were washed with water, and then equilibrated with Transfer buffer (0.58% Tris-base, 0.293% glycine, 0.0375% SDS and 20% methanol) prior to transfer of proteins to a nitrocellulose membrane using a semi-dry transfer cassette (BioRad, 170-3940) at 13 V for 60 minutes.

For NuPAGE gels, gels were run at 130 V for one and a half to two hours using 1X MOPS running buffer (Invitrogen, NP001). Gels were then washed with water and transferred using the iBlot Gel Transfer system (Invitrogen, IB1001) to nitrocellulose membrane (Invitrogen iBlot Transfer Stack,

nitrocellulose, IB3010-01) for 13 minutes at 20 V.

To check protein transfer, membranes were stained with 0.3% Ponceau solution (Sigma, P3504) in 1% Glacial Acetic Acid, and destained in TBST (TBS buffer supplemented with 0.1% Tween-20 (Sigma, P1379).

For blocking non-specific protein binding, membranes were incubated with either 5% skimmed milk (Marvel) or 3% BSA (Sigma, A3059) in TBST for one hour at room temperature or overnight at 4°C, depending on the primary antibody used.

Primary antibodies were incubated at the appropriate dilution in either TBST supplemented with 5% powdered skimmed milk or 3% BSA (Bovine Serum Albumine), for one hour at room temperature – except for anti-GFP, which required two hours incubation.

Membranes were then washed four times for five minutes with TBST, and incubated with a secondary antibody at the appropriate dilution for one hour at room temperature. Secondary antibodies were coupled to horseradish peroxidase (HRP), which produces light upon exposure to ECL substrate. After that, membranes were washed again four times for five minutes in TBST, before adding ECL substrate (GE Healthcare, RPN2109) and exposing the membrane to photographic film in a dark room (GE Healthcare, 28-9068).

Primary antibodies used were as follows: anti-Chs2 (lab collection, 1:200), anti-

Cyk3 (lab collection, 1:250), anti-Hof1 (lab collection, 1:200), anti-MYC 9E10 (1:1000, Cancer Research UK), anti-Inn1 (lab collection, 1:500), anti-Strep (iBa Life Sciences, 2-1507-001, 1:1000), anti-His (Qiagen, 34660, 1:2000) and PAP (Sigma, P1291, 1:5000).

Secondary antibodies used were as follows: anti-rabbit-HRP (Fisher, GZNA93401, 1:10000), anti-sheep-HRP (Sigma, A3415, 1:10000) and anti-mouse-HRP (Vector Labs, PI-2000, 1:10000).

2.3.7 Immunoprecipitation of protein complexes.

Aliquots of 300 µg of rabbit antisheep IgG (Sigma, S-1265) were coupled to Dynabeads M-270 Epoxy (Invitrogen, 143.01) at 4°C as described by the manufacturer.

To prepare yeast popcorn, 250 ml cultures of the strains of interest were centrifuged at 200 × g for three minutes and washed with 50 ml of 20 mM HEPES-KOH pH 7.9 buffer. Cells were then washed again with 10 ml of 100 mM HEPES-KOH pH 7.9, 50 mM potassium acetate, 10 mM magnesium acetate, 2 mM EDTA. After the wash, the pellet was weighed and re-suspended in three volumes of lysis buffer supplemented with protease inhibitors (2x Complete protease inhibitor (Roche, 11575400), 1% protease inhibitor cocktail (Sigma, P8215)), as well as phosphatase inhibitors (2 mM sodium β-glycerophosphate, 2 mM sodium fluoride) and

also 1 mM DTT as a reducing agent. Cell suspension was then transferred drop by drop into liquid nitrogen, which formed the so-called 'yeast popcorn', and was then stored at -80°C.

2.5 grams of cell popcorn were ground in a coffee mill in presence of dry ice. When cell breakage had reached 70-80% as judging from microscopic examination, broken cells were resuspended in lysis buffer supplemented with protease and phosphatase inhibitors, and DTT. Unbroken cells were removed by centrifugation at 16100 × g for 30 minutes; and supernatant was clarified by ultracentrifugation at 100000 × g for 60 minutes. After ultracentrifugation, a sample was collected as cell extract, and the rest was split into two aliquots and each was incubated with 100 µl of IgG-coated magnetic beads at 4°C for two hours on a rotating wheel.

Afterwards, beads were pelleted using a magnetic rack (Invitrogen, 14302D), and washed four times with 1 ml of wash buffer: 100 mM HEPES-KOH pH 7.9, 100 mM potassium acetate, 10 mM magnesium acetate, 2 mM EDTA, 0.1% NP-40, 2x Complete protease inhibitor (Roche), 1% protease inhibitor cocktail (Sigma), 2 mM sodium β-glycerophosphate and 2 mM sodium fluoride.

Finally, proteins were eluted by boiling the beads for five minutes in 50 µl of 1X Laemmli buffer, and the eluates were frozen in dry ice and stored at -80°C.

2.3.8 Growth of *E. coli* cultures for protein expression.

An overnight culture of LB media supplemented with 30 µg/ml kanamycin (Sigma, K1377) and 30 µg/ml chloramphenicol (Sigma, C0378) was inoculated from the appropriate *E. coli* Rosetta glycerol stock and grown overnight at 37°C.

Cultures were diluted the next morning in one litre of LB media supplemented with 30 µg/ml kanamycin (Sigma, K1377) and 30 µg/ml chloramphenicol (Sigma, C0378), and protein expression was induced at an OD₆₀₀ of 0.6 by addition of a final concentration of 1 mM of β-D-1-thiogalactopyranoside (IPTG) (Fisher, 10021793). Protein expression was performed for two hours at 37°C, upon which cells were pelleted and frozen at -20°C.

2.3.9 *E. coli* native purification.

Pellets from 500 ml culture of *E. coli* expressing each protein fragment tagged with either StrepTag or 6His, plus appropriate controls, were thawed at room temperature and resuspended in 10 ml lysis buffer (50 mM Tris-HCl pH 8, 10% glycerol, 0.1% NP-40, 10 mM MgCl₂, 150 mM NaCl, 5 mM β-mercaptoethanol, 1 mg/ml lysozyme, 1X HALT protease inhibitors, 1X Roche protease inhibitors) and incubated for 20 minutes on a tilting platform at room temperature. Unbroken cells were removed by centrifugation at 16100 × g for 10 minutes.

Cell extracts were mixed with 1 ml of Strep-Tactin Superflow Resin (iBa Life Sciences, 2-1206-002) equilibrated with lysis buffer, and incubated on a tilting platform for one hour at 4°C. Resin was centrifuged to collect the flow-through, and 10 ml of ice-cold wash buffer (50 mM Tris-HCl pH 8, 10% glycerol, 0.1% NP-40, 10 mM MgCl₂, 150 mM NaCl, 5 mM β-mercaptoethanol, 1X HALT protease inhibitors, 1X Roche protease inhibitors) was added to the resin and left to wash for 10 minutes on a tilting platform at 4°C. This wash was repeated two more times, after which protein was eluted in 2 ml of elution buffer (50 mM Tris-HCl pH 8, 10% glycerol, 0.1% NP-40, 10 mM MgCl₂, 150 mM NaCl, 5 mM β-mercaptoethanol, 1X HALT protease inhibitors, 1X Roche protease inhibitors, 25 mM desthiobiotin). 10 ml of His lysis buffer (50 mM Tris-HCl pH 8, 10% glycerol, 0.1% NP-40, 10 mM MgCl₂, 150 mM NaCl, 5 mM β-mercaptoethanol, 20 mM imidazole, 1X HALT protease inhibitors, 1X Roche protease inhibitors) was added to eluate.

Eluate was incubated with 1 ml Ni²⁺-NTA resin (Qiagen, 30210), equilibrated in His lysis buffer for one hour on a tilting platform at 4°C. Resin was centrifuged to collect the flow-through, and washed with 10 ml of ice-cold wash buffer (50 mM Tris-HCl pH 8, 10% glycerol, 0.1% NP-40, 10 mM MgCl₂, 150 mM NaCl, 5 mM β-mercaptoethanol, 20 mM imidazole, 1X HALT protease inhibitors, 1X Roche protease inhibitors). Resin was

centrifuged, and after adding further 4 ml of wash buffer resin was allowed to set in a PolyPrep column (BioRad, 731-1550). Final protein was eluted in five 0.5 ml washes with elution buffer (50 mM Tris-HCl pH 8, 10% glycerol, 0.1% NP-40, 10 mM MgCl₂, 150 mM NaCl, 5 mM β-mercaptoethanol, 250 mM imidazole, 1X HALT protease inhibitors, 1X Roche protease inhibitors).

2.3.10 *E. coli* denaturing purification.

Cell pellet was thawed on ice and resuspended as 5 ml of buffer A per gram of cell pellet (10 mM Tris pH 8, 100 mM NaH₂PO₄, 8 M guanidinium chloride), leaving it to incubate for one hour at room temperature on a tilting platform.

Insoluble fraction was removed by centrifugation at 16100 x g for 30 minutes, and cleared lysate was incubated with 1 ml of Ni²⁺-NTA resin equilibrated in buffer A for one hour at 4°C on a tilting platform. After centrifuging the resin to get rid of the flow through, resin was washed once with 10 ml of buffer A, transferred to a PolyPrep column (BioRad, 731-1550) and washed again with 5 ml of buffer A. Two consecutive 10 ml washes were done with buffer C (10 mM Tris pH 6.3, 100 mM NaH₂PO₄, 8 M urea), and protein was eluted with four 1 ml washes with buffer E (10 mM Tris pH 4.5, 10 mM NaH₂PO₄, 8 M urea).

2.3.11 Antigen purification.

Antigen, purified in an *E. coli* denaturing purification as described above, was loaded onto a precast 4-12% ZOOM gel (Thermo, NP0330BOX) and stained with 0.25M KCl. Antigen band was cut with a scalpel, minced into small pieces and ground in a mortar with dry ice.

Ground band was recovered in cold coupling buffer (0.1 M NaHCO₃, 0.5 M NaCl, pH 8.3), and concentrated in a Nanosep centrifugal device, 300K MWCO (Pall, 516-8530).

Flow-through was precipitated with ice-cold TCA to a final concentration of 25%, centrifuged at 12000 × g for 30 minutes at 4°C. Pellet was washed with 500 μl of ice-cold 0.05 M HCl, pelleted again at the same settings, and washed with 500 μl of ice-cold acetone. After centrifuging the sample at the same settings, pellet was dried and resuspended in around 100 μl of coupling buffer supplemented with 0.2% SDS.

After resuspension, protein concentration was estimated visually by running a known volume of suspension in the same gel as different amounts of protein standards.

2.3.12 Antibody purification.

Antibodies were purified on a 5ml HiTrap NHS-Activated HP column (GE Healthcare, 17-0716-01) coupled with the corresponding antigen.

To couple the antigen, column was activated by washing with 6 ml of ice-cold 1 mM HCl. Immediately after, antigen was injected into the column with a syringe, and allowed to rest for 30 minutes at room temperature. Unreacted NHS groups were later blocked with 10 ml of blocking buffer (0.5 M ethanolamine, 0.5 M NaCl, pH 8.3), and column was left to rest for 30 minutes. Then, the following wash cycle was done, twice: 10 ml of 10 mM Tris-HCl pH 8, 10 ml of 0.1 M glycine pH 2, 10 ml of 10 mM Tris-HCl pH 8, 10 ml of 0.1 M triethylamine pH 11.5. Finally, column was washed with 30 ml of PBS.

To bind the antibody to the column, 15 ml of 2xPBS were mixed to 15 ml of serum, and final concentration of 0.1% NaN₃ to prevent microbial growth. The mix was filtered through a 0.2 µm syringe filter, and left to recirculate in the column overnight at 4°C.

The day after, column was washed with 50 ml of wash buffer (1xPBS, 0.5 M NaCl, 0.1% Triton X-100), and then with 50 ml of PBS. Antibody was eluted with 0.1 M glycine pH 2.6, and collected as 1 ml fractions in tubes containing 100 µl of 2 M Tris-HCl pH 8.5. After elution, column was washed with 10 ml of PBS, and serum solution was allowed to recirculate again. The same process was repeated twice more to recover as much antibody as possible.

2.4 Microscopy methods.

Pictures of cells and colonies on agar plates were taken after 24 hours (YPD medium) or 30 hours (YPGal medium) with a Nikon CoolPix 995 camera attached to a Nikon Eclipse E400 microscope.

Calcofluor-stained cells were observed live. To quantify primary septum deposition, we examined 100 cells with primary septum for each sample, and measure the relative signal intensity of the primary septum using Image J software.

Aniline-stained cells were observed live. To quantify secondary septum deposition, we examined 100 cells with secondary septum for each sample, and measure the relative signal intensity of the secondary septum using Image J software.

To observe GFP-tagged proteins, 900 µl of cells were mixed with 900 µl of 16% formaldehyde (Thermo, 28908) for 10 minutes in a rotating wheel at room temperature, and subsequently washed twice with 1xPBS. Finally, cells were resuspended in 1xPBS, covered in foil, and stored at 4°C for a maximum of 48 hours prior to microscopic observation.

Phase contrast and fluorescence microscopy images of cells grown in liquid culture were obtained with a Nikon A1R Microscope and an Orca R2 camera (Hamamatsu) with objective lens Plan Apo TIRF 100x oil DIC 1.49NA, and LightLine single-band filter set FITC Semrock.

The illumination source was the Nikon Intensilight C-HGFIE (ultrahigh pressure 130W mercury lamp), and we used NIS elements software. We analysed eleven z-sections with a spacing of 0.375 μm to facilitate the examination of the whole cell volume for all experiments. In all cases, the exposure time, sensor gain, and digital adjustments were the same for the control and experimental samples.

Time-lapse video microscopy was performed using DeltaVision system with Olympus IX-71 microscope and CoolSNAP HQ2 Monochrome camera. The objective lens was Plapon 60X0 1.42 NA. The illumination source was the 300W xenon system with liquid light guide, and we used Softworx Resolve 3D acquisition software. We analysed ten z-sections with a spacing of 0.4 μm .

The microscopy data were deconvolved, except for cells stained with calcofluor and aniline, using Huygens (SVI) according to the "Quick Maximum Likelihood Estimation" method and a measured point spread function. The deconvolved data set was viewed with Image J software.

3. RESULTS

3.1 Biochemical studies on chitin synthase 2 - purification and stability of Chs2 protein.

In order to understand more details of how cells lay down the essential primary septum between mother and daughter cells, we aimed to structurally characterise chitin synthase Chs2 enzyme. Understanding how Chs2 functions could improve treatment of diseases with fungal origin, as it would drive the rational drug design (Mandal *et al.* 2009) to inhibit the enzymatic activity of chitin synthase Chs2, which is essential during cell division in fungal pathogens, such as the budding yeasts *Candida albicans*, *Cryptococcus neoformans*, *Cryptococcus gattii* and *Ajellomyces dermatitidis*. The idea of targeting chitin activity as a therapeutic target has been used in the past, although there are no reports that any compound reached the clinic as they share modest antifungal properties (Aaltonen *et al.* 1994, Sudoh *et al.* 2000, Hwang *et al.* 2002, Ke *et al.* 2009).

A predicted structure for Chs2 has been proposed based on its similarity to other glycosyltransferases (Dorfmueller *et al.* 2014) however, the crystal structure of Chs2 has not yet been solved.

Integral membrane proteins account for 20-30% of all open-reading frames (ORFs) (Wallin and Von Heijne 1998) and over 60% of drug targets (Overington *et al.* 2006). However, reported structures of integral membrane proteins constitute less than 3% of

the deposited sequences in PDB (<http://www.rcsb.org/pdb/home/home.do>), highlighting the challenge of obtaining the crystal structure of a membrane protein. Those figures show the challenge that structural biology studies on membrane proteins represent. In order to solve crystal structure, proteins have to be expressed to a sufficient amount, which has been proven to be difficult for membrane protein targets (Tate 2001, Bill *et al.* 2011). After expression, membrane proteins have to be extracted from the hydrophobic membrane environment to solubilise them by use of detergents. This step is critical and a wide screening of detergents is often needed to find the one that is not only able to make the protein soluble but will work without altering its native conformation (Carpenter *et al.* 2008). The suitable detergent can be making the protein stable but in doing so it can impede protein-protein interactions needed for successful crystallisation process. Taken together, all these reasons explain why it is difficult to obtain high-resolution structural data for membrane proteins.

We chose three different truncations of Chs2 to be expressed. These included: full-length Chs2 (1-963aa) (Figure 3.1.A (i)), Chs2 protein lacking its N-terminal CDK-regulated tail (215-963aa) (Figure 3.1.A (ii)) and a fusion of full-length Chs2 protein with the C2 domain of Inn1 (C2-Chs2) (Figure 3.1.A (iii)), which has been shown to regulate Chs2 activity

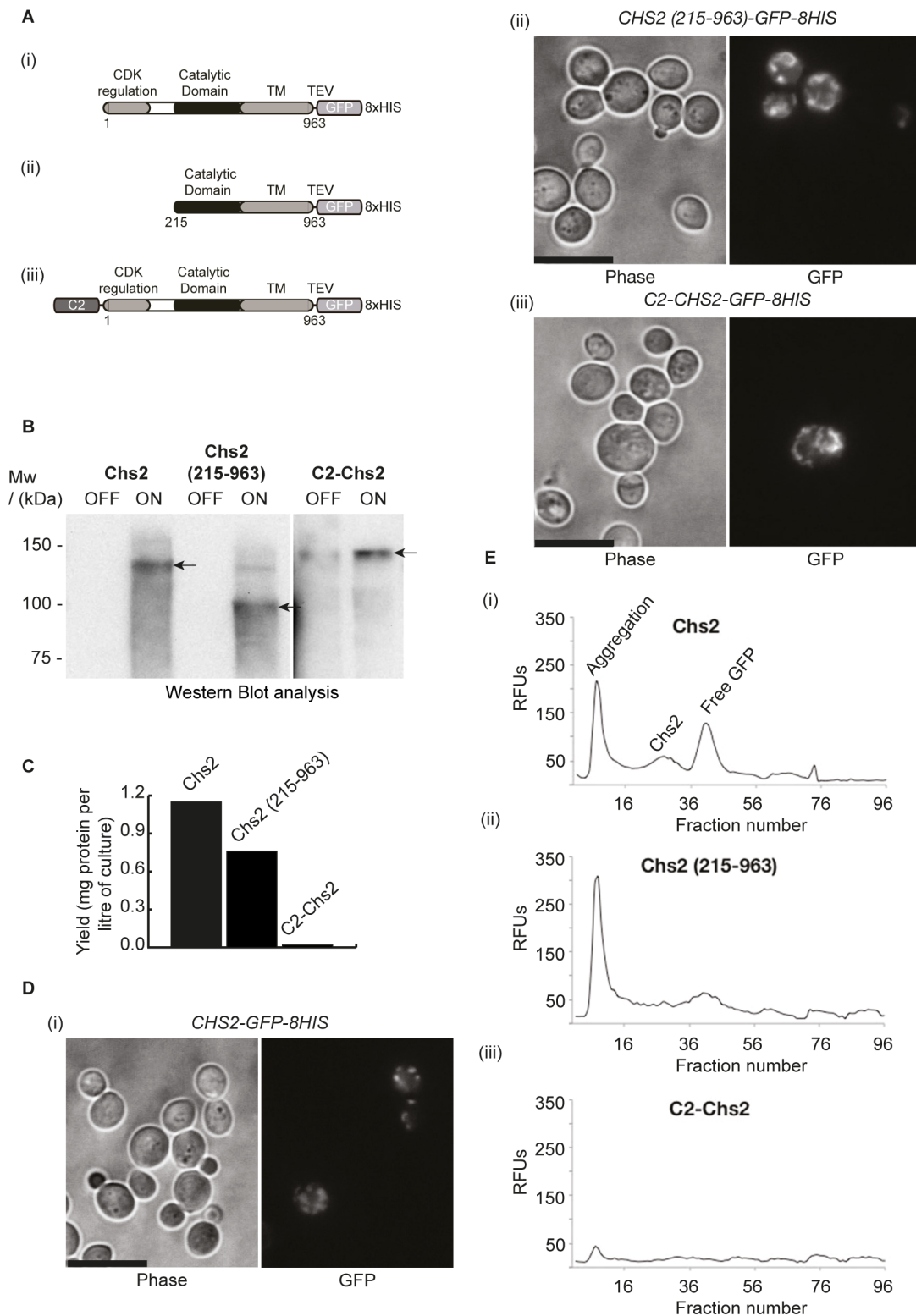


Figure 3.1: Expression and solubilisation of chitin synthase Chs2.

(A) Schematic drawing of the protein constructs used in this study: full-length Chs2 (Chs2-GFP-8His) (i), Chs2 lacking its N-terminal domain (Chs2-215-963-GFP-8His) (ii) and a fusion of Chs2 protein with C2 domain of Inn1 (C2-Chs2-GFP-8His) (iii). (B) Western Blot using anti-GFP antibodies showing the overexpression of the indicated constructs labelled with an arrow (C) Expression levels of the indicated constructs. (D) Fluorescence microscopy photos of full-length Chs2 (i) (YIMP457), Chs2 lacking its N-terminal domain (YIMP459) (ii) and a fusion of Chs2 protein with C2 domain of Inn1 (YIMP460) (iii). Scale bar corresponds to 10 μ m. (E) Fluorescence Size-Exclusion Chromatography (FSEC) profiles representing the purification of full-length Chs2 (i), Chs2 lacking its N-terminal domain (ii) and a fusion of Chs2 protein with Inn1 C2 domain (iii).

(Sanchez-Diaz *et al.* 2008, Nishihama *et al.* 2009, Devrekanli *et al.* 2012). It has been previously reported that the fusion of a highly crystallisable T4 lysozyme to the N-terminus of membrane protein beta 2 adrenergic receptor has facilitated its crystallogenesis (Zou *et al.* 2012). Therefore, we were hoping that adding well-structured C2 domain would make Chs2 more soluble.

Different Chs2 constructs were cloned in a 2 μ pDDGFP2 plasmid (Drew *et al.* 2008), allowing protein expression control from a galactose-inducible promoter; and were transformed into budding yeast FGY217 (*MATa*, *ura3-52*, *lys2 Δ 201*, *pep4 Δ*). This strain comes from PLY127 strain (Kuehn *et al.* 1996, Kota *et al.* 2007, Drew *et al.* 2008) and protein expression was induced upon addition of galactose to the media, as described in Materials and Methods. All constructs contained the protein of interest followed by a TEV cleavage site, a copy of yEGFP to monitor the purification process and an 8xHIS tag to allow protein purification (Figure 3.1).

Overexpression of desired Chs2 constructs was confirmed using immunoblotting with anti-GFP antibodies (Figure 3.1.B) and whole-cell GFP fluorescence counts (Figure 3.1.C). We showed that the full-length and the truncation lacking the N-terminal tail could be expressed, but the C2-Chs2 fusion was not expressed successfully (Figure 3.1.B and Figure 3.1.C).

Next, we assayed intracellular protein localisation using fluorescence microscopy. We could see that full-length Chs2 protein (1-963aa) was able to localise to the site of division, confirming that this construct could be correctly trafficked to the bud neck (Figure 3.1.D (i)). Truncation lacking N-terminal tail (Chs2 215-963aa) (Figure 3.1.D (ii)) and fusion of full-length Chs2 to C2 domain of Inn1 (C2-Chs2) (Figure 3.1.D (iii)) were localising as tubular structures in the cytoplasm, which could represent the ER, where Chs2 is synthesised (Teh *et al.* 2009) or the vacuoles, where Chs2 is degraded (Chuang and Schekman 1996, Chin *et al.* 2016). However, Chs2 degradation by vacuolar Pep4 protease is not possible, as this protein was deleted in our experimental strain (Drew *et al.* 2008).

Chs2 is a membrane protein; so in order to purify it, it has to be extracted from the plasma membrane and the stripped lipids have to be replaced by detergent molecules to stabilise the hydrophobic moieties. This step is critical for membrane protein purification, as solubilisation of membrane proteins usually requires screening different detergents to find the one that will keep the membrane protein stable in aqueous solution (Carpenter *et al.* 2008). To assess the solubility of the generated constructs, we used the Fluorescent Size-Exclusion Chromatography (FSEC) technique. FSEC relies on the separation of the GFP-tagged solubilised proteins by size in a gel filtration column and allows distinguishing

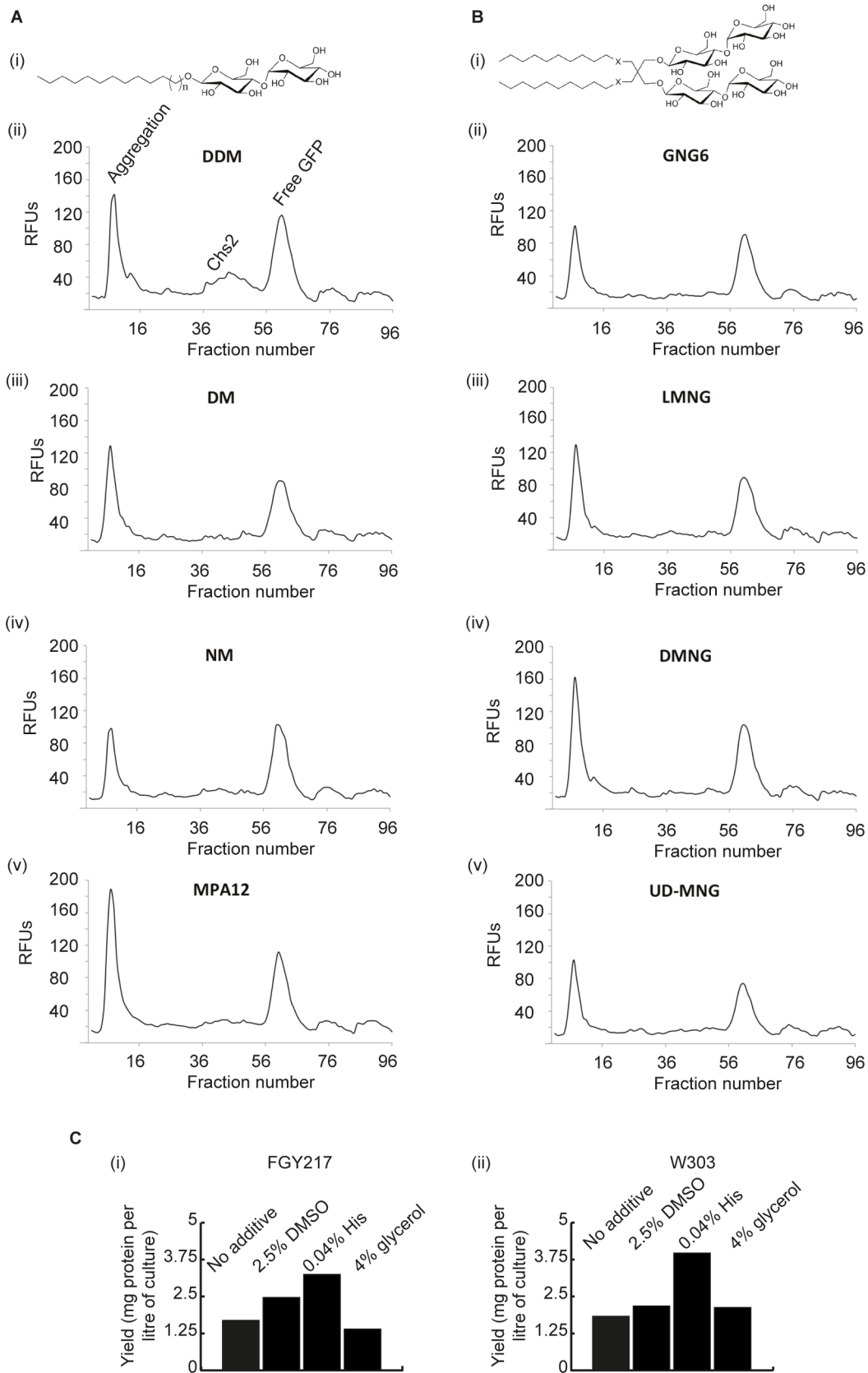


Figure 3.2: Assessment of Chs2 solubility in different detergents.

(A) FSEC profiles of full-length Chs2 protein, expressed from YIMP457 strain at 30°C for 22 hours, in presence of different maltoside detergents. (i) Structure of maltosides. (ii) N-Dodecyl- β -D-Maltopyranoside. (iii) n-Decyl- β -D-Maltopyranoside. (iv) N-Nonyl- β -D-Maltopyranoside. (v) 3-Decyloxypropyl-1- β -D-Maltopyranoside. **(B)** FSEC profiles of Chs2 protein, expressed from YIMP457 strain at 30°C for 22 hours, in presence of different glucose neopentyl glycols. (i) General structure of glucose neopentyl glycols. (ii) Octyl Glucose Neopentyl Glycol. (iii) Lauryl Maltose Neopentyl Glycol. (iv) Decyl Maltose Neopentyl Glycol. (v) Undecyl Maltose Neopentyl Glycol. **(C)** Influence of different metabolic additives on the expression of Chs2 protein in a FGY217-derived strain (YIMP457) (i) or an W303-derived strain (YIMP458) (ii).

between aggregated protein, soluble protein and free GFP, which could be a marker of protein degradation.

After solubilising membranes containing either full-length Chs2 (1-963aa) (Figure 3.1.E (i)), Chs2 lacking its CDK-regulated tail (215-963aa) (Figure 3.1.E (ii)) or a fusion of Chs2 with the C2-domain of Inn1 protein (C2-Chs2) (Figure 3.1.E (iii)) in dodecylmaltoside (DDM), we separated solubilised material by size in a gel-filtration column, collected it in a 96-well plate and read GFP fluorescence in a plate reader. We showed that we could solubilise full length Chs2 protein, but not truncation lacking its N-terminal CDK-regulated tail (215-963aa) or a fusion of full-length Chs2 with the C2-domain of Inn1 protein (C2-Chs2), as we could see three different peaks: an aggregation peak, corresponding to protein aggregation; a peak corresponding to soluble Chs2-GFP-8HIS; and a third peak corresponding to free GFP, that is related to protein degradation (Figure 3.1.E (i)). As for Chs2 (215-963aa) truncation (Figure 3.1.E (ii)) and C2-Chs2 fusion (Figure 3.1.E (iii)), only an aggregation peak was seen, so we decided to carry on with the full-length Chs2 construct.

In order to improve Chs2 solubilisation and stabilisation, the full-length Chs2-containing membranes were subjected to FSEC analysis with an array of different detergents based on alkyl maltopyranosides (Figure 3.2.A (i)) or glucose neopentyl glycols

(Figure 3.2.B (i)). We have tested: dodecylmaltoside (DDM) (Figure 3.2.A (ii)), decylmaltoside (DM) (Figure 3.2.A (iii)), nonylmaltoside (NM) (Figure 3.2.A (iv)) and monopodal amphiphile 12 (MPA-12) detergents (Figure 3.2.A (v)); as well as glucose neopentyl glycol 6 (GNG6) (Figure 3.2.B (ii)), lauryl maltose neopentyl glycol (LMNG) (Figure 3.2.B (iii)), decyl maltose-neopentyl glycol (DMNG) (Figure 3.2.B (iv)) and undecyl maltose-neopentyl glycol (UD-MNG) (Figure 3.2.B (v)) but none of them improved the solubilisation of Chs2 protein compared to DDM.

Finally, different metabolic additives were tested in order to improve full-length Chs2 expression levels (André *et al.* 2006, Newstead *et al.* 2007) (Figure 3.2.C (i)). Briefly, overnight cultures of FGY217 cells expressing full-length Chs2 protein (1-963aa) were diluted in to an OD₆₀₀ of 0.15 (0.33×10⁷ cells/ml), and upon induction of expression at an OD₆₀₀ of 0.6 (1.4×10⁷ cells/ml) by addition of galactose, required additives were added too. After 22 hours of expression induction, protein expression was assessed by whole-cell GFP counts.

The addition of glycerol to culture media to FGY217 cells expressing full-length Chs2 (1-963aa) did not improve the expression, and DMSO had only a discreet effect (Figure 3.2.C (i)). It had been shown that histidine addition to media could improve the expression of the target protein (André *et al.*

2006), probably by protecting the cell from oxidative stress (Murakami *et al.* 1997). Consistently, we found that addition of histidine to the culture expressing full-length Chs2 had increased the expression of Chs2 fusion more than twice (Figure 3.2.C (i)). The same results were obtained using a different budding yeast expression host, with a W303-based genetic background (Figure 3.2.C (ii)).

Six litres culture of *GAL-CHS2-GFP-8HIS pep4Δ* (YIMP458) expressing full-length Chs2 was grown at 30°C in medium lacking uracil supplemented with 0.1% glucose, and protein expression was induced upon addition of galactose to a concentration of 2% at an OD₆₀₀ of 0.6 (1.4×10⁷ cells/ml). Membranes were purified and subsequently solubilised in a PBS-based buffer containing

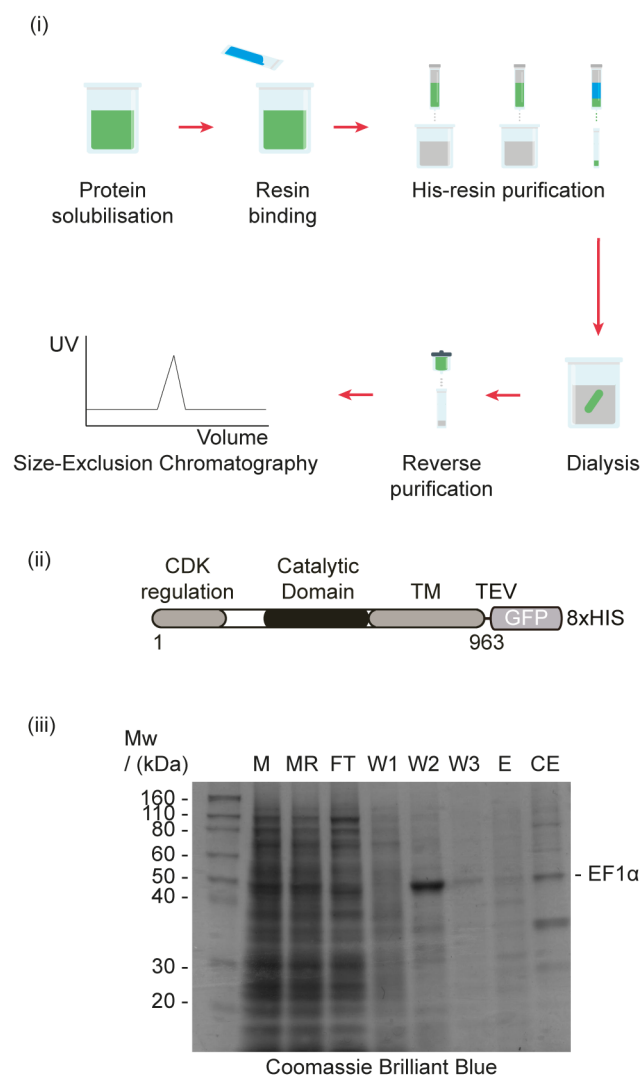
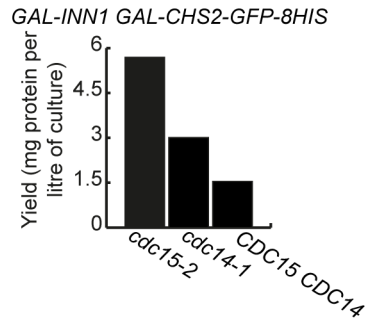


Figure 3.3: Expression and purification of Chs2 protein.

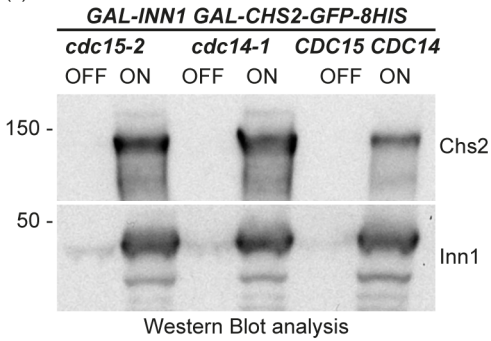
(i) Diagram of the purification process. (ii) Diagram of Chs2 construct used in this study. (iii) Coomassie Brilliant Blue stained gel after the purification of full-length Chs2 from YIMP458 strain upon the addition of 0.04% histidine. Lanes are labelled as M (membranes), MR (resolubilised membranes), FT (flow-through), W1 to W3 (washes with 10 mM, 30 mM and 50 mM of imidazole, respectively), E (elution) and CE (concentrated elution). Arrow indicates protein identified by mass spectrometry as ribosomal elongation factor 1-alpha.

A

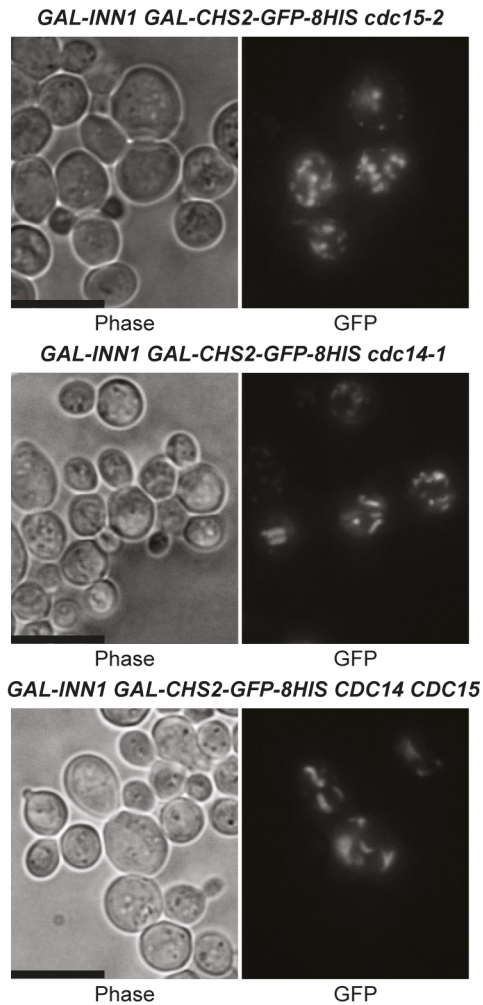
(i)



(ii)

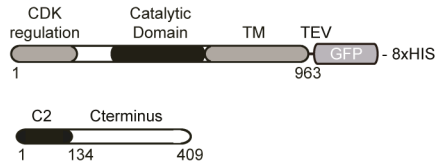


(iii)

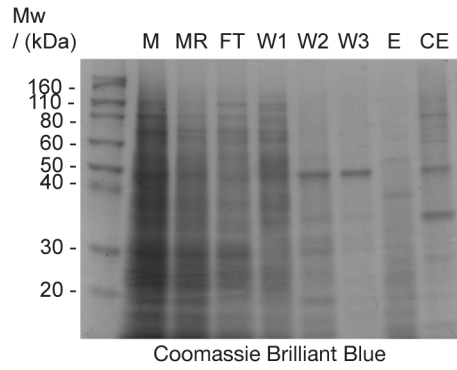


B

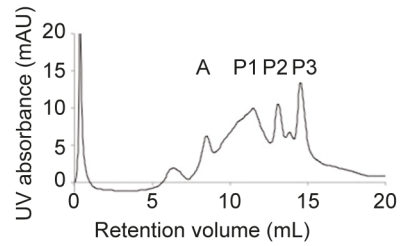
(i)



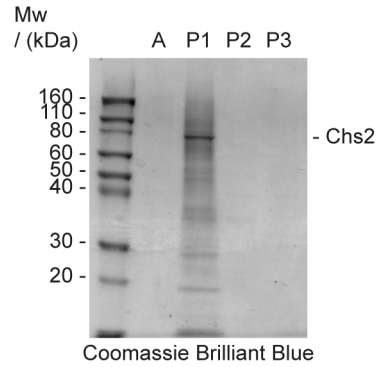
(ii)



(iii)



(iv)



(v)

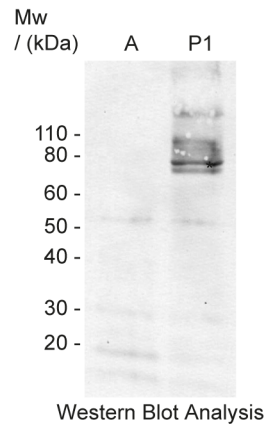


Figure 3.4: Purification of Chs2 after co-expression with Inn1 protein in *cdc15-2* or *cdc14-1* background.

(A) Co-expression of Inn1 protein together with Chs2 enhances overall Chs2 expression. (i) Expression levels of Chs2 in protein extracts derived from different strains: *cdc15-2 GAL-INN1 pep4Δ::ADE2 CHS2-GFP-8HIS* (YIMP462), *cdc14-1 GAL-INN1 pep4Δ::ADE2 CHS2-GFP-8HIS* (YIMP461) and *GAL-INN1 pep4Δ::ADE2 CHS2-GFP-8HIS* (YIMP463). (ii) Immunoblotting showing Chs2 and Inn1 expression levels in (i) using anti-Inn1 and anti-GFP antibodies. (iii) Examples of cells expressing full-length Chs2 constructs from *cdc15-2 GAL-INN1 pep4Δ::ADE2 CHS2-GFP-8HIS* (YIMP462), *cdc14-1 GAL-INN1 pep4Δ::ADE2 CHS2-GFP-8HIS* (YIMP461) and *GAL-INN1 pep4Δ::ADE2 CHS2-GFP-8HIS* (YIMP463). Scale bar corresponds to 10μm. **(B)** Purification of Chs2 full-length in a strain co-expressing Inn1 protein. (i) Diagram of overexpressed constructs used in this study. (ii) *cdc15-2 GAL-INN1 pep4Δ::ADE2 CHS2-GFP-8HIS* (YIMP462) was used and Chs2-containing membranes from six litres of culture were purified and run on a gel. Coomassie Brilliant Blue stained gel shows the different stages of the purification process: M (membranes), MR (resolubilised membranes), FT (flow-through), W1 to W3 (washes with 10 mM, 30 mM and 50 mM of imidazole, respectively), E (elution) and CE (concentrated elution). (iii) UV-trace of the SEC profile. Peaks are labelled as A (aggregation), and peaks one to three are labelled as P1, P2 and P3. Corresponding peaks from the SEC profile were run on a gel and stained with Coomassie Brilliant Blue (iv) or Western Blot analysis was performed with anti-Chs2 antibodies (v).

1% DDM (details in sections 2.3.2 and 2.3.4 in Materials and Methods). Solubilised Chs2 was bound to a nickel resin for two hours. After washing the resin to get rid of unspecifically bound protein with increasingly high concentrations of imidazole, fusion protein was eluted in 350 mM imidazole. Subsequently, eluate was digested with TEV protease to separate Chs2 from C-terminal GFP and 8HIS tags and dialysed to remove imidazole, as high concentrations of imidazole can destabilise proteins (Postis *et al.* 2009) and imidazole removal is necessary for the following reverse-purification. Tags were later eliminated by reverse purification on a nickel column and eluate was purified through Size-Exclusion Chromatography (SEC) (Figure 3.3.A (i)). SEC chromatography is used to separate proteins by size, to distinguish between the possible isoforms (monomers, dimers, aggregates, etc.) and to ensure all possible contaminants are separated from the protein of interest.

SEC purification did not yield any full-length Chs2 protein (Figure 3.3.A (ii)). A putative band eluted in the first nickel column

elution (Figure 3.3.A (ii)) was sent for mass spectrometry identification (details in section 2.3.4 in Materials and Methods), and was identified as a ribosomal elongation factor (EF1α).

Since Inn1 binds to and regulates Chs2 (Nishihama *et al.* 2009, Devrekanli *et al.* 2012, Foltman *et al.* 2016a), we postulated that the presence of Inn1 protein could be important to prevent degradation of Chs2. As shown earlier, expression of a fusion of the C2 domain of Inn1 with Chs2 (C2-Chs2) was not successful, so we decided to follow another approach. Full-length Chs2 protein was overexpressed from pDDGFP2-based plasmid, together with Inn1 protein expressed from a galactose-inducible promoter from a pRS305-based plasmid (pAD88).

Protein expression was carried out in budding yeast, but we used W303 genetic background. To try to purify proteins from cells that were going through cytokinesis synchronously, we used temperature-sensitive mutants that stop cell cycle at G2/M phase, with cells that are unable to downregulate

kinase activity associated to mitotic cyclins/Cdk1. One of those mutants was *cdc14-1*, that inactivates the special phosphatase Cdc14 at the restrictive temperature, as mentioned in the Introduction. In addition, we used *cdc15-2* mutant that blocks the activity of one of the key kinases that plays an essential role in the Mitosis Exit Network signalling cascade (Fitch *et al.* 1992, Taylor *et al.* 1997). The original idea was to inactivate one of them, Cdc14 or Cdc15, arrest cells at G2/M phase of the cell cycle to allow expression of protein of interest and release cells to collect the cell pellet when cells were going through cytokinesis to enrich the population of cells containing Chs2 at the site of division. Unfortunately, we have observed that cells did not express Chs2 after four hours induction in galactose at the restrictive temperature (37°C). Therefore, we decided not to use the original set up, but we used the same strains for protein production at the permissive temperature. We could see that protein expression after 22 hours at the permissive temperature was greater than the control strain lacking these mutations (Figure 3.4.A (i) and (ii)).

To test protein expression, 10 ml cultures of strains YIMP462 (*MATa pep4Δ cdc15-2 GAL-INN1 pDDGFP-CHS2-TEV-GFP-8HIS*), YIMP461 (*MATa pep4Δ cdc14-1 GAL-INN1 pDDGFP-CHS2-TEV-GFP-8HIS*) and YIMP463 (*MATa pep4Δ GAL-INN1 pDDGFP-CHS2-TEV-GFP-8HIS*) were grown overnight

at 24°C in medium lacking uracil supplemented with 2% glucose, diluted to an OD₆₀₀ of 0.15 the day after in medium lacking uracil supplemented with 0.1% glucose and allowed to grow at 24°C. Expression of the target protein was induced for 22 hours by addition of galactose to a final concentration of 2% (details in Section 2.2.8 in Materials and Methods). Using whole-cell GFP fluorescence counts and Western Blot analysis, we found that Chs2 expression was increased in *cdc15-2* strain for reasons that are unknown at this moment (Figure 3.4.A (i) and (ii)). Also, we could observe that full-length Chs2 localised to reticular structures (Figure 3.4.A (iii)), but not to the site of division. These structures could represent organelles such as the ER, where Chs2 is synthesised; or the vacuole, where it is degraded. Degradation of Chs2 should be minimised as protease Pep4, which is responsible for its degradation, is deleted in these cells (Chuang and Schekman 1996, Zhang *et al.* 2006, Teh *et al.* 2009).

We carried out large-scale protein expression using the strain with the highest expression level for Chs2: YIMP462 (*pep4Δ cdc15-2 GAL-INN1 pDDGFP-CHS2-TEV-GFP-8HIS*). This strain produces a full-length Chs2 protein followed by a TEV cleavage site to allow tag removal, then a GFP cassette and an 8xHIS tag to allow purification. Protein induction was performed from a six litres culture. After preparation and solubilisation of the membranes with DDM, elution of full-length

Chs2 from the column showed a clear band (Figure 3.4.B (i) and (ii)). Further purification showed that this band could be eluted as a broad peak in Size-Exclusion Chromatography (SEC) purification. After Coomassie stain we determined the presence of a protein band in the fraction corresponding at peak 1 that runs at the expected size for Chs2 (Figure 3.4.B (iii)). We finally confirmed, using specific antibodies against Chs2, that such a band corresponds to Chs2 protein, as shown by Coomassie stain (3.4.B (iii)) and Western Blot (Figure 3.4.B (iv)); Chs2 band is labelled with an arrow). Unfortunately, the low yield obtained was not sufficient to undertake

structural studies.

To summarise we have been able to clone, express and purify soluble Chs2 protein using *S. cerevisiae* as a host organism by growing the cells at 24°C and inducing expression for 22 hours. We have determined that overexpression of Inn1 helped in the process.

3.2 Identification of Cyk3 protein as a component of the Ingression Progression Complex.

Dr. Magdalena Foltman in the laboratory of Dr. Alberto Sanchez-Diaz performed a systematic analysis of all

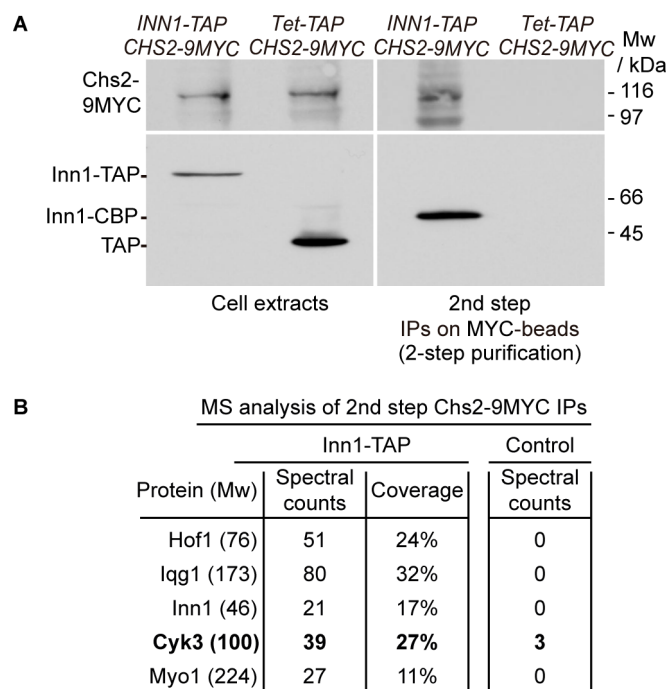


Figure 3.5: Ingression Progression Complexes (IPCs) are formed at the end of cytokinesis to coordinate actomyosin ring contraction, primary septum formation and membrane ingression (reproduced with permission of Dr. Magdalena Foltman).

(A) *INN1-TAP CHS2-9MYC* (YMF38) and control (YMF79) were grown at 24°C in YPD medium and synchronised in G1 phase with mating pheromone and then released for 105 minutes. Cell extracts were prepared before the immunoprecipitation of Inn1-TAP (or TAP in control) on IgG-beads. The isolated material was released from the beads by cleavage with TEV protease. After cleavage, part of the TAP tag (CBP, calmodulin-binding protein) remained fused to Inn1. Purified material was subjected to immunoprecipitation of Chs2-9MYC before analysis by SDS-PAGE and immunoblotting. (B) The protein composition of purified fractions including spectral counts and coverage as analysed by mass spectrometry.

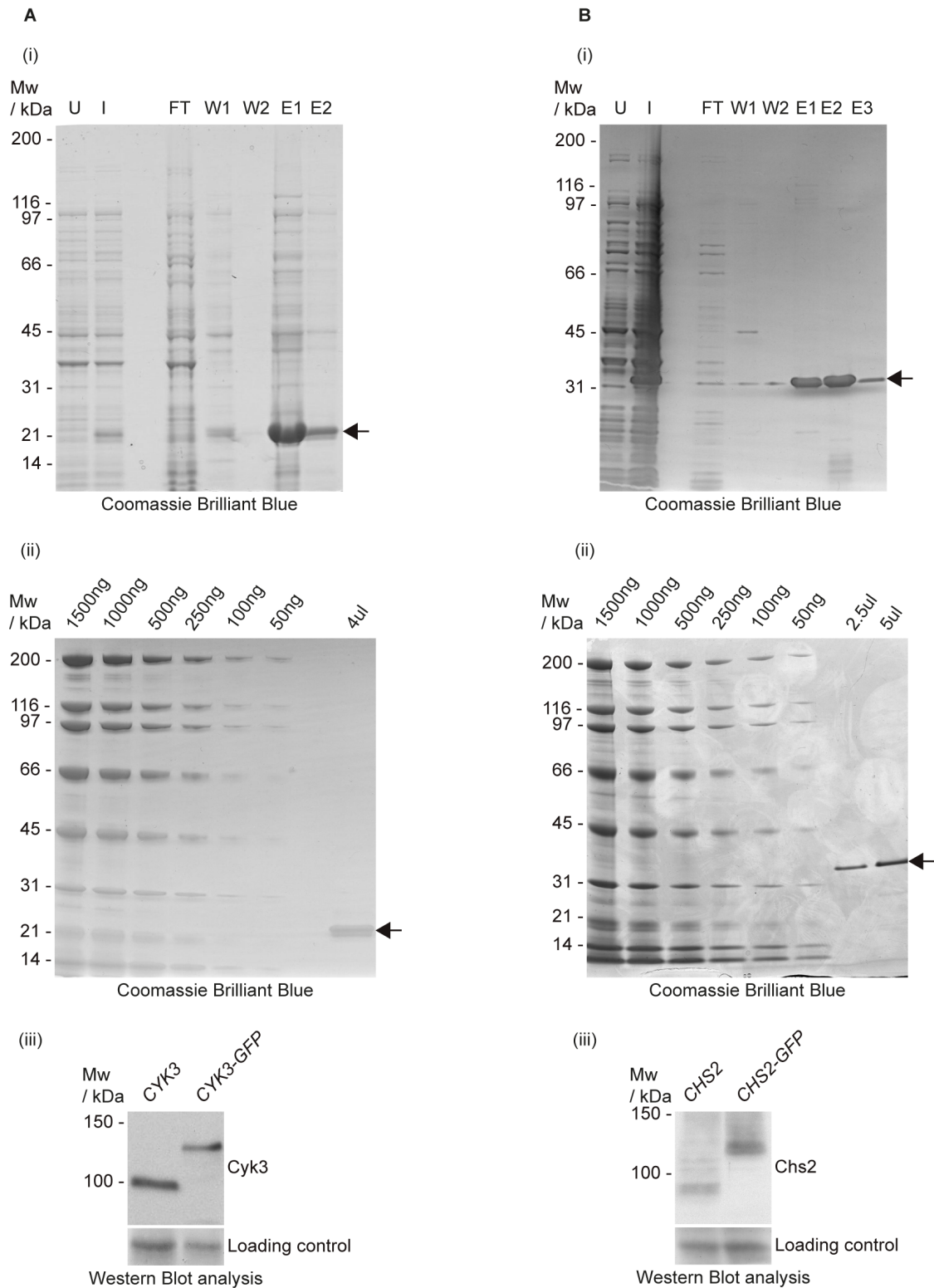


Figure 3.6: Raising anti-Cyk3, anti-Chs2 and anti-Hof1 antibodies.

(A) (i) A 25-kDa fragment of 6His-tagged Cyk3 was expressed and purified from *E. coli* and injected into sheep. Lanes in the gel are labelled as follows: U, uninduced; I, induced; FT, flow-through; W1-W2, washes; E1-E2, elutions. (ii) Serum was purified in a NHS-activated column with covalently bound antigen previously purified. (iii) Purified serum was tested by immunoblotting in wild type strain (W303-1a) and a *CYK3-GFP* strain (YASD2061). **(B)** (i) A 25-kDa fragment of 6His-tagged Chs2 was expressed and purified from *E. coli* and injected into rabbit. Lanes in the gel are labelled as follows: U, uninduced; I, induced; FT, flow-through; W1-W2, washes; E1-E3, elutions. (ii) Serum was purified in a NHS-activated column with covalently bound antigen previously purified. (iii) Purified serum was tested by immunoblotting in wild type strain (W303-1a) and a *CHS2-GFP* strain (YASD819).

In order to better understand the regulation of chitin synthase Chs2, we decided to raise antibodies against chitin synthase 2, as well as two other proteins that have been shown to influence Chs2 activity: Cyk3 and Hof1 (Oh *et al.* 2012, Meitinger *et al.* 2013, Oh *et al.* 2013). In order to do that, we cloned 25 kDa fragments of non-conserved regions of each protein in pET28c vectors (Novagen), which allowed us to conditionally overexpress the desired fragments upon the addition of IPTG to the culture media. These cloned fragments were tagged with 6HIS epitope to allow purification using nickel columns.

Material obtained upon denaturing purification of the following protein fragments: 6HIS-Chs2 (1-222aa), 6HIS-Cyk3 (101-322aa) and 6HIS-Hof1 (280-502aa) on the nickel columns, was sent to be injected into animal hosts: rabbit (Chs2) or sheep (Cyk3 and Hof1) (Figure 3.6.A (i), 3.6.B (i) and 3.6.C (i)). Antibodies were purified on a HiTrap NHS activated HP column, to which purified antigen was previously covalently bound (Figure 3.6.A (ii), 3.6.B (ii) and 3.6.C (ii)).

Purified antibodies were tested using Western Blot against protein extracts prepared from budding yeast cells expressing either a wild type or a tagged version of the protein of interest (Figure 3.6.A (iii), 3.6.B (iii) and 3.6.C (iii)). All three antibodies recognised their target proteins, and proved to be useful for further studies.

3.3 Chitin synthase Chs2 is able to directly interact with cytokinetic protein Cyk3.

It had been shown that overexpression of Cyk3 induces primary septum deposition between mother and daughter cells during cytokinesis (Meitinger *et al.* 2010, Devrekanli *et al.* 2012, Oh *et al.* 2012), there has been no evidence of the direct interaction of Chs2 with the cytokinetic protein Cyk3. In addition, defects associated to the lack of Cyk3 can be rescued by a hypermorphic allele of *CHS2*, *CHS2-V377I* (Devrekanli *et al.* 2012). Despite these evidences, there were no molecular details about how Cyk3 could regulate Chs2 activity.

In order to show whether Cyk3 could interact with Chs2, we decided to C-terminally tag *CYK3* at its wild type locus with a C-terminal TAP tag to efficiently immunoprecipitate Cyk3 protein (Cyk3-TAP). We transformed a diploid strain that contained Chs2-9MYC (YMF76) to generate *CYK3-TAP CHS2-9MYC*. Tetrad dissection from this diploid strain showed that these two alleles were synthetically lethal, which impeded further use of this strain (Figure 3.7.A (ii) and (iii)). In order to circumvent this problem, we decided to tag *CYK3* at its N-terminus as TAP-*CYK3* in diploid strain YIMP22, which also harboured *CHS2-9MYC* allele. When tetrads were dissected from the diploid YIMP22 (*CYK3/TAP-CYK3 CHS2/CHS2-9MYC*), we found that both alleles could be present at the

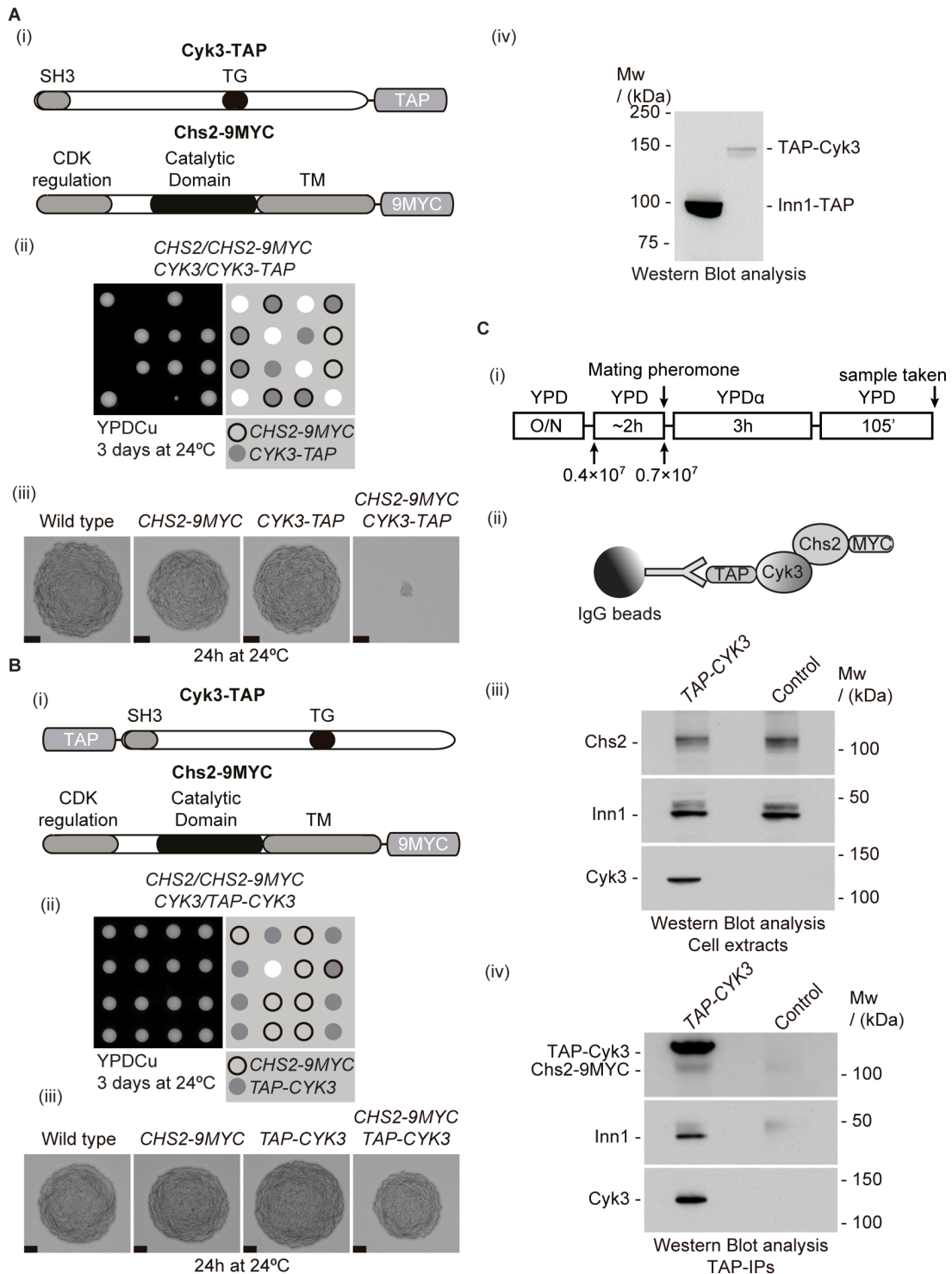


Figure 3.7: Cyk3 is able to interact with Chs2 in yeast extracts from cells undergoing cytokinesis.

(A) C-terminal tagging of *CYK3-TAP* and *CHS2-9MYC* is synthetically lethal. (i) Schematic diagram of the expressed constructs *Cyk3-TAP* and *Chs2-9MYC*. (ii) Tetrad dissection of diploid *CYK3/CYK3-TAP CHS2/CHS2-9MYC* (YMF76). (iii) Pictures of tetrads of the indicated genotypes after 24 hours of incubation on YPD plates at 24°C. Scale bar corresponds to 20µm. **(B)** (i) Schematic diagram of the expressed constructs *TAP-Cyk3* and *Chs2-9MYC*. (ii) Tetrad dissection of diploid *CYK3/TAP-CYK3 CHS2/CHS2-9MYC* (YIMP22). (iii) Pictures of tetrads of the indicated genotypes after 24 hours of incubation on YPD plates at 24°C. Scale bar corresponds to 20µm. (iv) Protein extracts from *CHS2-9MYC pep4Δ::ADE2 TAP-CYK3* (YIMP37) and *INN1-TAP pep4Δ ADE2+* (YASD2081) were run on a gel and Western Blot analysis with anti-TAP antibodies was performed. **(C)** *Cyk3* and *Chs2* co-immunoprecipitate. (i) *TAP-CYK3 CHS2-9MYC pep4Δ::ADE2* (YIMP37) and control (YIMP39) were grown in YPD, diluted and regrown to exponential phase and arrested in G1 phase by addition of mating pheromone. Cells were released from block, and allowed to progress until 105 minutes, when *Chs2* localisation peaks. (ii) Immunoprecipitation of *TAP-Cyk3* was performed in IgG-coated beads. Whole cell extracts (iii) and immunoprecipitation eluates (iv) were analysed by immunoblotting with anti-Inn1, anti-TAP and anti-MYC antibodies.

same time in the haploid progeny (Figure 3.7.B (i), Figure 3.7.B (ii), and 3.7.B (iii)). Furthermore, the expression of TAP-Cyk3 fusion was confirmed using Western Blot (Figure 3.7.B (iv)).

To check whether Cyk3 and Chs2 interact during cytokinesis, we decided to grow *TAP-CYK3 CHS2-9MYC* (YIMP37) and control cells (YIMP39). We synchronised them in G1 phase of the cell cycle by addition of mating pheromone, and then release them from the block synchronously for 105 minutes (Figure 3.7C (i) and 3.7C (ii)). Under these conditions, it has been shown that most cells are undergoing actomyosin ring contraction, plasma membrane ingression and extracellular matrix remodelling (Foltman *et al.* 2016a).

After performing the immunoprecipitation using IgG beads on cell extracts generated from control and *TAP-CYK3* cells (Figure 3.7.C (iii)) we determined that TAP-Cyk3 is able to interact with Chs2. An extra band was shown in the Chs2 Western Blot that corresponded to TAP-Cyk3, since TAP has the ability to recognise rabbit antibodies (Chs2 antibodies were raised in rabbit) (Figure 3.7.C (iv)). In addition we confirmed that Cyk3 binds to Inn1 as previously reported (Nkosi *et al.* 2013) (Figure 3.7.B (iii) and 3.7.B (iv)).

We could not rule out the possibility that this interaction could be mediated by another yeast protein bridging them together. In order to assess whether this interaction is

direct, we used a Rosetta *E. coli* strain expression system, in which the only eukaryotic proteins would be His-tagged full-length Cyk3 (6HIS-Cyk3) and a Strep-tagged fragment of Chs2 containing its catalytic domain (Strep-Chs2-215-629aa). This *E. coli* Rosetta strain allows co-expression of a chloramphenicol-resistant plasmid encoding tRNAs that are rare in prokaryotic cells, improving the expression (Scheich *et al.* 2007).

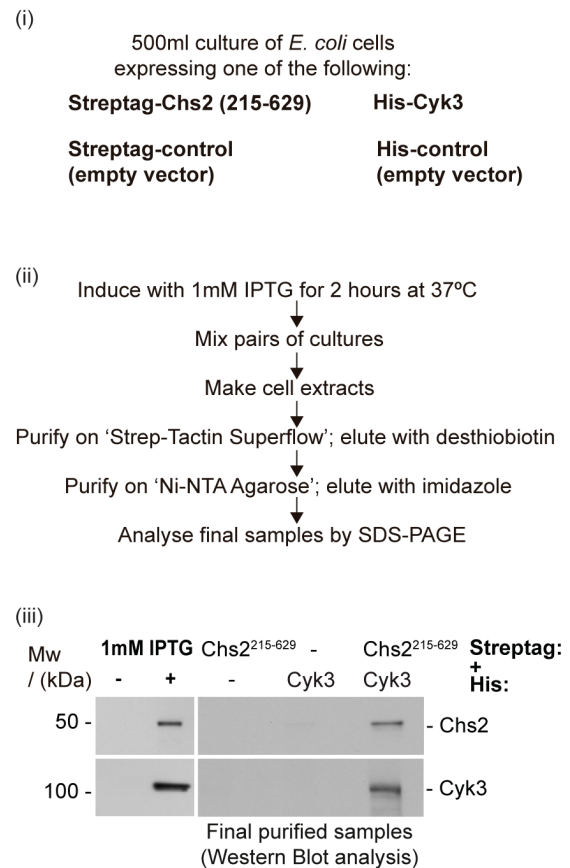


Figure 3.8: Chs2 and Cyk3 are able to directly interact when purified from an *E. coli* expression system.

(i) Indicated *E. coli* strains containing plasmids pMF36 (Strep-Chs2(215-629aa)); pET100 (Strep-empty); pMF22 (6His-Cyk3) and pET28c (6His-empty) were grown as indicated in (ii). (ii) Cultures were grown at 37°C, and protein induction was performed at an OD₆₀₀ of 0.6 upon addition of IPTG for two hours. Corresponding cultures were mixed and strep-tagged protein was purified, and eluates were further purified through their 6His-tag. Final eluates were analysed by immunoblotting with anti-His and anti-Strep antibodies (iii).

CYK3 was cloned in a pET28-based plasmid, and Strep-Chs2 (215-629aa) was cloned in a pET100-based plasmid. These plasmids allow protein expression upon addition of IPTG to the culture media. Alongside these constructs, *E. coli* Rosetta strains were transformed with empty plasmids as controls (Figure 3.8 (i)).

After growing 500 ml cultures for each construct and corresponding controls, protein expression was induced at an OD₆₀₀ of 0.6 by addition of IPTG to a final concentration of 1 mM for two hours at 37°C. Cell pellets were prepared by mixing the cultures and frozen at -20°C. Upon preparation of protein extracts, we did a two-step purification, first using Strep-tag and eluting with desthiobiotin, and then using HIS-tag and elute with imidazole (Figure 3.8 (ii)). We then used the final eluate and showed by immunoblotting that both proteins were present, proving that Cyk3 and Chs2 proteins are effectively able to interact directly (Figure 3.8 (iii)).

3.4 Generating conditional mutants to inactivate Cyk3. Lack of Cyk3 protein produces a cell division defect.

To determine the defects associated to the lack of Cyk3 and to understand Cyk3 function during cell division, we generated CYK3 conditional mutants. First we transformed cells to include a C-terminal auxin-inducible degron in CYK3 locus

(Nishimura *et al.* 2009, Kanemaki 2013, Nishimura and Kanemaki 2014) (Figure 3.9.A (i) and 3.9.A (ii)), which allows protein depletion upon addition of auxin to the culture media and expression of the rice E3 ubiquitin ligase OsTir1 (Figure 3.9.A (iii)). Two auxins are used together in our experiments: IAA (indole acetic acid) and NAA (naphthalene acetic acid).

To assess the defects caused by lack of Cyk3, *cyk3-aid* (YIMP81) and control (YNK40) cells were spotted onto YPD plates, or YP plates containing galactose to induce E3 ubiquitin ligase *UBR1* expression and 500 µM auxins (NAA and IAA) to induce *Cyk3-aid* degradation. As we could see *cyk3-aid* cells growing in restrictive conditions did not show a strong growth defect (Figure 3.9B (i)).

We repeated the experiment in liquid media, in which cells *cyk3-aid* (YIMP81) and control (YNK40) were grown in YPRaff media, diluted to 0.4×10⁷ cells/ml, and shifted to YPGal media supplemented with 500 µM NAA and IAA auxins at 0.7×10⁷ cells/ml. After this point, samples were taken every 90 minutes until 9 hours (details in section 2.2.6 in Materials and Methods). Microscopy and flow cytometry analysis showed that only a small proportion of cells showed a cell division defect (Figure 3.9.B (ii)). We assessed the efficiency of protein depletion by taking samples for immunoblotting at different stages. After running the samples in a protein gel and blotting it onto a nitrocellulose membrane,

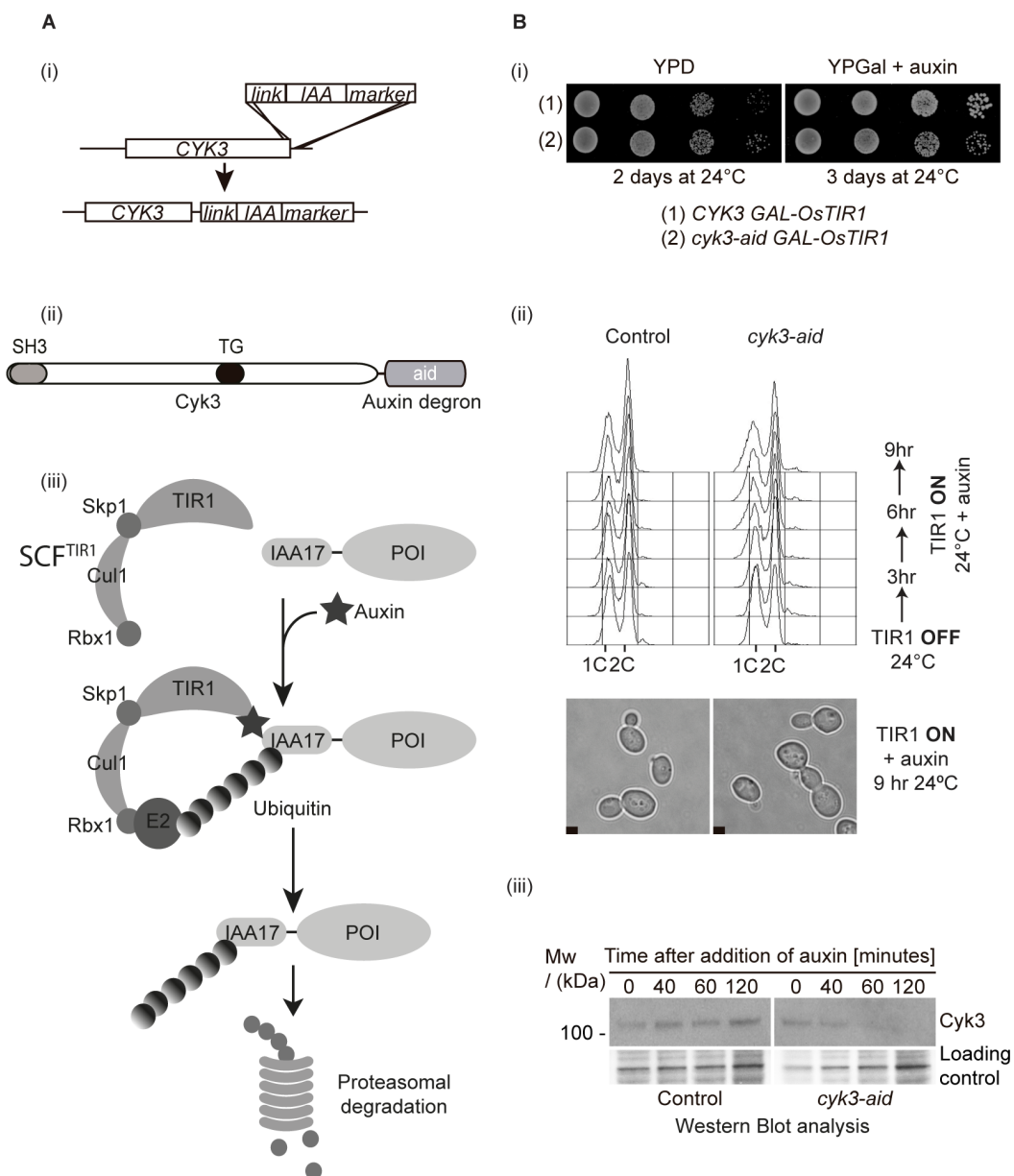


Figure 3.9: Degradation of Cyk3 using auxin degron does not yield a tight phenotype.

(A) (i) An auxin degron was integrated in the C-terminus of CYK3 in the wild type locus. (ii) Diagram of the expressed Cyk3-aid protein. (iii) Model of auxin-dependent degradation. Upon auxin binding to TIR1 in the SCF complex, auxin degron-tagged protein is recruited to the SCF^{TIR1} complex, leading to its polyubiquitylation and proteolysis by the proteasome. **(B)** (i) *cyk3-aid* GAL-OsTIR1 (YIMP81) and control (YNK40) cells were spotted onto YPD and YPGal plates containing NAA and IAA auxins and incubated at 24°C. (ii) *cyk3-aid* GAL-OsTIR1 (YIMP81) and control (YNK40) cells were grown in YPRaff medium at 24°C overnight, diluted the next morning and media changed to YPGal containing NAA and IAA auxins when cells were at exponential phase. Samples for FACS analysis and immunoblotting with anti-Cyk3 antibody (iii) were taken at the corresponding time points, and photos of cells were taken at the end of the experiment. Scale bar corresponds to 2µm.

protein detection was done using purified anti-Cyk3 antibody. We could see that depletion of Cyk3 protein happened within two hours after

galactose and auxin addition in *cyk3-aid* (YIMP81) (Figure 3.9.B (iii)).

In order to improve the degradation of Cyk3 protein, we decided to further modify Cyk3 and add a temperature-sensitive degron at the N-terminus, on top of the previously included auxin degron. Therefore we created a double-tagged allele with an N-terminal temperature-sensitive degron and a C-terminal auxin-inducible degron (Figure 3.10.A (i) and (ii)) (Dohmen *et al.* 1994, Labib *et al.* 2000, Sanchez-Diaz *et al.* 2004). The expression of this double degron fusion protein was controlled by the *CUP1*, copper inducible promoter. The temperature-inducible degron tag contains an ubiquitin that is rapidly cleaved when the fused protein is expressed, allowing an arginine to be the first residue of the protein. This feature is the key for the temperature degron, as the arginine is recognised by the E3 ubiquitin ligase Ubr1. After ubiquitin, tag follows with a thermosensitive version of mouse dihydrofolate reductase (DHFR^{ts}). Protein is able to carry out its function at 24°C, however at the restrictive temperature (37°C), DHFR^{ts} exposes lysine residues within the degron that can be now ubiquitylated by the E3 ubiquitin ligase Ubr1, which is able to recognise the arginine as the first residue of the fused protein and polyubiquitylated protein is degraded by the proteasome (Figure 3.10.A (iii)) (Dohmen *et al.* 1994, Labib *et al.* 2000, Sanchez-Diaz *et al.* 2004). It has been shown that double td-aid degron-tagged proteins are depleted also at 24°C upon inducing the

expression of E3 ubiquitin ligases Tir1 and Ubr1 and addition of 500 µM auxins (both NAA and IAA) to the culture media (Devrekanli *et al.* 2012).

In order to assess the efficiency of this novel allele, strains *td-cyk3-aid* (YMF335) and control (YIMP231) were spotted onto permissive YPDCu plates, or restrictive YP plates containing galactose to allow expression of E3 ubiquitin ligases Ubr1 and Tir1, as well as 500 µM NAA and IAA auxins to allow depletion of Td-cyk3-aid protein (Figure 3.10.B (i)). Under restrictive conditions, the double degron *td-cyk3-aid* (YMF335) showed a much tighter phenotype than previously described single *cyk3-aid* degron (YIMP81), presenting a strong growth defect (Figure 3.10.B (i)).

Also, double td-aid degron strains *td-cyk3-aid* (YMF335) and control (YIMP231) cells were grown in YPRaff media, diluted to 0.4×10^7 cells/ml, and shifted at 0.7×10^7 cells/ml to YPGal media supplemented with 500 µM NAA and IAA auxins, where samples were taken every 90 minutes during 9 hours. Upon analysis of the phenotype, we have shown that this mutant was tighter than the single *cyk3-aid* degron. We determined by flow cytometry an accumulation of cells with 4C DNA content at the end of the experiment. In addition we observed cell chains, which clearly showed a cytokinetic defect (Figure 3.10.B (ii)). These results suggested that these cells suffer a cytokinesis defect, as they replicate

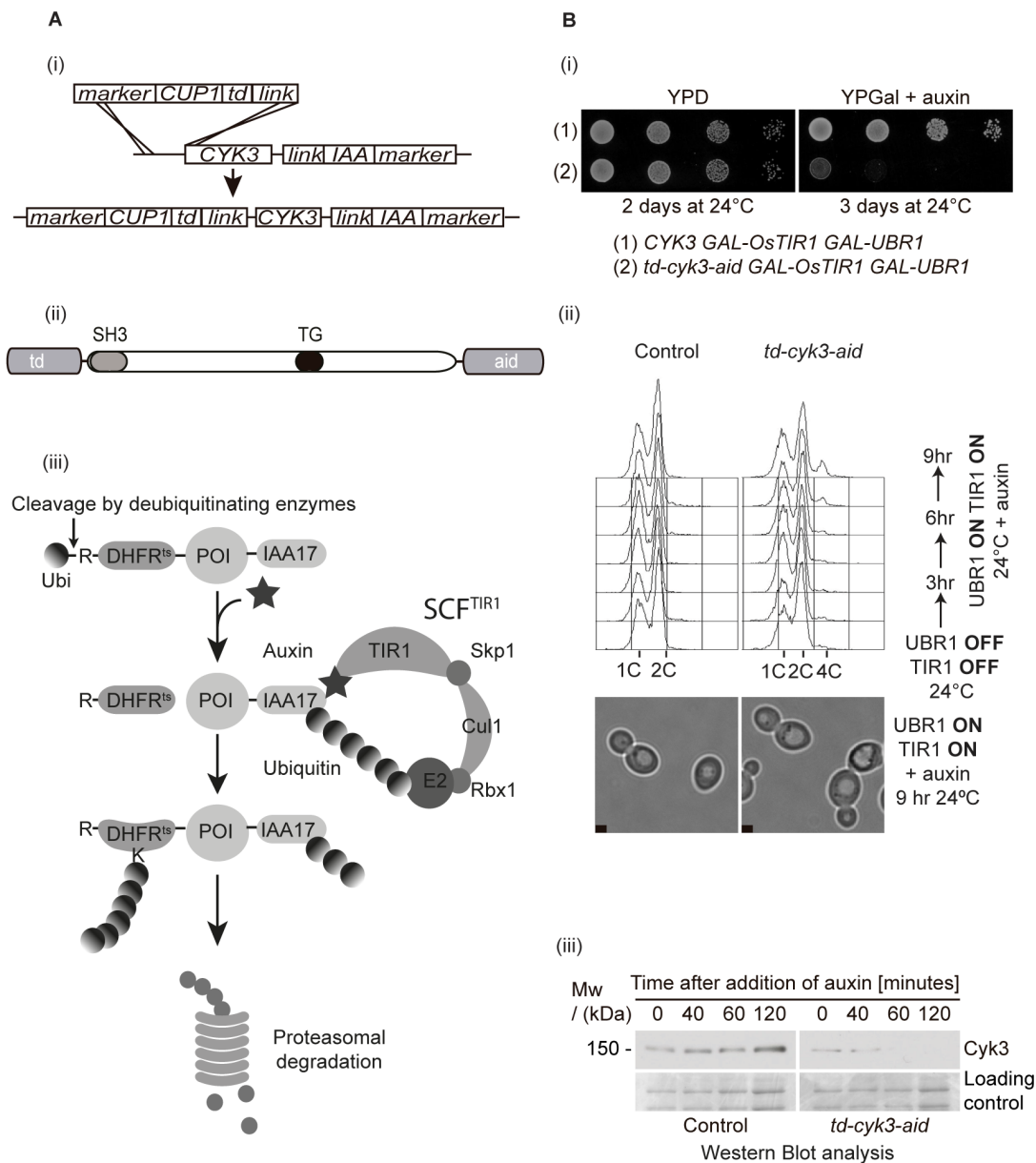


Figure 3.10: Double temperature and auxin degron (td-aid) provides an excellent tool for studying the role of Cyk3 protein.

(A) (i) A temperature-inducible degron (td-) was introduced in the N-terminus of a *cyk3-aid* strain. (ii) Diagram of the expressed Td-*cyk3-aid* protein. (iii) Degradation pathway of Td-*cyk3-aid* Auxin degron will degrade the fusion protein from the C-terminus as explained in Figure 3.9. The heat-inducible degron begins with a ubiquitin molecule that reveals an arginine upon cleavage. This arginine is bound by Ubr1, protein associated with E3 ubiquitin ligase Ubc2, which upon a degron conformational change usually occurring at 37°C, can induce polyubiquitylation of the degron and therefore proteasomal degradation of the fusion protein. In practice, degradation of double degron-tagged proteins could also happen at 24°C, depending on the strain (Devrekanli *et al.* 2012). **(B)** (i) *td-cyk3-aid GAL-UBR1 GAL-OsTIR1* (YMF335) and control (YIMP231) cells were spotted onto YPD and YPGal plates containing NAA and IAA auxins and incubated at 24°C for the corresponding number of days. (ii) *td-cyk3-aid GAL-UBR1 GAL-OsTIR1* (YMF335) and control (YIMP231) cells were grown in YPRaff medium at 24°C overnight, diluted the next morning and media changed to YPGal containing NAA and IAA auxins when cells were at exponential phase. Samples for FACS analysis and immunoblotting with anti-Cyk3 antibody (iii) were taken at the corresponding time points and photos of cells were taken at the end of the experiment. Scale bar corresponds to 2µm.

their DNA without separating mother and daughter cells. In this experiment, we assessed the efficiency of protein depletion by taking samples for immunoblotting during the course of the experiment. Protein depletion occurred within an hour of galactose and auxin addition (Figure 3.10.B (iii)).

3.5 Studying the defects associated with Cyk3-depleted cells.

To evaluate the defect of cells lacking Cyk3, we decided to use *td-cyk3-aid* strain (YMF335). To understand cytokinetic dynamics in Cyk3-depleted cells, we monitored Inn1 localisation, as a component of the actomyosin ring, at the site of division (Sánchez-Díaz et al., 2008).

td-cyk3-aid INN1-GFP (YIMP197) and control (YIMP207) cells were grown in YP supplemented with raffinose at 24°C, and synchronised in G1 phase with mating pheromone. After expression of ubiquitin ligases Ubr1 and Tir1 and addition of NAA and IAA auxins to inactivate Cyk3 protein, cells were released from G1 block at 24°C and allowed to progress while taking samples to monitor the immediate consequences of the lack of Cyk3 (Figure 3.11 (i), Figure 3.11 (ii) and Figure 3.11 (iii)).

We found that there was a temporary accumulation of binucleate cells in strains conditionally depleted for Cyk3 (Figure 3.11

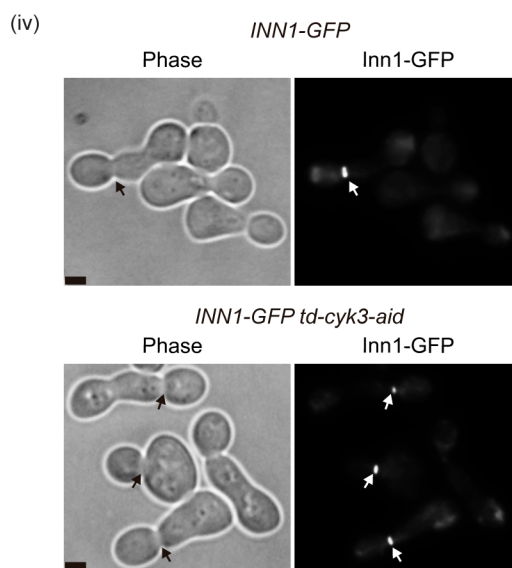
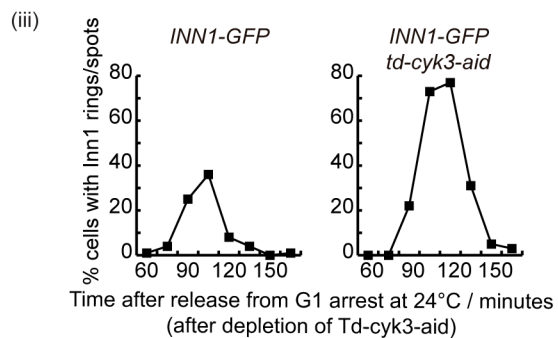
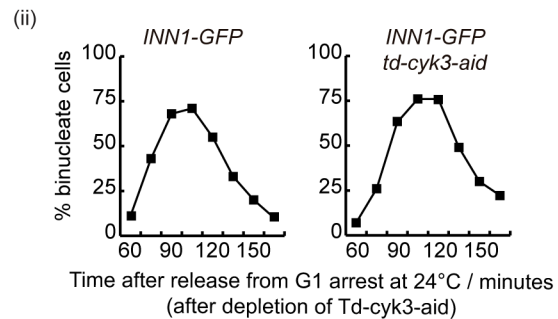
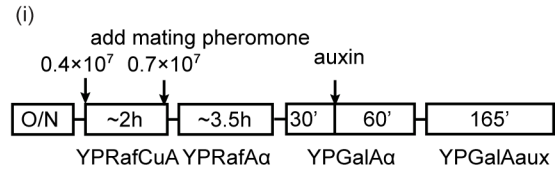


Figure 3.11: Upon the depletion of Cyk3 protein, a temporary accumulation of Inn1-GFP occurs, indicating a defect in cell division.

(i) *INN1-GFP td-cyk3-aid GAL-UBR1 GAL-OsTIR1* (YIMP197) and control (YIMP207) cells were grown in YPRaffCu at 24°C overnight. The day after, cells were diluted, and mating pheromone was added to synchronise cells in G1 phase of the cell cycle. Cells were then shifted to YPGal and NAA and IAA auxins were added to induce Td-cyk3-aid degradation; mating pheromone was washed out to allow cells progress through the cell cycle in the presence of NAA and IAA auxins. Samples were taken for both binucleate cells counting (ii) and fluorescence microscopy (iii). (iv) Examples of photos with Inn1-GFP localisation are shown. Scale bar corresponds to 2 μm.

(ii)). In addition, we showed an increase in the number of cells containing Inn1-GFP localised at the site of division (Figure 3.11 (iii) and

Figure 3.11 (iv)). It seemed that *Cyk3*-inactivated cells had no defect in the assembly or contraction of the actomyosin ring. All the

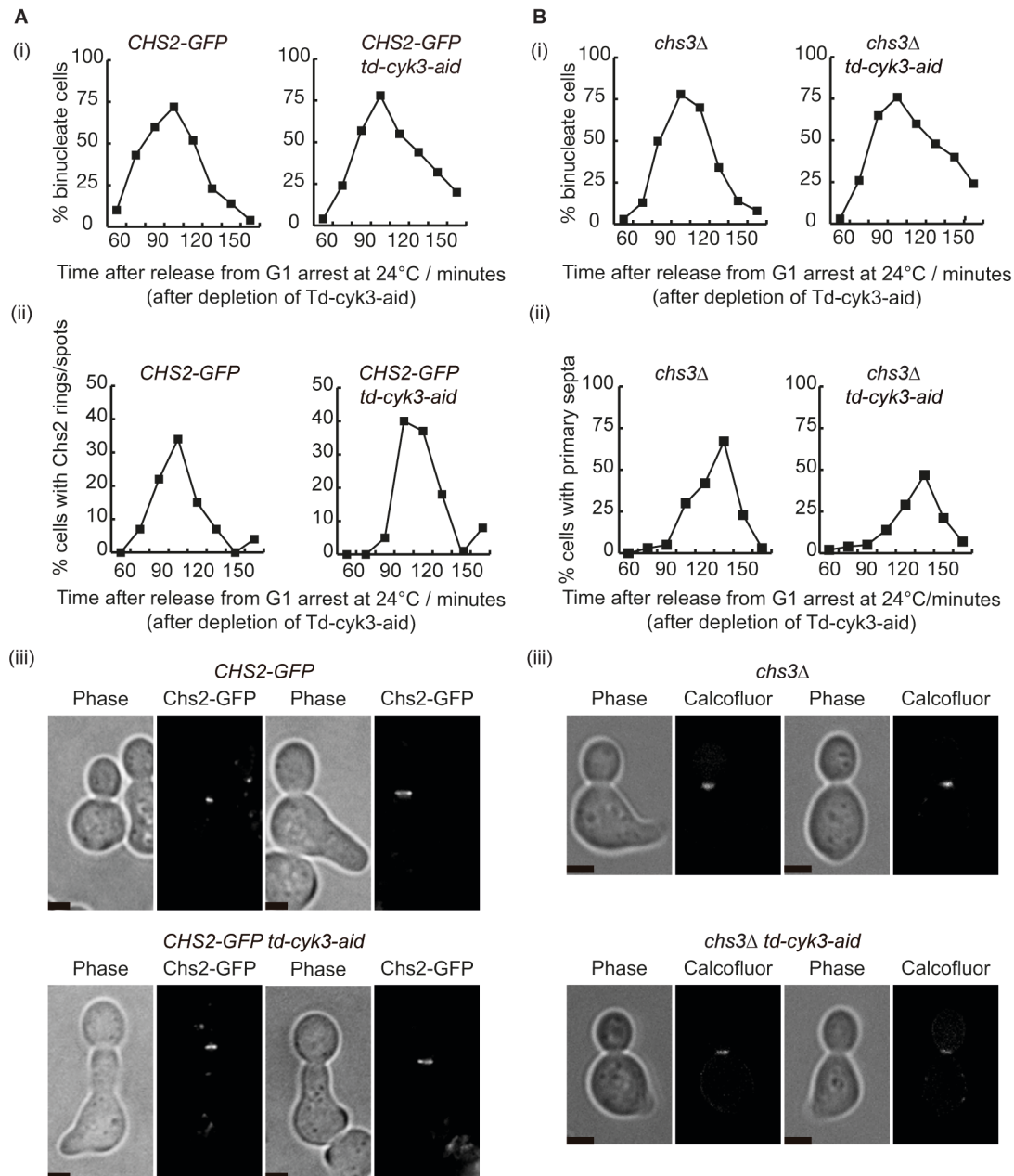


Figure 3.12: Upon the depletion of *Cyk3* protein, chitin synthase *Chs2* protein can localise at the site of division.

(A) Depletion of *Cyk3* does not affect *Chs2* localisation. (i) *CHS2-GFP td-cyk3-aid GAL-UBR1 GAL-OsTIR1* (YMF343) and control (*YIMP206*) cells were grown in YPRaffCu at 24°C overnight. The day after, cells were diluted, and mating pheromone was added to synchronise cells in G1 phase of the cell cycle. Cells were then shifted to YPGal and NAA and IAA auxins were added to induce Td-cyk3-aid degradation; mating pheromone was washed out to allow cells progress through the cell cycle in the presence of NAA and IAA samples. Samples were taken for both binucleate counting (i) and fluorescence microscopy (ii). (iii) Examples of photos with *Chs2-GFP* localisation. Scale bar corresponds to 2µm. **(B)** (i) *chs3Δ td-cyk3-aid GAL-UBR1 GAL-OsTIR1* (YIMP247) and control (*YIMP248*) cells were grown in YPRaffCu at 24°C overnight. The day after, cells were diluted, and mating pheromone was added to synchronise cells in G1 phase of the cell cycle. Cells were then shifted to YPGal and NAA and IAA auxins were added to induce Td-cyk3-aid degradation; mating pheromone was washed out to allow cells progress through the cell cycle in the presence of NAA and IAA auxins. Calcofluor was added 35 minutes after release to stain primary septa. Samples were taken for both binucleate cells counting (i) and fluorescence microscopy (ii). (iii) Examples of photos with calcofluor-stained primary septa are shown. Scale bar corresponds to 2µm.

results taken together suggest that cell division occurred slower in the absence of Cyk3.

As Cyk3 interacts with Chs2, we next studied whether lack of Cyk3 protein has any influence over the localisation of chitin synthase Chs2.

We grew *td-cyk3-aid CHS2-GFP* (YMF343) and control (YIMP206) cells in YP media supplemented with raffinose at 24°C and synchronised in G1 phase of the cell cycle with mating pheromone as described previously. After induction of expression of ubiquitin ligases Ubr1 and Tir1, together with the addition of NAA and IAA auxins, cells inactivated Td-cyk3-aid. Cells were then released from a G1 block and allowed to progress. Samples were taken to monitor cell cycle progression and Chs2-GFP localisation. We detected an increase in the amount of Chs2-GFP at the site of division upon degradation of Td-cyk3-aid compared to the control strain (Figure 3.12.A (i), Figure 3.12.A (ii) and Figure 3.12.A (iii)), which was consistent with the accumulation of Inn1-GFP at the cleavage site.

As it has been shown that Cyk3 has a positive influence on Chs2 synthesis of primary septum (Meitinger et al., 2010; Oh et al., 2012), the next step was to monitor the synthesis of primary septa at the site of division in cells lacking Cyk3. To finely detect chitin deposition under the microscope, we stained cells with calcofluor (Arcones et al. 2016). In addition, we used *CHS3*-deleted

cells, since Chs3 is the chitin synthase enzyme that makes most of the chitin content in the cell; and such content could disguise the presence of primary septum (Shaw et al. 1991, Bulawa 1992).

td-cyk3-aid chs3Δ (YIMP247) and control (YIMP248) were grown at 24°C in YP media supplemented with raffinose, and synchronised in G1 phase of the cell cycle by addition of mating pheromone. After inducing the expression of ubiquitin ligases Ubr1 and Tir1 and depletion of Td-cyk3-aid by addition of NAA and IAA auxins, cells were released from G1 block and cell cycle allowed to progress in the presence of calcofluor. Calcofluor had been added to the media 35 minutes after the release from G1 arrest to stain the primary septa, and samples were collected to visualise the primary septa and monitor cell cycle progression. Cells lacking Td-cyk3-aid had slightly decreased number of cells with primary septum, which could suggest a role of Cyk3 in the primary septum synthesis (Figure 3.12.B (i), Figure 3.12.B (ii) and Figure 3.12.B (iii)).

In conclusion, we have shown that we are able to conditionally deplete Cyk3 protein, and that Cyk3 protein is involved in cytokinesis at the level of primary septum synthesis.

3.6 Generating the tool to determine Cyk3 function.

Understanding the role of non-essential protein is challenging, as there are

no striking phenotypes associated to the lack of such proteins. It is therefore necessary to find a genetic combination in which the protein of interest becomes essential.

In order to understand more details of the role of Cyk3, a non-essential protein, in chitin synthase Chs2 regulation, we took advantage of the fact that this protein becomes essential in cells in which the C2 domain of Inn1 protein is fused to Hof1 ((Devrekanli *et al.* 2012) and Figure 3.13.A (i)). *cyk3Δ* cells grow as smaller colonies or die as clumps of cells, whereas when combined with *C2-HOF1* they die as a chain of cells confirming the cytokinetic defect (Figure 3.13.A (i) and Figure 3.13.A (ii)). It is important to highlight at this point that these cells die despite the presence of wild type Inn1. The lethality of a strain containing the fusion in the absence of functional *CYK3* was confirmed using conditional *td-cyk3-aid* degon.

Strains *C2-HOF1 td-cyk3-aid* (YMF356) and control (YMF334) were spotted onto permissive YDPCu or restrictive YPGalCu medium supplemented with NAA and IAA auxins. Upon depletion of Td-cyk3-aid, a complete abolition of growth was observed, reproducing the synthetic lethality observed in the tetrad dissection (Figure 3.13.A (i) and Figure 3.13.A (iii)).

We grew strain *C2-HOF1 td-cyk3-aid* (YMF356) and control strain (YMF334) asynchronously in medium containing raffinose, transferring the exponentially

growing culture to YPGalCu media supplemented with NAA and IAA auxins to induce degradation of Td-cyk3-aid for 9 hours. We studied DNA content by FACS and we could observe an accumulation of cells with higher than 2C DNA content. In addition, cell chains were observed, suggesting that these cells die because of a cytokinetic defect (Figure 3.13.A (iv)).

We next asked whether this lethality could be due to a lack of function of C2-Hof1 fusion, as it has been shown that simultaneous lack of Cyk3 and Hof1 is lethal (Korinek *et al.* 2000). To test this hypothesis, we combined *C2-HOF1* with deletions of genes that have been shown to be synthetic lethal with *hof1Δ*: *SHO1* and *RVS167* (Nkosi *et al.* 2013). We generated diploids containing double deletions, *C2-HOF1* and either *sho1Δ* (YIMP391) or *rvs167Δ* (YIMP210), and determined the progeny by tetrad dissection analysis. Marker analysis after tetrad dissection showed that haploid cells could harbour either deletion in the presence of the fusion (Figure 3.13.B (i) and Figure 3.13.B (ii)), suggesting that the *C2-HOF1* allele was functional.

Another possibility would be that C2-Hof1 fusion, even though it is expressed and functional, could be defective in its localisation. To address this possibility, localisation of C2-Hof1-GFP (YIMP409) and Hof1-GFP (YASDHOF1-1B) were followed at the site of division in an asynchronous culture in YDPCu

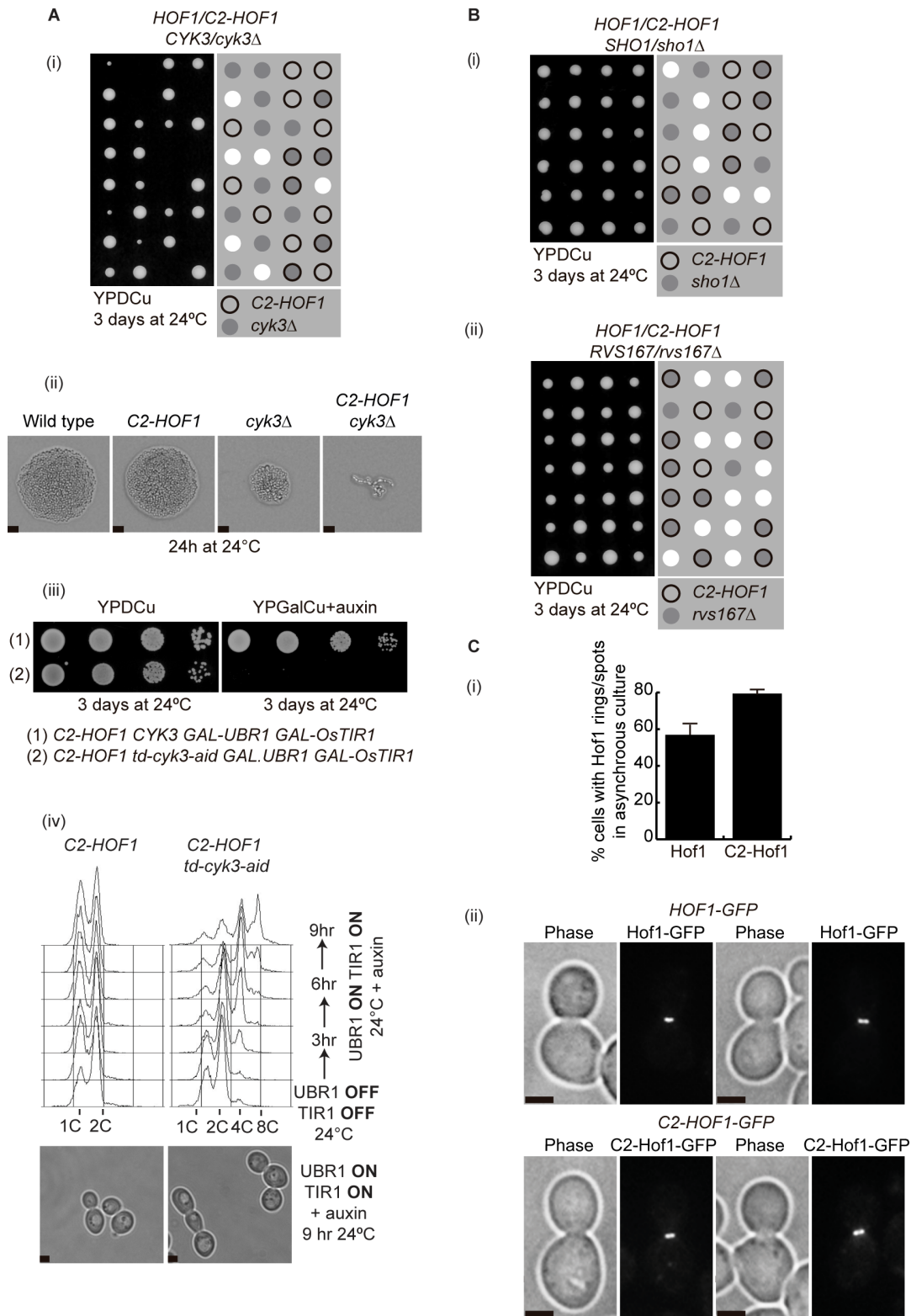


Figure 3.13: C2-HOF1 is synthetically lethal with *td-cyk3-aid*.

(A) (i) Tetrad dissection of diploid *HOF1/C2-HOF1* *CYK3/cyk3Δ* (YIMP237) shows synthetic lethality between *C2-HOF1* and *cyk3Δ* alleles. (ii) Pictures of the indicated genotypes taken after 24 hours of incubation in YPDCu at 24°C. (iii) *C2-HOF1* *td-cyk3-aid* *GAL-OsTIR1* *GAL-UBR1* (YMF356) and control (YMF334) strains were spotted at 24°C in YPDCu and YPGalCu plates supplemented with NAA and IAA auxins. (iv) *C2-HOF1* *td-cyk3-aid* *GAL-OsTIR1* *GAL-UBR1* (YMF356) and control (YMF334) strains were grown in YPRaff medium at 24°C overnight, diluted the next morning and media changed to YPGal with NAA and IAA auxins when cells were at exponential phase. Samples for FACS analysis were taken at the corresponding time points and photos of cells were taken at the end of the experiment. Scale bar corresponds to 2μm. (B) (i) Tetrad dissection of diploid *HOF1/C2-HOF1* *SHO1/sho1Δ* (YIMP391). (ii) Tetrad dissection of diploid *HOF1/C2-HOF1* *RVS167/rvs167Δ* (YIMP210). (C) (i) Asynchronous cultures of *C2-HOF1-GFP* (YIMP409) and *HOF1-GFP* (YASDHOF1-1B) were grown in YPDCu medium, and numbers of cells expressing Hof1-GFP or C2-Hof1-GFP was counted. (ii) Examples of photos with Hof1-GFP and C2-Hof1-GFP localisation are shown. Scale bar corresponds to 2μm.

at 24°C. After counting the percentage of cells with GFP signal at the site of division, we showed that the fusion could also be localised correctly to the site of division (Figure 3.13.C (i) and Figure 3.13.C (ii)).

Therefore, the observation that *CYK3* becomes essential in *C2-Hof1* presence represents an invaluable tool for studying *Cyk3* function.

3.7 SH3 domain of *Cyk3* is unable to interact with *Chs2*, but it is important for *Cyk3* localisation at the site of division.

We aimed to determine the function of *Cyk3* domains and their roles during cytokinesis. *Cyk3* contains an N-terminal SH3 domain, which has been shown to directly interact with *Inn1* protein (Nishihama *et al.* 2009, Palani *et al.* 2012, Nkosi *et al.* 2013), and a transglutaminase-like domain whose function is completely unknown (Figure 3.14 (i)).

Using conditions in which *CYK3* becomes essential, we wanted to assess the functionality of the SH3 domain of *Cyk3* (Figure 3.14.A (i) and (ii)). After deleting SH3 domain of *Cyk3* (*cyk3-SH3Δ*) in a strain harbouring *C2-HOF1*, we subjected this strain (YIMP35) to tetrad dissection and analysed the meiotic progeny. Cells harbouring *cyk3-SH3Δ* were substantially smaller than wild type, and similar to *cyk3Δ*. Also, cells died when combined with *C2-HOF1* allele, suggesting

that this domain is crucial for *Cyk3* function (Figure 3.14.A (iii) and (iv)). As these cells behave in tetrad dissection analysis similarly to *cyk3Δ* cells, we postulated that this domain could be important for the interaction of *Cyk3* with *Chs2*.

To investigate whether SH3 domain of *Cyk3* was important to interact with *Chs2*, we used yeast two-hybrid analysis. This technique involves cloning two genes encoding for proteins of interest, bait and prey, in two plasmids. Each plasmid synthesises a fusion protein with one half of a reporter gene. If both proteins are able to interact with one another, the reporter gene is expressed. In our case, it allowed cells to grow in media lacking histidine (Fields and Song 1989).

Cyk3 has been shown to interact through its SH3 domain with the C-terminus of *Inn1* protein (Nishihama *et al.*, 2009; Nkosi *et al.*, 2013). In agreement with the published literature, *Cyk3* was able to interact with the C-terminus of *Inn1* (Figure 3.14.B (i) and Figure 3.14.B (ii), see (3) and (5)). However, *Cyk3* SH3 domain was unable to interact either with a fragment of *Chs2* lacking its transmembrane domain (see (1) and (3)) or a fragment also lacking its CDK-regulated tail (see (2) and (3)) (Figure 3.14.B (i) and Figure 3.14.B (ii)).

To evaluate the importance of SH3 domain for *Cyk3* localisation, we kept *cyk3-SH3Δ* cells alive by adding a plasmid that would express wild type *CYK3* under *GAL* promoter (YMF475) and compared with control

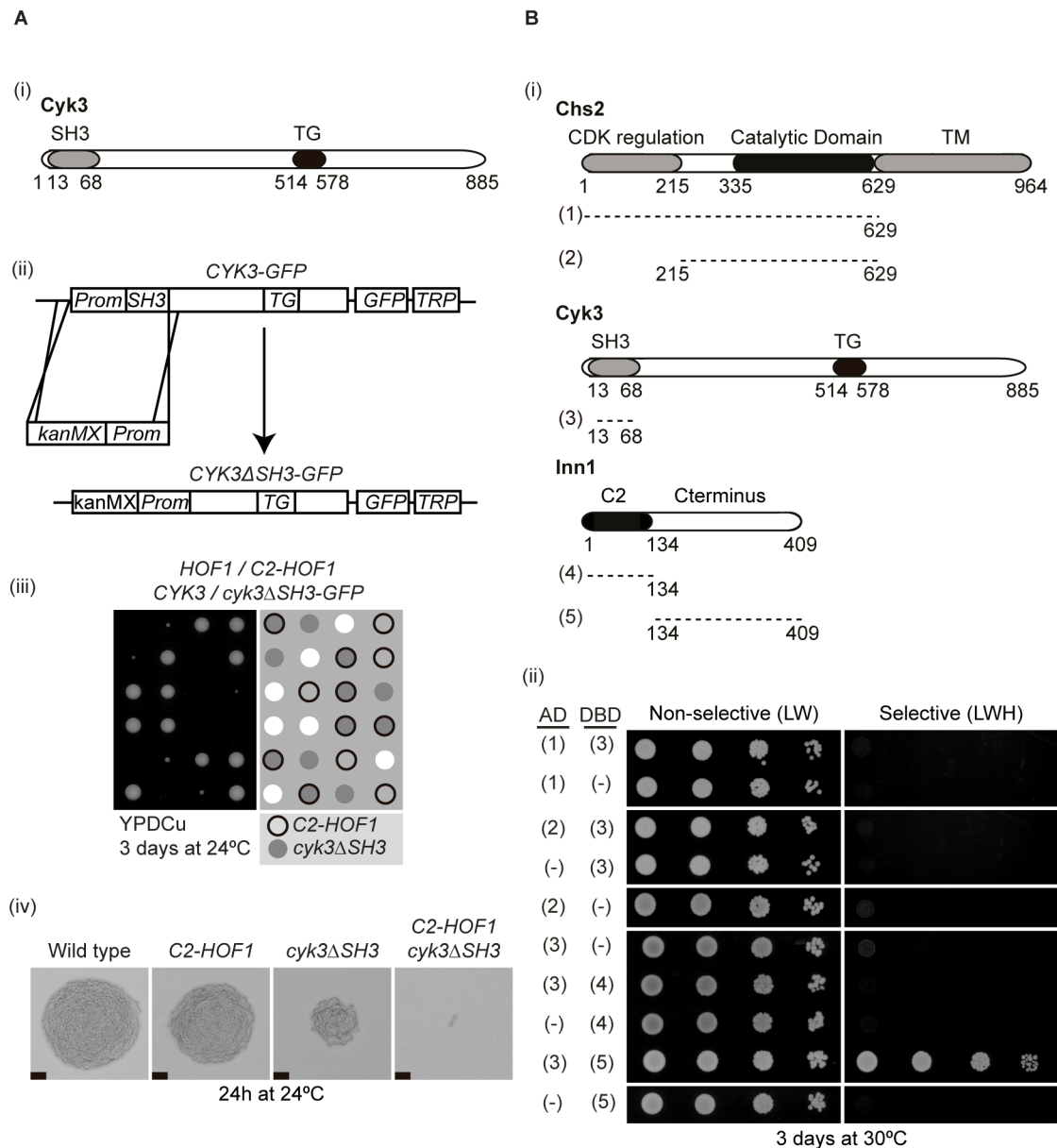


Figure 3.14: SH3 domain of Cyk3 does not bind to Chs2.

(A) (i) Diagram representing Cyk3 protein. (ii) SH3 domain was deleted inside *CYK3* in the wild type locus. (iii) Tetrad dissection of diploid *HOF1/C2-HOF1 CYK3/cyk3ΔSH3* (YIMP35). (iv) Pictures of tetrads of the indicated genotypes taken after 24 hours incubation on YPDCu plates at 24°C. Scale bar corresponds to 20µm. **(B)** Yeast two-hybrid analysis of Chs2 and Cyk3. (i) Diagram of the fragments of Chs2 and Cyk3 tested. (ii) Yeast two-hybrid analysis shows interaction between Cyk3 SH3 domain and Inn1 C-terminus (3-5), but not between Cyk3 SH3 domain and Chs2 (1-3, 2-3).

cells (YASD2061). After growing the cells in YP media supplemented with galactose and taking an asynchronous sample, we showed that this domain is important for the localisation of Cyk3, as cells lacking SH3 domain were unable to localise Cyk3 to the site of division in an asynchronous culture

(Figure 3.15.A (i) and Figure 3.15.A (ii)); even though the protein was indeed being expressed (Figure 3.15.A (iii)).

As Cyk3 is able to interact with Inn1 through its SH3 domain, and lack of SH3 domain prevents Cyk3 localisation, we wanted to investigate whether Cyk3 localisation would

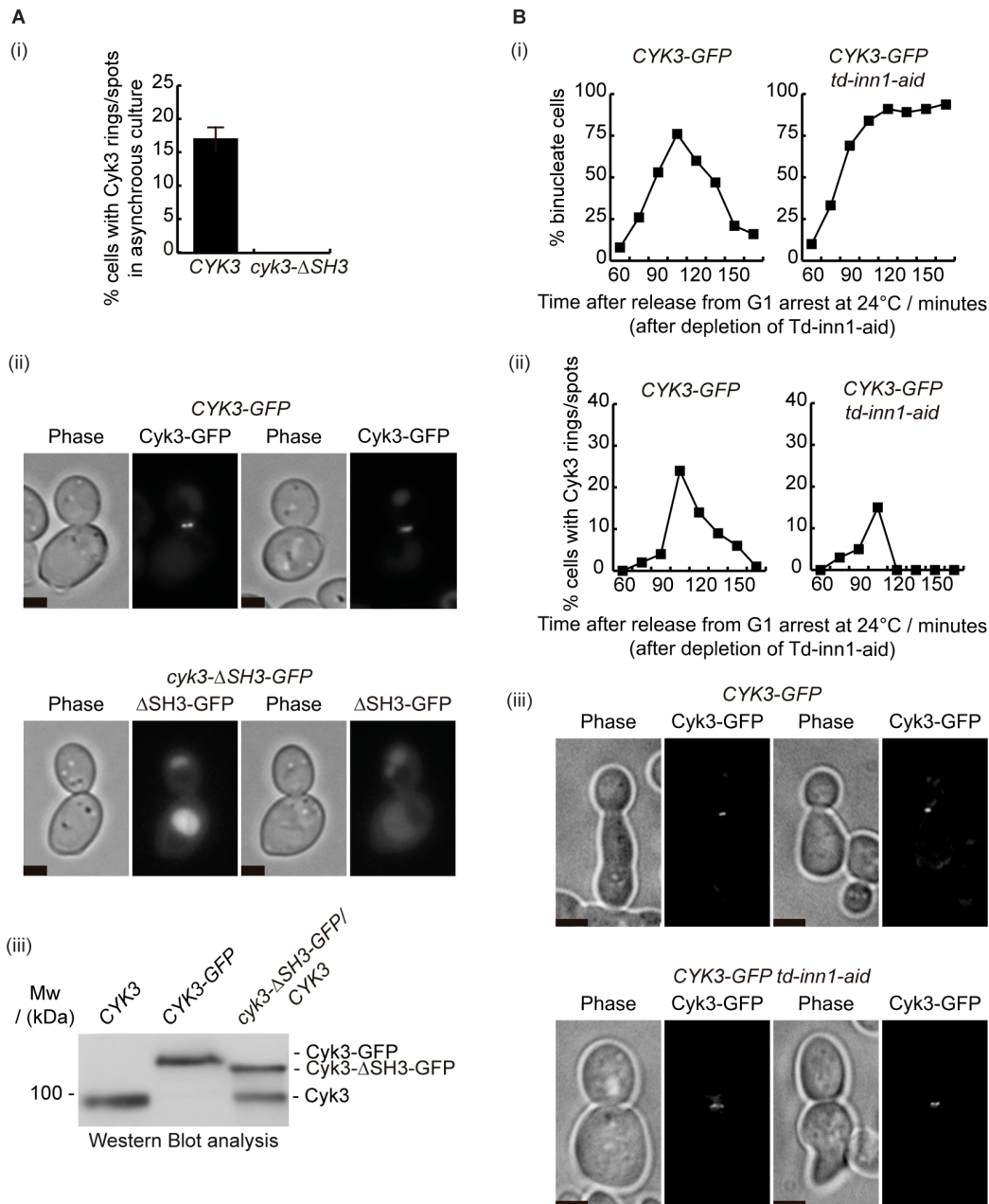


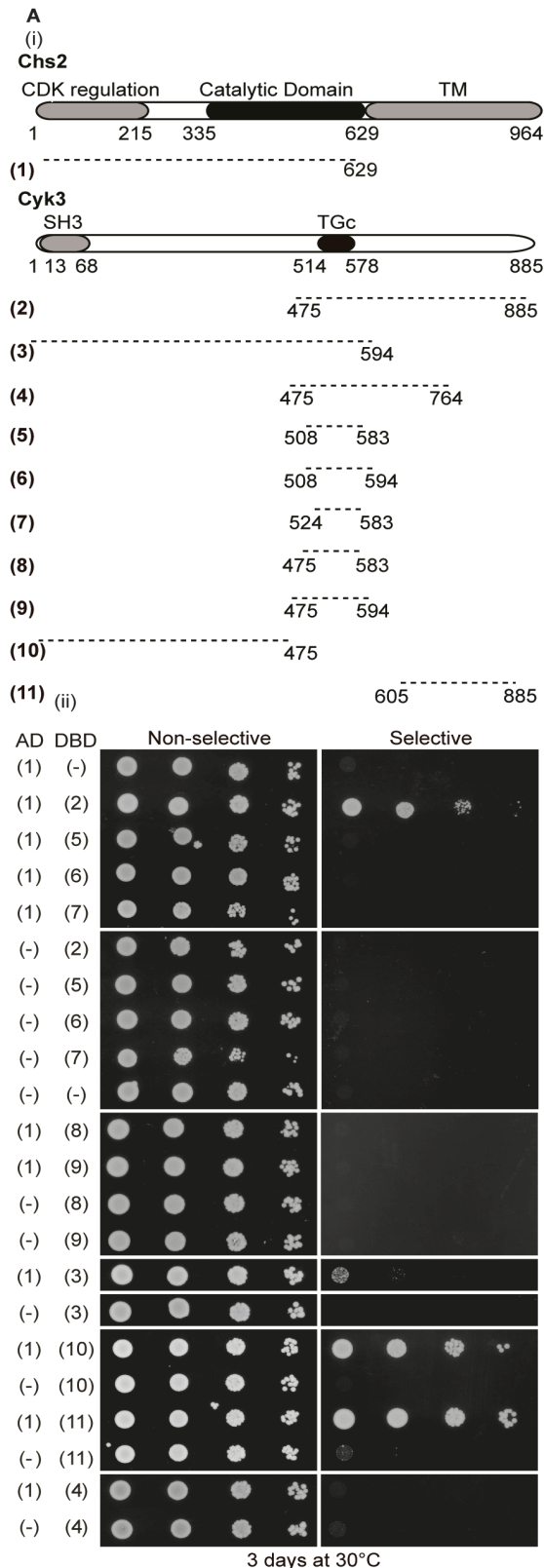
Figure 3.15: Lack of SH3 domain prevents localisation of Cyk3.

(A) (i) *cyk3ΔSH3-GFP GAL-CYK3* (YMF475) and control (YASD2061) cells were grown asynchronously in YPGal medium, and samples were taken for fluorescence microscopy (ii) and immunoblotting analysis with anti-Cyk3 antibody (iii). (ii) Examples of photos with Cyk3-GFP and *cyk3ΔSH3-GFP* localisation are shown. Scale bar corresponds to 2μm. **(B)** (i) *CYK3-GFP td-inn1-aid GAL-UBR1 GAL-OsTIR1* (YMF319) and control (YMF322) cells were grown in YPRaffCu medium at 24°C overnight. The day after, cells were diluted, and mating pheromone was added to synchronise cells in G1 phase of the cell cycle. Cells were then shifted to YPGal and NAA and IAA auxins were added to induce Td-inn1-aid degradation; mating pheromone was washed out to allow cells progress through the cell cycle in the presence of NAA and IAA auxins. Samples were taken for both binucleate counting (i) and fluorescence microscopy (ii). (iii) Examples of photos with Cyk3-GFP localisation are shown. Scale bar corresponds to 2μm.

be compromised in cells lacking Inn1 protein.

To do so, we grew *CYK3-GFP td-inn1-aid* (YMF319) and control (YMF322) cells in YP medium supplemented with raffinose.

Upon synchronising cells in G1 phase of the cell cycle by addition of mating pheromone, degradation of Inn1 protein was induced by the addition of NAA and IAA auxins to the culture



media. Cells were then released to synchronously progress through cell cycle, and samples were collected to monitor cell cycle progression and Cyk3-GFP localisation (Figure 3.15.B). As expected, in the absence of

Figure 3.16: Different fragments of Cyk3 are able to interact with a fragment of Chs2 containing the catalytic domain in a yeast two-hybrid assay.

(A) Fragment of Chs2 containing the CDK-regulated tail and the catalytic domain was assayed against different fragments of Cyk3. (i) Diagram of the different fragments used in this study. (ii) Yeast two-hybrid showing that Cyk3 (475-885aa), Cyk3 (1-594aa), Cyk3 (1-475aa), Cyk3 (605-885aa) are able to interact with Chs2 (1-629aa).

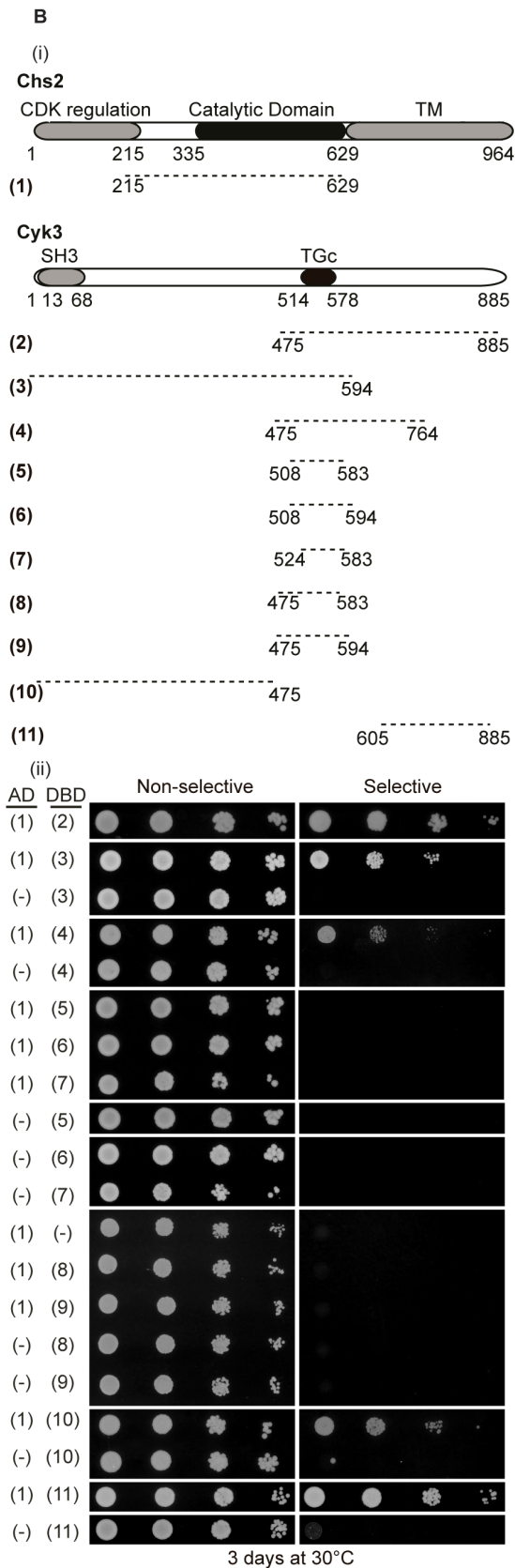
essential Inn1 protein cells accumulated as binucleate cells (Figure 3.15.B (i)), a sign of division failure. Importantly, the localisation of Cyk3 to the site of division was compromised, highlighting the importance of this interaction in cell division (Figure 3.15.B (i), Figure 3.15.B (ii) and Figure 3.15B (iii)).

In conclusion, we show that Cyk3 SH3 domain is indispensable for its correct bud-neck localisation and the SH3 functions, presumably, by stabilising its interaction with Inn1 at the site of division.

3.8 Cyk3 regulates the function of Chs2.

As we have previously shown, Cyk3 and Chs2 can interact in a direct manner during cytokinesis. Also, it has been shown that Cyk3 can influence Chs2 deposition of primary septum during cytokinesis (Meitinger *et al.* 2010, Devrekanli *et al.* 2012, Oh *et al.* 2012), so the next step was to determine which fragments of each protein were responsible for this interaction to occur. We have shown above that Cyk3 SH3 domain is unable to interact with Chs2. Different truncations of Cyk3 were designed and cloned into yeast two-hybrid vectors, in order to

assess which ones were able to interact with Chs2 (Figure 3.16).



First, we wanted to understand whether Cyk3 would be able to interact with a fragment of Chs2 lacking its transmembrane domain (Chs2 1-629aa; Figure 3.16.A (i)). Interactions are summarised in Figure 3.16A (i) and (ii), and show that Cyk3 is able to interact with Chs2 (1-629aa) through fragments (1-475aa), (1-594 aa), (605-885aa), and (475-885aa). As these fragments span the full-length of Cyk3 protein and partially overlap, this suggests that Cyk3 interacts with Chs2 through multiple contact points.

We have confirmed that we preserved Cyk3 interactions when using a slightly smaller fragment of Chs2, which lacks its transmembrane domain and CDK-regulated tail (Chs2 215-629aa). Interactions, summarised in Figure 3.16B (i) and (ii), show that the same interactions were found to occur when comparing to the longer fragment with one difference. Cyk3 fragment (475-764aa) was found to interact with Chs2 (215-629aa), but was unable to interact with the longer fragment of Chs2 (1-629aa). This could suggest a potential role of the N-terminal tail of Chs2 in the regulation of the protein interaction with Cyk3.

Figure 3.16: Different fragments of Cyk3 are able to interact with a fragment of Chs2 containing the catalytic domain in a yeast two-hybrid assay.

(B) A fragment of Chs2 only containing the catalytic domain was assayed against different fragments of Cyk3 (i) Diagram of the different fragments tested in this assay. (ii) Yeast two-hybrid showing that Cyk3 (475-885aa), Cyk3 (1-594aa), Cyk3 (1-475aa), Cyk3 (605-885aa) and Cyk3 (475-764aa) are able to interact with Chs2 (215-629aa).

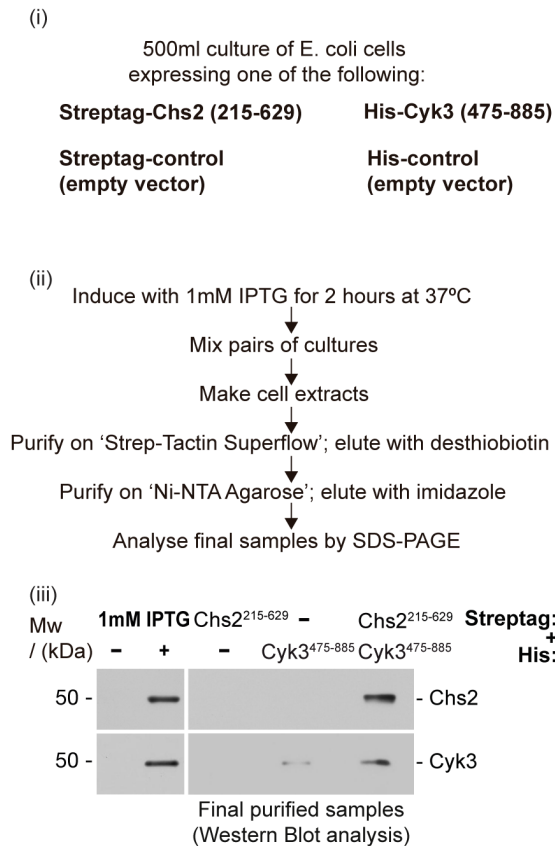


Figure 3.17: Chs2 and a fragment of Cyk3 are able to interact directly when purified from an *E. coli* expression system.

(i) Indicated *E. coli* strains containing plasmids pMF36 (Strep-Chs2(215-629aa)), pET100 (Strep-empty); pMF62 (6His-Cyk3(475-885aa)) and pET28c (6His-empty) were grown as indicated in (ii). (ii) Cultures were grown at 37°C, and protein induction was performed at an OD₆₀₀ of 0.6 upon addition of IPTG for two hours. Corresponding cultures were mixed and strep-tagged protein was purified, and eluates were further purified through their 6His-tag. Final eluates were analysed by immunoblotting with anti-His and anti-Strep antibodies (iii).

In order to determine whether fragment spanning amino acids 475-885aa of Cyk3 and fragment of Chs2 spanning amino acids 215-629 fragments would be able to directly interact, we used the same approach as previously to show interaction between Cyk3 and Chs2. We used Rosetta *E. coli* as an expression host in which the only eukaryotic proteins would be either Strep-Chs2 (215-629aa) or 6His-Cyk3 (475-885aa). Cyk3

fragment spanning amino acids 475-885aa was chosen, as it is similar to a fragment used in a previous study (Onishi *et al.* 2013) (amino acids 480-885aa).

After growing *E. coli* cultures, protein expression was induced at an OD₆₀₀ of 0.6 by addition of IPTG for two hours at 37°C. After preparing the protein extracts, purification was done first on a Strep column, and the material generated was loaded into a nickel column (details in section 2.3.7 of Material and Methods). Final elutions were loaded in a protein gel and subjected to immunoblotting analysis (Figure 3.17 (i) and Figure 3.17 (ii)), which showed that these two proteins are able to interact directly (Figure 3.17 (iii)).

The Cyk3 475-885aa fragment, which directly interacts with the catalytic domain of Chs2, contains a so-called transglutaminase-like domain. These types of domains are part of a large protein family that include proteins with active transglutaminase domains and others with transglutaminase-like domains, whose role is unknown (Lorand and Graham 2003). Active transglutaminase domains contain a catalytic triad including a cysteine, a histidine and an aspartic acid. Nevertheless, Cyk3, as others within the same subfamily, harbours a transglutaminase-like domain, which lacks the catalytic cysteine (Makarova *et al.* 1999).

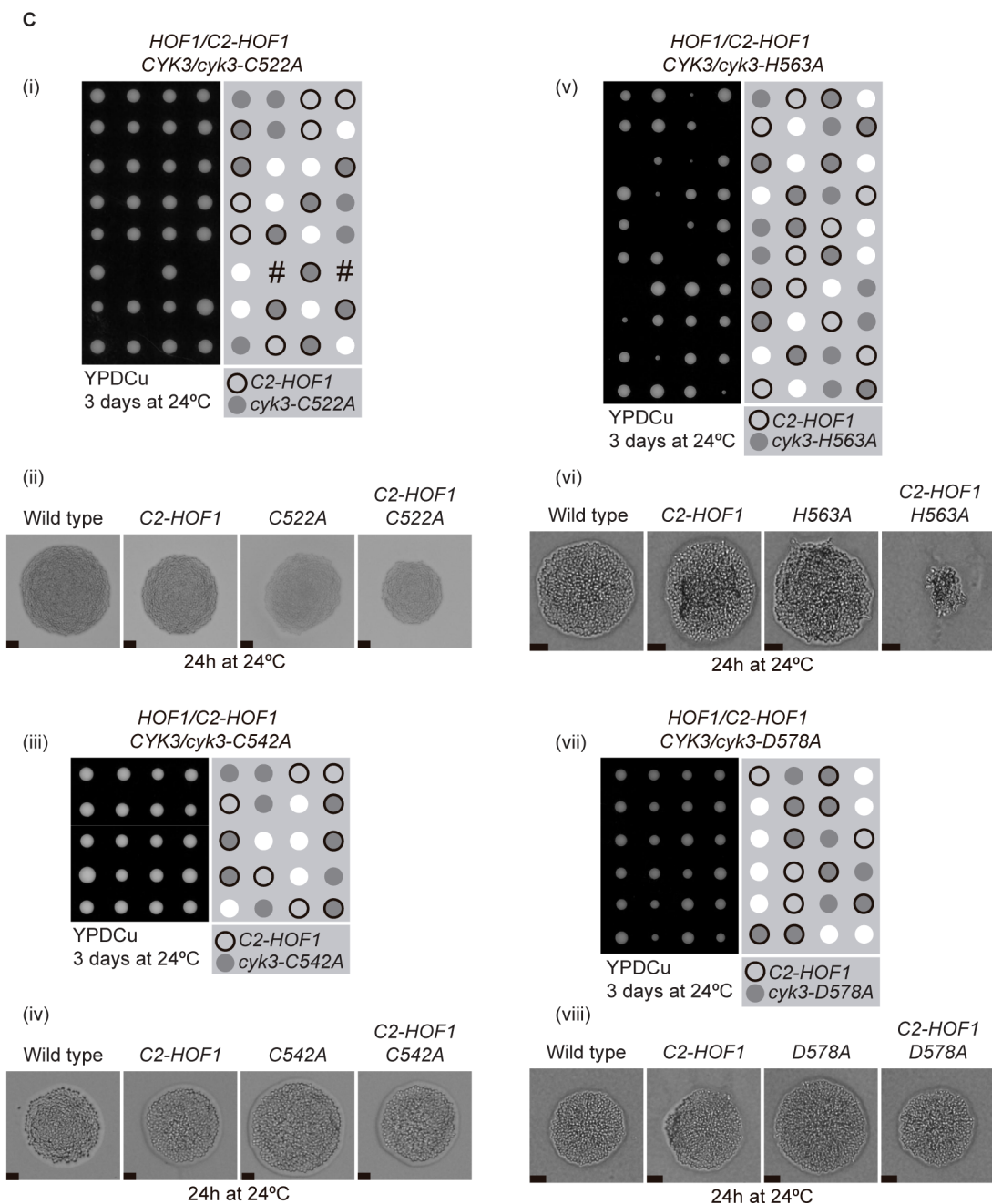
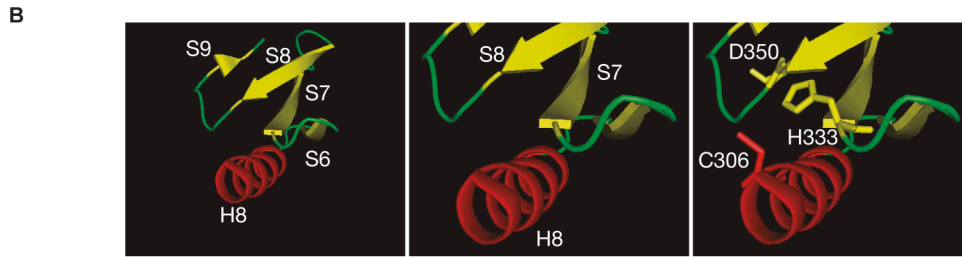
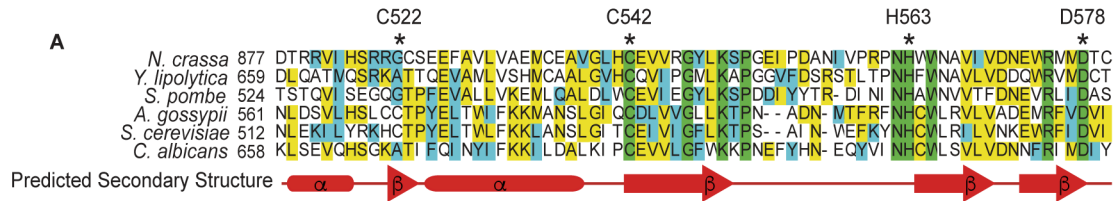


Figure 3.18: Conserved residues in the transglutaminase-like domain are important for *Cyk3* function.

(A) Alignment of the transglutaminase-like domain of *Cyk3* proteins from different fungi. (B) Tridimensional representation of the catalytic triad of the transglutaminase domain of PNGase (mouse PNGase; PDB 2F4M). (C) Tetrad dissection of diploid strains harbouring *C2-HOF1* fusion together with corresponding mutations (i) *cyk3-C522A* (YIMP9); (iii) *cyk3-C542A* (YIMP168); (v) *cyk3-H563A* (YIMP4); and (vii) *cyk3-D578A* (YIMP5). Pictures of tetrads of the indicated genotypes taken after 24 hours incubation on YPDCu plates at 24°C (ii), (iv), (vi) and (viii).

As *Cyk3* function becomes essential in cells harbouring *C2-Hof1* fusion protein, we aimed to identify key residues within this domain that could have a role in *Cyk3* function. We mutated the corresponding codons in *CYK3* gene sequence to change key residues for alanines within the catalytic triad. We next combined those mutated version of *CYK3* with *C2-HOF1* allele in diploid cells. Hence, if a residue would be important for *Cyk3* function, a haploid cell containing *C2-HOF1* and a mutated *CYK3* would die upon tetrad dissection.

To try to identify key residues within *Cyk3* transglutaminase-like domain, we compared it with other fungal *Cyk3* orthologs (Figure 3.18.A). We determined clearly two of the potential inactive triad: histidine 563 (H563) and aspartic acid 578 (D578). as they are located at the beginning or the end of β -strands (Figure 3.18.A). Interestingly, those residues are localised in close proximity in a 3D predicted protein structure (Figure 3.18.B). In addition, there are two other cysteins: C522, which is fully conserved, and a second one C542, which is not conserved but correspond

to the position of cysteins in the active triad (Figure 3.18.A) (Makarova *et al.* 1999).

Upon generation of the diploids, tetrad dissection and analysis of the meiotic progeny, mutations of either the previously described cysteins (C522 and C542) (YIMP9 and YIMP168) or the aspartic acid (D578) (YIMP5) to alanines did not yield any synthetic lethality phenotype when combined with *C2-Hof1* fusion in tetrad dissection analysis (Figure 3.18.C (i), Figure 3.18.C (ii) and Figure 3.18.C (iv)). However, mutation of histidine H563 to an alanine (YIMP4) reported a variable synthetic lethal or a synthetic sick phenotype (Figure 3.18.C (iii)).

We then assessed whether we could completely inactivate the function of this transglutaminase-like domain. Hence, we combined mutation of residues H563 and D578 within the transglutaminase-like domain into alanines (Figure 3.19.A). When combining this double mutant *cyk3-2A* with *C2-HOF1* allele in a diploid strain (YMF669), tetrad dissection showed a tight synthetic lethal phenotype when both alleles were combined, pointing out to a crucial role of the *Cyk3* transglutaminase-like domain (Figure 3.19.A).

To reproduce the same result using the *td-cyk3-aid* allele, we used a *C2-HOF1* strain harbouring the double *td-cyk3-aid* degon, in which we integrated a plasmid expressing an extra copy of either wild type *CYK3* or mutated *cyk3-2A* allele. Strains *C2-*

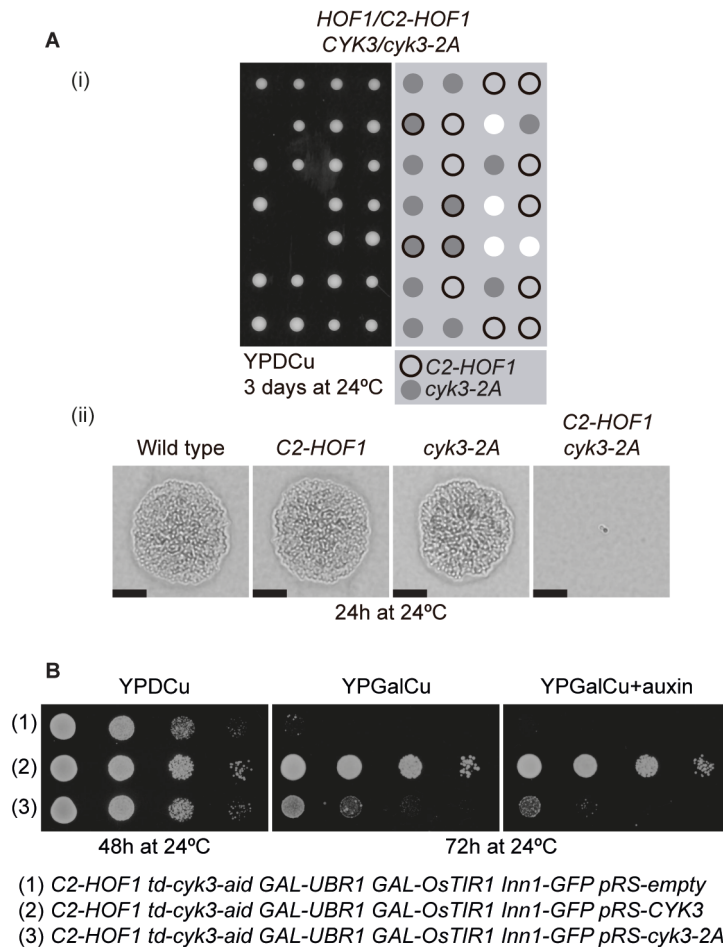


Figure 3.19: Simultaneous mutation of two conserved residues H563 and D578 to alanines (*cyk3-2A*) abolishes *Cyk3* function.

(A) Tetrad dissection of diploid strain YMF669 harbouring *C2-HOF1* fusion and *cyk3-2A* double mutant. Pictures of tetrads of the indicated genotypes taken after 24 hours incubation on YPDCu plates at 24°C. (B) Corresponding strains *C2-HOF1 td-cyk3-aid GAL-UBR1 GAL-OsTIR1 INN1-GFP* containing an empty plasmid (YIMP415), a plasmid expressing *Cyk3* (YIMP417) or a plasmid expressing *cyk3-2A* (YIMP416) were spotted on YPDCu, YPGalCu and YPGalCu supplemented with NAA and IAA auxins, and incubated for the corresponding number of days.

HOF1 td-cyk3-aid with an empty plasmid (YIMP415), a plasmid expressing wild type *CYK3* (YIMP417) or a plasmid expressing *cyk3-2A* (YIMP416) were spotted onto permissive YPDCu, or restrictive YPGalCu supplemented with 500 μ M NAA and IAA auxins, to induce *Td-cyk3-aid* degradation. We show that upon degradation of *Td-cyk3-aid*, only wild type *CYK3* could supply the function but not *cyk3-2A*, strongly suggesting that mutated H563A and D578A residues are crucial for *CYK3* function (Figure 3.19B).

It has been shown that overexpression of *Cyk3* is able to induce cells to lay down a thicker primary septum (Meitinger *et al.* 2010, Oh *et al.* 2012). Therefore, we asked whether this conserved transglutaminase-like domain is able to influence septum formation in budding yeast. In order to do that, we used *chs3 Δ* cells to avoid chitin background staining, as *Chs3* synthesises most of the chitin content within the cell (Shaw *et al.* 1991, Bulawa 1992). We overexpressed either wild type *CYK3* (YIMP235) or the mutant of *Cyk3* containing

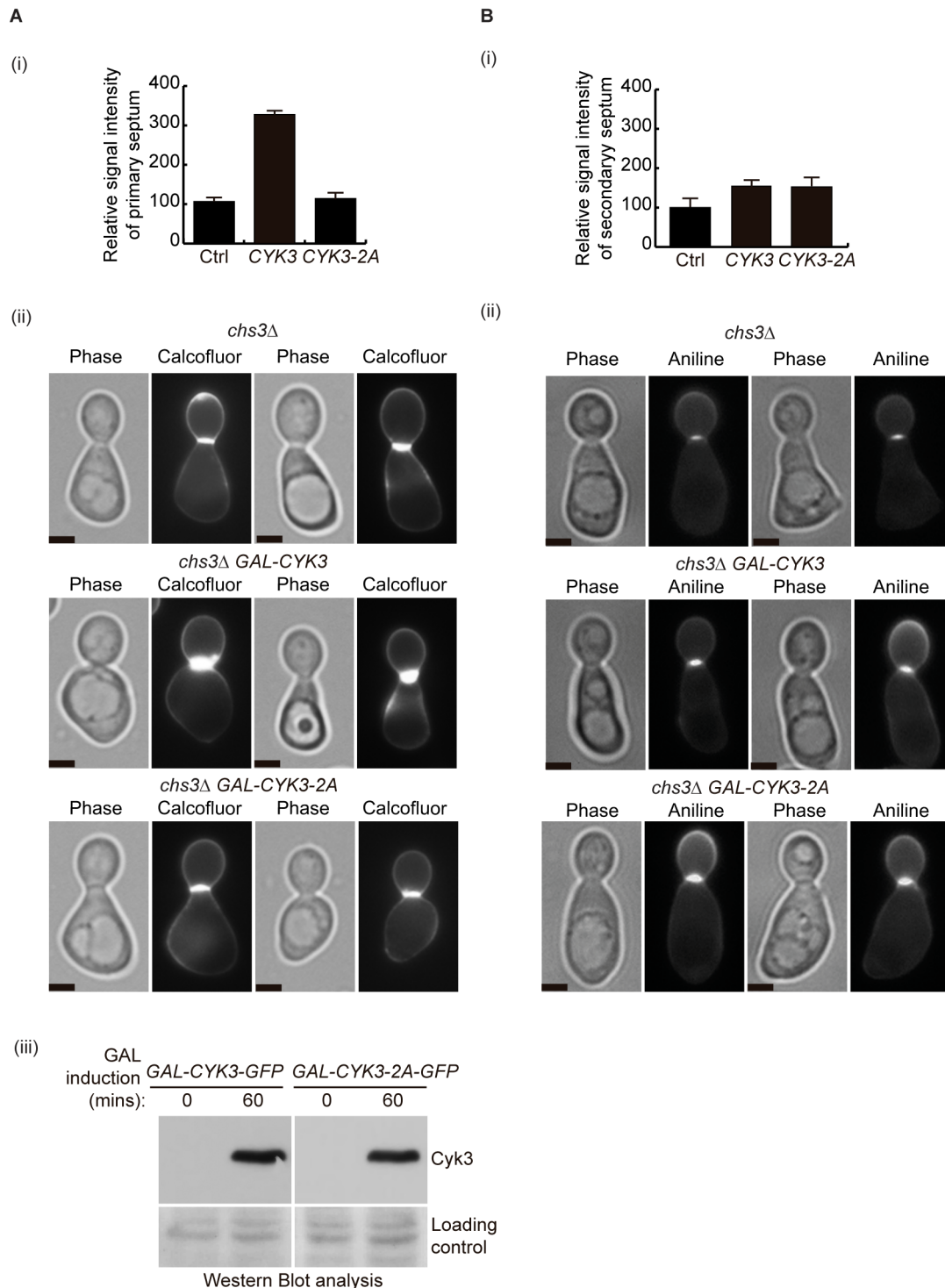


Figure 3.20: Overexpression of transglutaminase-like domain mutant *Cyk3-2A* unables cells to lay down thicker primary septa.

(A) Control (YMF505), *GAL-CYK3* (YIMP235) and *GAL-cyk3-2A* (YMF576) cells were synchronised in G1 phase of the cell cycle, protein overexpression was induced by media shift to galactose. Upon release from G1 block primary septa were stained by addition of calcofluor and samples were collected 135 minutes after the release from G1 phase to count number of cells containing stained primary septa. (i) Quantification of the relative intensity of the primary septum in corresponding mutants using control as 100%. (ii) Examples of photos with cells containing calcofluor stained primary septa are shown. Scale bar corresponds to 2µm. (iii) Immunoblotting showing the overexpression of the indicated proteins using anti-GFP antibody. **(B)** (i) Control (YMF505), *GAL-CYK3* (YIMP235) and *GAL-cyk3-2A* (YMF576) cells were synchronised in G1 phase of the cell cycle, protein overexpression induced by media shift to galactose. Upon release from G1 block secondary septa were stained by addition of aniline blue and samples were collected 135 minutes after the release. (i) Quantification of the relative intensity of the secondary septum. Control was set to 100%. (ii) Examples of photos with cells containing aniline blue stained secondary septa are shown. Scale bar corresponds to 2µm.

histidine-563 and aspartic acid-578 mutated to alanines (*cyk3-2A*) (YMF576), alongside a control strain expressing wild type levels of CYK3 (YMF505).

Cells were grown overnight in YPRaff, synchronised in G1 phase of the cell cycle by addition of mating pheromone, and shifted to the medium YPGal to induce the expression of the corresponding protein. After releasing cells from G1 block, chitin was stained with calcofluor and cells were collected at different time points after the release, to analyse the calcofluor staining at the bud neck, which reflected the primary septum formation in each strain.

In cells overexpressing wild type CYK3 there is a thicker deposition of primary septa, as it has already been shown that cells overexpressing *Cyk3* are able to lay down a thicker primary septa (Meitinger *et al.* 2010, Oh *et al.* 2012). Interestingly, the signal of cells overexpressing *cyk3-2A* was similar to the wild type (Figure 3.20.A (i) and Figure 3.20.A (ii)), which suggested that the transglutaminase-like domain plays a key role in the regulation of primary septum deposition. We confirmed by Western Blot analysis that protein amount of both *Cyk3* and *Cyk3-2A* was similar (Figure 3.20.A (iii)).

Meitinger *et al.* showed that cells overexpressing *Cyk3* protein deposited a thicker primary septum and, interestingly, those cells showed more dense areas around it, which might correspond to secondary septa

(Meitinger *et al.* 2010). To check that calcofluor staining was specific to the primary septum and that CYK3 overexpression selectively induced synthesis of the primary septum only, we used aniline blue, a dye that selectively binds to β -1,3 glucan, the main component of the secondary septum (Onishi *et al.* 2013).

chs3 Δ cells harbouring GAL-CYK3 (YIMP235) or GAL-*cyk3-2A* (YMF576), and control cells (YMF505) were grown overnight in YPRaff, synchronised in G1 phase of the cell cycle by addition of mating pheromone, and culture was shifted to medium YPGal to induce the overexpression of the protein. After releasing cells from G1 block, aniline blue was added after 35 minutes of the release and cells were collected at different time points after the release, to analyse in live cells the strength of the secondary septum signal in each strain (Figure 3.20.B).

Our results showed clearly a similar intensity of secondary septa between cells overexpressing mutant or wild type *Cyk3*, suggesting that the phenotype previously observed is effectively due to a different regulation in primary septum formation but not in secondary septa synthesis (Figure 3.20.B (i) and Figure 3.20.B (ii)).

These results also raise the question whether the observed thicker septa are due to a higher activity of *Chs2* protein, or a higher percentage of *Chs2* localisation. In order to address this question, we looked at *Chs2*

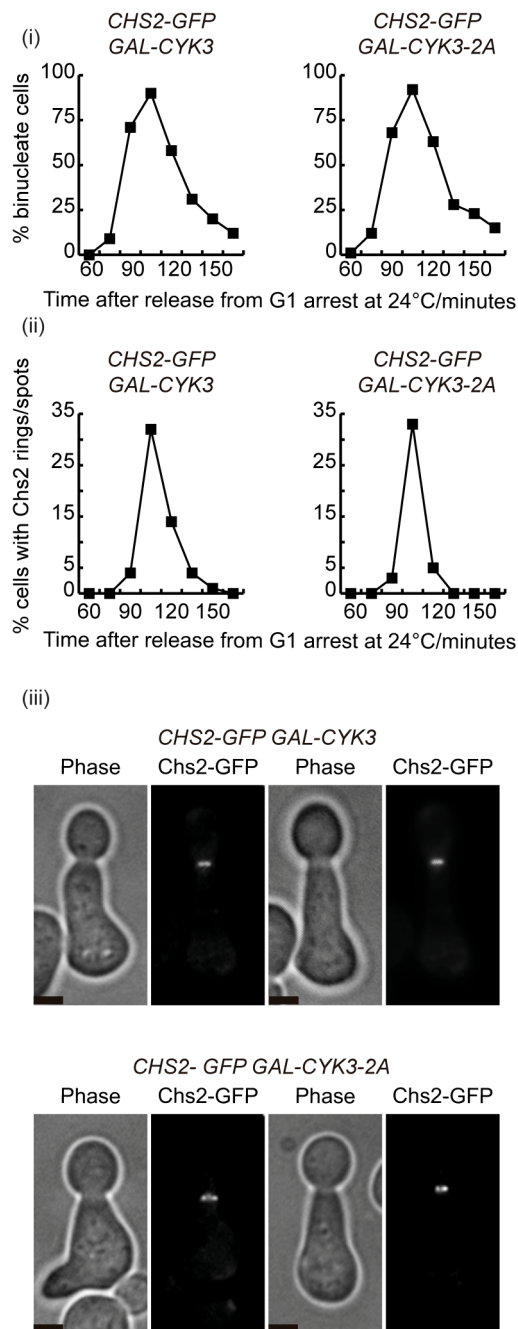


Figure 3.21: Deposition of thicker primary septa upon overexpression of Cyk3 is not due to Chs2 localisation.

(i) *GAL-CYK3* (YMF610) and *GAL-CYK3-2A* (YIMP423) strains were grown in medium containing raffinose, synchronised in G1 phase of the cell cycle, and protein overexpression was induced by media shift to galactose. Upon G1 release, samples were taken to monitor cell cycle progression (i) and Chs2-GFP localisation at the site of division (ii). (iii) Examples of cells with Chs2-GFP localisation are shown. Scale bar corresponds to 2µm.

localisation in cells overexpressing Cyk3 or Cyk3-2A.

To do that, we grew *CHS2-GFP GAL-CYK3* (YMF610) and *CHS2-GFP GAL-cyk3-2A* (YIMP423) cells in media containing raffinose, and induced a block in G1 phase of the cell cycle by addition of mating pheromone when cells were in exponential phase. After changing the carbon source to galactose to induce the overexpression of Cyk3 or Cyk3-2A, cells were released from G1 block and were allowed to progress through the cell cycle synchronously, while samples were taken to monitor Chs2-GFP localisation and cell cycle progression (Figure 3.21). Cell cycle progression occurred in a similar way in both strains (Figure 3.21). Furthermore, Chs2-GFP localisation peaked at 105 minutes upon release from G1 block in both strains, suggesting that these differences in primary septum deposition are due to Chs2 activity rather than a different localisation pattern at the site of division (Figure 3.21 (i), Figure 3.21 (ii) and Figure 3.21 (iii)).

Taken together, these results suggest that Cyk3 specifically controls primary septum synthesis through conserved residues lying within its transglutaminase-like domain.

3.9 Synthetic lethality of C2-HOF1 and lack of Cyk3 is rescued by a hypermorphic allele of CHS2 and reveals an unexpected role for Inn1 C-terminus.

We have shown that histidine H563 and aspartic acid D578 residues within Cyk3 transglutaminase-like domain are necessary to induce the synthesis of the primary septum by Chs2, so we wanted to address whether the synthetic lethality in cells harbouring *C2-HOF1* and *cyk3-2A* could be rescued with a hypermorphic allele of *CHS2* that promotes chitin synthase activity, namely *CHS2-V377I* (Devrekanli et al., 2012).

We dissected tetrads from a diploid strain harbouring *C2-HOF1 cyk3-2A CHS2-V377I* (YIMP466). Upon analysis of the meiotic progeny, we showed that the *CHS2-V377I* allele is able to rescue the lethality of *C2-HOF1 cyk3-2A*, strengthening the hypothesis of Cyk3 being involved in the regulation of primary septum synthesis by Chs2 as the triple mutant was alive (Figure 3.22.A (i) and Figure 3.22.A (ii)).

We then aimed to address whether a strain lacking full-length Cyk3 could reproduce the previous result. In order to do that, we dissected tetrads from a diploid strain harbouring *C2-HOF1 cyk3Δ CHS2-V377I* alleles (YIMP11). Analysis of the meiotic progeny showed that *CHS2-V377I* allele is also able to compensate for *C2-HOF1 cyk3Δ*

synthetic lethality (Figure 3.22.B (i) and Figure 3.22.B (ii)).

This result was reproduced using *cyk3-aid* conditional degron. We spotted strains YIMP257 (*C2-HOF1 cyk3-aid CHS2-V377I*), YIMP73 (*C2-HOF1 cyk3-aid*) and YIMP258 (*C2-HOF1 CHS2-V377I*) in permissive YPDCu or restrictive YPGalCu supplemented with NAA and IAA auxins. We found that *CHS2-V377I* was able to rescue defects associated to cells harbouring *C2-HOF1* fusion and lacking *CYK3* (Figure 3.22.B (iii)).

These experiments have shown that *CYK3* becomes essential in a *C2-HOF1* background due to defects in primary septum formation in a Chs2-related fashion. Understanding why *CYK3* becomes essential could help us to reveal the molecular details of this regulation.

One possibility could be that *CYK3* becomes essential because the presence of the C2 fusion blocks the arrival of wild type Inn1 to the site of division. Hence, Inn1 C-terminus would have the same function as Cyk3 and cells could cope with lack of one of these proteins, but not both (Figure 3.23A (i)). In order to answer this question, we used degron to deplete *td-inn1-aid* and *cyk3-aid* in a *C2-HOF1* background, while expressing the C-terminus from another locus. This strain YIMP250 (*C2-HOF1 cyk3-aid td-inn1-aid OsTIR1 pRS305-INN1-Cterminus-GFP*), with following controls YJW15 (*OsTIR1*), YIMP60

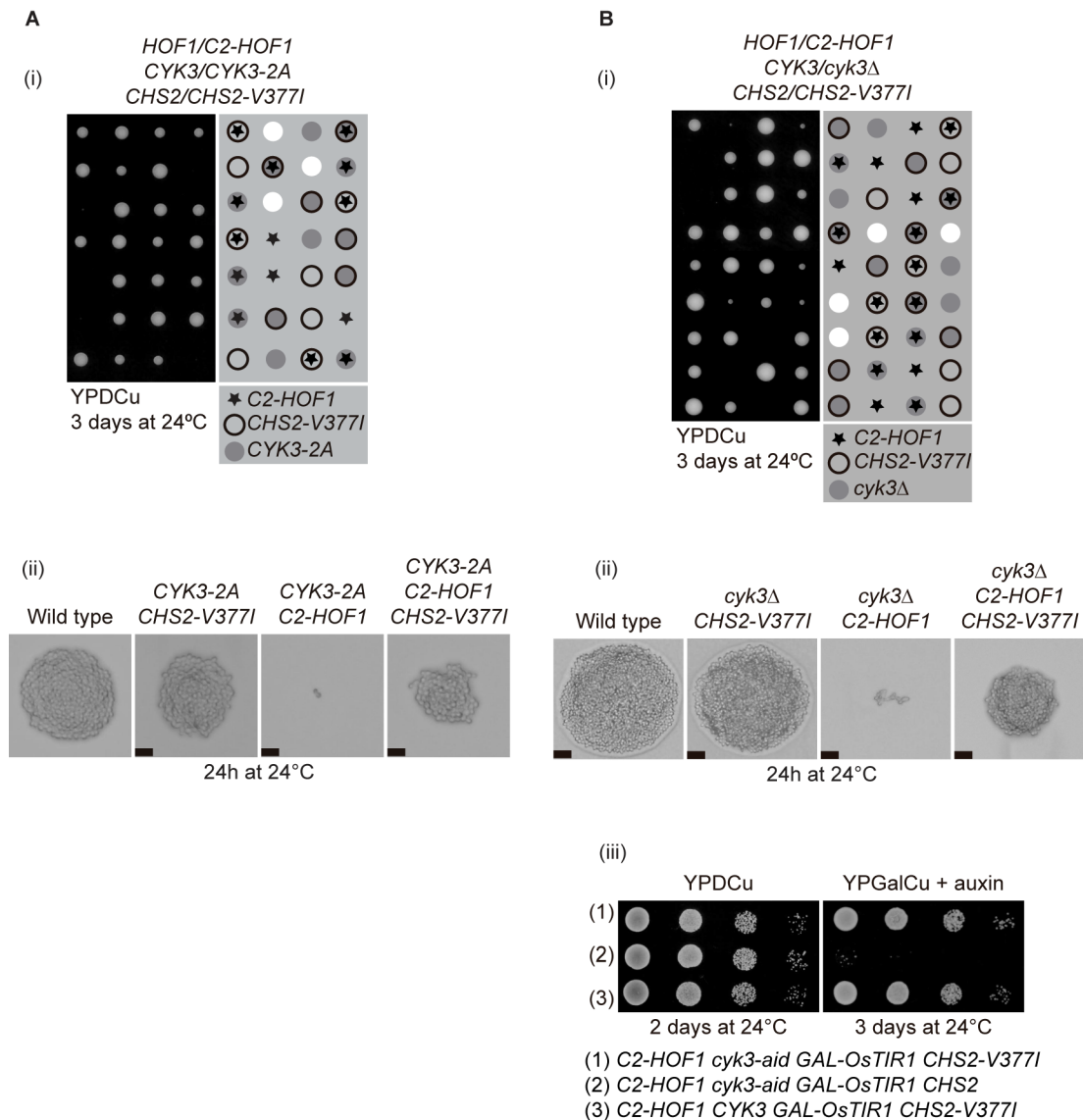


Figure 3.22: The synthetic lethal combination of *C2-HOF1* and the lack of *CYK3* is rescued by the hypermorphic allele of *Chs2*, *CHS2-V377I*.

(A) (i) Diploid strain *HOF1/C2-HOF1 CYK3/cyk3-2A CHS2/CHS2-V377I* (YIMP466) was sporulated, the meiotic progeny was analysed and (ii) photos of tetrads of the indicated genotypes were taken after 24 hours incubation on YPDCu plates at 24°C. Scale bar corresponds to 20µm. (B) Diploid strain *HOF1/C2-HOF1 CYK3/cyk3Δ CHS2/CHS2-V377I* (YIMP11) was sporulated, the meiotic progeny was analysed and (ii) photos of tetrads of the indicated genotypes were taken after 24 hours incubation on YPDCu plates at 24°C. Scale bar corresponds to 20µm. (iii) *C2-HOF1 cyk3-aid GAL-OsTIR1 CHS2-V377I* (YIMP257), *C2-HOF1 cyk3-aid GAL-OsTIR1* (YIMP73) and *C2-HOF1 GAL-OsTIR1 CHS2-V377I* (YIMP258) cells were spotted onto YPDCu plates and YPGalCu plates supplemented with NAA and IAA auxins, and plates were incubated at the corresponding temperature for the indicated number of days.

(*OsTIR1 cyk3-aid*), YIMP242 (*C2-HOF1 td-inn1-aid OsTIR1*), YIMP240 (*C2-HOF1 td-inn1-aid cyk3-aid OsTIR1*) and YIMP249 (*C2-HOF1 td-inn1-aid OsTIR1 pRS305-INN1-Cterminus-GFP*) were spotted onto YPDCu plates supplemented or not with NAA and IAA auxins and incubated at 24°C (Figure 3.23.A (ii)).

Ectopic expression of Inn1 C-terminus was unable to rescue the lethality from these cells, suggesting that these proteins do not share a common function (Figure 3.23.A (ii)).

In order to assess the possibility that expression of this *C2-HOF1* fusion would prevent the localisation of wild type Inn1, we

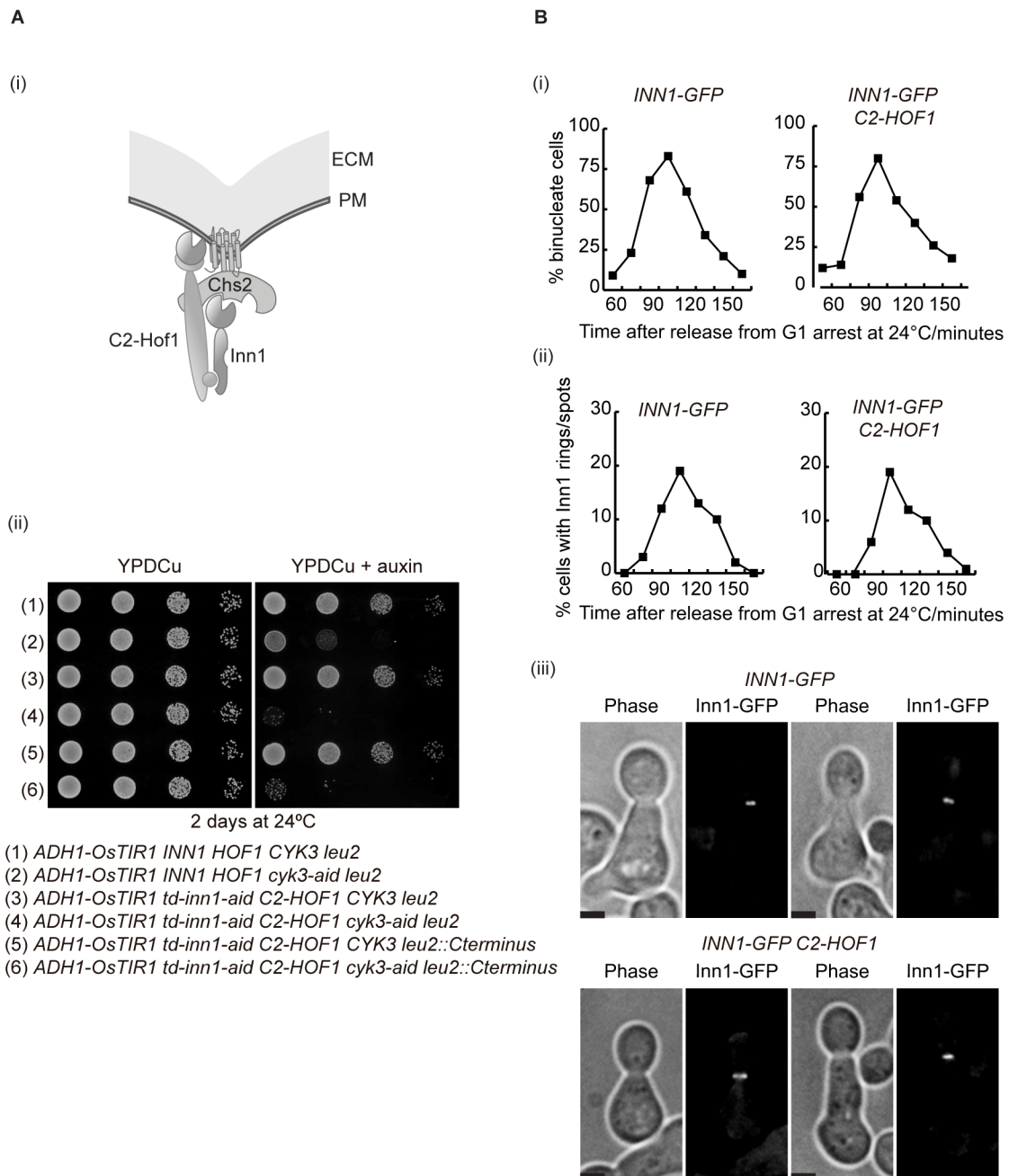


Figure 3.23: C-terminus of Inn1 and Cyk3 do not share a common function.

(A) (i) *C2-Hof1* fusion does not displace Inn1 from arriving at the site of division. (i) Diagram of the hypothesis. If *Cyk3* and *Inn1* C-terminus share the same function, cells would cope with lacking one, but not both. (ii) Corresponding strains *ADH1-OsTIR1* (YJW15), *ADH1-OsTIR1 cyk3-aid* (YIMP60), *td-inn1-aid ADH1-osTIR1 C2-HOF1* (YIMP242), *td-inn1-aid ADH1-OsTIR1 cyk3-aid C2-HOF1* (YIMP240), *td-inn1-aid ADH1-OsTIR1 C2-HOF1 INN1-Cterminus-GFP* (YIMP249) and *td-inn1-aid ADH1-OsTIR1 cyk3-aid C2-HOF1 INN1-Cterminus-GFP* (YIMP250) were spotted onto YPDCu plates and YPDCu plates supplemented with NAA and IAA auxins, and plates were incubated at the corresponding temperature for the indicated number of days. **(B)** *C2-Hof1* fusion does not block arrival of *Inn1* to the site of division. *C2-HOF1 INN1-GFP* (YIMP196) and control (YIMP207) cells were grown in YPRaffCu media, synchronised in G1 phase and allowed to progress through the cell cycle synchronously while monitoring cell cycle progression (i) and *Inn1-GFP* localisation (ii). Fluorescence microscopy pictures of the indicated strains are represented in (iii). Scale bar corresponds to 2µm.

grew *C2-HOF1 INN1-GFP* (YIMP196) and control *INN1-GFP* cells (YIMP207) to compare *Inn1* localisation. Briefly, after synchronising

cells in G1 phase of the cell cycle in medium containing raffinose, cells were released synchronously into the medium containing

galactose and samples were taken to follow cell cycle progression and Inn1-GFP localisation (Figure 3.23.B). Chromosome segregation occurred in a similar fashion in both strains and, more importantly, Inn1-GFP was able to localise at the site of division regardless of the presence of C2-Hof1 fusion (Figure 3.23B (i), 3.23B (ii) and 3.23B (iii)). This confirmed that Inn1 was able to localise at the site of division even in a *C2-HOF1* background.

A second option could be that, because two C2 domains would be present at the site of division in *C2-HOF1* cells (from C2-Hof1 and wild type Inn1), the Cyk3 presence would be necessary to regulate Chs2 function due to an excess of C2 activity, as C2 domain on its own could induce primary septum formation (Nishihama *et al.* 2009).

To test whether C2 domain of Inn1 could interact directly with Chs2 for this regulation, we used the same approach as previously explained (details in section 2.2.6 in Materials and Methods). Briefly, Rosetta *E. coli* cells were used to express either a fragment of Chs2 containing its catalytic domain as Strep-Chs2 (215-629aa), or 6HIS-tagged C2 domain of Inn1 (1-134aa). After mixing both cell pellets, including appropriate controls with empty plasmids, cell lysates were prepared and purification was carried out on Strep resin first, and eluate was loaded onto a nickel column. Final eluates showed that the C2 domain of Inn1 is able to directly interact with a

fragment of Chs2 containing its catalytic domain (Figure 3.24.A (i)).

To test the hypothesis of whether excess of C2 at the site of division is causing the defect, we wanted to inactivate one of the two C2 domains. We used a modified Inn1 protein, Inn1-K31A, which contains a residue of alanine instead of a lysine at position 31 within the C2 domain. That single change is enough to disrupt Inn1 C2 function (Sanchez-Diaz *et al.* 2008, Devrekanli *et al.* 2012) (Figure 3.24.A (ii)).

To test our hypothesis, we depleted both *td-inn1-aid* and *cyk3-aid* in a *C2-HOF1* background, while expressing from another locus a C2-inactive allele of Inn1. This strain YIMP142 (*C2-HOF1 cyk3-aid td-inn1-aid OsTIR1 pRS305- INN1-GFP-K31A-GFP*), with controls YJW15 (*OsTIR1*), YIMP60 (*cyk3-aid OsTIR1*), YIMP43 (*C2-HOF1 OsTIR1*), YIMP41 (*C2-HOF1 cyk3-aid OsTIR1*), YIMP149 (*td-inn1-aid OsTIR1 pRS305- INN1-GFP-K31A-GFP*) and YIMP147 (*C2-HOF1 td-inn1-aid OsTIR1 pRS305-INN1-GFP-K31A-GFP*), were spotted onto YPD plates or YPD plates supplemented with NAA and IAA auxins, and incubated at 24°C (Figure 3.24.A (iii)).

Expression of this C2-inactive allele could not rescue the lethality due to the lack of Cyk3 in a *C2-HOF1* background. This suggests that the two C2 domains are not the reason why *CYK3* becomes essential (Figure 3.24.A (iii)).

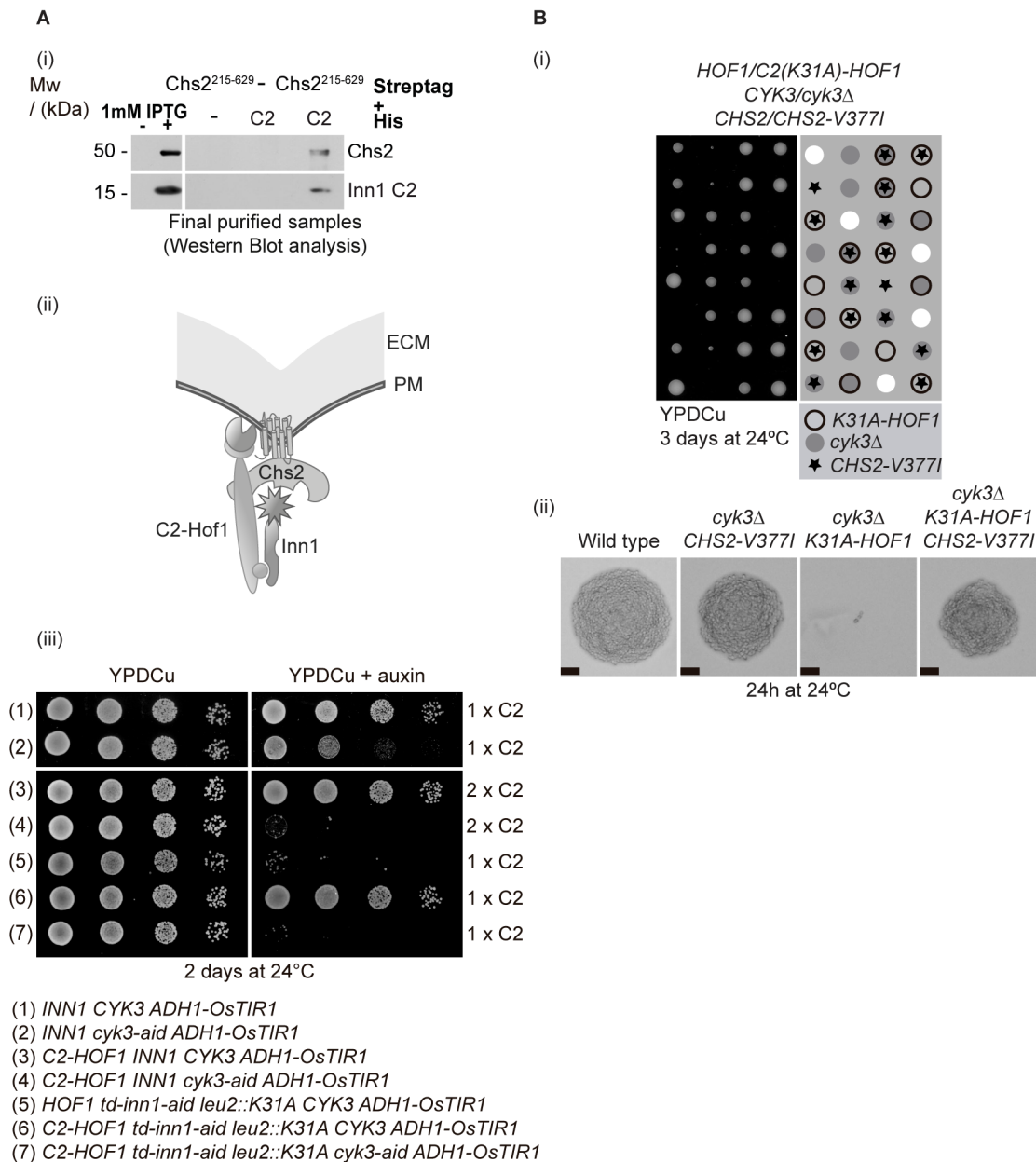
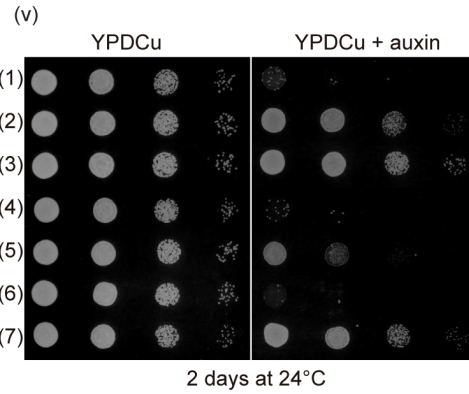
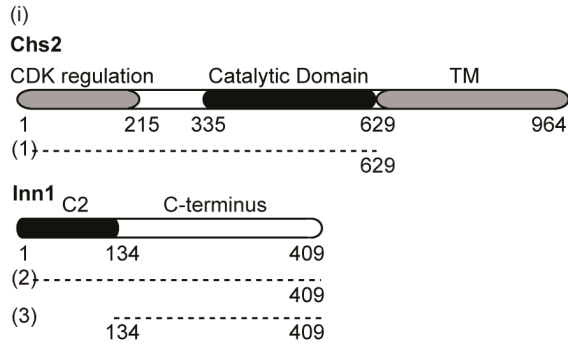


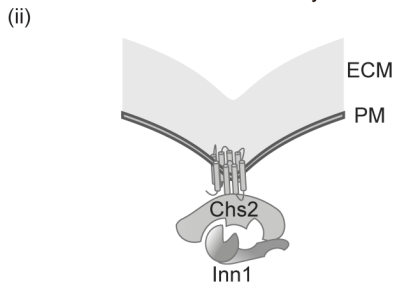
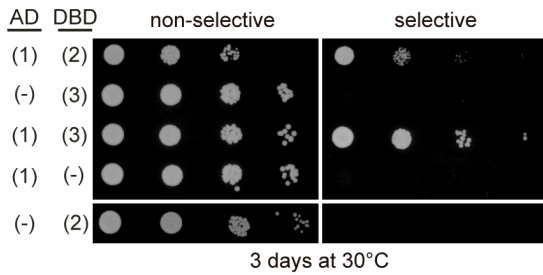
Figure 3.24: C-terminus of Inn1 is not able to compensate the lack of Cyk3 in C2-HOF1 cells.

(A) (i) Indicated *E. coli* strains containing plasmids pMF36 (Strep-Chs2(215-629aa)), pET100 (Strep-empty); pMFAD12 (6His-5xGA-C2) and pET28c (6His-empty) were grown at 37°C, and protein induction was performed at an OD₆₀₀ of 0.6 upon addition of IPTG for two hours. Corresponding cultures were mixed and strep-tagged protein was purified, and eluates were further purified through their 6His-tag. Final eluates were analysed by immunoblotting with anti-His and anti-Strep antibodies. (ii) Diagram of the hypothesis. As Inn1 C2 domain regulates Chs2 activity, we postulated that having two C2 domains at the site of division would require Cyk3 presence to counter-regulate an excess signalling. (iii) Corresponding strains *ADH1-OsTIR1* (YJW15), *ADH1-OsTIR1 cyk3-aid* (YIMP60), *C2-HOF1 ADH1-OsTIR1-9MYC* (YIMP43), *C2-HOF1 ADH1-OsTIR1-9MYC cyk3-aid* (YIMP41), *td-inn1-aid ADH1-osTIR1 K31A-GFP* (YIMP149), *td-inn1-aid ADH1-osTIR1 K31A-GFP C2-HOF1* (YIMP147) and *td-inn1-aid ADH1-osTIR1 K31A-GFP cyk3-aid C2-HOF1* (YIMP142) were spotted onto YPDCu plates and YPDCu plates supplemented with NAA and IAA auxins, and plates were incubated at the corresponding temperature for the indicated number of days. (B) (i) Diploid *HOF1/C2-K31A-HOF1 CYK3/cyk3Δ CHS2/CHS2-V377I* (YIMP12) was sporulated, and the meiotic progeny was analysed. (ii) Photos of tetrads of the indicated genotypes were taken after 24 hours incubation on YPDCu plates at 24°C. Scale bar corresponds to 20µm.

In order to assess whether inactivation of any strain in which the C2 domain fused to Hof1 of the C2 domains could produce the same effect, we dissected tetrads from a diploid strain in which the C2 domain fused to Hof1 protein was inactive: *HOF1/C2(K31A)-HOF1 CYK3/cyk3Δ CHS2/CHS2-V377I* (YIMP12).



- (1) *ADH1-OsTIR1 td-inn1-aid*
 (2) *ADH1-OsTIR1 td-inn1-aid CHS2-V377I*
 (3) *ADH1-OsTIR1 td-inn1-aid C2-HOF1*
 (4) *ADH1-OsTIR1 td-inn1-aid cyk3-aid*
 (5) *ADH1-OsTIR1 td-inn1-aid cyk3-aid CHS2-V377I*
 (6) *ADH1-OsTIR1 td-inn1-aid cyk3-aid C2-HOF1*
 (7) *ADH1-OsTIR1 td-inn1-aid cyk3-aid CHS2-V377I C2-HOF1*



HOF1/C2-HOF1
CYK3/cyk3Δ
INN1/inn1Δ
CHS2/CHS2-V377I

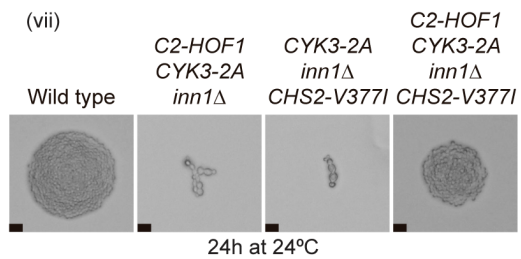
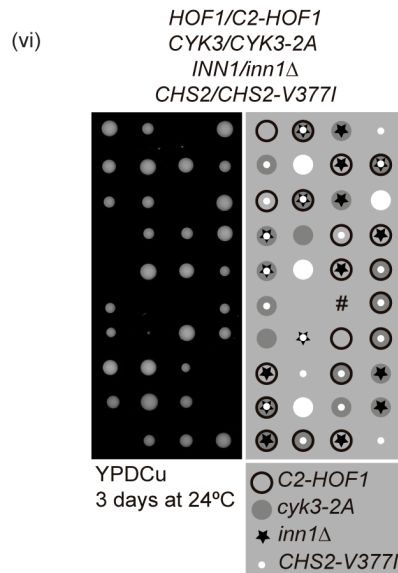
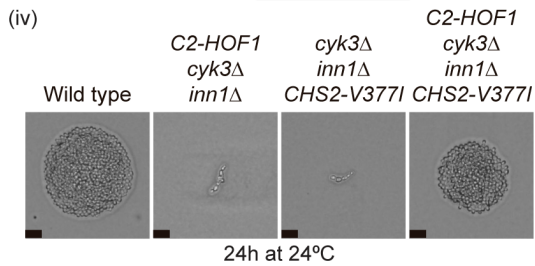
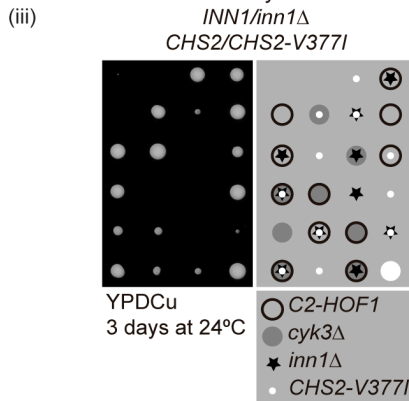


Figure 3.25: C-terminus domain of Inn1 is responsible for the synthetic lethality in C2-HOF1 cells lacking Cyk3 function because of misregulation of Chs2 protein.

(i) Diagram of the yeast two-hybrid fragments used in the assay and yeast two-hybrid interactions between Inn1 and Chs2. (ii) Diagram of the hypothesis. As Inn1 C-terminus can also interact with Chs2, we postulated that the presence of C-terminus of Inn1 could be the reason why C2-HOF1 cells lacking CYK3 die. (iii) Asci from diploid *INN1/inn1Δ HOF1/C2-HOF1 CHS2/CHS2-V377I CYK3/cyk3Δ* (YIMP390) were dissected, and meiotic progeny was analysed and (iv) photos of tetrads of the indicated genotypes were taken after 24 hours incubation on YPDCu plates at 24°C. Scale bar corresponds to 20µm. (v) shows representative pictures of the indicated colonies. (v) Corresponding strains *td-inn1-aid ADH1-osTIR1* (YIMP324), *td-inn1-aid ADH1-osTIR1 CHS2-V377I-hphNT* (YIMP325), *td-inn1-aid ADH1-osTIR1 C2-HOF1* (YIMP242), *td-inn1-aid ADH1-osTIR1 cyk3-aid* (YIMP306), *td-inn1-aid ADH1-osTIR1 cyk3-aid CHS2-V377I* (YIMP308), *td-inn1-aid ADH1-osTIR1 cyk3-aid C2-HOF1* (YIMP240) and *td-inn1-aid ADH1-osTIR1 cyk3-aid C2-HOF1 CHS2-V377I* (YIMP310) were spotted onto YPDCu and YPDCu supplemented with NAA and IAA auxins, and photos were taken after the indicated number of days. (vi) Diploid *HOF1/C2-HOF1 INN1/inn1Δ CYK3/CYK3-2A CHS2/CHS2-V377I* (YIMP388) was sporulated, and the meiotic progeny was analysed and photos of tetrads (vii) of the indicated genotypes were taken after 24 hours incubation on YPDCu plates at 24°C. Scale bar corresponds to 20µm.

When analysing the meiotic progeny, this fusion was still synthetic lethal in combination with *cyk3Δ*, which further suggests that the presence of two C2 domains is not the reason why *CYK3* becomes essential (Figure 3.24.B (i) and Figure 3.24.B (ii)).

Yeast two-hybrid analysis carried out in our laboratory showed that the C-terminus of Inn1 was also able to interact with the catalytic domain of Chs2, which could point out to a role of the C-terminus, additionally to the C2 domain, in the regulation of Chs2 activity (Figure 3.25 (i) and 3.25 (ii)).

To try the possibility that the C-terminus of Inn1 could also regulate Chs2, a diploid strain lacking both *Cyk3* and Inn1 C-terminus (*HOF1/C2-HOF1 INN1/inn1Δ CYK3/cyk3Δ CHS2/CHS2-V377I*) (YIMP390) was sporulated, and dissected tetrads were analysed. Indeed, cells harbouring *C2-HOF1* fusion could be rescued by deleting *CYK3* and *INN1* at the same time, as long as they also contained the *CHS2-V377I* allele. These cells, without C-terminus function or *Cyk3* function,

were able to survive when they were supplied with a constitutively active allele of *CHS2-V377I* (Figure 3.25 (iii) and Figure 3.25 (iv)).

To confirm this result, we used conditional degrons to deplete *td-inn1-aid* and *cyk3-aid* in a *C2-HOF1* background harbouring *CHS2-V377I* allele. Experimental strain YIMP310, together with corresponding controls YIMP324 (*OsTIR1 td-inn1-aid*), YIMP325 (*OsTIR1 td-inn1-aid CHS2-V377I*), YIMP242 (*OsTIR1 td-inn1-aid C2-HOF1*), YIMP306 (*OsTIR1 td-inn1-aid cyk3-aid*), YIMP308 (*OsTIR1 td-inn1-aid cyk3-aid CHS2-V377I*) and YIMP240 (*OsTIR1 td-inn1-aid cyk3-aid C2-HOF1*), were spotted on permissive YPDCu or restrictive YPDCu supplemented with NAA and IAA auxins and incubated at 24°C. We showed that we were able to reproduce the previous result, namely that cells lacking both *Cyk3* and Inn1 C-terminus can survive as long as they harbour the hypermorphic *CHS2* allele, *CHS2-V377I* (Figure 3.25 (v)).

Next, we aimed to address whether inactivation of transglutaminase-like domain

activity (*cyk3-2A*) could reproduce the same results as above. Hence, we obtained a diploid strain harbouring *HOF1/C2-HOF1 INN1/inn1Δ CYK3/cyk3-2A CHS2/CHS2-V377I* (YIMP388). After tetrad dissection, analysis of the meiotic progeny showed that the mutants *C2-HOF1 cyk3-2A inn1Δ* were rescued by introducing *CHS2-V377I* allele (Figure 3.25 (vi) and 3.25 (vii)).

Taken together, these results showed that both the transglutaminase-like domain of Cyk3 and the C-terminus domain of Inn1 collaborate to regulate the activity of chitin synthase Chs2.

3.10 Defects in primary septum deposition cause the lethality associated to depletion of Cyk3 in *C2-HOF1* cells

As it has been shown that cells lacking Chs2 function have an actomyosin ring that breaks abruptly and disassembles upon contraction (VerPlank and Li 2005), we aimed to investigate what happens to the actomyosin ring in *C2-HOF1* cells depleted from Cyk3. To do so, we first compared the kinetics of Myo1 at the site of division during cytokinesis.

To allow conditional Cyk3 depletion, we used the double degron strain *td-cyk3-aid* in a strain harbouring *C2-HOF1* fusion and C-terminally tagged *MYO1-GFP* to follow kinetics of the type-II myosin Myo1 by time-course microscopy. We grew *C2-HOF1 td-cyk3-aid MYO1-GFP* (YIMP209) and control (YIMP452)

cells in medium containing raffinose at 24°C, and synchronised them in G1 phase of cell cycle by addition of mating pheromone. After shifting the culture to medium containing galactose to induce expression of E3 ubiquitin ligases Ubr1 and Tir1 for 90 minutes and adding NAA and IAA auxins to induce depletion of Td-*cyk3-aid*, cells were released from G1 block at 24°C. Samples were collected to follow cell cycle progression and study Myo1-GFP localisation (Figure 3.26 (i)).

Flow cytometry found that controls cells went correctly through cell division, while *C2-HOF1 td-cyk3-aid* accumulated as binucleate cells at the end of the experiment, which confirmed that those cells had a cytokinetic defect (Figure 3.26 (ii)).

However, timing and localisation of Myo1-GFP was quite similar in control and *C2-HOF1 td-cyk3-aid MYO1-GFP* cells, which suggests that the actomyosin ring was assembled and disassembled in a similar fashion in both cells (Figure 3.26 (iii)).

To confirm these results, we decided to use time-lapse video microscopy to follow Myo1-GFP localisation in live cells. Control cells harboured *SPC42-eQFP*, which allowed us to mix both strain on the same IBIDI glass chamber and distinguished the identity of the cells throughout the time-lapse experiment. *C2-HOF1 td-cyk3-aid MYO1-GFP* (YIMP209)

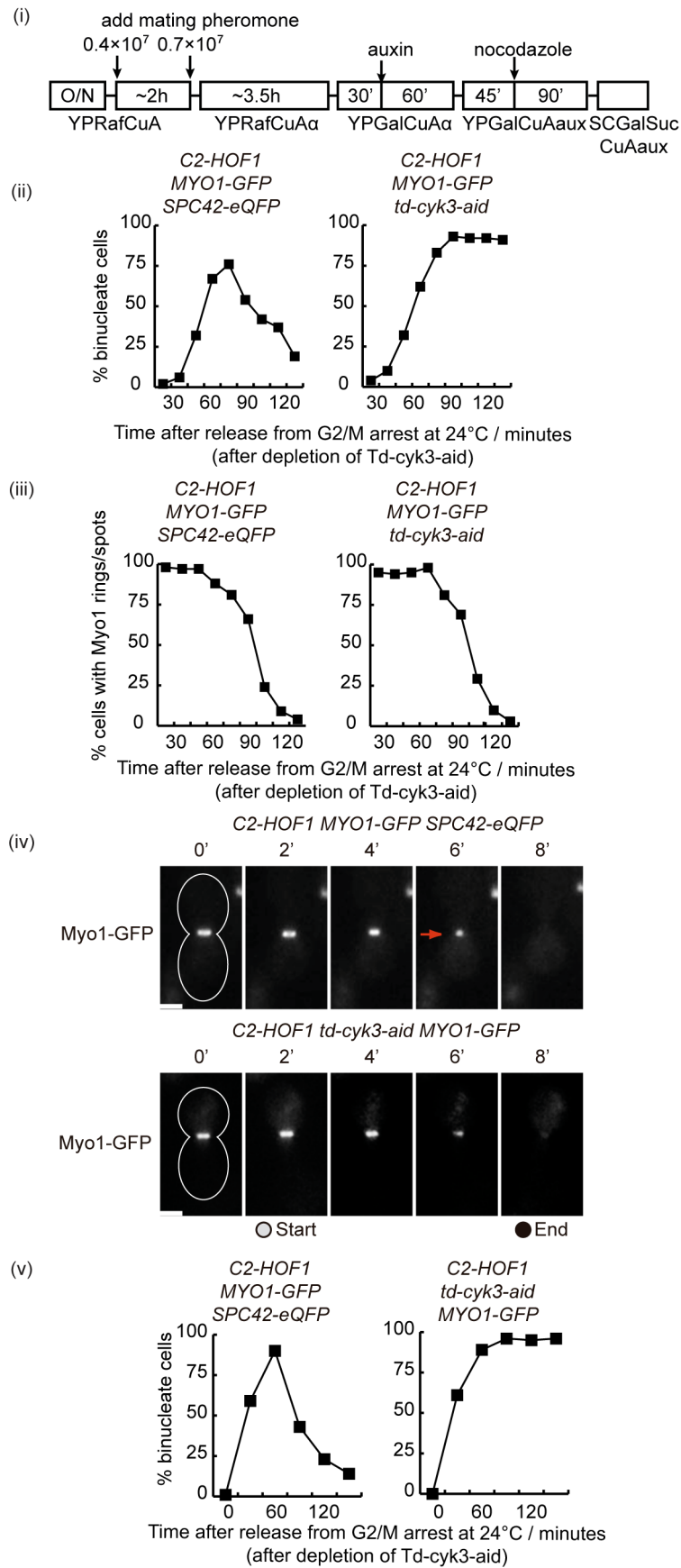


Figure 3.26: Actomyosin ring is assembled and disassembled in *C2-HOF1* cells lacking *Cyk3*.

(i) *C2-HOF1 td-cyk3-aid MYO1-GFP* (YIMP209) and control (YIMP452) were grown and arrested in G1 phase of the cell cycle with mating pheromone at 24°C in YPRaffCu. Cells were released from G1 arrest at 24°C in YPGal after depleting Td-Cyk3-aid. After cells had budded, nocodazole was added to synchronise the cells in G2/M-phase. Cells were then washed into fresh Synthetic Complete medium and allowed to complete mitosis at 24°C. Samples were taken in a time course to monitor chromosome segregation (ii) and Myo1-GFP localisation (iii). The same culture procedure was used to follow cells in time-lapse microscopy, although upon the release from G2/M cells were attached to a concanavalin-coated slide to examine the localisation of Myo1 every two minutes as cells completed mitosis at 24°C (see Materials and Methods for details). Contraction of the actomyosin ring in control cells ends as a “spot”, whereas in mutant cells, the actomyosin ring disappears before that stage. Examples of cells in which time-lapse analysis was used to follow the contraction of the Myo1-GFP ring. Scale bars indicate 2µm. A part of the cells released from G2/M were transferred to a flask instead of the time-lapse chamber, allowing us to take samples to monitor progression through the cell cycle (v).

and control *C2-HOF1 SPC42-eQFP MYO1-GFP* cells (YIMP452) were grown in medium containing raffinose, and mating pheromone was added when cells were at exponential phase to induce a G1 arrest. Afterwards, carbon source was changed to galactose for 90 minutes, and NAA and IAA auxins were added to induce the degradation of Td-cyk3-aid. After releasing cells from G1 in the presence of auxins, cells were allowed to progress into S phase for 45 minutes, and synchronised again in G2/M phase by addition of nocodazole to the media when cells had formed buds, indicating that they had been released from G1 phase and entered S phase. When cells had been synchronised in G2/M phase, indicated by the presence of large-budded cells, cells were washed in fresh synthetic complete (SC) medium containing NAA and IAA auxins. We next mixed strains together to ensure cells went through identical conditions during the time-lapse experiment. Cells were placed on a concanavalin-coated glass chamber to allow cells to get attached to the bottom of the glass (Sanchez-Diaz *et al.* 2008). During time-lapse microscopy, a z-

stack of images was taken to make sure that fluorescent signal across cells was fully analysed. We took pictures every two minutes to ensure we captured actomyosin ring contraction.

After examination of time-lapse video microscopy, we found that the contraction of the actomyosin ring occurred in a similar fashion in control and *C2-HOF1 td-cyk3-aid MYO1-GFP* cells, with a mean value of 5.54 minutes in control cells compared to 5 minutes in the mutant strain depleted of *Cyk3* and in the presence of *C2-Hof1* (Figure 3.26 (iv)). However, mutant cells never showed a single defined Myo1-GFP spot, as a sign of normal cytokinetic dynamics (Figure 3.26 (iv)). Signal at the site of division tended to disappear in mutant cells before showing a defined spot (Figure 3.26 (iv)). Furthermore, in parallel cell division defects were monitored after *Cyk3* depletion by studying the number of binucleate cells. We confirmed that mutant cells suffered a cell division defect (Figure 3.26 (v)).

Taken together, these results suggest that mutant strain conditionally depleted for

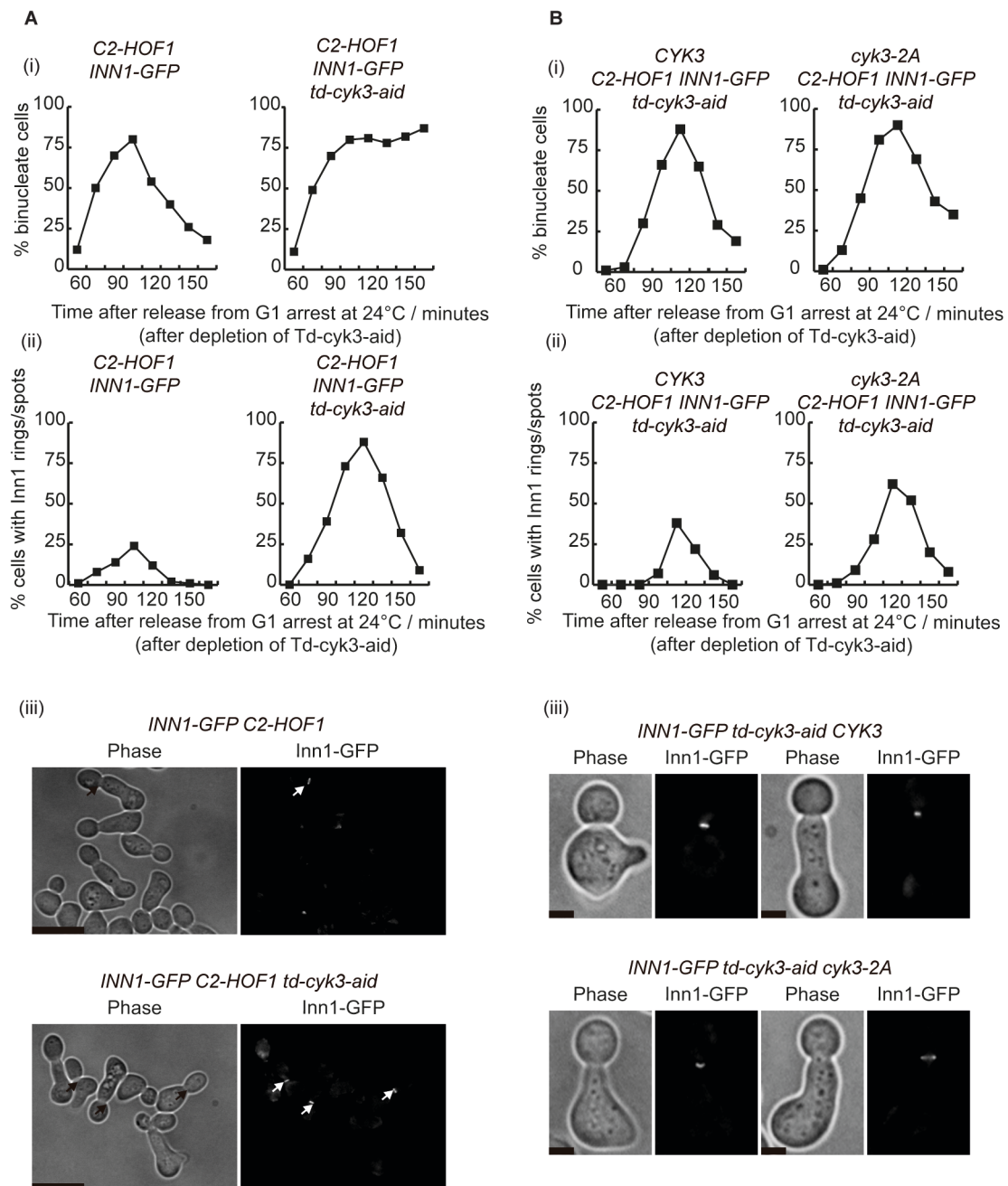


Figure 3.27: Inn1-GFP accumulates in cells lacking functional *CYK3* in the presence of *C2-HOF1*.

(A) *C2-HOF1 td-cyk3-aid INN1-GFP* (YIMP198) and control (YIMP196) cells were grown in YPRaffCu, synchronised in G1 phase of the cell cycle. Upon induction of Td-cyk3-aid degradation by addition of NAA and IAA auxins and changing the sugar source to galactose, samples were collected to monitor chromosome segregation (i) and Inn1-GFP localisation (ii). Examples of cells with Inn1-GFP localisation are shown in (iii). Scale bar corresponds to 2µm. **(B)** *C2-HOF1 td-cyk3-aid leu2::cyk3-2A INN1-GFP* (YIMP416) and control (YIMP417) cells were grown in YPRaffCu, synchronised in G1 phase of the cell cycle. Upon induction of Td-cyk3-aid degradation by addition of IAA and NAA auxins and changing the sugar source to galactose, samples were collected to monitor chromosome segregation (i) and Inn1-GFP localisation (ii). Examples of cells with Inn1-GFP localisation are shown in (iii). Scale bar corresponds to 2µm.

Cyk3 is able to correctly assemble, contract and disassemble an actomyosin ring.

As a next step we aimed to look at the localisation of another ingression progression complex component, Inn1, at the site of

division. We have shown that in wild type cells lacking Cyk3, there is a partial accumulation of Inn1 at the site of division.

C2-HOF1 INN1-GFP cells harbouring the previously described *td-cyk3-aid* double degon (YIMP198), as well as control cells

(YIMP196), were cultured in YP medium containing raffinose, addition of mating pheromone synchronised the cells in G1 phase of the cell cycle. After shifting the carbon source to galactose to induce expression of E3 ligases, and addition of auxins to induce depletion of Td-cyk3-aid, cells were released from G1 block at 24°C in the presence of NAA and IAA auxins and samples were collected to follow cell cycle progression and monitoring Inn1-GFP localisation (Figure 3.27.A).

Indeed, mutant cells conditionally depleted for Td-cyk3-aid accumulated as binucleate cells, whereas control cells were able to progress through the cell cycle and segregate their chromosomes as expected (Figure 3.27.A (i)). Furthermore, we observed under the microscope an accumulation of Inn1-GFP at the site of division in mutant cells. This result was in agreement with what was observed before (Figure 3.27.A (ii) and Figure 3.27.A (iii)).

Using the same experimental approach, we aimed to study whether this result would be reproducible by using the Cyk3-inactive version of the transglutaminase-like domain (*cyk3-2A*) expressed as an extra copy, instead of a full deletion of Cyk3 protein. *C2-HOF1 td-cyk3-aid* cells expressing either *CYK3* (YIMP417) or *cyk3-2A* (YIMP416) were cultured in medium containing raffinose and synchronised in G1 phase of the cell cycle by addition of mating pheromone. Upon shifting

the media to medium containing galactose to induce expression of E3 ligases and adding NAA and IAA auxins to induce depletion of Td-cyk3-aid, cells were released from G1 block at 24°C in the presence of auxins and samples were collected to follow cell cycle progression and monitoring Inn1-GFP localisation (Figure 3.27.B).

Inactivation of the transglutaminase-like domain that contains Cyk3 function induces accumulation of Inn1-GFP at the site of division (Figure 3.27B (ii) and (iii)).

Since there was no delay in actomyosin ring contraction in mutant cells, a possible explanation could be that Inn1 could localise earlier in the cell cycle in these cells. To address this question, we grew *C2-HOF1 td-cyk3-aid INN1-GFP* (YIMP198) and control cells (YIMP196) in medium containing raffinose and synchronised them in G2/M phase of the cell cycle by addition of nocodazole. After shifting the carbon source to galactose and adding NAA and IAA auxins to induce *td-cyk3-aid* depletion, cells were released from G2/M block in the presence of auxins (Figure 3.28).

Cell cycle progression happened in the expected fashion, as mutant cells accumulated as binucleate cells whereas control cells could progress through the cell cycle (Figure 3.28 (i)). Importantly, we could observe Inn1-GFP localisation at the site of division in 33% of *C2-HOF1 td-cyk3-aid INN1-GFP* cells arrested in G2/M phase with high mitotic CDK activity

against none in the control. This result could indicate that in these cells inactivation of *Cyk3* prompts earlier *Inn1* localisation (Figure 3.28 (ii) and Figure 3.28 (iii)).

As cells could localise *Inn1* earlier in the cell cycle, we investigated whether that

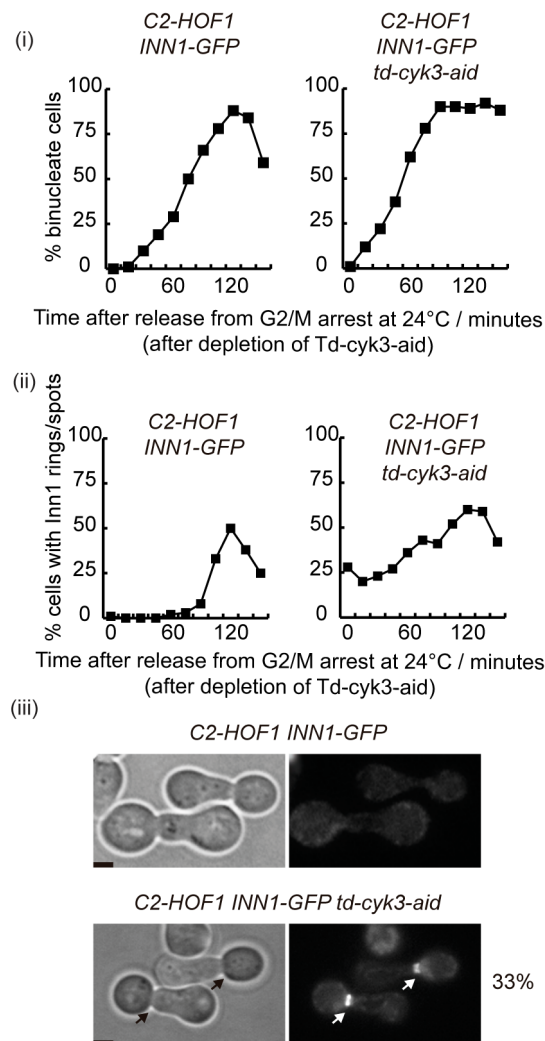


Figure 3.28: *Inn1* is able to localise prematurely in the site of division in cells devoid of *Cyk3* in a *C2-HOF1* background.

C2-HOF1 td-cyk3-aid INN1-GFP (YIMP198) and control (YIMP196) cells were grown in YPRaffCu, and synchronised in G2/M phase of the cell cycle by addition of nocodazole. Upon the induction of *Td-cyk3-aid* degradation by the addition of NAA and IAA auxins and changing the sugar source to galactose, samples were collected to count binucleate cells (i) and monitor *Inn1-GFP* localisation (ii). Examples of cells with *Inn1-GFP* localisation at time zero are shown in (iii). Scale bar corresponds to 2µm.

could have an implication in the synthesis of the primary septum between mother and daughter cells. We initially aimed to approach the problem by following *Chs2-GFP* localisation at the site of division in cells depleted of *Cyk3* and in the presence of *C2-HOF1*. However, cells harbouring *C2-HOF1 td-cyk3-aid CHS2-GFP* would die upon tetrad dissection from strain YIMP428 (*HOF1/C2-HOF1 CYK3/td-cyk3-aid CHS2/CHS2-GFP*) (Figure 3.29.A (i) and Figure 3.29.A (ii)).

We decided to follow primary septum synthesis instead by using calcofluor to stain *Chs2*-synthesised chitinous primary septa, in a *chs3Δ* strain to avoid background signal.

chs3Δ C2-HOF1 td-cyk3-aid (YIMP246) and control *chs3Δ C2-HOF1* cells (YIMP234) grown in YPRaff were synchronised in G1 phase of the cell cycle by addition of mating pheromone. Carbon source was then shifted to galactose and NAA and IAA auxins were added to induce depletion of *Td-cyk3-aid*. Cells were subsequently released from the G1 block in the presence of auxins, and calcofluor was added 35 minutes after the release to stain primary septa, while taking samples to monitor primary septa formation and cell cycle progression (Figure 3.29.B (i) and Figure 3.29.B (ii)).

In control cells, cell cycle progression happened as expected, with cells being able to progress through the cell cycle whereas mutant cells accumulated as binucleate cells (Figure 3.29.B (i)).

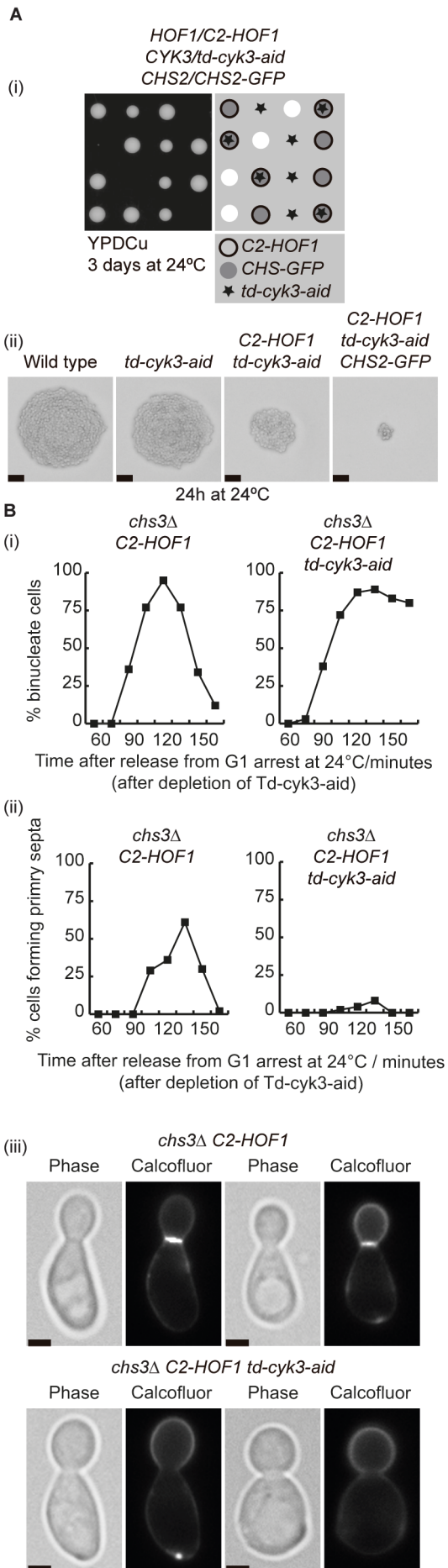


Figure 3.29: C2-HOF1 cells depleted for Cyk3 are unable to lay down primary septa.

(A) Diploid strain *C2-HOF1 td-cyk3-aid CHS2-GFP* (YIMP428) was sporulated, and meiotic progeny was analysed and photos of tetrads (ii) of the indicated genotypes were taken after 24 hours incubation on YPDCu plates at 24°C. (B) *C2-HOF1 td-cyk3-aid chs3Δ* (YIMP246) and control (YIMP234) cells were grown in YPRaffCu. Upon induction of Td-cyk3-aid degradation by addition of NAA and IAA auxins and changing the sugar source to galactose, cells were released from G1 block in the presence of NAA and IAA auxins, and calcofluor was added to stain the primary septa. Samples were taken for monitoring cell cycle progression (i) and primary septa staining by calcofluor (ii). Examples of cells with stained primary septa are shown in (iii). Scale bar corresponds to 2µm.

Importantly when analysing stained primary septa, we showed that, unlike control, mutant strain was unable to synthesise a primary septum between mother and daughter cells, showing that cells conditionally depleted for Td-cyk3-aid in the presence of C2-Hof1 are dying due to a defect in primary septum synthesis (Figure 3.29.B (ii) and 3.29.B (iii)).

Taken together, the results presented in this thesis show that Cyk3 protein plays a crucial role in the process of cytokinesis, not because of an action on the actomyosin ring assembly or contraction, but because of its role in the regulation of the primary septum formation by chitin synthase Chs2.

4. DISCUSSION

4.1 A protein complex coordinates cytokinesis in budding yeast.

Our data support a model in which Cyk3 regulates the activity of chitin synthase Chs2 (Figure 4.1).

These cytokinetic factors, together with the proteins Iqg1 and Myo1, form the Ingression Progression Complex (IPC) (Foltman *et al.* 2016a). Within these complexes, Cyk3 plays an important role stimulating chitin synthase Chs2 activity. The stability of IPC components

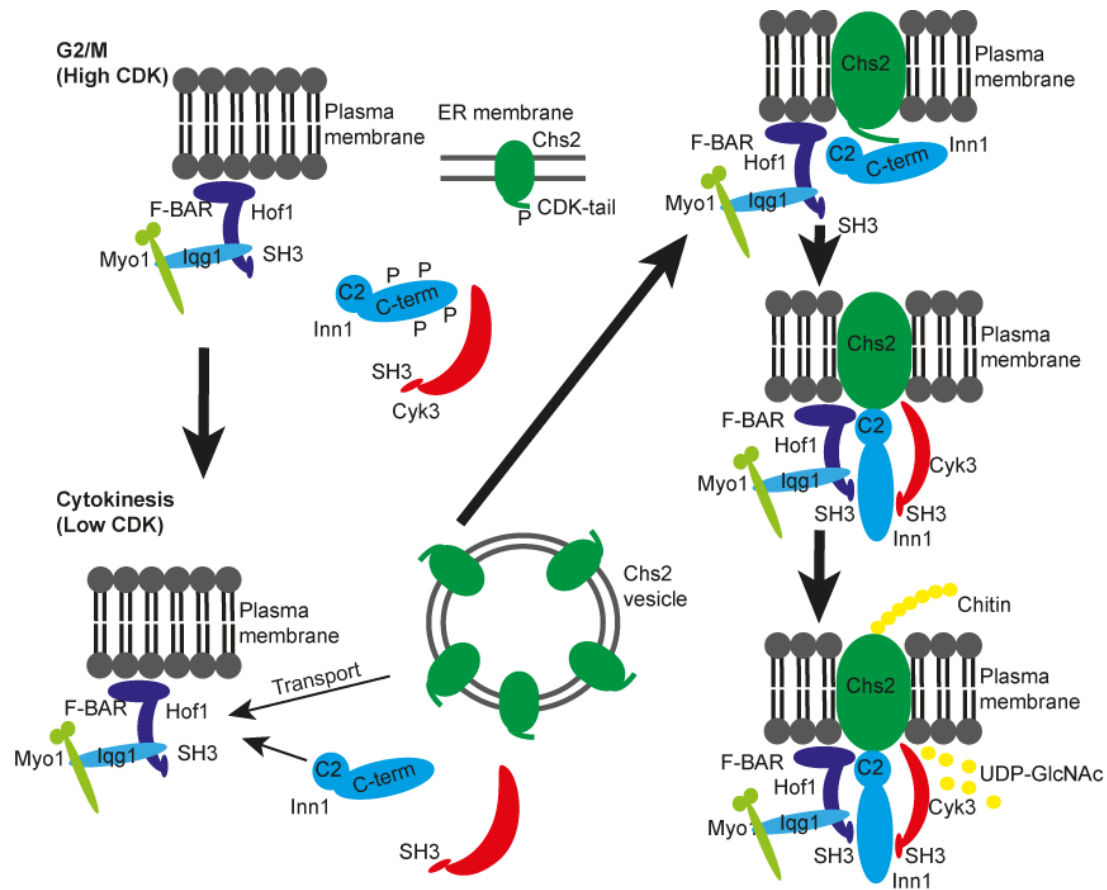


Figure 4.1: Model for the activation of chitin synthase Chs2.

Prior to cytokinesis exit, Chs2 protein is synthesised and stored in the ER membrane, while some other cytokinetic proteins are already localised at the site of division. Upon mitosis exit, Chs2 is incorporated into vesicles, then transported to the cleavage site and finally gets incorporated to the so-called IPCs. These complexes coordinate actomyosin ring contraction, plasma membrane ingression and primary septum deposition, in which Chs2 plays an essential role. The C-terminal end of Inn1 protein plays an unexpected inhibitory role to block the activity of Chs2. The protein Cyk3 is required to remove such block and allow Chs2 to make chitin.

Upon Cdc14 release by the mitotic exit network, Chs2 and cytokinetic factors such as Cyk3 and Inn1 are transported to the site of division (Teh *et al.* 2009, Meitinger *et al.* 2010, Chin *et al.* 2012, Oh *et al.* 2012), where cytokinetic protein Hof1 is located since G2 phase of the cell cycle (Vallen *et al.* 2000).

at the site of division depends on the scaffolding role of type-II myosin (Boyne *et al.* 2000, Wloka *et al.* 2013) as they show Myo1-dependent immobility, and depend on Myo1 to localise to the site of division (Sanchez-Diaz *et al.* 2008).

Table 4.1: Glycosyltransferase enzymes involved in cell division in different organisms (details in the main text).

Enzyme	Organism	Polymer	Lack of activity	Reference
Chs2	<i>S. cerevisiae</i>	Chitin	Cytokinesis failure	VerPlank and Li, 2005
Bgs1	<i>S. pombe</i>	Beta-glucan	Cytokinesis failure	Cortes et al., 2007
Chondroitin synthase	<i>C. elegans</i>	Chondroitin	Cytokinesis failure	Mizuguchi et al., 2013
Glucuronyl transferase-I	<i>M. musculus</i>	Chondroitin sulfate, heparan sulfate	Cytokinesis failure	Izumikawa et al., 2010

The multiple interactions between Myo1, Iqg1, Hof1, Inn1, Cyk3 and Chs2 form the IPCs (Foltman *et al.* 2016a) to coordinate actomyosin ring contraction, plasma membrane ingression and extracellular matrix remodelling. Although the enzymatic details of extracellular matrix remodelling are not conserved throughout evolution, the mechanism underlying it is. Extracellular matrix remodelling takes place thanks to special enzymes called glycosyltransferases, which can synthesise long sugar chains from UDP-sugar monomers; and lack of function of these enzymes result in cytokinesis failure and cell death in different organisms. Thus, blocking beta-glucan synthase Bgs1 function in *S. pombe* leads to the deposition of a discontinuous, non-symmetric septum, and eventually cell death (Cortes *et al.* 2007). In a similar way, RNAi blocking of a chondroitin synthase in *C. elegans* leads to early embryonic death due to cytokinetic failure (Mizuguchi *et al.* 2003). Finally, blocking of a glucuronyltransferase in *M. musculus* also leads to early embryonic death due to a

cytokinesis defect (Izumikawa *et al.* 2010) (Table 4.1).

4.2 Is Chs2 conserved throughout evolution?

In higher eukaryotes, the glycosyltransferases that harbours the most homology to Chs2 are the three human hyaluronan synthases (HAS), especially HAS3, which polymerises N-acetylglucosamine and glucuronic acid alternatively (Weigel 2002). In line with Chs2 role in cell division, it has been shown that hyaluronic acid (HA) synthesis by HAS increases during mitosis (Brecht *et al.* 1986).

It is interesting to note that only the specific glycosyltransferase enzyme is needed to provide synthesis of a certain polymer in the cell, as inducing *HAS2* expression in *Drosophila* is sufficient to drive synthesis of hyaluronan (Takeo *et al.* 2004). Inversely, supplying *Streptococcus equisimilis* SeHAS with N-acetylglucosamine leads to synthesis of short chitin oligomers (Weigel *et al.* 2015), suggesting that the synthesis of the

extracellular matrix is more conserved than initially anticipated. Accordingly, analysis of sequence identity shows a 30% sequence identity between ScChs2 and human HAS3. More importantly, key residues for Chs2 function are conserved in HsHAS3 such as K417, D441, D562, Q601, R604 and W605 (Nagahashi *et al.* 1995, Devrekanli *et al.* 2012), which are necessary for Chs2 chitin synthase activity (Figure 4.2).

induction of restrictive conditions (Figure 3.29). Interestingly, Chs2 enzyme has an ortholog in the pathogenic yeast *Candida albicans*, *CHS1*, which has been shown to be active when introduced in *S. cerevisiae* and rescues defects associated to the lack of ScCHS2 (Au-Young and Robbins 1990). Harboring a 50% homology with ScChs2, this enzyme is also essential (Munro *et al.* 2001), and hence constitutes a possible target against fungal

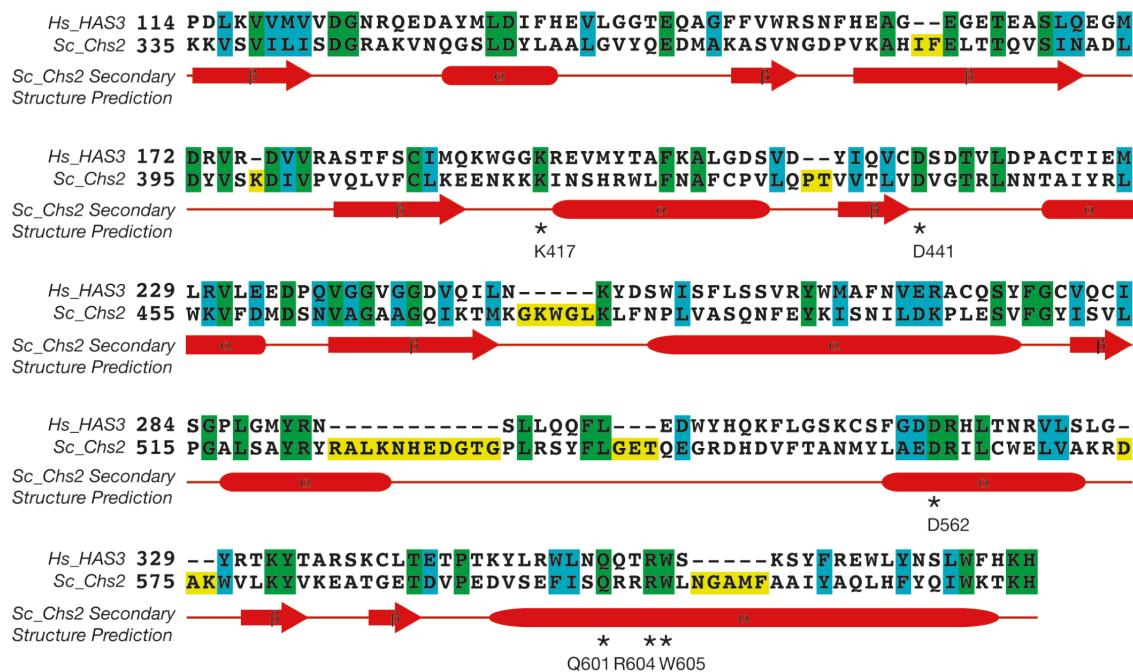


Figure 4.2: Hyaluronan synthases share homology with chitin synthase Chs2.

PSI-BLAST searches were used to search for sequence similarities between Chs2 and human proteins. Alignment of Chs2-335-625 containing catalytic domain with corresponding fragment from human hyaluronan synthase 3 (*HAS3*) was generated using 'ClustalW' and 'Boxshade' (<http://workbench.sdsc.edu/>). Amino acid sequence alignment shows that key residues in Chs2, shown previously to be important for in vitro activity or in vivo function, are conserved in HAS3. Those residues are marked with an asterisk. The structure-fold recognition server Protein Homology/Analogy Recognition Engine (PHYRE) (Kelley and Sternberg, 2009) and 'JPred' (Cole *et al.*, 2008) were used to search for Chs2 structural secondary prediction, which is shown below the amino acid sequence.

In budding yeast, Chs2 synthesises the essential primary septum between mother and daughter cells. We have shown, as previously reported, that impairment of the activity of Chs2 enzyme is lethal for the cells, as they accumulate as binucleate cells upon

pathogens. Although Chs2 function could be conserved in higher eukaryotes, the specific enzymatic details would be different between mammals and fungi, which makes Chs2 protein an excellent target for therapeutic intervention to avoid secondary effects.

The first drugs developed against Chs2 protein were analogs of its natural substrate, UDP-N-Acetylglucosamine; hence, they are competitive inhibitors. They are nikkomycins and polyoxins (Bago *et al.* 1996, Kathiravan *et al.* 2012). They exhibit a great potency *in vitro*; however, they are not suitable as drugs because of limitations *in vivo*, as they are not extremely stable and do not enter the cell easily. Due to their potency, there has been an effort to try to chemically modify these inhibitors to potentially assess these problems (Jackson *et al.* 2013).

The next generation of Chs2 inhibitors were non-competitive inhibitors. The first non-competitive inhibitor developed was RO-09-3143 (Sudoh *et al.* 2000), which inhibited both ScChs2 and its ortholog in *C. albicans* (CaChs1). Later, a group developed a coumarin derivative that proved to inhibit chitin synthase from *Candida tropicalis* at an IC₅₀ of 0.08mM (Ji *et al.* 2016). Coumarin have been proven an unvaluable backbone for drug design, as its benzopyrone structure has been shown to interact with a variety of enzymes and proteins through weak bond interactions, showing a potential as medicinal drugs in a wide range of substrates (Peng *et al.* 2013).

These inhibitory molecules were a result of trial-and-error assays, of trying different batteries of compounds to assess whether any of them would indeed behave as an inhibitor.

Although a structure of Chs2 has been proposed by modelling with glycosyltransferase NodC from *Rhizopus* (Dorfmueller *et al.* 2014), NodC synthesises oligosaccharides only up to five monomers long, and lacks both Chs2 N-terminal domain and a C-terminal transmembrane domain. This way, it would be interesting to understand Chs2 structure in a more direct manner, by crystallising the protein. Hence, better understanding Chs2 structure would provide us a framework to specifically design drugs that would target pockets within its structure, thus inhibiting enzyme activity and avoiding undesirable side effects.

4.3 Working with membrane protein Chs2, a not-so-easy task.

Determining the structure of a membrane protein like Chs2 is extremely challenging. One of the key problems related to integral membrane proteins is the difficulty in expressing significant amounts of material required for structural biology. Eukaryotic membrane proteins often have some specific membrane lipid requirements for stability of their transmembrane alpha helices, and also require specific post-translational modifications that make prokaryotic cell overexpression inappropriate. Amongst higher eukaryotes, yeast cells meet the requirements for overexpression of membrane proteins, while being cheaper to work with than mammalian or insect cells.

We tried several constructs to assess the overexpression of Chs2, as it has been shown that several constructs and homologs often need to be assayed to obtain sufficient protein expression (Carpenter *et al.* 2008). Surprisingly, we found that fusion of the well-structured C2-domain of Inn1 protein to Chs2 was very badly expressed (Figure 3.1).

As recombinant protein expression may vary greatly from one organism to the other, we also tried using methylotrophic yeast *Pichia pastoris* as a host to express and purify fusion C2 domain of Inn1 to hypermorphic allele of *CHS2*, *CHS2-V377I* (Devrekanli *et al.* 2012, Byrne 2015), as *P. pastoris* can be grown to extremely high cell densities, so the amount of material obtained per litre of culture is maximised. We used *P. pastoris* SMD1163 (*his4*, *pep4*, *prb1*), which lacks different proteases that may degrade the fusion protein; and protein was expressed as a *C2-CHS2-V377I-MYC-8HIS* from pPICZA plasmid, which allows protein expression upon shifting the carbon source of the media from glycerol to methanol. However, this *C2-CHS2-V377I-MYC-8HIS* fusion protein aggregated upon size-exclusion chromatography (SEC) purification.

However, when purifying Chs2 from a *S. cerevisiae* strain that also overexpresses Inn1 as a separate protein, Chs2 remained soluble and stable (Figure 3.4), suggesting that it is the covalent fusion of the C2-domain that renders it unstable. Hence, in line with our

finding that Inn1 interacts with Chs2 through its C2 and C-terminal domain (Foltman *et al.* 2016a), it is probably the contact between full-length Inn1 and Chs2 proteins that makes the complex more stable.

Interestingly, Chs2 expressed better in cells overexpressing Inn1 protein, in cells which also harboured temperature sensitive point mutations in Cdc14 and Cdc15 proteins involved in mitotic exit (Figure 3.4). As Chs2 expresses during G2/M and accumulates in the ER (Pammer *et al.* 1992), it could be that these mutants would not have full function. This would lead to a delayed mitotic exit and, hence, a longer time for Chs2 accumulation in the ER.

Even though we managed to purify Chs2, the obtained amount was not sufficient for crystallisation studies. As we purified Chs2 protein from membranes from a six-litre culture, we could try to obtain more protein by using a fermentor. Using a fermentor, the grow-up of larger volumes of culture is possible, ranging typically from 15 to 50 litres. This would increase the amount of protein expressed. Furthermore, fermentors allow monitoring of parameters such as the dissolved oxygen or the pH of the media, which could dramatically maximise the amount of protein obtained. Also, the position of the tag plays an important role in protein functionality, so placing the tag in the N-terminus could potentially help with protein expression and stability. Finally, it has been

shown that GST-tag can facilitate protein folding (Harper and Speicher 2011), so changing from an 8HIS-tag to a GST-tag could also potentially help with protein expression and stability.

4.4 Cyk3 as a crucial cytokinetic regulator.

The role of SH3-containing protein Cyk3 during cytokinesis in *S. cerevisiae* is undoubtedly important. In agreement with the available literature (Korinek *et al.* 2000, Meitinger *et al.* 2010, Devrekanli *et al.* 2012), Cyk3 is a non-essential protein in *S. cerevisiae* (Figure 3.9, Figure 3.10, Figure 3.13.A (ii)), with *cyk3Δ* cells forming smaller colonies than wild type cells and a percentage of cytokinesis failure. The importance of Cyk3 in fission yeast *S. pombe* is similar, as cells lacking SpCyk3 harbour some cytokinetic defects, such as multi-nucleated and multi-septated cells (Pollard *et al.* 2012, Ren *et al.* 2015). Another SH3 domain-containing protein, Imp2, localises to the site of division later than Cyk3 in cytokinesis (Ren *et al.* 2015). In *S. pombe*, the genetic interactions between the SH3 domain of Imp2 and Cyk3 and Fic1 are different (Ren *et al.* 2014), suggesting a different mechanism of action than their budding yeast counterparts Cyk3 and Inn1, which collaborate to regulate Chs2 chitin synthase (Nishihama *et al.* 2009, Devrekanli *et al.* 2012, Foltman *et al.* 2016a). It could be possible that whereas Cyk3, Inn1 and Hof1

form a trimeric complex coordinating cytokinesis in budding yeast, SH3-domain containing proteins Cyk3 and Imp2 could form different complexes and hence provide different signals.

However, Cyk3 becomes essential in budding yeast *Kluyveromyces lactis* (Rippert *et al.* 2014). KICyk3 similarity is higher with ScCyk3 (61%) than with SpCyk3 (51%). This difference in the importance of Cyk3 amongst species could be due to a different organisation of the cytokinetic regulators. While in *S. cerevisiae* both the contraction of an actomyosin ring and the synthesis of a primary septum are needed for successful cytokinesis, actomyosin ring constriction seems to be dispensable in *K. lactis* (Rippert *et al.* 2014). Hence, Cyk3, promoting primary septum formation, could play a more important role in this budding yeast.

It should also be noted that in budding yeast *C. albicans*, Cyk3 is an essential protein. Lack of CaCyk3 function leads to cytokinesis failure (Reijntj *et al.* 2010), hence suggesting a potential therapeutic target in *C. albicans*. Unlike Chs2, Cyk3 is a soluble protein, which would make it easier to work with to solve a structure upon which rationally design putative inhibitors to kill its function.

Cyk3 harbours an SH3 domain and a transglutaminase-like domain. In agreement with the literature (Jendretzki *et al.* 2009), SH3 domain in the N-terminus of the protein is necessary for its correct localisation (Figure

3.15). Cyk3 interacts through this SH3 domain with PXXP motifs in the C2-domain containing protein Inn1 (Nishihama *et al.* 2009, Nkosi *et al.* 2013); hence, this interaction could be important for Cyk3 correct localisation. Interestingly, conditional depletion of Inn1 prevented Cyk3-GFP targeting to the site of division to the level of a wild type strain (Meitinger *et al.* 2010) (Figure 3.15.B). However, Cyk3-GFP was still able to localise to some level. It is not surprising that the correct localisation of some of these proteins do not rely on a single interaction (Foltman *et al.* 2016a), as this mechanism ensures a correct protein localisation and function, so other proteins could be responsible for Cyk3 correct localisation. We have showed that Cyk3 is able to interact with Chs2 in a direct manner, through multiple points of contact (Figure 3.7, Figure 3.8 and Figure 3.16). Although we have shown that the localisation of Chs2 is not compromised by the lack of Cyk3 (Figure 3.12.A), we cannot rule out the possibility that Cyk3 localisation could also depend on Chs2. Finally, it has also been shown that Cyk3 harbours a proline-rich motif that can interact with the SH3 domain of Hof1 protein (Labeledzka *et al.* 2012). As Hof1 arrives earlier to the site of division (Vallen *et al.* 2000), it could be possible that this interaction could stabilise Cyk3 protein at the site of division. The possibility that Chs2 and Hof1 could have a role in Cyk3 localisation could be

tested in the future by using conditional degrons to deplete Chs2 or Hof1.

Cyk3 also harbours a transglutaminase-like domain, which we have shown to be able to stimulate chitin production by chitin synthase Chs2 (Figure 3.20.A). Transglutaminase-like domains do not have a clear molecular function (Makarova *et al.* 1999), but it has been shown that lack of functional protein band 4.2 in erythrocytes, which carries such domain, produces a phenotype of hemolysis and is unable to capture CD48 membrane protein (Bruce *et al.* 2002, Dahl *et al.* 2004). We have shown that Cyk3 is not responsible for maintaining Chs2 at the site of division (Figure 3.12.A), but it could affect Chs2 activity by stabilising the protein in an active conformation. As transglutaminases catalyse protein crosslinking reactions, it could be possible that despite lacking the catalytic cysteine, transglutaminase-like domain containing proteins could have a strong affinity towards certain protein motifs, stabilising Chs2 in an active conformation. This way, Cyk3 could promote Chs2 activity.

It is also interesting to point out that Cyk3 (475-764aa), containing the transglutaminase-like domain, is able to interact with Chs2 protein only when it lacks its N-terminal tail Chs2 (1-215aa) (Figure 3.16). Hence, Chs2 activity stimulation by Cyk3 should happen once this N-terminal tail has been removed. It has been shown that partial

protease treatment of Chs2 releases its full enzymatic activity (Martinez-Rucobo *et al.* 2009); however, no cellular protease has been found in yeast that physiologically removes this domain. However, a serine protease was shown in moth *Manduca sexta* to interact with MsChs2 chitin synthase (Broehan *et al.* 2007), and this synthase was also activated by proteolytic treatment, just like ScChs2 (Martinez-Rucobo *et al.* 2009). Hence, the proteolytic activation option cannot be ruled out.

Another option is that interaction of Chs2 with another cytokinetic protein removes the inhibition caused by its N-terminal tail and the C-terminal domain of Inn1 protein (Foltman *et al.* 2016a), allowing Chs2 to become active.

This protein could be Cyk3, which could remove the inhibitory role that Inn1 C-terminus plays against Chs2, while also interacting with Chs2 through different points of contact (Foltman *et al.* 2016a). Inn1 would interact with Chs2 at the end of mitosis, with Inn1 C-terminus keeping Chs2 inactive. Upon Cyk3 arrival to the site of division, Cyk3 would remove the inhibitory Inn1 C-terminus, and collaborate with Inn1 C2 domain to activate the catalytic domain of Chs2 and hence start the deposition of primary septum.

The precise residues involved in Inn1 and Cyk3 binding to Chs2 could be solved by protein painting (Luchini *et al.* 2014), which could help us to understand in deeper detail

the complex interactions and regulation of IPCs.

In conclusion, we have shown that chitin synthase Chs2 is tightly regulated by Cyk3 protein. Evolutionary conservation of cytokinesis mechanism amongst fungi makes extracellular matrix remodelling an interesting target against fungal pathogens.

5. CONCLUSIONS

- Hemos expresado y purificado la proteína quitín sintasa Chs2 utilizando células de *Saccharomyces cerevisiae*.
- Hemos producido y purificado anticuerpos funcionales contra las proteínas con función clave durante la citoquinesis Chs2, Cyk3 y Hof1.
- Las proteínas Chs2 y Cyk3 son capaces de unirse directamente.
- El dominio SH3 de Cyk3 es esencial para la localización de la proteína Cyk3 en el lugar donde se lleva a cabo la división celular.
- Hemos creado un mutante condicional de tipo degrón para inactivar de forma eficiente la proteína Cyk3.
- La proteína Cyk3 regula la actividad de la quitín sintasa Chs2.
- El dominio similar a transglutaminasa es esencial para que la proteína Cyk3 pueda controlar la actividad de Chs2.
- El extremo C-terminal de Inn1 interacciona con Chs2 y nuestros resultados apuntan a un papel regulador negativo del extremo C-terminal de Inn1 sobre la actividad quitín sintasa de Chs2.
- Los defectos asociados a la falta de Cyk3 en células portadoras de la fusión C2-HOF1 son rescatados por el alelo hipermórfico de *CHS2*, *CHS2-V377I*.
- Las células portadoras de la fusión C2-HOF1 en las que se inactiva Cyk3 mueren debido a la falta de formación del septo primario entre la célula madre y la célula hija.

- We have expressed and purified chitin synthase protein Chs2 using *Saccharomyces cerevisiae* cells.
- We have raised and purified functional antibodies against proteins with a key function during cytokinesis, Chs2, Cyk3 and Hof1.
- Chs2 and Cyk3 proteins are able to directly interact.
- The SH3 domain of Cyk3 is essential for the localisation of Cyk3 protein to the site of division.
- We have created a degron conditional mutant to efficiently inactivate Cyk3 protein.
- Cyk3 protein regulates the chitin synthase activity of Chs2.
- Cyk3 transglutaminase-like domain is essential for Cyk3 protein to control Chs2 activity.
- C-terminal domain of Inn1 interacts with Chs2, and our results point to a negative regulator role of the C-terminal domain of Inn1 on chitin synthase activity by Chs2.
- Defects associated with lack of Cyk3 in cells harbouring C2-HOF1 fusion are rescued by hypermorphic allele of *CHS2*, *CHS2-V377I*.
- Cells harbouring C2-HOF1 fusion where Cyk3 is inactivated die because of a lack of formation of the primary septum between mother and daughter cells.

-

6. RESUMEN

En la levadura *Saccharomyces cerevisiae*, la contracción del anillo de actomiosina durante la citoquinesis va acompañada de la formación de una capa especial de matriz extracelular producida por la enzima quitín sintasa Chs2. Esta quitín sintasa es esencial y sintetiza el denominado septo primario de quitina entre la célula madre y la célula hija durante la citoquinesis en *S. cerevisiae*. Ambos procesos están relacionados porque defectos en la contracción del anillo impide la formación del septo primario y, del mismo modo, el bloqueo de la síntesis del septo afecta a la contracción del anillo.

Para entender mejor el funcionamiento de esta enzima, en el laboratorio nos planteamos una caracterización estructural de la misma. Para ello, expresamos en *S. cerevisiae* la proteína Chs2 fusionada a la proteína GFP y a una cola de histidinas, lo cual permitía su visualización y purificación. Tras comprobar que sólo la construcción de la proteína completa y una versión de la proteína que carecía del dominio N-terminal de Chs2 se expresaban a un rendimiento aceptable, encontramos que sólo la proteína completa era solubilizable en el detergente dodecil maltósido. La utilización de otros detergentes no mejoró el proceso de solubilización, pero sí la adición de chaperonas químicas al medio, especialmente la adición de histidina. Sin embargo, los niveles de degradación asociados a la purificación de la proteína Chs2

eran demasiado elevados. Trabajos previos del laboratorio habían mostrado que la proteína Chs2 interaccionaba directamente con la proteína Inn1, por ello nos planteamos que la coexpresión de Chs2 e Inn1 podían mejorar el rendimiento. Efectivamente, los niveles de proteínas que fuimos capaces de aislar fueron mayores, sin embargo, la concentración de proteína Chs2 que obtuvimos no fue suficiente para llevar a cabo estudios estructurales.

Paralelamente, el laboratorio del Dr. Alberto Sánchez Díaz de la Universidad de Cantabria estaba interesado en conocer el mecanismo molecular por el que las células de *S. cerevisiae* regulan la actividad de la quitín sintasa Chs2. Evidencias generadas por nuestro laboratorio y otros apuntaban a que la proteína Inn1 podría tener un papel importante en la regulación de Chs2. Por ello, la Dra. Magdalena Foltman a través de una purificación de proteínas aisló un conjunto de proteínas que son capaces de interaccionar al mismo tiempo con Chs2 e Inn1 durante la citoquinesis. Entre esas proteínas estaba la proteína Cyk3, cuya implicación en la citoquinesis estaba descrita en la literatura. Así, células con la función de Cyk3 comprometida sufrían defectos en la división celular; y la sobreexpresión de Cyk3 provocaba la síntesis de un septo primario más grueso. Sin embargo, se desconocían los detalles moleculares de cuál era el papel que Cyk3 jugaba durante la citoquinesis, por ello

decidimos centrar nuestros estudios en la proteína Cyk3.

Ya que se había descrito la influencia de Cyk3 en la actividad quitín sintasa, decidimos comprobar si Cyk3 era capaz de interactuar con Chs2. Para ello, células expresando Cyk3 fusionado con la etiqueta TAP en su extremo N-terminal, y Chs2 con la etiqueta 9MYC, se recolectaron mientras realizaban citoquinesis de manera síncrona. Después de obtener extractos proteicos de estas células, se inmunoprecipitaron dichos extractos en resina cubierta de inmunoglobulina G, comprobando que ambas proteínas interactúan específicamente en células haciendo citoquinesis. Posteriormente, para comprobar si estas dos proteínas interactúan de forma directa, utilizamos un sistema de expresión procariota. Células de *E. coli* expresando Cyk3-6HIS o Strep-Chs2-215-629 (fragmento que contiene el dominio catalítico de Chs2) fueron mezcladas y los extractos proteicos fueron purificados primero por la etiqueta de Strep y luego por la cola de histidinas. Así, comprobamos que estas dos proteínas interactúan de forma directa.

Para entender mejor la función de Cyk3, decidimos incorporar en el extremo 3' de la región codificante de *CYK3* una etiqueta de degradación de auxina (-aid), que permite la degradación de la proteína de fusión mediante la expresión de una ubiquitina ligasa y la adición de auxinas al medio. Sin embargo, ya

que la reducción en la cantidad de Cyk3 no era notable, y el defecto en el fenotipo no era demasiado pronunciado, decidimos, añadir en el extremo 5' de la región codificante de Cyk3 una etiqueta de degradación de temperatura (-td). Esta etiqueta permite la degradación de la proteína mediante la expresión de una ubiquitina ligasa y un aumento de temperatura en la que crecen las células de 24°C a 37°C. La inactivación del doble degradón de Cyk3 provocó claramente un defecto en citoquinesis. Por tanto, generamos una herramienta importante para analizar la función de Cyk3.

La inactivación de Cyk3 provoca un incremento de la localización de Inn1 y Chs2, lo que se podría explicar porque las células sufren un retraso durante la citoquinesis. Sin embargo, la falta de Cyk3 produce un ligero defecto en la síntesis del septo primario entre la célula madre y la célula hija durante la citoquinesis, lo que apuntaría de nuevo a un papel relevante para Cyk3 en la regulación de la formación de ese septo primario.

El estudio de proteínas no esenciales como Cyk3 es complicado porque se deben encontrar las condiciones en las que esas proteínas se vuelvan esenciales y así poder estudiar los defectos asociados a su falta. La proteína Cyk3 se convierte en esencial en células que portan la fusión del dominio C2 de Inn1 y la proteína Hof1. Esta fusión es completamente funcional, proporcionando la función completa de Hof1, ya que esta fusión

no es letal sintética con otras deleciones de genes con las que, sin embargo, la deleción de Hof1 sí lo es. Por tanto, quisimos caracterizar los defectos asociados a células portadoras de la fusión C2-Hof1, en las que inactivamos Cyk3.

Cyk3 tiene un dominio SH3 en su extremo N-terminal y un dominio similar a un dominio transglutaminasa que se encuentra en el centro de su secuencia. La deleción del dominio SH3 provoca graves defectos en la división celular; y la combinación de este alelo con la fusión C2-Hof1 es letal sintética. Igualmente, este dominio es imprescindible para la correcta localización de Cyk3 en el sitio de división.

El mapeo de los sitios de interacción de Cyk3 con dos fragmentos de Chs2 reveló que Cyk3 es capaz de interactuar mediante múltiples puntos de contacto a lo largo de dos fragmentos de Chs2 que contiene el dominio catalítico. Además, uno de los fragmentos de Cyk3 (475-764aa) es incapaz de interactuar con un fragmento de Chs2 que contiene también su extremo N-terminal (1-629aa), sugiriendo que el extremo N-terminal de Chs2 impide la interacción entre ambas proteínas. De las truncaciones de Cyk3, se eligió el fragmento Cyk3-475-885, que se conocía por la literatura que era soluble, para comprobar en ensayos de interacción en proteína recombinante expresada en *E. coli* que la interacción con Chs2 se produce de forma directa, del mismo modo que con la proteína

completa. Este fragmento contiene el dominio similar a transglutaminasa, con dos residuos clave conservados: una histidina y un ácido aspártico. La mutación de ambos residuos eliminó la función de Cyk3, ya que la combinación de este alelo con *C2-HOF1* resultó en una letalidad sintética. Este alelo, al contrario que la versión salvaje, es incapaz de inducir la síntesis de septo primario cuando se sobreexpresa, de forma independiente a la localización de la quitín sintasa Chs2. La letalidad sintética del alelo mutante con *C2-HOF1* era rescatada por un alelo hipermórfico de Chs2; entender cómo ocurría ese rescate, podría darnos pistas sobre la regulación de esta proteína. Hemos comprobamos que el dominio C-terminal de Inn1 interacciona con Chs2 y nuestros resultados apuntan a un papel regulador negativo del extremo C-terminal de Inn1 sobre la actividad quitín sintasa de Chs2.

Nuestros experimentos indican que Cyk3 tiene un papel en la regulación de la actividad de Chs2 porque las células *C2-HOF1* desprovistas de Cyk3 son incapaces de llevar a cabo la formación del septo primario, lo que explica la razón por la que esas células mueren.

7. REFERENCES

- Aaltonen, L. A., *et al.* (1994). Replication errors in benign and malignant-tumors from hereditary nonpolyposis colorectal-cancer patients. Cancer Res **54**(7): 1645-1648.
- Abel, A. M., *et al.* (2015). IQGAP1: Insights into the function of a molecular puppeteer. Molecular Immunology, Elsevier Ltd. **65**: 336-349.
- Adams, D. J. (2004). Fungal cell wall chitinases and glucanases. Microbiology. **150**: 2029-2035.
- Adell, M. A. Y., *et al.* (2016). ESCRT-III and Vps4: a dynamic multipurpose tool for membrane budding and scission. FEBS J.
- Agbulut, O., *et al.* (2007). Green Fluorescent Protein Impairs Actin-Myosin Interactions by Binding to the Actin-binding Site of Myosin. The journal of biological Chemistry. **282**: 10465-10471.
- Alberts, A. S. (2001). Identification of a Carboxyl-terminal Diaphanous-related Formin Homology Protein Autoregulatory Domain. Journal of Biological Chemistry. **276**: 2824-2830.
- Almonacid, M., *et al.* (2011). Temporal Control of Contractile Ring Assembly by Plo1 Regulation of Myosin II Recruitment by Mid1/Anillin. Current Biology, Elsevier Ltd. **21**: 473-479.
- André, N., *et al.* (2006). Enhancing functional production of G protein-coupled receptors in *Pichia pastoris* to levels required for structural studies via a single expression screen. Protein Science. **15**: 1115-1126.
- Arabidopsis (2000). Analysis of the genome sequence of the flowering plant *Arabidopsis thaliana* Nature. **408**: 1-20.
- Arasada, R. and T. D. Pollard (2014). Contractile Ring Stability in *S. pombe* Depends on F-BAR Protein Cdc15p and Bgs1p Transport from the Golgi Complex. CellReports, The Authors. **8**: 1533-1544.
- Arcones, I., *et al.* (2016). Maintaining protein homeostasis: early and late endosomal dual recycling for the maintenance of intracellular pools of the plasma membrane protein Chs3. Mol Biol Cell **27**(25): 4021-4032.
- Au-Young, J. and P. W. Robbins (1990). Isolation of a chitin synthase gene (*CHS1*) from *Candida albicans* by expression in *Saccharomyces cerevisiae*. Molecular microbiology **4**(2): 197-207.
- Bago, B., *et al.* (1996). Effect of Nikkomycin Z, a chitin-synthase inhibitor, on hyphal growth and cell wall structure of two arbuscular-mycorrhizal fungi. Protoplasma. **192**: 90-92.
- Balasubramanian, M. K., *et al.* (2004). Comparative analysis of cytokinesis in budding yeast, fission yeast and animal cells. Curr Biol **14**(18): R806-818.
- Bardin, A. J. and A. Amon (2001). Men and sin: what's the difference? Nature reviews. Molecular cell biology **2**(11): 815-826.
- Barr, F. A. and U. Gruneberg (2007). Cytokinesis: placing and making the final cut. Cell **131**(5): 847-860.

- Barrett, T. B., *et al.* (1983). Polyploid nuclei in human artery wall smooth muscle cells. Proc Natl Acad Sci U S A **80**(3): 882-885.
- Beams, H. W. and T. C. Evans (1940). Some effects of colchicine upon the first cleavage in *Arbacia punctulata*. The Biological Bulletin. **79**: 188-198.
- Beaucher, M., *et al.* (2007). Metastatic ability of *Drosophila* tumors depends on MMP activity. Developmental biology **303**(2): 625-634.
- Bender, A. and J. R. Pringle (1989). Multicopy suppression of the *cdc24* budding defect in yeast by *CDC42* and three newly identified genes including the ras-related gene RSR1. PNAS. **86**: 9976-9980.
- Berger, S., *et al.* (1995). Do de-N-glycosylation enzymes have an important role in plant cells? Biochimie. **77**: 751-760.
- Bertin, A., *et al.* (2008). *Saccharomyces cerevisiae* septins: supramolecular organization of heterooligomers and the mechanism of filament assembly. Proc Natl Acad Sci U S A **105**(24): 8274-8279.
- Bi, E. (2001). Cytokinesis in budding yeast: the relationship between actomyosin ring function and septum formation. Cell Struct Funct **26**(6): 529-537.
- Bi, E. and J. Lutkenhaus (1991). FtsZ ring structure associated with division in *Escherichia coli*. Nature. **354**: 161-164.
- Bi, E., *et al.* (1998). Involvement of an Actomyosin Contractile Ring in *Saccharomyces cerevisiae* cytokinesis: 1-12.
- Bill, R. M., *et al.* (2011). Overcoming barriers to membrane protein structure determination. Nature biotechnology, Nature Publishing Group: 1-6.
- Blaauw, B., *et al.* (2013). Mechanisms modulating skeletal muscle phenotype. Compr Physiol **3**(4): 1645-1687.
- Bloom, J., *et al.* (2011). Global Analysis of Cdc14 Phosphatase Reveals Diverse Roles in Mitotic Processes. Journal of Biological Chemistry. **286**: 5434-5445.
- Boveri, T. (2008). Concerning the origin of malignant tumours by Theodor Boveri. Translated and annotated by Henry Harris. J Cell Sci **121 Suppl 1**: 1-84.
- Boyne, J. R., *et al.* (2000). Yeast myosin light chain, Mlc1p, interacts with both IQGAP and Class II myosin to effect cytokinesis. Journal of cell science. **113**: 4533-4543.
- Brecht, M., *et al.* (1986). Increased hyaluronate synthesis is required for fibroblast detachment and mitosis. Biochem. J. **239**: 445-450.
- Bremmer, S. C., *et al.* (2012). Cdc14 Phosphatases Preferentially Dephosphorylate a Subset of Cyclin-dependent kinase (Cdk) Sites Containing Phosphoserine. The journal of biological Chemistry. **287**: 1662-1669.
- Broehan, G., *et al.* (2007). A chymotrypsin-like serine protease interacts with the chitin synthase from the midgut of the tobacco hornworm. J Exp Biol **210**(Pt 20): 3636-3643.
- Bruce, L. J., *et al.* (2002). Absence of CD47 in protein 4.2-deficient hereditary spherocytosis

- in man: an interaction between the Rh complex and the band 3 complex. Blood **100**(5): 1878-1885.
- Bulawa, C. (1992). *CSD2*, *CSD3*, and *CSD4*, genes required for chitin synthesis in *Saccharomyces cerevisiae*: the *CSD2* gene product is related to chitin synthases and developmentally regulated proteins in *Rhizobium* species and *Xenopus laevis*. Molecular and cellular biology. **12**: 1764-1776.
- Byrne, B. (2015). *Pichia pastoris* as an expression host for membrane protein structural biology. Current Opinion in Structural Biology, Elsevier Ltd. **32**: 9-17.
- Carpenter, E. P., *et al.* (2008). Overcoming the challenges of membrane protein crystallography. Current Opinion in Structural Biology, Elsevier Ltd. **18**: 581-586.
- Caussinus, E. and C. Gonzalez (2005). Induction of tumor growth by altered stem-cell asymmetric division in *Drosophila melanogaster*. Nat Genet **37**(10): 1125-1129.
- Chalfie, M., *et al.* (1994). Green fluorescent protein as a marker for gene expression. Science **263**(5148): 802-805.
- Chambers, R. (1922). A Micro Injection Study on the Permeability of the Starfish Egg. J Gen Physiol **5**(2): 189-193.
- Chambers, R. and M. J. Kopac (1937). The coalescence of living cells with oil drops. I. *Arbacia* eggs immersed in sea water. Journal of cellular and comparative physiology. **9**: 331-343.
- Chang, F., *et al.* (1996). Isolation and characterization of fission yeast mutants defective in the assembly and placement of the contractile actin ring. J Cell Sci **109** (Pt 1): 131-142.
- Chant, J. and I. Herskowitz (1991). Genetic Control of Bud Site Selection in Yeast by a Set of Gene Products That Constitute a Morphogenetic Pathway. Cell. **65**: 1203-1212.
- Chant, J. and J. R. Pringle (1995). Patterns of Bud-Site Selection in the Yeast *Saccharomyces cerevisiae*. The journal of cell Biology. **129**: 751-765.
- Chia, W., *et al.* (2008). *Drosophila* neuroblast asymmetric divisions: cell cycle regulators, asymmetric protein localization, and tumorigenesis. J Cell Biol **180**(2): 267-272.
- Chin, C. F., *et al.* (2012). Dependence of Chs2 ER export on dephosphorylation by cytoplasmic Cdc14 ensures that septum formation follows mitosis. Mol Biol Cell **23**(1): 45-58.
- Chin, C. F., *et al.* (2016). Timely Endocytosis of Cytokinetic Enzymes Prevents Premature Spindle Breakage during Mitotic Exit. PLOS Genetics. **12**: e1006195.
- Choi, W. J., *et al.* (1994). Are yeast chitin synthases regulated at the transcriptional or the posttranslational level? Mol Cell Biol **14**(12): 7685-7694.
- Chuang, J. S. and R. W. Schekman (1996). Differential trafficking and timed localization of two chitin synthase proteins, Chs2p and Chs3p. J Cell Biol **135**(3): 597-610.

- Colman-Lerner, A., *et al.* (2001). Yeast Cbk1 and Mob2 activate daughter-specific genetic programs to induce asymmetric cell fates. Cell **107**(6): 739-750.
- Conklin, E. G. (1916). Effects of Centrifugal Force on the Polarity of the Eggs of *Crepidula*. Proc Natl Acad Sci U S A **2**(2): 87-90.
- Cortes, J. C., *et al.* (2007). The (1,3)beta-D-glucan synthase subunit Bgs1p is responsible for the fission yeast primary septum formation. Mol Microbiol **65**(1): 201-217.
- Cueille, N., *et al.* (2001). Flp1, a fission yeast orthologue of the *S. cerevisiae* CDC14 gene, is not required for cyclin degradation or rum1p stabilisation at the end of mitosis. Journal of cell science. **114**: 2649-2664.
- Dahl, K. N., *et al.* (2004). Protein 4.2 is critical to CD47-membrane skeleton attachment in human red cells. Blood **103**(3): 1131-1136.
- De Virgilio, C., *et al.* (1996). *SPR28*, a sixth member of the septin gene family in *Saccharomyces cerevisiae* that is expressed specifically in sporulating cells. Microbiology. **142**: 2897-2905.
- Deibler, M., *et al.* (2011). Actin Fusion Proteins Alter the Dynamics of Mechanically Induced Cytoskeleton Rearrangement. PloS one. **6**: e22941.
- Devrekanli, A., *et al.* (2012). Inn1 and Cyk3 regulate chitin synthase during cytokinesis in budding yeasts. J Cell Sci **125**(Pt 22): 5453-5466.
- Dobbelaere, J. and Y. Barral (2004). Spatial coordination of cytokinetic events by compartmentalization of the cell cortex. Science **305**(5682): 393-396.
- Dohmen, R. J., *et al.* (1994). Heat-inducible degron: a method for constructing temperature-sensitive mutants. Science **263**(5151): 1273-1276.
- Dong, Y. P., D; Bretscher, A (2003). Formin-dependent actin assembly is regulated by distinct modes of Rho signaling in yeast. Journal of cell biology **161**(6): 1081-1092.
- Dorfmueller, H. C., *et al.* (2014). A Structural and Biochemical Model of Processive Chitin Synthesis. Journal of Biological Chemistry. **289**: 23020-23028.
- Douglas, C. M., *et al.* (1994). The *Saccharomyces cerevisiae* *FKS1* (*ETG1*) gene encodes an integral membrane protein which is a subunit of 1,3-β-D-glucan synthase. PNAS. **91**: 12907-12911.
- Drew, D., *et al.* (2008). GFP-based optimization scheme for the overexpression and purification of eukaryotic membrane proteins in *Saccharomyces cerevisiae*. Nat Protoc. **3**: 784-798.
- Drgonová, J., *et al.* (1996). Rho1p, a Yeast Protein at the Interface Between Cell Polarization and Morphogenesis. Science. **272**: 277-279.
- Duncan, A. W. (2013). Aneuploidy, polyploidy and ploidy reversal in the liver. Semin Cell Dev Biol **24**(4): 347-356.
- Echard, A., *et al.* (2004). Terminal cytokinesis events uncovered after an RNAi screen. Curr Biol **14**(18): 1685-1693.

- Elder, J. H. and S. Alexander (1982). Endo- β -N-Acetylglucosaminidase F: Endoglycosidase from *Flavobacterium meningosepticum* that cleaves both high-mannose and complex glycoproteins. PNAS. **79**: 4540-4544.
- Epp, J. A. and J. Chant (1997). An IQGAP-related protein controls actin-ring formation and cytokinesis in yeast. Curr Biol **7**(12): 921-929.
- Ettinger, A. W., *et al.* (2011). Proliferating versus differentiating stem and cancer cells exhibit distinct midbody-release behaviour. Nat Commun, Nature Publishing Group. **2**: 503-512.
- Fang, X., *et al.* (2010). Biphasic targeting and cleavage furrow ingression directed by the tail of a myosin II. J Cell Biol **191**(7): 1333-1350.
- Fields, S. and O.-k. Song (1989). A novel genetic system to detect protein-protein interactions. Nature **340**: 245-246.
- Finnigan, G. C., *et al.* (2016). Detection of protein-protein interactions at the septin collar in *Saccharomyces cerevisiae* using a tripartite split-GFP system. Molecular biology of the Cell: 1-58.
- Fitch, I., *et al.* (1992). Characterization of four B-type cyclin genes of the budding yeast *Saccharomyces cerevisiae*. Mol Biol Cell **3**(7): 805-818.
- Fitzpatrick, P. J., *et al.* (1998). DNA replication is completed in *Saccharomyces cerevisiae* cells that lack functional Cdc14, a dual-specificity protein phosphatase. Molecular & general genetics : MGG **258**(4): 437-441.
- Foltman, M., *et al.* (2016a). Ingression Progression Complexes Control Extracellular Matrix Remodelling during Cytokinesis in Budding Yeast. PLOS Genetics. **12**: e1005864.
- Foltman, M., *et al.* (2016b) Synchronization of the budding yeast *Saccharomyces cerevisiae*. Methods in Molecular Biology **1064-3745** 1940-6029 **1369**, 279-291
- Fortier, M., *et al.* (2017). Incomplete cytokinesis/binucleation in mammals: The powerful system of hepatocytes. Methods Cell Biol **137**: 119-142.
- Frenette, P., *et al.* (2012). An Anillin-Ect2 Complex Stabilizes Central Spindle Microtubules at the Cortex during Cytokinesis. PloS one. **7**: e34888.
- Fujiwara, K. and T. D. Pollard (1976). Fluorescent antibody localization of myosin in the cytoplasm, cleavage furrow, and mitotic spindle of human cells. J Cell Biol **71**(3): 848-875.
- Fujiwara, K. and T. D. Pollard (1978). Simultaneous localization of myosin and tubulin in human tissue culture cells by double antibody staining. J Cell Biol **77**(1): 182-195.
- Fujiwara, T., *et al.* (2005). Cytokinesis failure generating tetraploids promotes tumorigenesis in p53-null cells. Nature **437**(7061): 1043-1047.
- Gentric, G. and C. Desdouets (2014). "Polyploidization in liver tissue." Am J Pathol **184**(2): 322-331.

- Gietz, D., *et al.* (1992). Improved method for high efficiency transformation of intact yeast cells. Nucleic Acids Res. **20**(6): 1425.
- Glomb, O. and T. Gronemeyer (2016). Septin Organization and Functions in Budding Yeast. Front Cell Dev Biol **4**: 123.
- Gottlin-Ninfa, E. and D. B. Kaback (1986). Isolation and Functional Analysis of Sporulation-Induced Transcribed Sequences from *Saccharomyces cerevisiae*. Molecular and cellular biology. **6**: 2185-2197.
- Gray, J. (1931). A textbook of Experimental Cytology. London: Cambridge University Press.
- Guizetti, J., *et al.* (2011). Cortical Constriction During Abcission Involves Helices of ESCRT-III-Dependent Filaments. Science. **331**: 1616-1620.
- Guo, S. and K. J. Kemphues (1996). A non-muscle myosin required for embryonic polarity in *Caenorhabditis elegans*. Nature **382**(6590): 455-458.
- Harper, S. and D. W. Speicher (2011). "Purification of proteins fused to glutathione S-transferase." Methods Mol Biol **681**: 259-280.
- Hartwell, L. H., *et al.* (1970). Genetic control of the cell-division cycle in yeast. I. Detection of mutants. Proc Natl Acad Sci U S A **66**(2): 352-359.
- Henne, W. M., *et al.* (2007). Structure and analysis of FCHo2 F-BAR domain: a dimerizing and membrane recruitment module that effects membrane curvature. Structure **15**(7): 839-852.
- Hettasch, J. M. G., C S (1994). Analysis of the Catalytic Activity of Human Factor XIIIa. The journal of biological chemistry. **269**: 28309-28313.
- Hiramoto, Y. (1956). Cell division without mitotic apparatus in sea urchin eggs. Experimental cell research **11**(3): 630-636.
- Hiramoto, Y. (1965).Mechanics of cleavage in the sea urchin egg." Jpn J Med Sci Biol **18**(6): 320-321.
- Holaway, B. L., *et al.* (1987). Transcriptional regulation of sporulation genes in yeast. Molecular & general genetics : MGG **210**(3): 449-459.
- Homem, C. C. and J. A. Knoblich (2012). *Drosophila* neuroblasts: a model for stem cell biology. Development **139**(23): 4297-4310.
- Hu, C. K., *et al.* (2012). Midbody assembly and its regulation during cytokinesis. Molecular biology of the Cell. **23**: 1024-1034.
- Huang, J., *et al.* (2016). Curvature-induced expulsion of actomyosin bundles during cytokinetic ring contraction. Elife **5**.
- Huxley, H. and J. Hanson (1954). Changes in the cross-striations of muscle during contraction and stretch and their structural interpretation. Nature **173**(4412): 973-976.
- Hwang, E. I., *et al.* (2002). Obovatols, new chitin synthase 2 inhibitors of *Saccharomyces cerevisiae* from *Magnolia obovata*. The Journal of antimicrobial chemotherapy **49**(1): 95-101.
- Inoue, H., *et al.* (1990). High efficiency transformation of *Escherichia coli* with plasmids. Gene **96**(1): 23-28.

- Iwase, M., *et al.* (2007). Shs1 Plays Separable Roles in Septin Organization and Cytokinesis in *Saccharomyces cerevisiae*. Genetics. **177**: 215-229.
- Iwase, M., *et al.* (2006). Role of a Cdc42p effector pathway in recruitment of the yeast septins to the presumptive bud site. Mol Biol Cell **17**(3): 1110-1125.
- Izumikawa, T., *et al.* (2010). Impairment of Embryonic Cell Division and Glycosaminoglycan Biosynthesis in Glucuronyltransferase-I-deficient Mice. Journal of Biological Chemistry. **285**: 12190-12196.
- Jackson, K. E., *et al.* (2013). Polyoxin and nikkomycin analogs: recent design and synthesis of novel peptidyl nucleosides. Heterocyclic Communications. **19**: 375-386.
- Jakobsen, M. K., *et al.* (2013). Phosphorylation of Chs2p regulates interaction with COPII. Journal of cell science **126**(Pt 10): 2151-2156.
- James, P., *et al.* (1996). Genomic libraries and a host strain designed for highly efficient two-hybrid selection in yeast. Genetics **144**(4): 1425-1436.
- Jaspersen, S. L., *et al.* (1999). Inhibitory phosphorylation of the APC regulator Hct1 is controlled by the kinase Cdc28 and the phosphatase Cdc14. Curr Biol **9**(5): 227-236.
- Jaspersen, S. L., *et al.* (1998). A late mitotic regulatory network controlling cyclin destruction in *Saccharomyces cerevisiae*. Mol Biol Cell **9**(10): 2803-2817.
- Jendretzki, A., *et al.* (2009). Cyk3 acts in actomyosin ring independent cytokinesis by recruiting Inn1 to the yeast bud neck. Mol Genet Genomics **282**(4): 437-451.
- Ji, Q., *et al.* (2016). Synthesis and biological evaluation of novel phosphoramidate derivatives of coumarin as chitin synthase inhibitors and antifungal agents. European Journal of Medicinal Chemistry, Elsevier Masson SAS. **108**: 166-176.
- Kamei, T., *et al.* (1998). Interaction of Bnr1p with a novel Src homology 3 domain-containing Hof1p. Implication in cytokinesis in *Saccharomyces cerevisiae*. J Biol Chem **273**(43): 28341-28345.
- Kamm, K. E. and J. T. Stull (1985). The function of myosin and myosin light chain kinase phosphorylation in smooth muscle. Annu Rev Pharmacol Toxicol **25**: 593-620.
- Kanemaki, M., *et al.* (2003). Functional proteomic identification of DNA replication proteins by induced proteolysis in vivo. Nature **423**(6941): 720-724.
- Kanemaki, M. T. (2013). Frontiers of protein expression control with conditional degrons. Pflugers Arch **465**(3): 419-425.
- Kathiravan, M. K., *et al.* (2012). The biology and chemistry of antifungal agents: A review. Bioorganic & Medicinal Chemistry, Elsevier Ltd. **20**: 5678-5698.
- Ke, S., *et al.* (2009). 1,3,4-Oxadiazoline derivatives as novel potential inhibitors targeting chitin biosynthesis: design, synthesis and biological evaluation. Bioorganic & medicinal chemistry letters **19**(2): 332-335.

- Kechad, A., *et al.* (2012). Anillin Acts as a Bifunctional Linker Coordinating Midbody Ring Biogenesis during Cytokinesis. Current Biology, Elsevier Ltd. **22**: 197-203.
- Kim, J. and P. Sudbery (2011). *Candida albicans*, a major human fungal pathogen. The Journal of Microbiology. **49**: 171-177.
- Kimura, K., *et al.* (1996). Regulation of myosin phosphatase by Rho and Rho-associated kinase (Rho-kinase). Science **273**(5272): 245-248.
- Kitajima, J., *et al.* (1995). Identification and distribution of peptide:N-glycanase (PNGase) in mouse organs. Archives of biochemistry and biophysics. **319**: 393-401.
- Kitayama, C., *et al.* (1997). Type II myosin heavy chain encoded by the *myo2* gene composes the contractile ring during cytokinesis in *Schizosaccharomyces pombe*. J Cell Biol **137**(6): 1309-1319.
- Korinek, W. S., *et al.* (2000). Cyk3, a novel SH3-domain protein, affects cytokinesis in yeast. Curr Biol **10**(15): 947-950.
- Kosako, H., *et al.* (2000). Rho-kinase/ROCK is involved in cytokinesis through the phosphorylation of myosin light chain and not ezrin/radixin/moesin proteins at the cleavage furrow. Oncogene **19**(52): 6059-6064.
- Kota, J., *et al.* (2007). Membrane chaperone Shr3 assists in folding amino acid permeases preventing precocious ERAD. The journal of cell Biology. **176**: 617-628.
- Kronstad, J. W., *et al.* (2011). Expanding fungal pathogenesis: *Cryptococcus* breaks out of the opportunistic box. Nature reviews. Microbiology **9**(3): 193-203.
- Kuehn, M. J., *et al.* (1996). Amino acid permeases require COPII components and the ER resident protein Shr3p for packaging into transport vesicles in vitro. The journal of cell Biology. **135**: 585-595.
- Kuilman, T., *et al.* (2014). Identification of Cdk targets that control cytokinesis. The EMBO Journal.
- Labeledzka, K., *et al.* (2012). Sho1p connects the plasma membrane with proteins of the cytokinesis network through multiple isomeric interaction states. J Cell Sci **125**(Pt 17): 4103-4113.
- Labib, K., *et al.* (2000). Uninterrupted MCM2-7 function required for DNA replication fork progression. Science **288**: 1643-1647.
- Lewis, W. H. (1939). The role of a superficial plasmagel layer in changes of form, locomotion and division of cells in tissue cultures. Archiv für Experimentelle Zellforschung **23**: 1-7.
- Lipka, E., *et al.* (2014). The Phragmoplast-Orienting Kinesin-12 Class Proteins Translate the Positional Information of the Preprophase Band to Establish the Cortical Division Zone in *Arabidopsis thaliana*. The Plant Cell. **26**: 2617-2632.
- Lippincott, J. and R. Li (1998). Dual function of Cyk2, a cdc15/PSTPIP family protein, in regulating actomyosin ring dynamics and septin distribution. J Cell Biol **143**(7): 1947-1960.

- Lorand, L. and R. M. Graham (2003). Transglutaminases: crosslinking enzymes with pleiotropic functions. Nat Rev Mol Cell Biol **4**(2): 140-156.
- Losick, V. P. (2016). Wound-Induced Polyploidy Is Required for Tissue Repair. Adv Wound Care (New Rochelle) **5**(6): 271-278.
- Luchini, A., *et al.* (2014). Protein painting reveals solvent-excluded drug targets hidden within native protein-protein interfaces. Nat Commun **5**: 4413.
- Lyu, Z., *et al.* (2016). Influence of FtsZ GTPase activity and concentration on nanoscale Z-ring structure in vivo revealed by three-dimensional superresolution imaging. Biopolymers.
- Mabuchi, I. (1973). A myosin-like protein in the cortical layer of the sea urchin egg. J Cell Biol **59**(2 Pt 1): 542-547.
- Mabuchi, I. (1974). A myosin-like protein in the cortical layer of cleaving starfish eggs. Journal of biochemistry **76**(1): 47-55.
- Mabuchi, I. and M. Okuno (1977). The effect of myosin antibody on the division of starfish blastomeres. J Cell Biol **74**(1): 251-263.
- Madaule, P. A., R; Myers, M (1987). Characterization of two members of the *rho* gene family from the yeast *Saccharomyces cerevisiae*. PNAS **84**: 779-783.
- Makarova, K. S., *et al.* (1999). A superfamily of archaeal, bacterial, and eukaryotic proteins homologous to animal transglutaminases. Protein science : a publication of the Protein Society **8**(8): 1714-1719.
- Mandal, S., *et al.* (2009). Rational drug design. European journal of pharmacology **625**(1-3): 90-100.
- Marsland, D. L., J. V. (1954). The mechanisms of cytokinesis: Temperature-pressure studies on the cortical gel system in various marine eggs. Journal of experimental zoology **125**(3): 507-539.
- Martinez-Rucobo, F. W., *et al.* (2009). Yeast chitin synthase 2 activity is modulated by proteolysis and phosphorylation. The Biochemical journal **417**(2): 547-554.
- Matsumura, F., *et al.* (2001). Role of myosin light chain phosphorylation in the regulation of cytokinesis Cell Struct Funct **26**(6): 639-644.
- Mayer, B. J. (2001). SH3 domains: complexity in moderation. J Cell Sci **114**(Pt 7): 1253-1263.
- Meitinger, F., *et al.* (2011). Phosphorylation-dependent regulation of the F-BAR protein Hof1 during cytokinesis. Genes Dev **25**(8): 875-888.
- Meitinger, F., *et al.* (2013). Dual function of the NDR-kinase Dbf2 in the regulation of the F-BAR protein Hof1 during cytokinesis. Mol Biol Cell **24**(9): 1290-1304.
- Meitinger, F., *et al.* (2010). Targeted localization of Inn1, Cyk3 and Chs2 by the mitotic-exit network regulates cytokinesis in budding yeast. Journal of cell science **123**(Pt 11): 1851-1861.
- Mendes Pinto, I., *et al.* (2012). Actin depolymerization drives actomyosin ring contraction during budding yeast cytokinesis. Developmental cell **22**(6): 1247-1260.

- Mercer, E. H. and L. Wolpert (1958). Electron microscopy of cleaving sea urchin eggs. Experimental cell research **14**(3): 629-632.
- Micanovic, R., *et al.* (1994). Role of Histidine 373 in the catalytic activity of coagulation factor XIII. The journal of biological Chemistry. **269**: 9190-9191.
- Miki-Noumura, T. and H. Kondo (1970). Polymerization of actin from sea urchin eggs. Experimental cell research **61**(1): 31-41.
- Miller, D. P., *et al.* (2015). Dephosphorylation of Iqg1 by Cdc14 regulates cytokinesis in budding yeast. Molecular biology of the Cell. **26**: 2913-2926.
- Minet, M., *et al.* (1979). Uncontrolled septation in a cell division cycle mutant of the fission yeast *Schizosaccharomyces pombe*. Journal of bacteriology **137**(1): 440-446.
- Mishima, M., *et al.* (2002). Central Spindle Assembly and Cytokinesis Require a Kinesin-like Protein/RhoGAP Complex with Microtubule Bundling Activity. Developmental cell. **2**: 41-54.
- Mishima, M., *et al.* (2004). Cell cycle regulation of central spindle assembly. Nature **430**(7002): 908-913.
- Mishra, M., *et al.* (2012). Cylindrical cellular geometry ensures fidelity of division site placement in fission yeast. J Cell Sci **125**(Pt 16): 3850-3857.
- Mishra, M., *et al.* (2013). In vitro contraction of cytokinetic ring depends on myosin II but not on actin dynamics. Nature cell biology **15**(7): 853-859.
- Mitchinson, J. M. (1953). Microdissection experiments on sea-urchin eggs at cleavage. Journal of Experimental Biology **30**: 515-524.
- Mizuguchi, S., *et al.* (2003). Chondroitin proteoglycans are involved in cell division of *Caenorhabditis elegans*. Nature **423**(6938): 443-448.
- Mohl, D. A., *et al.* (2009). Dbf2–Mob1 drives relocalization of protein phosphatase Cdc14 to the cytoplasm during exit from mitosis. The journal of cell Biology. **184**: 527-539.
- Moravcevic, K., *et al.* (2015). Comparison of *Saccharomyces cerevisiae* F-BAR domain structures reveals a conserved inositol phosphate binding site. Structure **23**(2): 352-363.
- Müller, S., *et al.* (2006). Two Kinesins Are Involved in the Spatial Control of Cytokinesis in *Arabidopsis thaliana*. Current Biology. **16**: 888-894.
- Müller, S. and G. Jürgens (2015). Plant cytokinesis—No ring, no constriction but centrifugal construction of the partitioning membrane. Seminars in Cell and Developmental Biology, Elsevier Ltd: 1-9.
- Mullins, J. M. and J. J. Biesele (1977). Terminal phase of cytokinesis in D-98S cells. The journal of cell Biology. **73**: 672-684.
- Muñoz, J., *et al.* (2013). Extracellular cell wall $\beta(1,3)$ glucan is required to couple septation to actomyosin ring contraction. The journal of cell Biology. **203**: 265-282.
- Munro, C. A., *et al.* (2001). Chs1 of *Candida albicans* is an essential chitin synthase

required for synthesis of the septum and for cell integrity. Molecular microbiology **39**(5): 1414-1426.

Murakami, K., *et al.* (1997). Protection by histidine against oxidative inactivation of AMP deaminase in yeast. Biochemistry and molecular biology international. **42**: 1063-1069.

Nagahashi, S., *et al.* (1995). Characterization of Chitin Synthase 2 of *Saccharomyces cerevisiae*. The journal of biological Chemistry. **270**: 13961-13967.

Nakayama, Y. and T. Inoue (2016). Antiproliferative Fate of the Tetraploid Formed after Mitotic Slippage and Its Promotion; A Novel Target for Cancer Therapy Based on Microtubule Poisons. Molecules **21**(5).

Naylor, S. G. and D. O. Morgan (2014). Cdk1-dependent phosphorylation of Iqg1 governs actomyosin ring assembly prior to cytokinesis. Journal of cell science. **127**: 1128-1137.

Newstead, S., *et al.* (2007). High-throughput fluorescent-based optimization of eukaryotic membrane protein overexpression and purification in *Saccharomyces cerevisiae*. Proc Natl Acad Sci U S A **104**(35): 13936-13941.

Nishihama, R., *et al.* (2009). Role of Inn1 and its interactions with Hof1 and Cyk3 in promoting cleavage furrow and septum formation in *S. cerevisiae*. J Cell Biol **185**(6): 995-1012.

Nishimura, K., *et al.* (2009). An auxin-based degron system for the rapid depletion of proteins in nonplant cells. Nature methods **6**(12): 917-922.

Nishimura, K. and M. T. Kanemaki (2014). Rapid Depletion of Budding Yeast Proteins via the Fusion of an Auxin-Inducible Degron (AID). Curr Protoc Cell Biol **64**: 20 29 21-20 29 16.

Nkosi, P. J., *et al.* (2013). Hof1 and Rvs167 have redundant roles in actomyosin ring function during cytokinesis in budding yeast. PloS one **8**(2): e57846.

Nurse, P., *et al.* (1976). Genetic control of the cell division cycle in the fission yeast *Schizosaccharomyces pombe*. Molecular & general genetics : **MGG 146**(2): 167-178.

O'Conallain, C., *et al.* (1999). Regulated nuclear localisation of the yeast transcription factor Ace2p controls expression of chitinase (CTS1) in *Saccharomyces cerevisiae*. Molecular & general genetics : **MGG 262**(2): 275-282.

Oh, Y., *et al.* (2012). Mitotic exit kinase Dbf2 directly phosphorylates chitin synthase Chs2 to regulate cytokinesis in budding yeast. Molecular biology of the Cell. **23**: 2445-2456.

Oh, Y., *et al.* (2013). Targeting and functional mechanisms of the cytokinesis-related F-BAR protein Hof1 during the cell cycle. Molecular biology of the Cell. **24**: 1305-1320.

Ohkura, H., *et al.* (1995). The conserved *Schizosaccharomyces pombe* kinase plo1, required to form a bipolar spindle, the actin ring, and septum, can drive septum formation in G1 and G2 cells. Genes & Development. **9**: 1059-1073.

- Oliferenko, S., *et al.* (2009). Positioning cytokinesis. Genes Dev **23**(6): 660-674.
- Onishi, M., *et al.* (2013). Distinct roles of Rho1, Cdc42, and Cyk3 in septum formation and abscission during yeast cytokinesis. The Journal of cell biology **202**(2): 311-329.
- Osman, M. A. and R. A. Cerione (1998). Iqg1p, a yeast homologue of the mammalian IQGAPs, mediates cdc42p effects on the actin cytoskeleton. J Cell Biol **142**(2): 443-455.
- Overington, J. P., *et al.* (2006). How many drug targets are there? Nature reviews. **5**: 993-996.
- Palani, S., *et al.* (2012). Cdc14-dependent dephosphorylation of Inn1 contributes to Inn1-Cyk3 complex formation. Journal of cell science. **125**: 3091-3096.
- Pammer, M., *et al.* (1992). *DIT101* (*CSD2*, *CAL1*), a cell cycle-regulated yeast gene required for synthesis of chitin in cell walls and chitosan in spore walls. Yeast **8**(12): 1089-1099.
- Paoletti, A. and F. Chang (2000). Analysis of mid1p, a protein required for placement of the cell division site, reveals a link between the nucleus and the cell surface in fission yeast Mol Biol Cell **11**(8): 2757-2773.
- Peng, X. M., *et al.* (2013). Current developments of coumarin compounds in medicinal chemistry. Curr Pharm Des **19**(21): 3884-3930.
- Perry, M. M., *et al.* (1971). Actin-like filaments in the cleavage furrow of newt egg. Experimental cell research **65**(1): 249-253.
- Pickett-Heaps JD, N. D. (1966). Organization of microtubules and endoplasmic reticulum during mitosis and cytokinesis in wheat meristems. Journal of cell science **1**: 109-120.
- Piekny, A., *et al.* (2005). Cytokinesis: welcome to the Rho zone. Trends in Cell Biology. **15**: 651-658.
- Plummer, T. H. J., *et al.* (1987). Detection and quantification of peptide-N4-(N-acetyl- β -glucosaminyl)asparagine amidases. European Journal of Biochemistry. **163**: 167-173.
- Pollard, L. W., *et al.* (2012). Fission yeast Cyk3p is a transglutaminase-like protein that participates in cytokinesis and cell morphogenesis. Molecular biology of the cell **23**(13): 2433-2444.
- Pollard, T. D. (2010). Mechanics of cytokinesis in eukaryotes. Curr Opin Cell Biol **22**(1): 50-56.
- Postis, V. L. G., *et al.* (2009). A high-throughput assay of membrane protein stability. Molecular Membrane Biology. **25**: 617-624.
- Pruyne, D., *et al.* (2004). Stable and dynamic axes of polarity use distinct formin isoforms in budding yeast. Mol Biol Cell **15**(11): 4971-4989.
- Queralt, E. and F. Uhlmann (2008). Cdk-counteracting phosphatases unlock mitotic exit. Curr Opin Cell Biol **20**(6): 661-668.
- Rancati, G., *et al.* (2008). Aneuploidy Underlies Rapid Adaptive Evolution of Yeast Cells Deprived of a Conserved Cytokinesis Motor. Cell, Elsevier Inc. **135**: 879-893.

- Rappaport, R. (1961). Experiments concerning the cleavage stimulus in sand dollar eggs. J Exp Zool **148**: 81-89.
- Rappaport, R. (1967). Cell division: direct measurement of maximum tension exerted by furrow of echinoderm eggs." Science **156**(3779): 1241-1243.
- Reijntjens, P., *et al.* (2010). *Candida albicans* SH3-domain proteins involved in hyphal growth, cytokinesis, and vacuolar morphology. Current genetics **56**(4): 309-319.
- Ren, L., *et al.* (2014). The Cdc15 and Imp2 SH3 domains cooperatively scaffold a network of proteins that redundantly ensure efficient cell division in fission yeast. Molecular biology of the Cell: 1-30.
- Ren, L., *et al.* (2015). The Cdc15 and Imp2 SH3 domains cooperatively scaffold a network of proteins that redundantly ensure efficient cell division in fission yeast. Molecular biology of the Cell. **26**: 256-269.
- Rhyu, M. S., *et al.* (1994). Asymmetric distribution of numb protein during division of the sensory organ precursor cell confers distinct fates to daughter cells. Cell **76**(3): 477-491.
- Rippert, D., *et al.* (2014). Regulation of cytokinesis in the milk yeast *Kluyveromyces fragilis*. BBA - Molecular Cell Research, Elsevier B.V. **1843**: 2685-2697.
- Roberts-Galbraith, R. H., *et al.* (2009). The SH3 domains of two PCH family members cooperate in assembly of the *Schizosaccharomyces pombe* contractile ring. J Cell Biol **184**(1): 113-127.
- Roberts-Galbraith, R. H., *et al.* (2010). Dephosphorylation of F-BAR protein Cdc15 modulates its conformation and stimulates its scaffolding activity at the cell division site. Mol Cell **39**(1): 86-99.
- Rodriguez-Rodriguez, J. A., *et al.* (2016). Mitotic Exit Function of Polo-like Kinase Cdc5 Is Dependent on Sequential Activation by Cdk1. Cell Rep **15**(9): 2050-2062.
- Sagot, I., *et al.* (2002). An actin nucleation mechanism mediated by Bni1 and Profilin. Nature cell Biology.
- Sanchez-Diaz, A., *et al.* (2004). Rapid depletion of budding yeast proteins by fusion to a heat-inducible degron. Sci STKE **2004**(223): PL8.
- Sanchez-Diaz, A., *et al.* (2008). Inn1 couples contraction of the actomyosin ring to membrane ingression during cytokinesis in budding yeast. Nature cell biology **10**(4): 395-406.
- Sanchez-Diaz, A., *et al.* (2012). The Mitotic Exit Network and Cdc14 phosphatase initiate cytokinesis by counteracting CDK phosphorylations and blocking polarised growth. The EMBO journal **31**(17): 3620-3634.
- Sanders, S. L. and C. M. Field (1995). Bud-site selection is only skin deep. Current Biology. **5**: 1213-1215.
- Santoro, A., *et al.* (2016). Molecular mechanisms of asymmetric divisions in

- mammary stem cells. EMBO Rep **17**(12): 1700-1720.
- Sburlati, A. and E. Cabib (1986). Chitin synthetase 2, a presumptive participant in septum formation in *Saccharomyces cerevisiae*. The Journal of biological chemistry **261**(32): 15147-15152.
- Scheich, C., *et al.* (2007). Vectors for co-expression of an unrestricted number of proteins. Nucleic Acids Res **35**(6): e43.
- Schmidt, M., *et al.* (2002). In budding yeast, contraction of the actomyosin ring and formation of the primary septum at cytokinesis depend on each other. Journal of cell science **115**(Pt 2): 293-302.
- Schmidt, S., *et al.* (1997). The Spg1p GTPase is an essential, dosage-dependent inducer of septum formation in *Schizosaccharomyces pombe*. Genes Dev **11**(12): 1519-1534.
- Schroeder, T. E. (1973). Actin in dividing cells: contractile ring filaments bind heavy meromyosin. Proc Natl Acad Sci U S A **70**(6): 1688-1692.
- Seko, A., *et al.* (1991). Peptide:N-Glycosidase Activity Found in the Early Embryos of *Oryzias latipes* (Medaka fish). The journal of biological Chemistry. **266**: 22110-22114.
- Shannon, K. B. and R. Li (1999). The Multiple Roles of Cyk1p in the Assembly and Function of the Actomyosin Ring in Budding Yeast. Molecular biology of the Cell. **10**: 283-296.
- Shannon, K. B. and R. Li (2000). A myosin light chain mediates the localization of the budding yeast IQGAP-like protein during contractile ring formation. Current Biology. **10**: 727-730.
- Shaw, J. A., *et al.* (1991). The function of chitin synthases 2 and 3 in the *Saccharomyces cerevisiae* cell cycle. J Cell Biol **114**(1): 111-123.
- Shimada, A., *et al.* (2007). Curved EFC/F-BAR-domain dimers are joined end to end into a filament for membrane invagination in endocytosis. Cell **129**(4): 761-772.
- Shou, W., *et al.* (2002). Cdc5 influences phosphorylation of Net1 and disassembly of the RENT complex. BMC Molecular Biology. **3**: 1-14.
- Sikorski, R. S. and P. Hieter (1989). A system of shuttle vectors and yeast host strains designed for efficient manipulation of DNA in *Saccharomyces cerevisiae*. Genetics **122**: 19-27.
- Silverman, S. J., *et al.* (1988). Chitin synthase 2 is essential for septum formation and cell division in *Saccharomyces cerevisiae*. PNAS. **85**: 4735-4739.
- Smith, G. R., *et al.* (2002). GTPase-Activating Proteins for Cdc42. Eukaryotic cell. **1**: 469-480.
- Song, S. and K. S. Lee (2001). A novel function of *Saccharomyces cerevisiae* CDC5 in cytokinesis. The journal of cell Biology. **152**: 451-469.
- Stoepel, J., *et al.* (2005). The mitotic exit network Mob1p-Dbf2p kinase complex localizes to the nucleus and regulates

- passenger protein localization. Mol Biol Cell **16**(12): 5465-5479.
- Strasburger, E. (1913). Pflanzliche Zellen- und Gewebelehre. In: Von Wettstein R (ed) Zellen- und Gewebelehre, Morphologie und Entwicklungsgeschichte. B. G. Teubner, Leipzig: 1-174.
- Sudoh, M., *et al.* (2000). Identification of a novel inhibitor specific to the fungal chitin synthase. Inhibition of chitin synthase 1 arrests the cell growth, but inhibition of chitin synthase 1 and 2 is lethal in the pathogenic fungus *Candida albicans*. The Journal of biological chemistry **275**(42): 32901-32905.
- Sugiyama, K., *et al.* (1983). Demonstration of a new glycopeptidase, from jack-bean meal, acting on aspartylglucosylamine linkages. Biochemical and Biophysical Research Communications. **112**: 155-160.
- Sun, S. C. and N. H. Kim (2013). Molecular mechanisms of asymmetric division in oocytes. Microsc Microanal **19**(4): 883-897.
- Suzuki, T., *et al.* (2000). *PNG1*, a yeast gene encoding a highly conserved peptide:N-glycanase. The journal of cell Biology. **149**: 1039-1051.
- Takahashi, N. (1977). Demonstration of a new amidase acting on glycopeptides. Biochemical and Biophysical Research Communications. **76**: 1194-1201.
- Takaine, M., *et al.* (2009). Fission yeast IQGAP arranges actin filaments into the cytokinetic contractile ring. The EMBO Journal, Nature Publishing Group. **28**: 3117-3131.
- Takeo, S., *et al.* (2004). In vivo hyaluronan synthesis upon expression of the mammalian hyaluronan synthase gene in *Drosophila*. J Biol Chem **279**(18): 18920-18925.
- Tate, C. G. (2001). Overexpression of mammalian integral membrane proteins for structural studies. FEBS letters. **504**: 94-98.
- Tatsumoto, T., *et al.* (1999). Human ECT2 is an exchange factor for Rho GTPases, phosphorylated in G2/M phases, and involved in cytokinesis. The journal of cell Biology. **147**: 921-927.
- Taylor, G. S., *et al.* (1997). The activity of Cdc14p, an oligomeric dual specificity protein phosphatase from *Saccharomyces cerevisiae*, is required for cell cycle progression. J Biol Chem **272**(38): 24054-24063.
- Tebbs, I. R. and T. D. Pollard (2013). Separate roles of IQGAP Rng2p in forming and constricting the *Schizosaccharomyces pombe* cytokinetic contractile ring. Molecular biology of the Cell. **24**: 1904-1917.
- Teh, E. M., *et al.* (2009). Retention of Chs2p in the ER requires N-terminal CDK1-phosphorylation sites. Cell Cycle **8**(18): 2964-2974.
- Tian, C., *et al.* (2014). Stepwise and cooperative assembly of a cytokinetic core complex in *Saccharomyces cerevisiae*. Journal of cell science **127**(Pt 16): 3614-3624.
- Trautmann, S., *et al.* (2001). Fission yeast Clp1p phosphatase regulates G2/M transition and coordination of cytokinesis with cell cycle progression. Current Biology. **11**: 931-940.

- Traverso, E. E., *et al.* (2001). Characterization of the Net1 Cell Cycle-dependent Regulator of the Cdc14 Phosphatase from Budding Yeast. Journal of Biological Chemistry. **276**: 21924-21931.
- Vallen, E. A., *et al.* (2000). Roles of Hof1p, Bni1p, Bnr1p, and myo1p in cytokinesis in *Saccharomyces cerevisiae*. Mol Biol Cell **11**(2): 593-611.
- Vedyaykin, A. D., *et al.* (2016). New insights into FtsZ rearrangements during the cell division of *Escherichia coli* from single-molecule localization microscopy of fixed cells. MicrobiologyOpen: n/a-n/a.
- VerPlank, L. and R. Li (2005). Cell cycle-regulated trafficking of Chs2 controls actomyosin ring stability during cytokinesis. Mol Biol Cell **16**(5): 2529-2543.
- Visintin, R., *et al.* (1998). The phosphatase Cdc14 triggers mitotic exit by reversal of Cdk-dependent phosphorylation. Mol Cell **2**(6): 709-718.
- Wallin, E. and G. Von Heijne (1998). Genome-wide analysis of integral membrane proteins from eubacterial, archaean, and eukaryotic organisms. Protein Science. **7**: 1029-1038.
- Watts, F. Z., *et al.* (1987). The yeast *MYO1* gene encoding a myosin-like protein required for cell division. Embo J **6**(11): 3499-3505.
- Weigel, P. H. (2002). Functional Characteristics and Catalytic Mechanisms of the Bacterial Hyaluronan Synthases. IUBMB Life. **54**: 201-211.
- Weigel, P. H., *et al.* (2015). Hyaluronan synthase assembles chitin oligomers with -GlcNAc(α 1-)UDP at the reducing end. Glycobiology: 1-39.
- White, E. A. and M. Glotzer (2012). Centralspindlin: At the heart of cytokinesis. Cytoskeleton. **69**: 882-892.
- White, J. G. and G. G. Borisy (1983). On the mechanisms of cytokinesis in animal cells. J Theor Biol **101**(2): 289-316.
- Wloka, C., *et al.* (2013). Immobile myosin-II plays a scaffolding role during cytokinesis in budding yeast. The Journal of cell biology **200**(3): 271-286.
- Wolpert, L. (1960). The mechanics and mechanism of cleavage. International Review of Cytology **10**: 163-216.
- Wu, J.-Q. and T. D. Pollard (2005). Counting cytokinesis proteins globally and locally in fission yeast. Science. **310**: 310-314.
- Yabe, T., *et al.* (1998). Mutational analysis of chitin synthase 2 of *Saccharomyces cerevisiae*. Identification of additional amino acid residues involved in its catalytic activity. Eur J Biochem **258**(3): 941-947.
- Yang, D., *et al.* (2007). Increased polyploidy in aortic vascular smooth muscle cells during aging is marked by cellular senescence. Aging Cell **6**(2): 257-260.
- Yatsu, N. (1908). Some experiments on cell-division in the egg of *Cerebratulus lacteus*. Annotationes Zoologicae Japonenses **6**(4): 267-276.

- Yatsu, N. (1912). Observations and experiments on the Ctenophore egg. I. The structure of the egg and experiments on cell-division. Journal of the College of Science, Imperial University of Tokyo **32**(3): 1-21.
- Yellman, C. M. and G. S. Roeder (2015). Cdc14 Early Anaphase Release, FEAR, Is Limited to the Nucleus and Dispensable for Efficient Mitotic Exit. PloS one. **10**: e0128604.
- Yi, K. and R. Li (2012). Actin cytoskeleton in cell polarity and asymmetric division during mouse oocyte maturation. Cytoskeleton **69**(10): 727-737.
- Yoshida, S. and T.-e. Akio (2002). Budding yeast Cdc5 phosphorylates Net1 and assists Cdc14 release from the nucleolus. Biochemical and Biophysical Research Communications. **294**: 687-691.
- Yoshida, S., *et al.* (2006). Polo-like kinase Cdc5 controls the local activation of Rho1 to promote cytokinesis. Science **313**(5783): 108-111.
- Yu, F., *et al.* (2006). *Drosophila* neuroblast asymmetric cell division: recent advances and implications for stem cell biology. Neuron **51**(1): 13-20.
- Yu, H. and K. Schulten (2013). Membrane sculpting by F-BAR domains studied by molecular dynamics simulations. PLoS Comput Biol **9**(1): e1002892.
- Zhang, G., *et al.* (2006). Exit from mitosis triggers Chs2p transport from the endoplasmic reticulum to mother-daughter neck via the secretory pathway in budding yeast. J Cell Biol **174**(2): 207-220.
- Zhang, Y. V., *et al.* (2010). Stem cell dynamics in mouse hair follicles: a story from cell division counting and single cell lineage tracing. Cell Cycle **9**(8): 1504-1510.
- Ziman, M. and D. I. Johnson (1994). Genetic Evidence for a Functional Interaction between *Saccharomyces cerevisiae* CDC24 and CDC42. Yeast. **10**: 463-474.
- Zou, Y., *et al.* (2012). N-terminal T4 lysozyme fusion facilitates crystallization of a G protein coupled receptor. PloS one **7**(10): e46039.